Addis Ababa University
አዲስ አበባ ዩኒቨርሲቲ
Seek Wisdom, Elevate your Intellect and Serve Humanity

ETHIOPIAN INSTITUTE OF WATER RESOURCES

Characterization of Major Alluvial Aquifers of Ethiopia and Determination of their Vulnerability to Climate Variability and Land use Changes

Ph.D. Dissertation

By: Tesema Kebede Seifu

Department: Water Resources Engineering and Management

(Specialization: - Groundwater Management)

Supervisors:

Tenalem Ayenew (Ph.D., Professor, AAU)

Taye Alemayehu (Ph.D., Assistant professor, AAU)

Tekalegn Ayele Woldesenbet (Ph.D., Associate professor, AAU)

June, 2024

Addis Ababa University, Addis Ababa, Ethiopia

Addis Ababa University

Characterization of Major Alluvial Aquifers of Ethiopia and Determination of their Vulnerability to Climate and Land cover Changes

Tesema Kebede Seifu

A dissertation submitted to the Ethiopian Institute of Water Resources

Presented in the Fulfillment of the Requirement for the degree of Doctor of Philosophy in Water Resources Engineering and Management (Specialization on Groundwater Management)

Addis Ababa University, Addis Ababa, Ethiopia

June, 2024

Dedication

I would like to dedicate my work to my beloved sister Mrs. Dirshaye Kebede Seifu for her unconditional love and support. She instilled in me a desire to learn and made sacrifices so that I could have access to quality education from an early age. Also, this is dedicated to my close friends who have always supported me throughout my college years.

Statement of Declaration

I hereby certify that I am the sole author of this dissertation. I certify that, to the best of my knowledge and belief, my dissertation does not infringe any copyright or proprietary rights, and that any ideas, techniques, quotations, or other material from the work of others contained in my dissertation will be published or otherwise fully acknowledged by standard attribution practices.

I declare that this is the true copy of my dissertation, including all final revisions, as approved by my doctoral committee and the study office, and that this dissertation has not been submitted to any university or institution for a higher degree.

Declaration

I, the undersigned, swear that this is my original work, that it has never been presented or promoted at this or any other university, and that all resources utilized for the dissertation have been acknowledged.

Tesema Kebede Seifu

Signature: 

Date: 16/11/2023

This dissertation has been submitted for examination with my approval as supervisor committee:

Main Advisor:

Tenalem Ayenew (Ph.D. Professor, AAU)

Signature: 

Date: 16/11/2023

Co Advisors:

Taye Alemayehu (Ph.D., Assistant Professor, AAU)

Signature: 

Date: 17/11/2023

Tekalegn Ayele Woldesenbet (Ph.D., Associate Professor, AAU)

Signature: 

Date: 28/11/2023

Table of Contents

LIST OF FIGURES

LIST OF TABLES

LIST APPENDIXES

Appendix Figures

Appendix Tables

LIST OF ABBREVIATION

AI	Aridity index
AETc	Actual crop evapotranspiration
AHP	Analytical hierarchy process
CMIP6	Coupled Model Inter-comparison Project-6
CMCC	ESM2- Euro-Mediterranean Centre on Climate Change with Climate and Earth System Models
DMI	De Martone Aridity Index
DTC	Decision tree classifier
$\delta D/\delta\ ^{2}H$	Stable isotope of hydrogen (Deuterium)
D-excess	Deuterium excess
EC	Eastern catchment
ETc	Crop evapotranspiration
ETo	Potential evapotranspiration
FGOALS-g3	Flexible Global Ocean-Atmosphere-Land System Model Grid-Point Version GCM Global climate model
GBC	Gradient boaster classifier
GWPZ	Groundwater potential zone
KNC	k-Neighbors classifier
LULC	Land use land cover
MCDM	multi-criteria Decision-Making
MIROC6	Model for Interdisciplinary Research on Climate version 6
MODIS	Moderate Resolution Imaging Spectroradiometer
MLA	Machine learning algorithm
NDVI	Natural difference vegetation index
$\delta^{18}O$	Stable isotope of oxygen (oxygen atoms have a mass of 18 (8 protons and 10 neutrons)
RFC	Random Forest classifier
ROC	Receiver operating curve
RCP	Representative concentration pathways

TZ^+	Total cations
TDS	Total dissolved solids
TWI	Topographic wetness index
TRI	Topographic roughness index
UNEP	United Nations Environment Program
V-SMOW	Vienna Standard Mean Ocean Water
WMO	World Meteorological Organization
WC	Western catchment

ACKNOWLEDGMENT

First of all, I would like to thank almighty God, for letting me through all the difficulties. I have experienced your guidance day by day. It's you who gave me permission to complete my degree. I will continue to have faith in you for my future.

I would like to acknowledge and give my deepest thanks to my supervisors Prof. Tenalem Ayenew, Dr. Taye Alemayehu, and Dr. Tekalegn Ayele for their continued support and encouragement. I would like to thank department committee members for letting my defense for their support throughout my study period. The author also thanks all governmental organizations, for providing the necessary data for this research work. The author also wants to give special gratitude to the professionals in the Somali Reginal State and Dire-Dawa administration water bureau for their valuable support during data collection.

It would not have been possible to complete this thesis without the support of my classmates Mrs. Kidist Demissie.

I would like to express my sincere gratitude and unconditional love to my dear sister, Mrs. Dirshaye Kebede, for her invaluable support and inspiration during a period when I was losing hope.

Finally, I express my sincere appreciation for the learning opportunities offered by Haramaya University Institute of Technology (HIT).

List of original papers

1. Seifu, T. K., Ayenew, T., Woldesenbet, T. A., & Alemayehu, T. (2022). Identification of groundwater potential sites in the drought-prone area using geospatial techniques at Fafen-Jerer sub-basin, Ethiopia. Geology, Ecology, and Landscapes, 1-13. https://doi.org/10.1080/24749508.2022.2141993
2. Seifu, T. K., Ayenew, T., Alemayehu, T., & Woldesenbet, T. A. (2023). Groundwater potential mapping using GIS and remote sensing with multi-criteria decision-making in Shinile sub-basin, eastern Ethiopia. Songklanakarin Journal of Science & Technology, 45(1). https://web.s.ebscohost.com/
3. Seifu, T. K., Eshetu, K. D., Woldesenbet, T. A., Alemayehu, T., & Ayenew, T. (2023). Application of advanced machine learning algorithms and geospatial techniques for groundwater potential zone mapping in Gambela Plain, Ethiopia. Hydrology Research. https://doi.org/10.2166/nh.2023.083
4. Seifu T.K (2023) Hydrogeochemical and Stable isotope characteristics of the major alluvial region of Ethiopia Accepted
5. Seifu T.K., Woldesenbet T.A., Alemayehu T., & Ayenew T. (2023) Aquifer vulnerability analysis using original and Modified DRASTIC method on alluvial aquifer zones, Ethiopia https://doi.org/10.1007/s12524-024-01818-0
6. Seifu T.K., Woldesenbet T.A., Alemayehu T., & Ayenew T. (2023) Spatio-temporal change of Land use/land cover and vegetation using multi-MODIS satellite data, western Ethiopia. https://doi.org/10.1155/2023/7454137
7. Seifu, T. K., & Demessie Eshetu, K. (2024). Characterizing the aridity indices and potential evapotranspiration using CMIP6-GCMs in two distinct regions of Ethiopia. Journal of Water and Climate Change, jwc2024394. https://doi.org/10.2166/wcc.2024.394
8. Seifu T.K.(2023) Climate and land use impact on Groundwater of Alluvial regions, Ethiopia: Under review

GENERAL ABSTRACT

Water is an essential resource for the sustainability of life. Goals for access to clean water, the growth of the energy sector, and food security can all be met with the help of climate-resilient groundwater management. Nonetheless, not much study has been done to evaluate Ethiopia's groundwater resources. The purpose of this study was to examine the physical attributes of Ethiopia's principal alluvial aquifers and determine how sensitive they were to changes in the country's climate and land cover. Geographic information systems (GIS), remote sensing, the analytic hierarchy process (AHP) method of multicriteria decision-making (MCDM), and machine learning algorithms (MLAs) were all utilized in the first segment. The hydro-geological, climatic, and land use land cover (LULC) characteristics were explored as potential influencing variables for groundwater in the study regions. Following that, the stable isotope and geochemical analysis were employed to better understand the groundwater and the underlying geological components. Examination of aquifer vulnerability using a modified DRASTIC index was the third technique implemented. The study's other main emphasis was the effect of changing climate and land cover on groundwater. Independent research on LULC and climate change was also conducted in this part. Lastly, the study looked at how groundwater is affected by changes in climate and land cover together. According to the groundwater potential analysis, 81.93% of Fafen-Jerer, 22.35% of Gambela, and 17.38% of Shinile are classified as low and very low potential zones. The high and very high groundwater potential zone covers 4.32% of Fafen-Jerer, 55.52% of Gambela, and 64.8% of the Shinile sub-basin. The key criteria highly influencing groundwater potential in the research areas are geomorphology, rainfall, and geology. The geochemical analysis indicates that the predominant cation and anion concentrations are $Ca^{2+} > Na^{+} > Mg^{2+} > K^{+}$ and $SO_4^{2-} > HCO_3^{-} > Cl^{-} > NO_3^{-}$ respectively. The groundwater in the study sites is slightly alkaline and quite hard. Mixed (Na-Mg-Ca) water is the most prevalent water type kind in the research area. The primary hydrochemical process is the interaction between rocks and water. The isotope analysis revealed that groundwater samples of hydrogen and oxygen isotopic compositions were mostly concentrated close to the meteoric water line. The results demonstrate that precipitation has been found to have more enriched isotope compositions than groundwater at both locations (Dire Dawa and Jigjiga). The LULC's findings show that croplands have reduced, whereas forests have increased significantly in coverage in the western catchment (WC). The LULC shift for the eastern catchment (EC) indicates an increase in area coverage of grasslands, croplands, and urban areas,

and a reduction in shrublands, and barren. Climate research reveals that climate change will be a major concern for water supplies in the studied regions. Over the reference period (1981-2010), the WC and EC had annual temperature rises of 1.5 and 0.06 ºC, and annual precipitation declines of 15.73 and 3.68 mm/year respectively. These changes in these core climatic parameters continue to affect future cases. According to the UNEP aridity index (AI) and De Martone aridity index (DMI) results the aridity indices also followed a downward trend for the past periods. These changes shift the climate characters from humidity conditions to semi-arid and arid climates. According to the study, the effect of climatic change is more pronounced in the WC than in the EC. The results of the current period's climate change show that it is particularly robust in the study regions' dry corners. The effect of climate on groundwater will be pronounced in these regions by the end of 2070. The outputs of this research should provide a significant understanding of Ethiopian alluvial aquifer zones for future studies in paleoclimatology, hydrogeology, meteorology, and geomorphology. The study's findings might be useful for water resource and environmental management, as well as policy and decision-making.

Keywords: Alluvial aquifers, Aridity Indices, GCM, Geospatial, Groundwater potential; Isotope-Geochemistry, MODIS

CHAPTER 1

GENERAL INTRODUCTION

1.1. Background and Justification

Water is one of the most important necessities for overrun life on earth (Vardhan et al., 2019; Young & Haveman, 1985). Scientists have investigated water as a resource since research began (Gerlak & Mukhtarov, 2015). There are more than a dozen methods of assessing and researching water resources, ranging from regional to specific spatial coverage (AL-Washali et al., 2016; Gerlak & Mukhtarov, 2015; Hamza et al., 2015; Koop & van Leeuwen, 2015; Leavesley, 1994; Nika et al., 2020; Yasin et al., 2021). Assessment methods vary by region, purpose, available technology, time, and economic values. The climate is the main driver of water resources which is an important part of the ecosystem. Life exists almost everywhere on the surface of the earth due to the favoring of this natural gift, the climate(Edwards, 2011; Urry, 2015). Today, climatic unpredictability and land cover changes are the two main issues affecting water supplies (Beillouin et al., 2022; Ty et al., 2022; Wang et al., 2022).

Intergovernmental Panel on Climate Change (IPCC) estimates that since 1880, global temperature increased by about 1 degree Celsius, by 2050 it is projected to be 1.5 degrees Celsius, and by 2100 2-4 degrees Celsius (Kumar, 2012). There are several signs that the natural environment has changed as a result of climatic changes. High-magnitude floods, prolonged droughts, flow variability, temperature rise, and reduced rainfall are among these influences (Clarke et al., 2022; Kourtis et al., 2022). Climate change plays a considerable role in farming practices, water resources management, and even public health. The climate change consequences are not only affecting the surface water resources but also the subsurface system (Hanifehlou et al., 2022; Swain et al., 2022). Climate change touches the subsurface water resources in two basic ways: one by recharge variability and the other by changing the level of groundwater depth (Berhail, 2019; Hashemi et al., 2015). It is important to understand climate conditions more precisely than approximately to plan adaptive measures.

The growing problem of climate change in many parts of the world is aridity (Wallén, 1967). While temperature and rainfall are the main determinants of aridity, other elements also have a role. The air's moisture content affects the soil's water balance. Water has a propensity to evaporate into the

air when the moisture content of the soil is higher than that of the air. The degree of aridity/dryness of a climate in a given location is expressed by a numerical indicator called the Aridity Index (AI) (Bešťáková et al., 2023; dos Santos et al., 2022). The UNCCD definition of Desertification is “land degradation brought on by a variety of variables, such as climate fluctuations and human activity, in dry sub-humid, semi-arid, and arid regions” (Ambalam, 2014). The degree to which a system (e.g., an arid or a semi-arid ecosystem or land) is susceptible to adverse effects of desertification intensified by climate changes is stated as vulnerability. A system's susceptibility to climatic fluctuation depends on its sensitivity, adaptability, and the kind, rate, and extent of desertification it experiences (Eze & Onokala, 2022; Imbrenda et al., 2022).

The other major parameter that affects the water resources system is the land cover change (Kabite, et al., 2018; Chimdessa et al., 2019). Many studies report that land-use change has become a very serious problem in environmental dynamics (Birhanu et al., 2019; Choto & Fetene, 2019; Gashaw et al., 2018). In addition to altering the surface water resources, land-use change influences recharge to the subsurface system and affects groundwater storage. Therefore, for integrated water management, it is essential to consider simultaneously the climate and land-use changes impact (Yan et al., 2019). The combined effects of land-use change and climate on water resources in general and groundwater resources, in particular, is the concern of scholars today (Elias et al., 2018; Guzha et al., 2018; Wu et al., 2020).

The study areas are covered by quaternary sediment as a major geologic material. The report shows that almost one-fourth of the landmass of the country is covered by quaternary aquifers (Kebede, 2013). Alluvial and terrace deposits include sand, silt, clay, and gravel, and together they make up the Quaternary aquifer. These aquifers are generally unconfined, and composition of gravel, sand, silt, and clay, deposited by a river in a river channel, banks, or floodplain (Kassune et al., 2018). Aquifers that are alluvial possibly very fruitful (Owen & Dahlin, 2005), and can be taken as simple-layer groundwater bodies (Di Lorenzo & Galassi, 2013). There are two types of alluvial formations: those dispersed throughout alluvial plains are the first and the other alluvial which strips along with river courses (Ayenew et al., 2008).

It is anticipated that Africa will use more groundwater in the next decades as a result of the continent's rapidly growing population and increased abstraction for various purposes (Pavelic, P. 2012). Ethiopia relies largely on groundwater for industry, animal production, and drinking.

Aquifers provide more than 80% of the water supply (Kebede et al., 2005; Khadim et al., 2020). Even though most people's lives depend on groundwater, not many thorough hydrogeological investigations have been done on the alluvial aquifers and related sediment zones (Ayenew et al., 2008). Over-extraction lowers the water table, which impacts the streamflow that feeds into the aquifer, harming the ecology and the sustainability of water resources. Additionally, the overall groundwater trends in alluvial aquifers can be influenced by a variety of factors, including the climate, agricultural practices, land use, and land cover.

Because high-quality water is required for home and agricultural usage, groundwater quality must get the same consideration as quantity (Yousefi et al. 2018). The World Health Organization (WHO, 2016) indicated that an estimated 663 million people globally, mostly in developing nations, rely on tainted or dangerous water for cooking and drinking. According to reports, the study region's water resources contain certain ingredients that are not advised by standards for national and international organizations (Smedley, P. 2001; Tilahun & Merkel, 2010). The primary features of the groundwater in the region are its high amounts of nitrate and chloride, high dissolved solids content, high salinity, and hardness. Understanding the quality of the water used for drinking and irrigation, as well as any possible detrimental effects on human health and plant development, is essential to preventing quality concerns, maximizing agricultural output, and protecting public health. The primary issue affecting water quality is also the impending effects of climate change and land use and land cover changes. Furthermore, future population increase is predicted to necessitate drilling more water wells, which in turn draws more animals and causes organic wastes to build up at water sites, especially in arid places.

In the majority of the research locations, there is a serious deficiency of hydrogeological data. There is no widely accessible systematic database. A lot of work has gone into gathering relevant data for this study from academic institutions, governmental and non-governmental organizations, and other sources. Climate models are the leading modern techniques for making climate predictions on seasonal to decadal time scales and for making projections of future climate (Kattsov et al., 2013). Remote sensing satellite data have efficient applications in detecting structural geology and mapping inaccessible areas. Digital elevation model (DEM) data, Geographic Information System (GIS), Landsat, Aster, and other satellite imagery, are rapid and cost-effective methods for geological mapping and interpretation. These instruments offer data on vast and unreachable

regions in a brief amount of time for the evaluation, observation, and administration of groundwater resources. Isotope and hydro-chemical methods are some of the approaches to investigate the character of groundwater. The isotope methods give insight into detecting the origin, inflow zones, and rates of groundwater (Ayenew et al., 2008; Kebede and Zewdu, 2019).

The area for this study was selected because of its aquifer types (alluvial sediment), its climatic nature (highly variable climate nature), its water availability (potable water scarcity), and its economic importance. The techniques used to investigate alluvial aquifers were based on a multidisciplinary data-layer analysis that considers land cover, hydrogeological data, stable isotopes-geochemistry, geology, geomorphology, drainage lines, soil type, and structural lineaments. Water availability, composition, sensitivity to natural calamities, and climate and LULC change are the four main factors that determine the characteristics of alluvial groundwater. Because of this, the research focuses on these environmental and hydroclimatic aspects to investigate the features of alluvial groundwaters.

1.2. Statement of the problem

Water is one of the most important elements needed for life on Earth to exist. However, it is anticipated that human activity will cause 1.0°C greater global warming than pre-industrial levels; it will likely vary from 0.8°C to 1.2°C. If the current pace of growth in global warming persists, it is expected to reach 1.5°C by 2030–2052 (IPCC, 2019). According to the IPCC (2019) report, in Africa, from total water resources available, agriculture takes about 85% of the water, and the other portions 10% and 5% used for domestic supply and industrial purposes respectively.

Groundwater is one of the main sources of domestic water supply for Ethiopia. Among the main aquifers; alluvial aquifers are very good sources of groundwater due to their important hydro-geologic formations (Macdonald et al., 2019). Alluvial aquifers are advantageous over other aquifers due to their abundant yields and shallow depths. The shallow depths and high porosity nature of the aquifers make them particularly vulnerable to pollution and water level fluctuations due to seasonal variations in precipitation. Additionally, overexploitation of groundwater resources from alluvial aquifers can impose pressures on surface water courses and wetlands (Mansour et al., 2012).

Hydro-climatic characteristics determine the occurrence, origin, distribution, and flow of groundwater. Identification of the different hydro-climatic parameters and their assessment are necessary for predicting groundwater potential and planning. The groundwater resources of the country have many challenges due to its unpredicted amount and the argument about its potential. Different studies attempt to reflect this evidence and suggest the measures that should be taken to come up with the solutions. Some studies were carried out to investigate the Ethiopian aquifers in general. Most of the previous studies concentrated at the basin level and focused on the specifically identified area and small numbers of studies were carried out on some specific aquifers. Generally, most of the Ethiopian alluvial aquifers are not given the required attention by scholars. Given the fact that alluvial aquifers are the main sources of water supply, the coming climate and land cover change may threaten the ecosystems of the alluvial regions of the country. Previously there were few overall studies in the alluvial aquifers' zones of Ethiopia. However, these studies use different methods and for different purposes. Using a specific approach to study the alluvial aquifers would make a more significant difference from the techniques used and the outcomes found by previous studies. This study plans to meet these research gaps by characterizing the major alluvial aquifers of Ethiopia and determining their vulnerability to pollution, climate, and land cover changes.

1.3. Research Questions

The study aimed to address several key questions concerning the groundwater dynamics in alluvial aquifers and their interactions with various geological, structural, morphological, and climatic factors. These questions included:

- What are the relationships between the groundwater potential of alluvial aquifers and the geological, structural, morphological, and climate factors?
- How does groundwater interact with the geological materials in alluvial regions?
- What is the vulnerability of alluvial aquifers to pollution from natural causes?
- How vulnerable are alluvial aquifers to climate and land cover changes?

1.4. Objectives

The primary objective of this study is to comprehensively characterize the major alluvial aquifers in Ethiopia by examining their geological and structural characteristics, and their relationships with

regional aquifers, and assessing their vulnerability to pollution, climate and land cover changes. The study is guided by the following specific objectives:

- Understanding the groundwater potential of the research regions involves looking at the many geological, structural, morphological, and climatic factors.
- Examining the interactions between groundwater and geological materials in alluvial zones, as well as their hydrogeochemical and isotopic properties.
- Modeling the vulnerability of alluvial aquifers to pollution using modified DRASTIC models.
- Determining the vulnerability of alluvial aquifers to climate and land cover changes.

1.5. Significance of the study

The study of aquifers plays a crucial role in understanding the subsurface component of the hydrologic system. The findings and applications derived from this study will hold significant importance not only for the specific study areas but also on a nationwide scale. Helping the study regions manage their water resources sustainably is the main goal of this project. By unraveling the geological setups, identifying sources, and examining the interaction between groundwater, and rock formations, as well as assessing the impacts of climate and land cover changes on hydrogeology, valuable insights can be gained. The implications of this research extend beyond the study areas and will be invaluable for researchers studying Ethiopian aquifers. The output of this study can provide a foundation of knowledge and data that enrich future research endeavors in the field. The study's outcomes can guide evidence-based decision-making, inform policies, and support the implementation of sustainable practices for the correct management and protection of alluvial areas.

1.6. Scope of the study

The main goal of this study is to investigate the alluvial aquifers in Ethiopia for future water supply development.

- The study is concentrated on alluvial regions in the western (Gambela plain) and Eastern (Fafen-Jerer and Shinile sub-basins) Ethiopia.
- The study examined the stable isotope, and geochemical characteristics of groundwater for only eastern catchment areas.

- In characterizing the aquifers, pollution susceptibility, climate variability, and land-use change's impact on the groundwater resources based on the principle of vulnerability and aridity was a concern.

1.7. Limitations of the study

Due to the field of study and the nature of the research questions developed, this research is a quantitative research type. The research has the following limitations.

- The study was limited to major alluvial aquifers regions (Gambela plain, Fafen-Jerer, and Shinile sub-basins).
- The sample size of the stable isotope study was relatively small. Besides economic constraints, instability, and security issues were the other constraints for data collection.
- The availability of data is the other limitation of any research in developing countries, which also posed problems for this study. Too little and unavailable evidence or previous research on the study regions was also another limitation.

1.8. Structure of the dissertation

This dissertation is compiled into eight chapters. The first chapter presents the general introduction section. This section includes the background of the study, the statement of problems, objectives, the scope and limitations of the study. The literature review section of the dissertation is discussed in the second chapter. Chapter three covers the general methodology section for the research which is presented in the order of the objectives. From chapter four to chapter seven, the document presents the main parts of the thesis. The published, accepted, and online manuscripts on the review are included in these chapters. The synthesis, conclusion, recommendation, and related future works are presented in chapter eight. Lastly, the paper presents the references and appendixes used in this research.

CHAPTER 2

LITERATURE REVIEW

2.1. Water Resources Development in Ethiopia

Water is essential for the survival of all life forms. The development of water resources is a component of 17 Sustainable Development Goals (SDGs) of the UN, comprising 64% of the goals. Goal numbers 6, 7, 13, 14, and 15 all directly relate to water resources. Water resource development should therefore take precedence to achieve the development aim in a sustainable future. The fundamentals of the global objective are to guarantee that by 2030, everyone has equitable access to safe and fairly priced drinking water as well as appropriate and equitable sanitation and hygiene (Hák, et al., 2016).

Large bodies of water, such as lakes, rivers, swamps, and subterranean aquifers, are abundant in Ethiopia. However, due mostly to the depletion and underuse of these water resources, Ethiopian philosophy does not reflect this level of prosperity. With a population of over 120 million, just 38% of Ethiopians have access to sources of clean drinking water, and only 12% make use of better sanitation facilities. Ethiopia is currently experiencing an acute water crisis, primarily due to a severe drought, a lack of financing and support from the government, and inadequate resources for water management and sanitation (Hendrix, M. 2012). Since agriculture accounts for more than 80% of the economy, farmers are especially susceptible to shocks due to the highly erratic rainfall, which also limits their capacity to apply modern technologies that boost productivity (Hagos et al., 2012). Understanding the temporal and spatial variability of a region's water resources is essential for designing effective agricultural and water resource projects (Tilahun, K. 2006).

In all of Ethiopia's climatic zones, groundwater is a vital resource that provides around 80% of the domestic water needs of both urban and rural inhabitants (Mengistu et al., 2021). Despite being one of the most drought-affected countries in the world, hardly little research has ever been done to characterize the groundwater resources of semi-arid portions of Ethiopia. For Ethiopia's semi-arid future to develop, studying the features of groundwater resources is therefore vitally important. With an emphasis on the primary alluvial aquifer zones in western and eastern Ethiopia, this chapter covers the literature on characterizing the alluvial aquifer and points out research gaps on groundwater in alluvial regions.

2.2. Understanding the groundwater potential

2.2.1. Remote sensing and groundwater

Due to resource scarcity, ground-based hydrometeorological observations are often scarce in developing countries such as Ethiopia, and remote sensing is the best option for application. Digital Elevation Model (DEM), LANDSAT, Sentinel 2, MODIS, ASTER, and other satellites cover the Earth's surface, capturing surface images and providing freely usable surface data (Onačillová et al., 2022; Safaei et al., 2021; Yoo et al., 2022). As a result, large terrestrial datasets of satellite imagery are progressively used around the world (Knoche et al., 2014; Renzullo et al., 2014).

Since the advent of remote sensing, GIS, along with advances in computer technology, has become a very useful tool to assess surface properties at spatial and temporal scales. Satellite data have previously been used in several water resource assessment studies (Ranghetti & Boschetti, 2021; Xue et al., 2022). These data are used by several academics to map and analyze land and water resources, as well as to estimate changes in lake water volume. (Baltodano et al., 2022; Sun et al., 2022). Others used satellite imagery combined with GIS to map different attributes of the Earth (Nagy & Lăzăroiu, 2022; Remondino et al., 2022; Tariq et al., 2022). Remote sensing data has also been used previously for water resource allocation, flooding assessment, and land, and water productivity studies (Kidd et al., 2009). The application of remote sensing is one of the new technologies used in many parts of the world for the development and management of water resources (Ayad & Saeid, 2022; Duan et al., 2021; Kana et al., 2022). Satellite remote sensing applications in hydrology are the emergence of globally available satellite imagery (Brierley et al., 2022; Hata et al., 2022; Ioana-Toroimac et al., 2022; Tegos et al., 2022).

Groundwater is a hidden resource and its explorations by drilling test and stratigraphy analysis methods are either cost or time-consuming and also often require skilled manpower. The best and most cost-effective solutions to these problems are using remote sensing (RS) and geographical information systems (GIS) for assessing and managing groundwater resources (Mallick et al., 2014). Since the invention of technology, geologists have utilized data from remote sensing for structural interpretation and regional mapping (van der Meer et al., 2012). A combination of geospatial techniques (remote sensing and GIS) for the identification of geological structures of the earth has become an important tool in evaluating, monitoring, and conserving resources (Shah & Lone, 2019). Remote sensing techniques are now being gradually used to prepare geological maps

and obtain the basic geological information on which further detailed work is based (Bhan & Krishnanunni, 1983).

Geological mapping has already made use of GIS and remote sensing techniques in many parts of the world (Lk et al., 2019; Mohamed et al., 2021; Radaideh et al., 2016; Souza et al.,1997; Yamusa et al., 2018). Visual Interpretation of satellite data is the basic application of remote sensing in groundwater exploration. Remote sensing facilitates the preparation of lithological, structural, and geomorphological maps, with various resolutions of the images. These data show major rock groups, structures like folds, faults, lineaments, and fractures, and different landforms, due to their synoptic coverage and multispectral capability (Souza et al., 1997; Bahiru, 2011; Mogaji, et al., 2011; Kebede et al.,2020). With the help of data covering large and inaccessible areas becoming available quickly, remote sensing's spectral, spatial, and temporal capacity has created an extremely useful tool for gathering, storing, translating, enhancing, displaying, and analyzing spatial data (Balakrishnan, 2019). Visual interpretation of remote-sensing images is achieved efficiently and effectively way using basic interpretation keys or elements (O'Callaghan, 1980). Some studies in Ethiopia use satellite data for geological investigations (Gintamo, 2017; Romilly & Gebremichael, 2011). Many scholars have created important methods for using remote sensing in geological study throughout the past few decades. Below, a summary of some of these works is presented. Gintamo (2017) has worked on groundwater potential using geospatial techniques: in the South Rift Valley of Ethiopia. Using GIS and integrated remote sensing methods, he tried to identify and categorize prospective groundwater zones.

2.3. Stable isotope and geochemistry of groundwater

Previously water resources managers, as well as scholars, have always looked at groundwater and surface water as two separate entities, due to this reason, hydrologic science concentrates only on determining the surface water resource quantity (Kalbus et al., 2006; Ivkovic et al., 2009). But to quantify water resources accurately, one must consider the interplay between surface and subsurface systems when using a problem-solving approach that simulates internal variables like groundwater levels and the interactions between saturated and unsaturated zones. (Rassam et al., 2013). When groundwater flows from one system to the other, it interacts with the surrounding geological material and rock system. The solubility of geologic and rock material aids in this interaction (Walter et al., 2017). The types and concentrations of the different types of minerals carried in

solution in the groundwater are primarily determined by several factors, including the chemistry of the rock, interactions between surface and groundwater, the geologic setting of the paths, and any additional sources (Yousif, et al., 2018). Dissolution/precipitation, ion exchange reactions, oxidation, and reduction are all examples of chemical processes that occur during rock-water contact. Igneous, metamorphic, and sedimentary rocks are the three broad categories of rocks. Minerals in these rocks will dissolve entirely or partially in water depending on their chemical weathering resistance (Dehnavi et al., 2011). Water-rock interaction is the interaction of an aqueous solution with a rock, which includes chemical and physical processes. These interactions not only induce mineral changes but also influence the chemical composition and quality of water above and below the Earth's surface (Morán-Ramírez et al.,2016). Isotope and geochemical approaches are among the main techniques to study the interaction of groundwater with the surrounding materials.

2.3.1. Isotope method

Disparities in the isotopic composition of water samples from rainfall, stream runoff, and groundwater show the interaction between these components of hydrology (Bhat & Jeelani, 2018). Isotopes in groundwater hydrology offer a transparent window into the processes of aquifer migration and dispersion. Complementary information on the kind, source, and age of groundwater is provided by isotope hydrology. If the aquifer's isotope concentration remains constant, it will serve as a reflection of the water's origin, specifically the time, place, and methods of recharging. The evolution of an isotope's composition via groundwater pathways also provides insight into the water's past, specifically the processes of mixing, salinization, and discharge (Terwey, 1984). The isotope technique is one of the methodologies used for surface-groundwater interaction studies (Ayenew et al., 2013; Kebede et al., 2005, 2018; Kebede & Travi, 2012; Levin et al., 2009).

Because stable isotope composition sheds light on groundwater sources and recharge processes, it offers a comprehensive knowledge of water resource systems (Z. Bedaso & Wu, 2021a). The stable isotope of water occurs in two hydrogen (^{1}H – protium, and ^{2}H - deuterium) and three oxygen (^{16}O, ^{17}O, ^{18}O) forms. Vienna Standard Mean Ocean Water, or V-SMOW, is the globally recognized standard for reporting isotope ratios of water (Coplen, 1996). Water with stable isotopes ($\delta^{18}O$ and $\delta^{2}H$) is a reliable tool for assessing surface water–groundwater exchanges both qualitatively and quantitatively. This is because surface waters are often heavier than groundwater owing to isotopic fractionation during evaporation (Jung et al., 2019; Rodgers et al., 2005). Stable isotopes can be an

excellent indicator of water circulation in the aquifers. Stable isotopes also proved to be useful tools in hydrogeological studies, providing valuable insights into water dynamics in a given basin (Kebede et al., 2018; Kebede & Travi, 2012; Terwey, 1984).

Many studies show that isotope signatures are one of the methods of surface-subsurface interaction investigation. In addition, an isotope signatures study confirms that the electric conductivity of water shows also the interaction between the surface and surface system (Gomaa, 2020; Johnson et al., 2015; Kassune et al., 2018b; Rusydi, 2018). Some research works are presented below in this regard (Kebede and Travi, 2012). The study conducted by Kebede and Zewdu (2019) examined the application of 222Rn and $\delta^{18}O$-$\delta^{2}H$ isotopes in identifying the source of water and measuring groundwater inflow rates in Beseka Lake.

2.3.2. Geochemical method

Understanding the dynamics of hydrogeological systems and identifying the hydrogeochemical evolution processes are frequently used to investigate the interactions of fluids with rocks or sediments to gain an understanding of aquifer heterogeneity and connectivity, as well as physical and chemical processes that influence water chemistry. Groundwater chemistry is the result of the interaction between water and rocks from different geological eras (Yousif et al., 2018). The comparison of different geochemical data aided in the understanding of the rock-water interaction, dissolution pattern, and ion exchange mechanism. Water percolation via rocky lithology and long-term rock-water interaction may result in greater solute concentrations, showing the importance of surrounding rocks in controlling water quality (Morán-Ramírez et al., 2016). Groundwater's chemical composition reflects the marks of rock-water interaction and chemical reactions. As a result, groundwater chemistry can be utilized to discover rock-water interactions or chemical processes (Dehnavi et al., 2011).

2.4. Modeling groundwater vulnerability

2.4.1. Concept of vulnerability

Vulnerability is a condition created by physical, social, economic, and environmental factors or processes that make a person, community, asset, or system more vulnerable to the effects of a hazard. The degree of susceptibility to the unfavorable consequences of change and the inability to adapt is known as its vulnerability (Al-Kalbani et al., 2014; Metzger et al., 2006).

Margat initially developed the notion of groundwater vulnerability in the late 1960s, and it is described as the proclivity for pollutants to enter the groundwater system. This concept encompasses both innate and particular vulnerabilities. The intrinsic vulnerability reveals a vulnerability to all pollutants, whereas the particular vulnerability is determined by combining the inherent vulnerability with the unique contaminant features (Wei, A., et al., 2021). Growing water demand and resource vulnerabilities are directly affected by population growth, socio-economic growth, and related land cover changes. Being vulnerable is a theoretical concept that is challenging to measure directly. Water resource systems and vulnerability assessment are two complicated concepts (dual complexity), making it challenging but essential to estimate. The degree of vulnerability to negative consequences of climate change, especially climate unpredictability, and extremes, or unable to handle them.

There are several studies worldwide that focus on the vulnerability of water resources (Ahmed et al., 2022; Chishugi et al., 2021; Wang, et al., 2022). This study demonstrates and concludes that the relationship between climate, LULC, and water resources is strong and that the effects of each will affect complaints. Many researchers also have studied the effects of climate and LULC on groundwater resources (El-Magd et al., 2022; Geris et al., 2022; Pinsri et al., 2022). Some studies in Ethiopia show that LULC and climate change are causing problems for water resources (Abera et al., 2022; Bogale & Erena, 2022; Geris et al., 2022; Ketema et al., 2022; Maja et al., 2023; Semaw et al., 2022; Tolche et al., 2021). Depending on the situation, a variety of vulnerability assessment methodologies are applied. Process-based approaches, statistical methods, and overlay and index methods are extensively used to estimate groundwater risk in various parts of the world (Patel, P. et al., 2022).

2.4.2. DRASTIC Model

The most crucial techniques for examining vulnerability mapping are the overlay and index processes if field data is unavailable and remote cases. This method takes into account all of the elements that influence groundwater vulnerability in a certain place. This technique uses a variety of physical and hydrological characteristics to limit the transport of pollutants that damage groundwater quality through the unsaturated zone until the water table is reached (Patel, P. et al., 2022). DRASTIC is a weighing and grading system that measures vulnerability using seven parameters: groundwater depth (D), net recharge (R), aquifer media (A), soil media (S), topography

(T), influence of the vadose zone media (I), and aquifer hydraulic conductivity (C) (Aller et al. 1987). This DRASTIC Model is based on the following assumptions: 1) The aquifer would get polluted by a surface pollution source. 2) Following precipitation, the pollutants should be mobile enough to mix with the recharging water and reach the water table.

2.5. Climate and Land cover change

2.5.1. Climate Change Impact

In reality, temperature increases have direct influences on natural systems; the glaciers' retreat indicates a high sensitivity to global warming (Nistor, 2019). The climate system's intrinsic internal processes (internal variability) or changes in man-made or natural external variables (external variability) can cause change. The United Nations Framework Convention on Climate Change (UNFCCC) defines climate change as "an increase in the natural climatic change seen over comparable periods, coupled with a shift in climate that is either directly or indirectly attributable to human activities changing the composition of the global atmosphere" (Stone, 2014).

Climate is the average state of the atmosphere and the underlying land or water in a particular region over a specific period. Climate change is a significant variation in the mean state of climate parameters over extended periods (decades or longer). Previous climate change studies focus mostly on surface water resource systems due to limited observational data of the subsurface and the inaccessibility of most resources for data acquisition (Taylor, et al., 2009). Climate change affects groundwater by altering the recharge and discharge and also by changing the quality and quantity of the subsurface hydrologic cycle (C. P. Kumar, 2015). The linkage between climate change and the sub-surface water resources system is one of the upcoming issues of science (Nistor, 2019; Nistor et al., 2016, 2017). Climate change directly affects surface water resources by varying air temperature, precipitation, and evapotranspiration, the relationship between the changing climate variables and the impact of climate change on groundwater is more complicated and poorly understood. The effect of climate on subsurface systems is analyzed through the direct interaction of surface water resources with subsurface systems (Singh, et al., 2010).

2.5.2. Climate Models

Nowadays, the study of future climatic impact on hydrology involves a two-step approach: (i) climate model outputs are used to generate local climate conditions such as precipitation and

temperature, which is known as ‘downscaling’; (ii) downscaled local climate data are used as input to a hydrological model to project the hydrological changes according to future climate (Tisseuil et al., 2010). Climate models are numerical representations used to simulate the past, present, and future of climate systems expressed as computer codes and run on powerful computers (Deidda et al., 2013). Mogaji, and others, (2013) study used GCM under A2, A1B, and B1 emission scenarios, regional Modeling of Climate Change Impacts on Groundwater Resources Sustainability in Peninsular Malaysia. This work used an integrated strategy using GIS-based geostatistical approaches, model forecasting accuracy optimization, and empirical modeling equations to simulate the suite of GCM outputs for impact investigations. Results suggest that recharge reduction in the area is evidence of water resource scarcity in the 2020s. Coarse spatial resolutions are the major limitations of the GCMs that are unable to capture the mesospheric processes and dynamics driving the occurrence of such physical processes (Segele et al., 2009).

2.5.3. Land Use land cover and water resources

Land use change and surface water resources are directly related, but the subsurface system is indirectly affected by the land use change. The effect of land use on surface water resources is straightforward. Rainfall serves as the primary source of surface water precipitation on Earth's surface, occurring naturally. After having these natural phenomena, it is the role of surface condition that can change it to surface run-off or infiltration to the subsurface system. Numerous studies have already demonstrated how land use/land cover affects water supplies and the environment (Birhanu et al., 2019; Chimdessa et al., 2019; Choto & Fetene, 2019; Hasan et al., 2020; Liu et al., 2017; Negese, 2021; Singh et al., 2010). Some studies indicate that land use/ cover change impacts on groundwater resources (Singh et al., 2010).

2.5.4. Aridity and Aridity Index

Aridity is a climatic characteristic measured by temperature and precipitation variables and has a significant impact on many aspects of life. It is a climatic state for which we need to know the average conditions of a region, and it is necessary to evaluate if there is a lack of moisture in the existing vegetation (Paniagua et al., 2019). There are different approaches to state whether the land is arid or not. The approaches include Classical, Index, and water balance techniques. This study applied the index approach which suggests using a variety of standard indices that have been created throughout time from earlier classical research and include one, two, or more meteorological factors

to designate areas with varying degrees of aridity. Such indexes have been given by Koppen, de Martone, Emberger, Angstrom, etc. The two basic index techniques that were selected for this particular research are presented below.

De Martone Aridity Index (DMI)

The application of the De Martone Aridity Index has a large use in climate and agricultural studies. This index was proposed by De Martone (1925, 1926) and is appropriate for moisture determination at the local scale (Deniz, et al., 2011). For its applicability in environmental studies, the De Martone Aridity Index is frequently used, both for temporal and spatial analyses (Baltas, 2007; Nistor et al., 2016). Little works are done related to climate aridity in Ethiopia (Abrha & Hagos, 2019; Gebremedhin et al., 2019; N. Tadesse et al., 2015; Y. Tadesse et al., 2018). Gebremedhin and others (2019) study on aridity indices in Raya Valley, Ethiopia.

UNEP Aridity Index (AI)

This index as proposed by UNEP (1992) estimates PET using the straightforward Thornthwaite (1948) formula, which only needs information on air temperature. The UNEP index is popularly known as the aridity index, and FAO also uses it (Ludwig et al., 2021; Zarei & Mahmoudi, 2021). The UNEP Aridity Index (AI) divides aridity into five categories based on the availability of precipitation over atmospheric water demand. Several researchers used to assess aridity using the UNEP index (Adelodun et al., 2022; Mihi et al., 2022; Straffelini & Tarolli, 2023). UNEP index measures aridity using the ratio of precipitation (P) to potential evapotranspiration (PET).

2.6. The Major alluvial aquifers of the country

In Ethiopia, the alluvial sediments are found in large distributions in the Gambella area, the Main Ethiopian Rift, and the southern Afar transition zone areas (Chernet et al., 1998; Kebede, 2013; Mechal et al., 2017) (Figure 2.1). Abbay river basin (Kassune et al., 2018), and in river courses of different parts of the country as a whole. In the areas mentioned above, the main source of water supply is groundwater. The benefits of utilizing groundwater from alluvial deposits over surface water are as follows: (the water quality is typically better and more stable than river water; storage from groundwater systems permits abstraction even when run-off is low; and the development cost is cheaper) (Mansour et al., 2012). Alluvial aquifers in semi-arid regions are called Wadi aquifers. The word “Wadi” is used to refer Wadi channel and the related alluvial aquifers (Maliva & Missimer, 2012). Wadi is an Arabic term defined as “a stream bed, boulder ravine, gully, valley, or

dry wash". The property of Wadi aquifers shows that they cover limited geographic extent and thickness, and thus have lower storage volumes (Maliva & Missimer, 2012). According to the report from (Kebede et al., 2018) wadi bed length exceeds 30, 000 km across Ethiopia, and 3 billion cubic meters of groundwater storage is available. Wadi is the most important aquifer in pastoral areas like Borena, lower Omo, Ogaden, the western border area, and Afar depression in supporting livelihoods. The report shows that the main sources of considerable good quality water supply in the study area are from shallow alluvial aquifers (Kebede, 2013). Salinity is the major problem in the groundwater of the Shinile zone. Most of the Woreda in the Shinile zone are dominantly coved by alluvial deposits composed of sand, silt, and clay with gravel with high to moderate groundwater potential (Kebede, 2013).

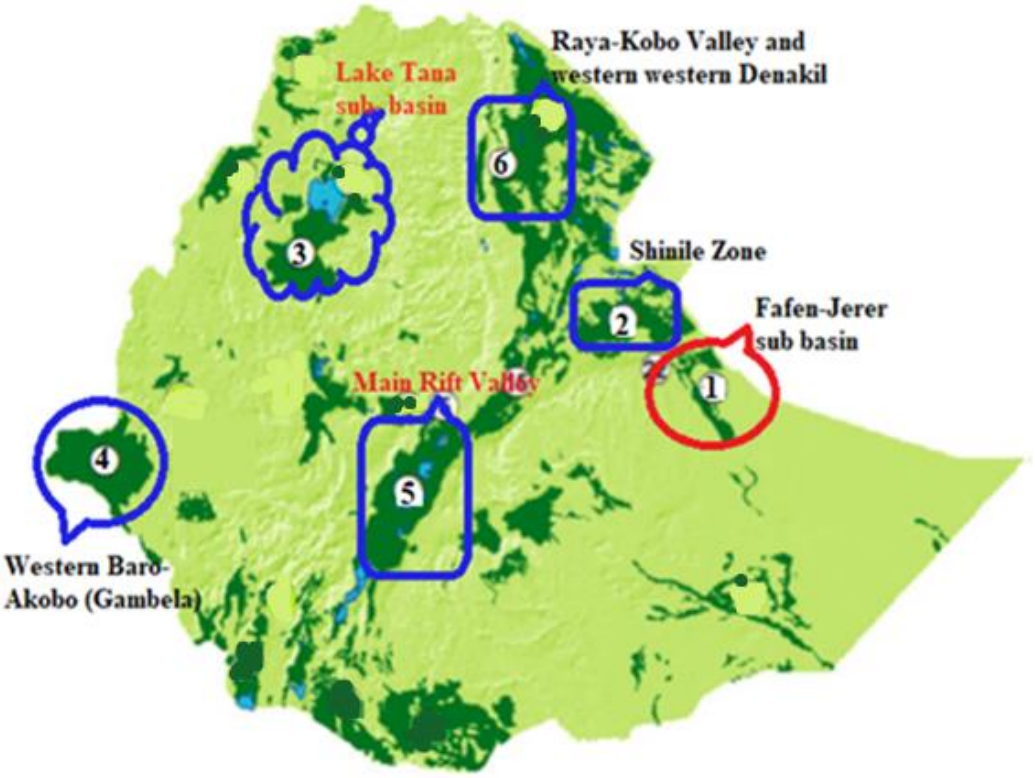

Figure 2. 1 The alluvial aquifer zones modified from (Kebede, 2013)

The study areas for this particular research are selected based on data availability for the specific methods, the area of least researched by previous scholars, and the water resources problems in the region. The different geological study reports that the western lowland plain areas of the Baro-Akobo River basin are covered by quaternary sediment (Alemayehu et al., 2016). There are four hydro-stratigraphic units in the Baro-Akobo River basin, one of these groups is a quaternary alluvial

aquifer. Alluvial aquifer in the basin is found in the western low-lying area. The alluvial in the Gambela area consists of course material and is highly productive(Kebede, 2013). The alluvial vast plains of the Baro-Akobo River basin have moderate productivity (Awulachew et al., 2007).

Generally, reports from different scholars show that alluvial and colluvial deposits are distributed in the rift valley floor and along the major river valleys in the country. These sediments have moderate to high permeability in much of the area (MoWR, 2002). Quaternary alluvial sediment is distributed largely in the Rift Valley, the southern part of the country (like the Gofa basin, Borena area, Ririba valley, and Omo area), in the northwestern margin area of Rehad and Tekeze and Humer plain, alluvial plains in the Tendaho, Dubti, and Asaiyata areas of lower Awash basin (Ayenew, et al., 2008), lower catchments Wabi Shebelle river, alluvial in Bonga area, alluvial sediments of the lake Alemaya-Adele plain. The Afar depression areas are also covered by alluvial sediments. Bidu, Delalu, and Kori Woreda in the eastern Afar regional state are mainly dominated by alluvial aquifers. Due to the movements of alluvial deposits from highland to lowland areas, in the depression area the alluvial aquifers are thick (Ayenew, 2006). Study shows the alluvial deposit in the Danakil depression has moderate to high groundwater potential. There are alluvial plains in Belesa, Lalibela, Taba village, and Sekota areas in the Tekeze river basin that have shallow or deep groundwater (Seifu, 2012). The aquifers in the central part of the country are associated with permeable alluvial deposits (Ketema et al., 2016). The most prevalent unit covering the Kola Diba well field in Dembia Wereda is alluvial sediments, in North Gonder Zone. These extensive alluvial sediments in the northeastern, northwestern, and southern margins of the area cover almost 71 percent of the total area (Kassune, et al., 2018). There are moderate and highly potential alluvial aquifers in the Sirinka and Woydo area underlaid by a basaltic rock in the Sunuta Sub-Basin (Begashaw & NT., 2017).

2.6.1. Hydrogeology of the study areas

The Ethiopian aquifers are classified based on productivity as low, moderate, high, and very high productivity. The majority of Ethiopia's landmass is covered by aquifers with moderate productivity. Most of the country's north and central highland regions are covered by these aquifers. The eastern portion of Ethiopia is home to highly productive aquifers. The primary aquifers with high productivity include the rift valley areas of the Afar region, the south-eastern highlands, the Borena areas, the eastern Gojam, the south-eastern Ogaden areas, the Shinile areas, and the main

rift valley areas. Aquifers of low productivity cover substantial areas of Ethiopia's western, southern, and northern basement terrain of Ethiopia (Deyassa et al., 2014). These low-productivity zones are distributed in Tigrayi, Benshangul, western Borena, and western Gojam (Kebede, 2013). Very high productivity zones are also distributed in rift-valley and Shinile areas.

The aquifers in Ethiopia are also grouped as continuous, discontinuous, dual permeable aquifers, and geothermal. Continuous aquifer cover is distributed in the eastern and the western extreme parts of Ethiopia. Gambela plain, Ogaden area, Shinile zone, and rift vally areas are the main parts that are covered by continuous aquifers. These discontinuous aquifers dominate the main central area of Ethiopia. Particularly the eastern part Abay basin, the southwestern part of the Tekeze basin, the headwater zones of the Awash, Omo-gibe, and Rift vally basins, and the eastern border area of the Denakil basin covered by the discontinuous aquifers. The alluvial regions selected for this specific study are highly productive areas with different productivity levels.

The geology of the Fafen-Jerer sub basin is composed of Tertiary and younger sediment, and Oligocene Miocene volcanic. The western area is dominated by Oligocene Miocene volcanic rocks, while the majority of the eastern region is composed of Tertiary and younger sediments (Ismail & Abdelsalam, 2012). The aquifer in Fafen-Jerer is specifically known as the Wadi beds. Wadi refers to the bed or valley of a stream in parts of northern Africa and Southwest Asia that are often dry, save during the rainy season. According to a study, alluvial deposits—which may be as thick as thirty meters and span an area of over three thousand square kilometers—are almost exclusively located on the banks of perennial rivers, where seasonal flooding is responsible for their formation. These sediments consist of well-sorted sandy silts and clays with distinct layers of uncommon gravel and coarse sands. The aquifer qualities of the deposits are moderate to good, particularly those of the sandy lenses. Silty units have high retention qualities and, except for deposits with extremely fine grain, give water to wells gradually but consistently.

For Gambela plain sediments, the transmissivity reaches 120 m^2/day, and the yield can vary from 0.01 to 2.5 l/s. The depth of water varies from 13.8 to 30.1 meters below the surface (Kebede, 2013). The total recharge of groundwater in the Gambela plain was previously estimated at 128 *10^6 m^3/year. The total volume of groundwater in the basin area is estimated to be 200 km^3.

The quaternary formation covers most of the Shinile sub-basin, especially the central parts of the region. The northern stripes and the upper catchment boundary region are partially covered with

tertiary volcanic material (Kebede, 2013). The Shinile zone is very highly productive compared to the others. The yield of wells in the Shinile zone ranges from 1-28 l/s with an average yield of 13 l/s (Kebede, 2013).

CHAPTER 3

MATERIALS AND METHODS

3.1. Descriptions of the study area

The study was focused on alluvial aquifers which include the Fafen-Jerer sub-basin, Gambela plain, and Shinile sub-basin. These areas were selected as study regions due to their geological nature, climate, and economic importance. Additionally, these areas have not been given proper attention by previous researchers. Descriptions of each of the study areas considered are given in the following sections.

3.1.1. Geographical Location and Accessibility

Fafen-Jerer sub-basin: The Fafen-Jerer sub-basin is situated in the Wabi Shebelle river basin which is in the southeastern part of the country (Figure 3.1). Administratively the region is a part of the Oromia regional state and Somali regional state. The Fafen-Jerer sub-basin has a mean surface area of about 17390 sq. km which is bounded by longitudes from 42° 23' to 44° 11' E and latitudes from 7° 34' to 9° 35' N (Awulachew *et al.*, 2007; Kebede *et al.*, 2017). The sub-basins of the Fafen and Jerer are lengthy regions that stretch NW-SE. Karamara Mountain (2150 m) is one of the features in the north, which stretches along the NW-SE direction separating the Jerer valley in the east from the Fafen valley in the west. The altitude in the study region varies from 780 m at the outlet to about 2450 m above sea level on the escarpment. To access the sub-basin, there is a major asphalt road from Addis Ababa to the study area through Adama – Harer- Jigjiga covers about 620km. There is also another road from Jigjiga to Gode through Deghabur which is the second town in the study region. There is also a daily flight from Addis Ababa to Jigjiga.

Shinile sub-basin: The Shinile sub-basin is found in the southeastern corner of the Awash River basin (Figure 3.1). Administratively the region is a part Somali regional state and Dire Dawa administration. The geographic location of the sub-basin ranges from $41^0$19’ to $43^0$17’E longitude and from $9^0$24’ to $10^0$55’ N latitude covering 19963sq.km area (Figure 3.1). Within the study region, the height ranges from about 2750 m on the escarpment to 450 m near the outflow. In this area, drainage generally flows from southeast to northwest. There is a major asphalt road from Addis Ababa to the study area through Adama – Dire Dawa covers about 456km. The Shinile town is 20km north of Dire Dawa city. Additionally, there is a daily flight from Addis Ababa to Dire Dawa.

Gambela Plain: The Baro-Akobo River basin is the river basin of the country and is part of the southwestern Ethiopian Plateau. The basin is one of the smallest river basins with an area of 75,721 km^2. Administratively the region is a part Gambela regional state. Geographically the basin is located between 5º27' to 10º52'N Latitude and 33º00' to 36º17'E Longitude (Alemayehu *et al.*, 2016). The Gambela plain area's geographical longitude ranges from $33^0$00 to $34^0$48'E and latitude from $7^0$18' to $8^0$35'N, covering an area of 18222 sq. km. The elevation of the plain ranges from 403 to 846m above sea level (Figure 3.1). The region borders with Oromia regions to the northeastern, the Southwestern Peoples' Regional State in the southeastern, and the South Sudan Republic to the west. The area is accessed through Addis Ababa- Ambo- Nekemte- Gambela. Additionally, there is a daily flight from Addis Ababa to Gambela.

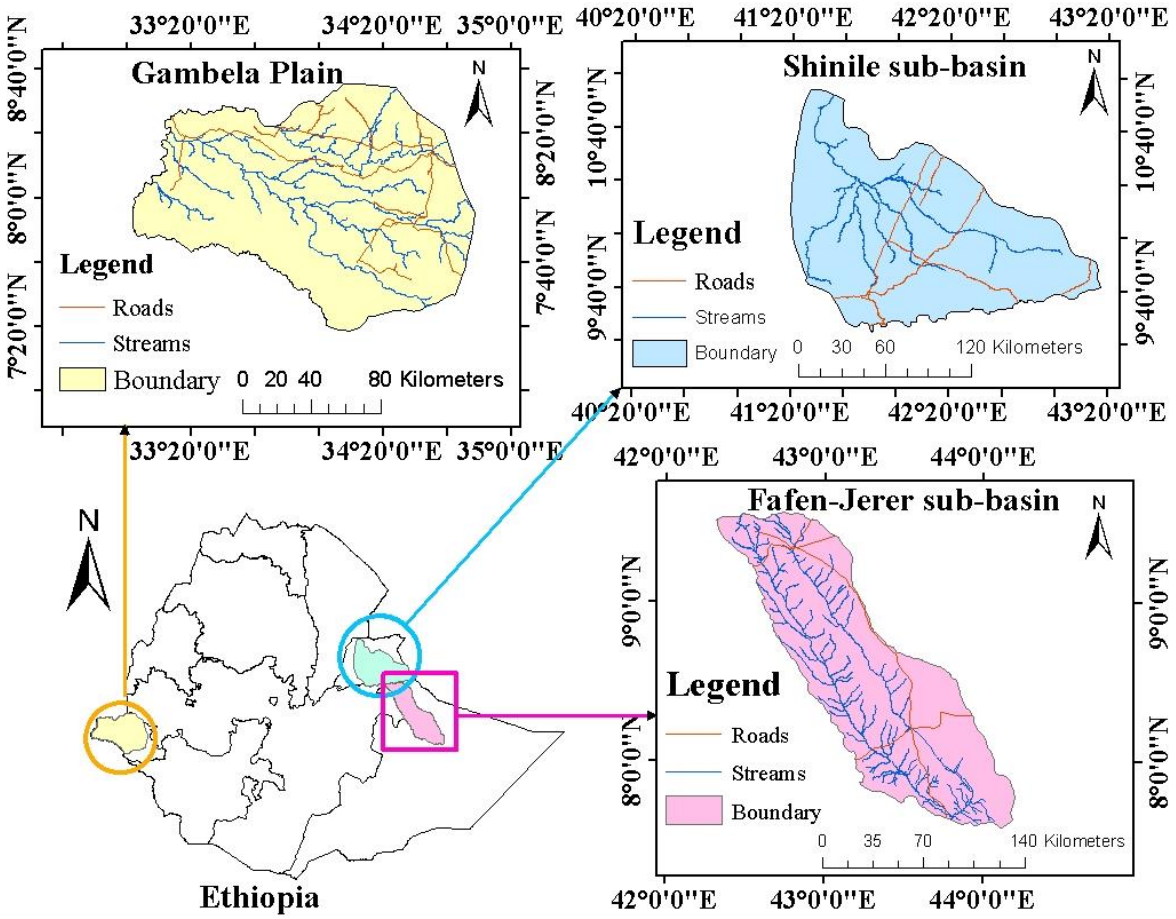

Figure 3. 1 Location of study areas

3.1.2. Geology and hydrology

Fafen-Jerer sub-basin: The geological formation of the Wabi-Shebelle basin is composed of Mesozoic Sedimentary Aquifers (Abebe and Foerch, 2006; Kebede, 2013). The basin is underlain by a very thick succession of Late Paleozoic, Mesozoic, and Cenozoic (Tertiary) sedimentary rocks. It is characterized by flat to undulating plain geomorphology, where the surface geology is a Mesozoic sedimentary deposit with a thickness that varies from less than 200 m to more than 1000 m below ground. The lithologic units identified in the area consist of Tertiary Mesozoic sedimentary rocks with intercalation of sandstones, limestones, and gypsum, which, in general, is named "Jesoma sandstone" (Godfrey et al., 2019).

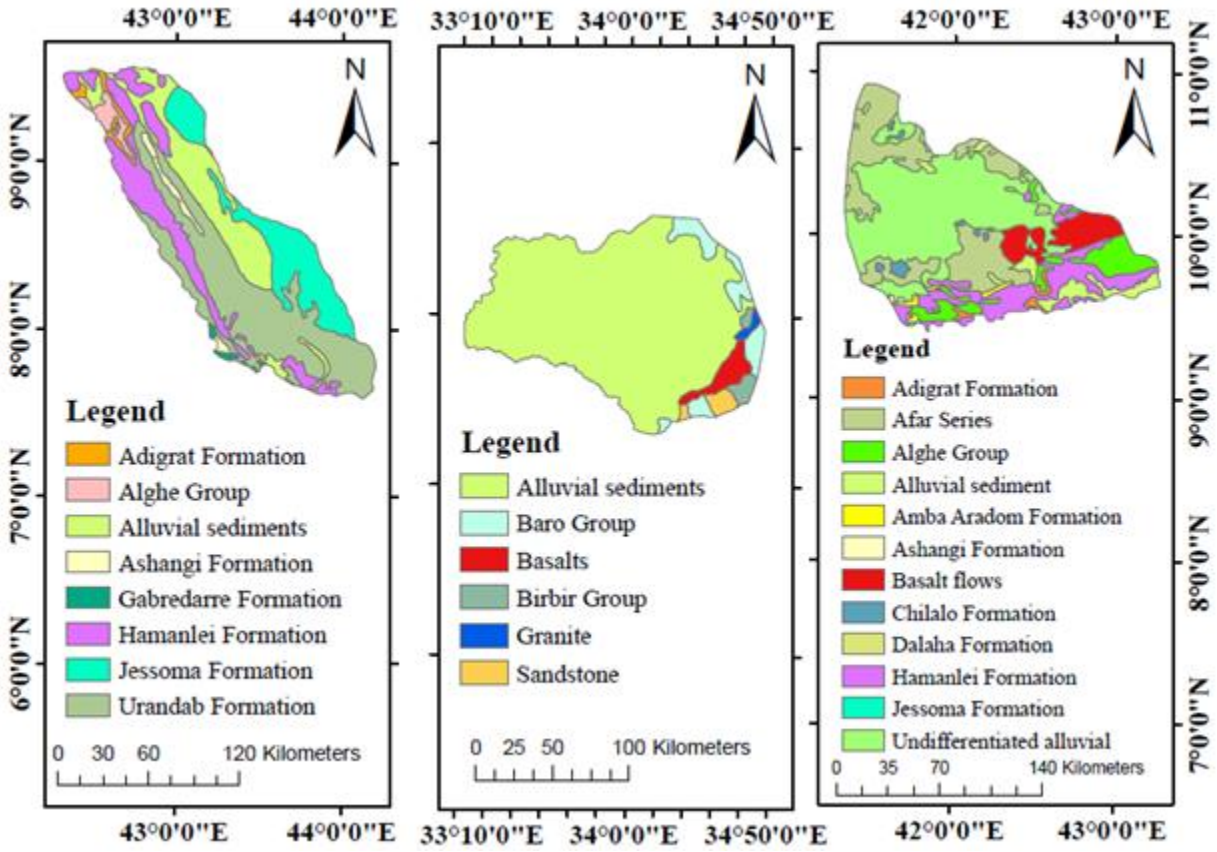

Figure 3. 2 Geologic units

Specifically, the Fafen-Jerer sub-basin is dominated by alluvial and fan deposits of seasonal floods and stream beds (Abebe and Foerch, 2006). In the eastern part of the study area (Jigjig plain), silty-clay deposits derived from limestone and basement rocks constitute the alluvial deposits (Kebede,

2013). The Jigjiga Plain is made up of limestone covered with a thick layer of loose materials (Abebe and Foerch, 2006) (Figure 3.2).

The Fafen and Jerer rivers are Ethiopia's easternmost rivers, located in the Wabi-Shebelle region and the country's southeast. Both rivers originate in the northern highlands and flow southward to meet the main river. Fafen River starts from Amora Mountain whereas the Jerer River starts from the Jigjiga plains. Except during extremely rainy seasons when they flow into the Wabi-Shebelle, both rivers are drying up and entering the desert.

Shinile sub-basin: The central catchment of the Shinile sub-basin is formed by Tertiary and younger sediment, while the surrounding area of the sub-basin is bordered by Miocene Quaternary volcanic rocks (Ismail & Abdelsalam, 2012) (Figure 3.2). The Mesozoic sequences, basalt ridges, quaternary to recent lava sheets, and recent alluvial sediments make up the Shinile area's geology. Gravels, pebbles, and coarse sand make up the alluvium. There are isolated dunes, and dunes scattered throughout the alluvial sediments. There are two main sources of recharging. The majority of recharge originates from the first source, which is lost streams, and the second source is mountain block recharge, which enters through aquifers and travels laterally beneath the southern mountains. Most of the groundwater shows a water table condition while some wells exhibit artesian conditions. The quaternary sediments are composed of alluvium (sand, silt, and clay and their inter-bedding) river gravels, fans, and travertine. No surface water was found that flows throughout the year. Groundwater is the main potable water supply in the region. Dire Dawa, Melkajebdu and Aysha are the only meteorological stations in the region.

Gambela plain: The majority of the western plain of the Gambela plain is typically covered in Tertiary and younger sediment, while the eastern margins are primarily composed of Precambrian crystalline rocks. (Ismail & Abdelsalam, 2012). The four hydro stratigraphic units of Gambela plain identified by MWR (1972) are (a) the aquifers of the Basement complex, (b) the alluvial aquifers of the Holocene, (c) the Quaternary alluvio lacustrine aquifer, and (d) the regional sandstone aquifers of the Pliocene Alwero formation.

The basement complex is located on the eastern edge of the plain (Figure 3.2). These rocks consist of schistose and high-grade poly-deformed rocks (granulites and gneisses) intruded by plutonic rocks with gabbroic to granitic compositions (Deyassa et al., 2014). Holocene alluvium that was deposited alongside river courses and in direct hydraulic continuity with the rivers makes up the

Holocene alluvial aquifer. The Gambela plain has quaternary alluvio lacustrine aquifers, primarily in the western sector. This alluvium aquifer was deposited during the Holocene, starting in the Upper Pleistocene (Kebede, 2013).

The Plio-Quaternary deposit that begins at the plain of Illubabor (the easternmost region) and extends beneath the Gambela Plain to the border between Ethiopia and Sudan is comprised of regional aquifers. Throughout the entire aquifer complex, three recharge sources are identifiable. These include lateral groundwater inflow from the crystalline highlands, direct infiltration from rainfall, and infiltration from channels and flood plains (Kebede, 2013).

About 80% of the plain is made up of alluvial-lacustrine deposits of sand, silt, clay, diatomite, limestone, and beach sand (Kebede, 2013). The remaining 20% of the territory on the eastern border is covered by late to post-tectonic granite, Makonnen basalts, Enticho sandstone, Birbir group, Baro group, and other geological features. The major rivers in the region include; the Baro, Gilo, and Akobo rivers. The drainage pattern is oriented from east to west (Figure 3.3).

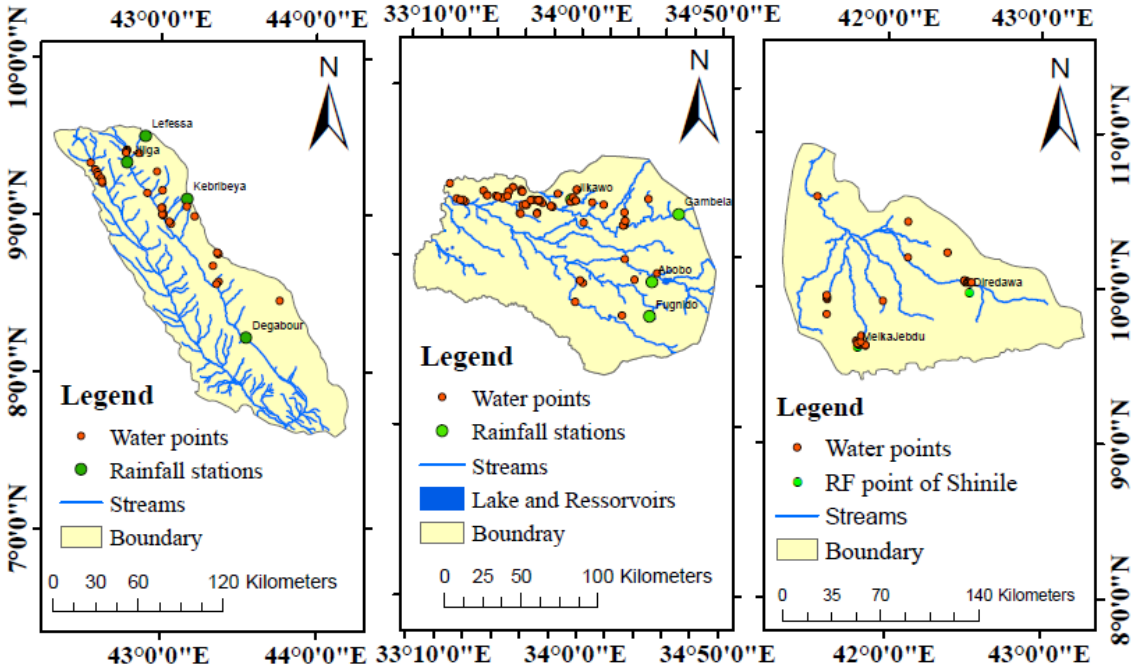

Figure 3. 3 Hydrogeologic points

3.1.3. Climate

The climatic and geographical features of Ethiopia are varied, encompassing equatorial rainforests with abundant rainfall and humidity in the south and southwest, the Afro-Alpine on the summits of the Simien and Bale Mountains, and lowlands in the northeast, east, and south-east that resemble deserts. The two extreme climate conditions the lowlands area in the eastern region and the equatorial rain forest in the western region are partially reflected in the climates of the study regions. The study regions generally warm to hot, semi-arid zone includes those areas with an altitude of 500-1,500 m, average annual rainfall generally of around 600 mm (but as high as 1,600 mm in the western lowlands of Gambela), and an average annual temperature range of 20-28ºC;

Fafen-Jerer sub-basin: this area is a lowland part of eastern Ethiopia. The climatic conditions of the area are arid and semi-arid (Berhane, 2013). The region can be divided into two areas based on the seasons of the year: the northwestern, and the southeastern. The rainfall pattern for both is bimodal but the timings differ slightly. The average precipitation ranges from 300mm in the southern corner to 800mm in the northwestern mountain region. The mean temperature in the area ranges from 20 º C in the upper catchment to 25ºC in the lower catchment (Deghabur).

Shinile sub-basin: the Shinile sub-basin experiences a bimodal rainfall pattern brought about by the wind system coming from the Indian Ocean from September to November and from March to May. The most reliable rainy months are April and May. The climate is semi-arid in the upper catchment to arid in the lower catchment around Aysha. The mean annual rainfall ranges from 200mm to 800 mm and the average temperature range is from 28 to 38 ºC.

Gambela Plain: the Gambela plain is a part of the equatorial forest and experiences an unimodal rainfall pattern brought about by wind systems coming from the Indian Oceans and merging with those from the Atlantic to give continuous rain from March or April to October or November. In terms of agroecology, the area is mostly lowland (Kolla), with a small number of midlands (Weyna-Dega). The average temperature of the region ranges from 24.5 º C at the central to 28 º C at the eastern corner and the mean annual rainfall ranges from 1000mm in Jikawo in the west to 1400 mm in the northeastern area.

3.1.4. Soil and LULC

The soil texture classification of Ethiopia shows loam is a dominant texture followed by sandy loam and clay. Clay, sandy loam, and loamy sand soils are the dominant soil textures in the study regions (Brehanu, 2013). Clay soil dominates most parts of the Gambela plain and sandy loam and loamy sand are the main constituents in the Shinile sub-basin.

The LULC of the research regions includes urban areas, wetlands, bare lands, forests, croplands, grasslands, shrublands, and water bodies (Figure 3.4). Grassland makes up more than half of the landmass in each location. The other land covers that make up a sizable portion are forest and shrublands. Shrublands and bare lands are unique to the Fafen and Shinile sub-basin, whereas forests, wetlands, and water bodies make up the Gambela plain's land cover (Figure 3.4).

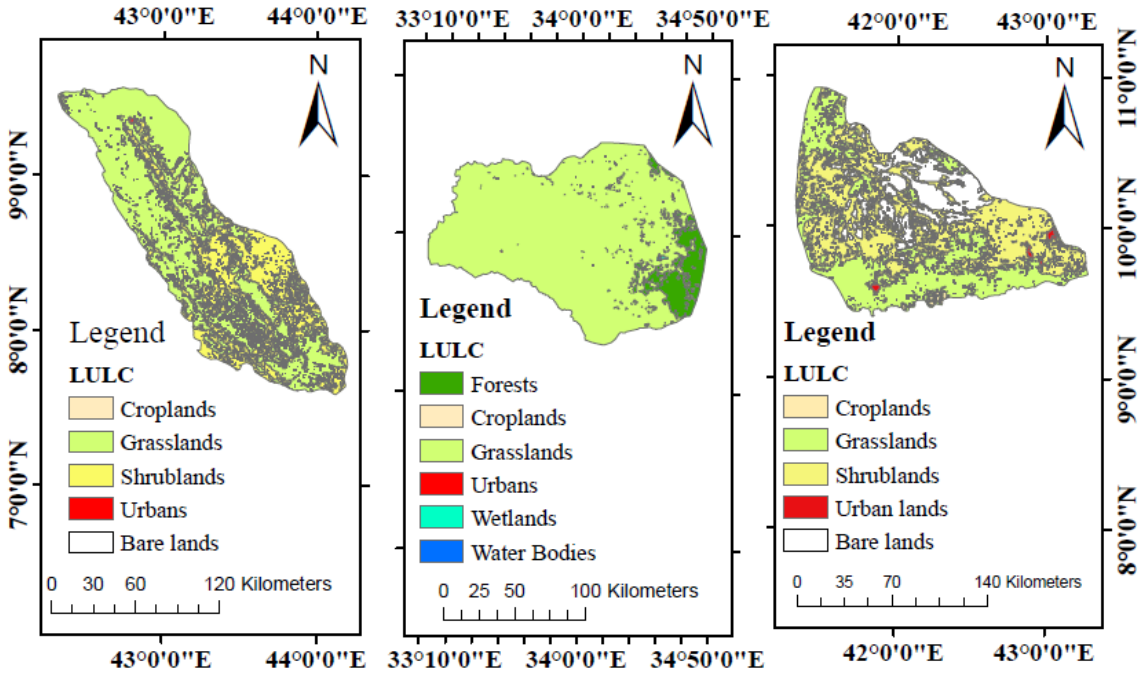

Figure 3. 4 The land use land cover

3.2. Research Methodology

This study's primary goal was to examine the features of Ethiopia's principal alluvial aquifers from the perspectives of hydroclimatic, structural, geological, and geological analysis, as well as to determine how land use land cover and climate change have affected them. To accomplish the main goal data from satellite imagery, historical records, and field observations were carried out. Satellite products of Landsat, Sentinel 2 imagery, and MODIS satellite land use land cover products were

used for land cover analysis. SRTM DEM for elevation, drainage, lineament, and other geological Insite were also applied. Available historical records of meteorological data for 30 years were collected from the National Meteorological Agency. Groundwater data and other hydrological data of the study regions were collected from the Ministry of Water and other governmental organizations. To accomplish the aforementioned primary goal, four fundamental objectives have been prepared. The detail-specific works that summed up this primary objective are presented in the figure (Figure 3.5).

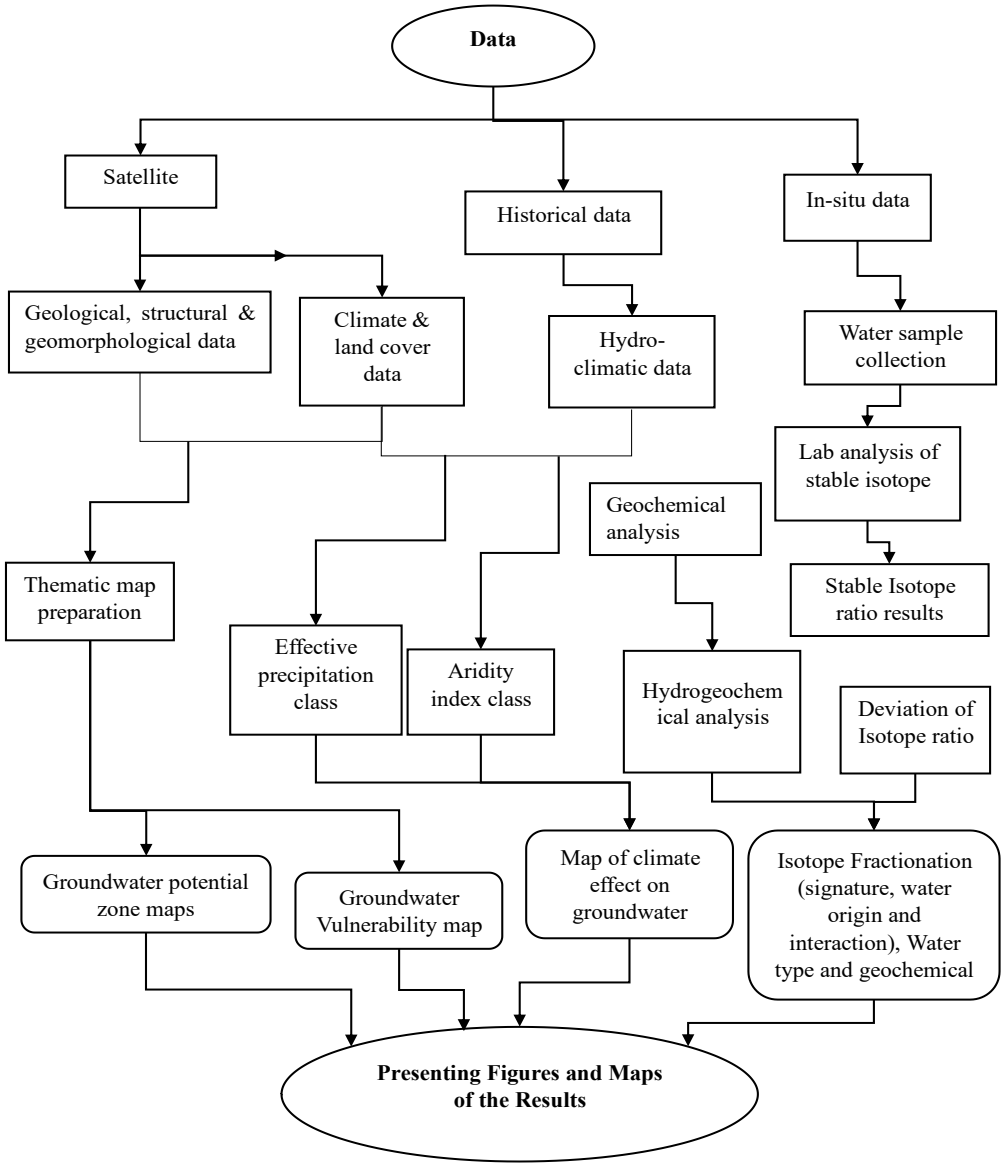

Figure 3. 5 Methodology flowchart of the dissertation

3.2.1. Understanding the Groundwater Potential

To achieve the first objective geological map of the areas, satellite imagery and ASTER DEM were used. The method involved the compilation of literature related to various aspects of geology, geomorphology, LULC, hydro-metrological parameters, extraction of geological and geomorphological structures from satellite imageries (Sentinel 2, DEM), collecting ground truth (well location), and finally analysis and interpretation of results with mapping of different geological structures of the study areas.

Required Data and sources

- Remote sensing (RS) imagery and derived products, such as Digital Elevation Models (DEMs), and Sentinel 2 image for mapping geological structures.
- Both DEM and satellite images were freely downloaded from USGS/NASA servers.
- The Topo-sheet of the area was collected from the Ethiopian Mapping Agency.
- The geological map was collected from Ethiopia Geological Survey.
- Field observations using GPS (Global Positioning System) were conducted to get the ground truth points for image classification and accuracy assessment for the geological and structural elements.

Data Processing

The initial satellite image data were pre-processed and upgraded to extract the geographic aspects of the study region so that the information and coordinate projection systems meet the required position.

An analytical hierarchy process (AHP) with multi-criteria decision-making (MCDM) was used to develop the criteria weights by pairwise ranking to identify the groundwater potential zone. The AHP model known as the Saaty method was originally developed by Saaty (1990). All of the map themes were presented in UTM Projection Zone 31, Datum WGS84 with precise resolution. The prepared groundwater potential map for the study areas and validation with existing bore-well data and flow direction of the basin conclude this part of the study. The whole analytical process is shown in the figure (Figure 3.6).

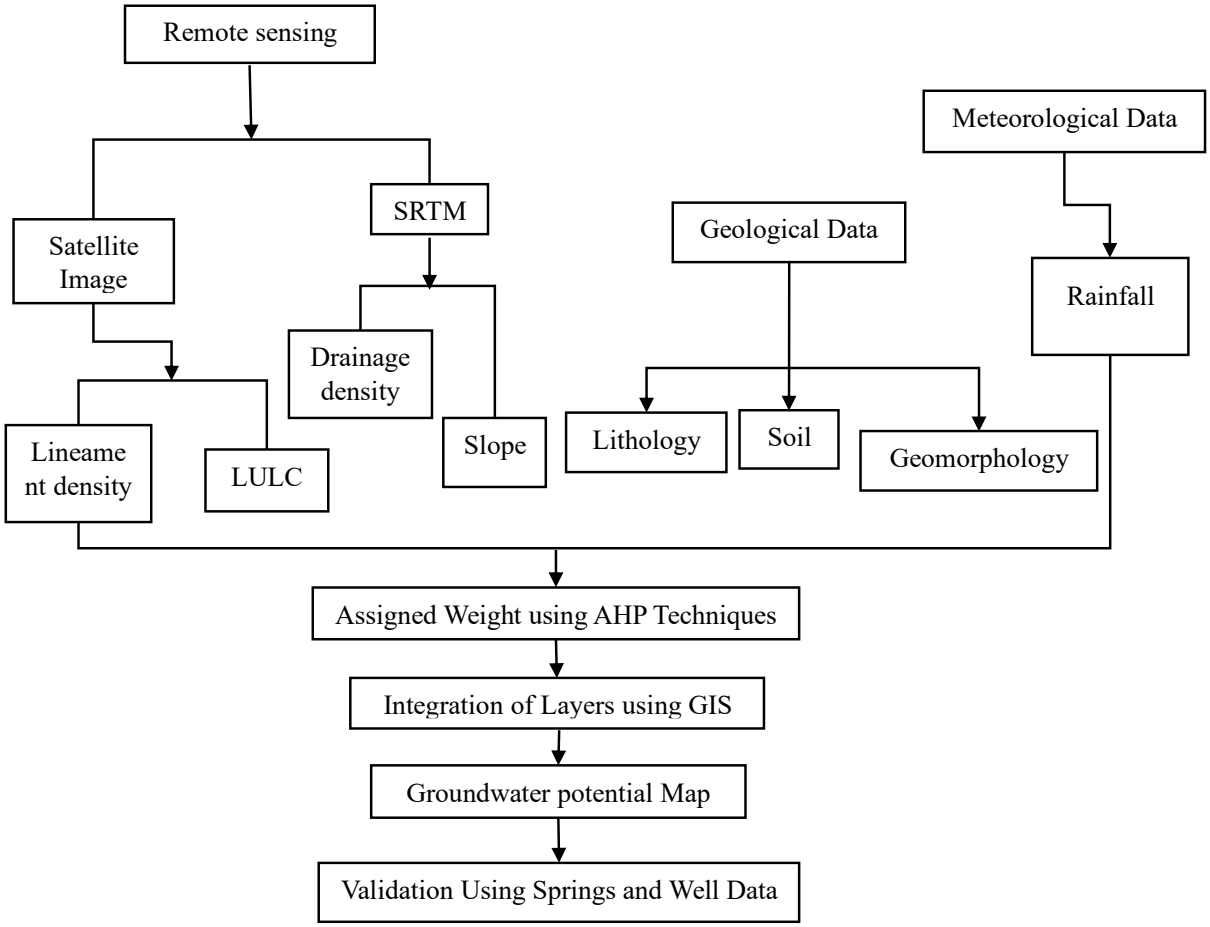

Figure 3. 6 Flow chart for groundwater potential zonation

3.2.2. Stable isotopes geochemistry

To achieve this goal, stable isotopes and geochemical parameters of the water were used to analyze the origins of groundwater and how it interacts with the rock in the alluvial aquifers. The whole procedure of the study is presented in the flow chart (Figure 3.7).

Required Data and sources

Field surveys were carried out to collect water samples (well, and precipitation) including basic information, such as groundwater usage, well-depth, and water level for the study areas. Additionally, the fieldwork includes measuring the physical parameters of water: temperature, electrical conductivity, and pH.

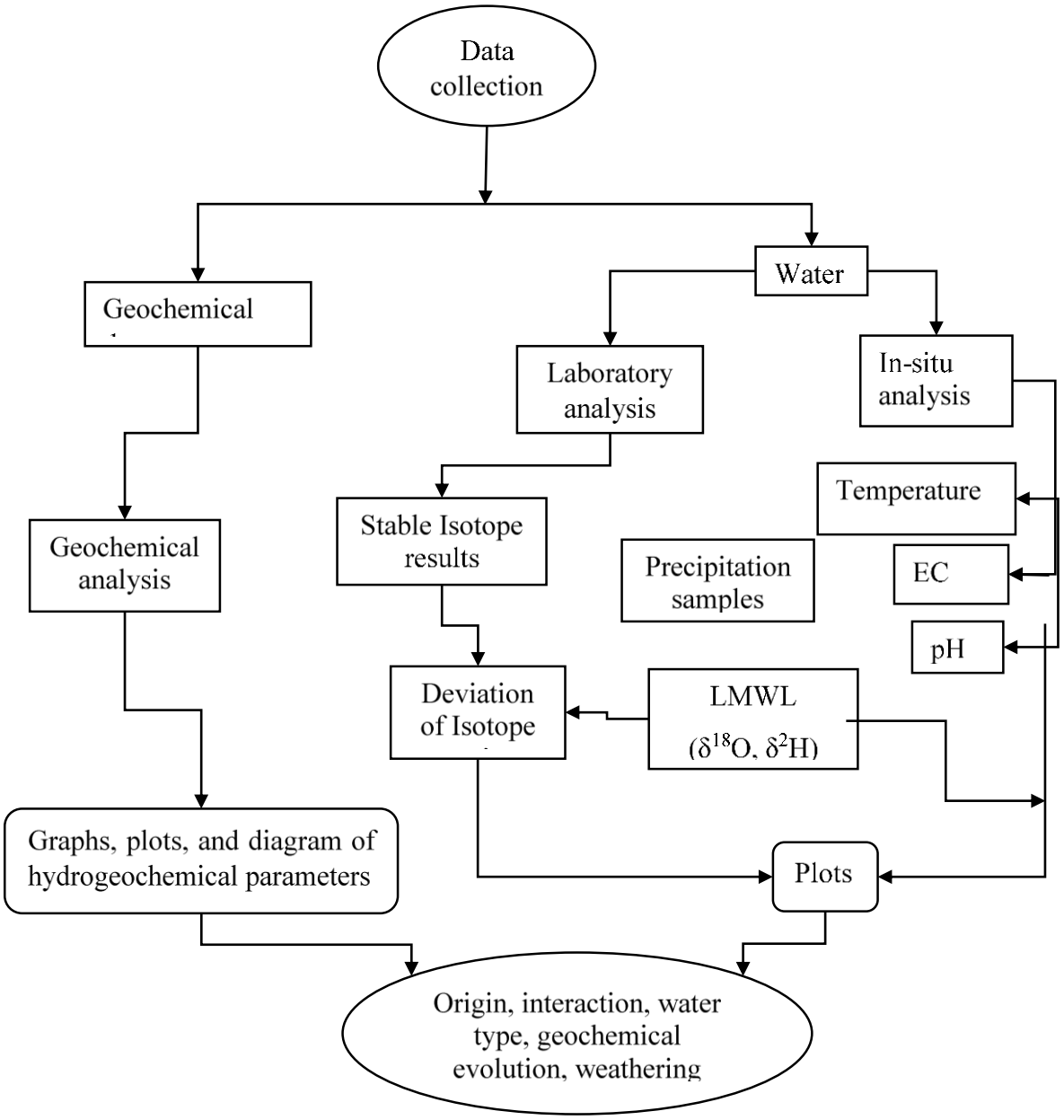

Figure 3. 7 Flow chart for hydrogeochemical and stable isotope analysis

Isotope analysis and interpretation

The analysis was performed at Saskatchewan University, Hillslope Hydrology Lab, Canada. The stable isotope contents ($\delta^{18}O$ and $\delta^{2}H$) were performed by McDonnell Hillslope Hydrology Lab on a Los Gatos Research liquid water Off-Axis Integrated-Cavity Output Spectroscopy (Off-Axis ICOS) unit and post-processed using LIMS for Lasers, Canada. The isotopic ($\delta^{18}O$, $\delta^{2}H$)

compositions of groundwater (well), precipitation, and river water were used to identify the interaction, recharge sources, zones of recharge, and groundwater flow (Terwey, 1984; Seifu *et al.*, 2002).

3.2.3. Intrinsic vulnerability

One of the problems with water supply in many parts of the world is water quality. Groundwater can sometimes naturally mitigate the effects of pollution in particular aquifer types. Although groundwater is very resistant to pollution, it can be challenging to rehabilitate after it has been contaminated. The term "groundwater vulnerability" refers to the natural characteristics of the water that control how easily the imposed contaminated load might negatively impact it. DRASTIC is a well-known and commonly utilized parametric vulnerability mapping approach. It was developed in the United States as part of an EPA (Environmental Protection Agency) initiative to help managers, planners, and administrators. DRASTIC may be used in a broad variety of places because of its low deployment cost and ease of data collection (Aller et al. 1987).

The goal of the research at this step was to assess the alluvial aquifer's possible risk zone for pollution exposure. The DRASTIC index considers seven geological, hydrological, and environmental parameters: depth to water table (D), net Recharge (R), aquifer media (A), soil media (S), topography (T), vadose zone impact (I), and hydraulic conductivity (C). The study applied the modified DRASTIC model by introducing lineament and LULC (DRASTIC_LU). Each of these DRASTIC criteria was assigned ratings and weights based on their proportional significance to groundwater contamination vulnerability. To compare the findings obtained, the natural break categorization method was used to split the assessment region into five ranks: very low, low, medium, high, and very high susceptibility zones. The model was validated using nitrate and TDS data from the study area (Figure 3.8).

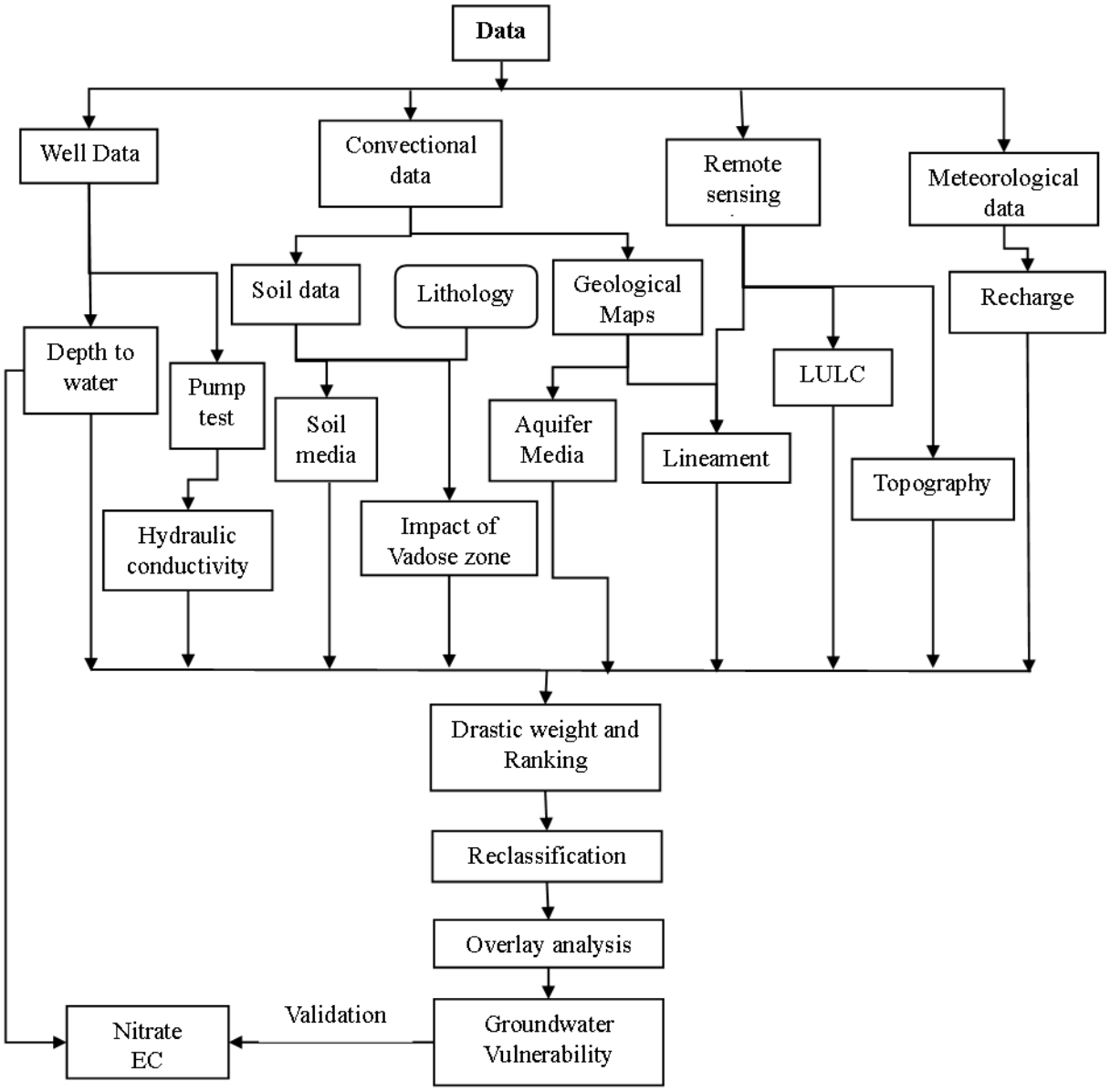

Figure 3. 8 Flow chart for DRASTIC method

3.2.4. Climate and LULC changes

This objective aims to present a study to identify the areas of alluvial aquifers most susceptible to climate change and land-use change with the application of the climate aridity index and water availability.

Required data and sources

Hydro-climatic parameters and land cover data of the study areas were collected and used as input data to evaluate the climate and LULC effect. The temporal frames for the climate data were 1981–2010, 2011–2040, and 2041–2070. Historical land use land cover dynamics was developed from satellite remote sensing images (MODIS satellite). Freely available satellite data were downloaded from the USGS /website https://earthexplorer.usgs.gov/ of Earth Explorer. Global climate model data (GCM) was utilized to generate future climate parameters (precipitation, temperature) (Figure 3.9).

Instrument and procedure

Both linear and non-linear bias correction methods were used to avoid overestimating or underestimating the climate variables (temperature and precipitation data). The method used for this study was the New Implemented Spatial-Temporal on Regions–Climate Effect on Groundwater (NISTOR-CEGW) method. The method combines effective precipitation with the De Martone Aridity Index, both at spatial and temporal scales to determine and depict the effect of climate change on groundwater (Nistor, et al., 2016).

Due to data scarcity Thornthwaite method was used for evapotranspiration (ETo) estimation (Allen, et al. 1998). Ordinary Kriging interpolation for areal mapping of climate parameters (temperature, precipitation, and ETo) was applied. After the classification of the land cover, the Kc value for each land cover class for ETc calculation (using FAO standard). ETc value was determined by multiplying the values of crop coefficient Kc by ET_0 for each type of crop. The effective precipitation values are determined by considering ETc values and the total precipitation values.

De Martone's aridity index (DMI) was used to characterize the climate of the area and to determine the “humidity–aridity” at the regional scale. The method was proposed by De Martone (1925, 1926) and is widely used for climatological, agricultural, and hydrological studies. The climatic classification was based on the DMI values.

In this part of the study, the method narrates the values of the De Martone Aridity Index and the precipitation amount with the groundwater recharge of the study areas. The method suggests that the areas of low effective precipitation values and low De Martone Aridity Index values represent areas susceptible to climate change effects on groundwater recharge.

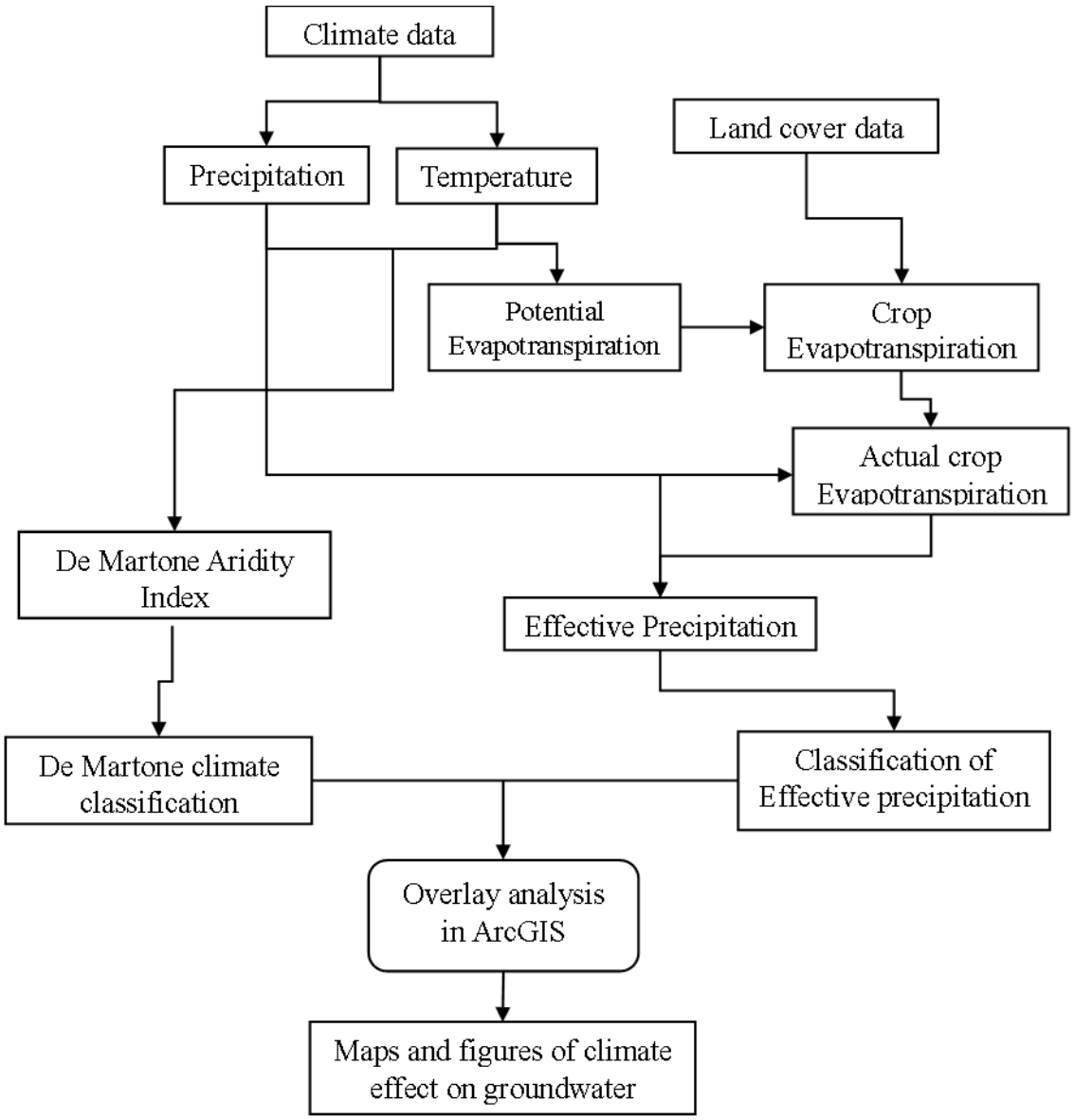

Figure 3. 9 Flow chart for climate and land cover changes

CHAPTER 4

GROUNDWATER POTENTIAL ANALYSIS

Abstract

An essential initial step in looking into groundwater resources in dry and semi-arid areas is analyzing the groundwater potential zone. The groundwater potential mapping approach, based on geographic databases and remote sensing and has seen significant advancements recently, is presented in this study as state-of-the-art. The study applied analytic hierarchy process (AHP) models and four machine learning algorithms: random forest classifier (RFC), gradient boosting classifier (GBC), decision tree classifier (DTC), and K-neighbor classifier (KNC). To capture the groundwater potential zone eleven influencing factors were collected, such as geology, geomorphology, slope, soil, lineament density, drainage density, land use land cover, normalized difference vegetation index, topographic wetness index, topographic roughness index, and rainfall. Groundwater potential zone (GWPZ) was categorized into five classes from very low to very high potential areas. According to the results 81.93% (14395.4sq.km) of Fafen-Jerer, 22.35% (4072.7sq.km) of Gambela, and 17.38% (3466.2sq.km) of Shinile are classified as low and very low potential zones. The high and very high GWPZ covers 4.32% (759.2sq.km) of Fafen-Jerer, 55.52% (10115.7sq.km) of Gambela, and 64.8% (12926.7sq.km) of Shinile sub-basin. A high and very high potential zone resulted in a large coverage in the Gambela and Shinile sub-basins, whereas a low and very low potential area gets huge area coverage in the Fafen-Jerer. The study was validated using water point (water level) data in the study regions. The validation of the AHP model was performed by the area under the curve (AUC) of the receiver operating curve (ROC) which resulted from 87.0%, 78.2%, and 94.1% for Fafen-Jerer, Gambela, and Shinile sub-basin respectively. The authentication of the machine learning models shows 93.4, 92.5, 72.4, and 87.7% values of AUC for RFC, GBC, DTC, and KNC, respectively. The result shows that rainfall, geology, and geomorphology are the primary factors influencing the GWPZ. The outcome might promote improved groundwater management alternatives in other areas with a comparable condition.

Keywords: AHP, Groundwater potential, GIS, Remote sensing, Machine learning

4.1. INTRODUCTION

According to the United Nations Educational, Scientific, and Cultural Organization (UNESCO), water resources are crucial environmental components as well as a key driver of social and economic development. Policies and management options with the best decision-making choices are required to guarantee it's the quality, renewal, and sustainable use of water resources (Koncagül, E. 2015). Several literatures indicate that groundwater is the main source of domestic water supply globally (Silva et al., 2020; Liu et al., 2020). As a result, groundwater becomes the primary driving factor for development and food security in arid and semi-arid regions (Hoogesteger, 2022). The investigation of groundwater resources in these regions, however, is hampered by a lack of data availability and accessibility.

Ethiopia is a developing country where about 80% of the population is dependent on agriculture, which is the backbone of the economy (Baye, 2017; Zerssa et al., 2021). Groundwater is the main source of domestic water supply in many parts of the country. Nonetheless, estimates of Ethiopian groundwater resource potential vary significantly in the literature, particularly in recent years. The literature estimates the groundwater potential range from 2.6 to 1000 billion cubic meters (Berhanu et al., 2014; Kebede, 2013). This indicates that there is still a great deal of doubt regarding Ethiopia's hydrogeological study. In most parts of Ethiopia, the main challenge in investigating water resources is a lack of required meteorological, hydrological, and geomorphological data. The problem varies by region, but it is more severe in arid and semi-arid regions (Ayenew et al., 2008; Berehanu et al., 2017).

Some well-known and previously used groundwater investigation procedures, such as drilling and stratigraphic analysis, are now used exclusively worldwide (Campo et al., 2020; Regenspurg et al., 2018). However, these methods require a huge time and financial investment. The other method of groundwater investigation is numerical modeling, which requires uniformly distributed ground truth data for validation (Singh, 2014). To address these issues, researchers used emerging technology to investigate groundwater resources (Prasad et al., 2020). Numerous scholars employed models to map the possibilities for groundwater. Models like frequency ratio (Razandi et al., 2015), statistical models (Azma et al., 2021), ensemble models, and logistic regression (Farzin et al., 2021) are the main techniques. However, the majority of these techniques require substantial amounts of ground truth data, making them unsuitable in cases when there is a lack of data. The most efficient

method for studying groundwater in places with a lack of data is to use a geographic information system (GIS) and remote sensing (RS) technology with an analytical hierarchy process (AHP) (Bera et al., 2020; Jothimani et al., 2021; Yariyan et al., 2022; Ifediegwu, 2022). Machine learning models were used recently to map the potential of the groundwater in a region (Yariyan et al., 2022). There hasn't been much groundwater research done in Ethiopia despite the availability of the best techniques and methods for assessing groundwater potential.

The primary challenges of water resource distribution in the research regions are fluctuating climatic conditions and frequent droughts. The region is distinguished by semi-arid conditions, poor water sources, and erratic weather patterns. The little rainfall does not provide enough water to satisfy the needs of agriculture. Additionally, the study regions were neglected by the researchers due to their remote location. Data availability is the main challenge for researchers in the regions. Although thousands of people in the research region are impacted by recurring drought occurrences, there was no published work has been done concerning groundwater potential.

The current study used the geospatial approach of finding groundwater potential zones by examining several thematic layers that impact groundwater resources. The aforementioned approach is novel in the selected research area and has not been tried in a comparable oasis region. Thus, the purpose of this work is to investigate the groundwater potential using AHP approaches in conjunction with GIS and remote sensing. In addition, machine learning algorithms (MLAs) were applied for Gambela plain compared with the AHP technique. The use of four MLA models and AHP to assess each model's efficiency for groundwater potential site prediction is the study's primary innovation. The objectives of this research were to: (i) determine the importance of the geological, morphological, and hydro-climatic aspects in evaluating groundwater; (ii) identify and evaluate the factors affecting groundwater; (iii) assess the efficiency of the AHP technique for the GWPZ study; and (iv) evaluate the effectiveness of MLAs in identifying GWPZ. The potential availability of groundwater in specific areas depends on factors that govern resources. Thus, with the use of ground truth data, traditional maps, and remote sensing data using ArcGIS, this chapter highlights the key influencing factors of alluvial groundwater supply and their respective roles.

4.2. MATERIALS AND METHODS

4.2.1. Details of Data Collected

The following data were collected from various organizations for the present study

- Geological map (JPG format) of the study region was collected at the scale of 1:50000 from the Ethiopia Geological Survey.
- Rainfall data was collected from the National Metrological Agency (NMA).
- Groundwater data was collected from the Ministry of Water and Ethiopia Water Works Design Supervision enterprise.
- Soil data (shapefile format) has been collected from the Ministry of Water.
- Land use land cover data collected from Ethiopia geospatial information agency
- Satellite data both sentinel 2 imagery and SRTM DEM data were collected from the USGS Earth Explorer website (https://earthexplorer.usgs.gov).

4.2.2. Data collection and thematic layers preparation

To generate the groundwater potential zone map of the areas different parameters that influence groundwater potential were produced using GIS and remote sensing. The parameters used for this study include geology, geomorphology, soil, LULC, slope, drainage density, lineaments density, NDVI, topographic wetness index (TWI) topographic roughness index (TRI), and Rainfall. Remote sensing application directly used for map preparations for the above-listed parameters with digital format. Each thematic map was divided into 5 to 10 sub-classes based on the specific cases of the thematic layer.

The geology of the study areas was developed from a published geologic map of Ethiopia (1996). The map was taken in “PDF” and “JPG” format. Georeferencing these maps to UTM 37 coordinates was performed in ArcGIS. After dereferencing, the map changes to “TIFF” format by digitizing for detail analysis. The parameters like slope, drainage density, topographic wetness index (TWI), and topographic roughness index (TRI), were produced from the shuttle radar topography mission (SRTM) digital elevation model (DEM) of 30m-by-30m resolution from the USGS website. For rectifying and mapping these parameters the ArcGIS arc toolbox environment was used. The map of geology and soil were generated from the respective map of the study area (JPG and PDF format) by digitizing using GIS software. There are different geological materials in the study regions. The

common geological material is quaternary alluvial and lacustrine sediment, which has major area coverage. The soil textural class in the study regions includes clay, loam, loamy sand, and sandy loam. Clay soil type is the main soil which has a large area coverage compared to the others.

LULC and NDVI maps were produced from satellite Sentinel 2 imagery. Sentinel-2 is an Earth observation satellite from the Copernicus Programme that obtains optical imagery at high spatial resolution (10 m to 60 m) over land surface. Supervised classification was used to classify LULC of each area based on previously developed LULC with update. The value of NDVI index which describes the difference between visible and near-infrared reflectance of vegetation cover to determine the density of green leaf. NDVI was calculated from the red band (band 4) and near-infrared band (band 8) of sentinel 2 imagery. Converting and geo-referencing all the available data into Universal Transverse Mercator (UTM) zone 37 was the initial step of manipulation. The Rockwork 16, ERDAS Imagine, Surfer, and ArcGIS software were used in this study for the data processing.

Geology

The shallow alluvial-lacustrine sediments cover the studied regions. Alluvial terrain is said to make up as much as 25% of the nation's total geographical area. The Danakil basin, the Gambela plain region, the Tana sub-basin, the eastern Awash basin, the southern Omo valley, and the center portion of the major Ethiopian rift are the primary locations where the sediment is found. (Kebede, 2013). Alluvio- lacustrine deposits of sand, silt, clay, diatomite, limestone, and beach sand are the major geological features in the study region. The areal coverages of these geological parameters were different for each region. In addition to quaternary sediments, the study areas are occupied by different geological features. The feature covers more than 80% of the area in Gambela Plain 19.71% area coverage on Fafen Jerer and more than 45% area coverage in the Shinile sub-basin. Moreover, due to geographical similarity and closeness the Fafen-Jerer and Shinile sub-basins share similar geological features like (Ashangi Formation, Jessoma Formation, Hamanlei Formation, and Alghe Group) (Figure 4.1, & Table 4.1). The other geological parameters are specific to the specific regions. The table below describes the geological materials in the study regions.

- Urandab formation: Oxfordian-Kmmerdgian marl and shaly limestone is another major feature in the Fafen Jerer sub-basin which covers 37.68% of the area.

- Afar Series: Alkaline basalt with subordinate alkaline and peralkaline silicic (rhyolitic dome and flows and ignimbrites) is one of the main features in the Shinile sub-basin covering 25-30%.
- Jessoma formation: Cretaceous-Paleocene sandstone is the other major geologic feature in southeastern Ethiopia (Ogaden basin). The Jessoma formation covers 18.29% of the eastern part of the Fafen-Jerer sub-basin.
- Hamanlei Formation (17.43%): Oxfordian limestone and shale are also found in Fafen Jerer as the main formation and also have large coverage in the upper catchment of the Shinile sub-basin.
- Basalt flows, spatter cones, and hyaloclastites (Qb): Transitional type between alkaline and tholeiitic found small areal coverage in the Shinile sub-basin.

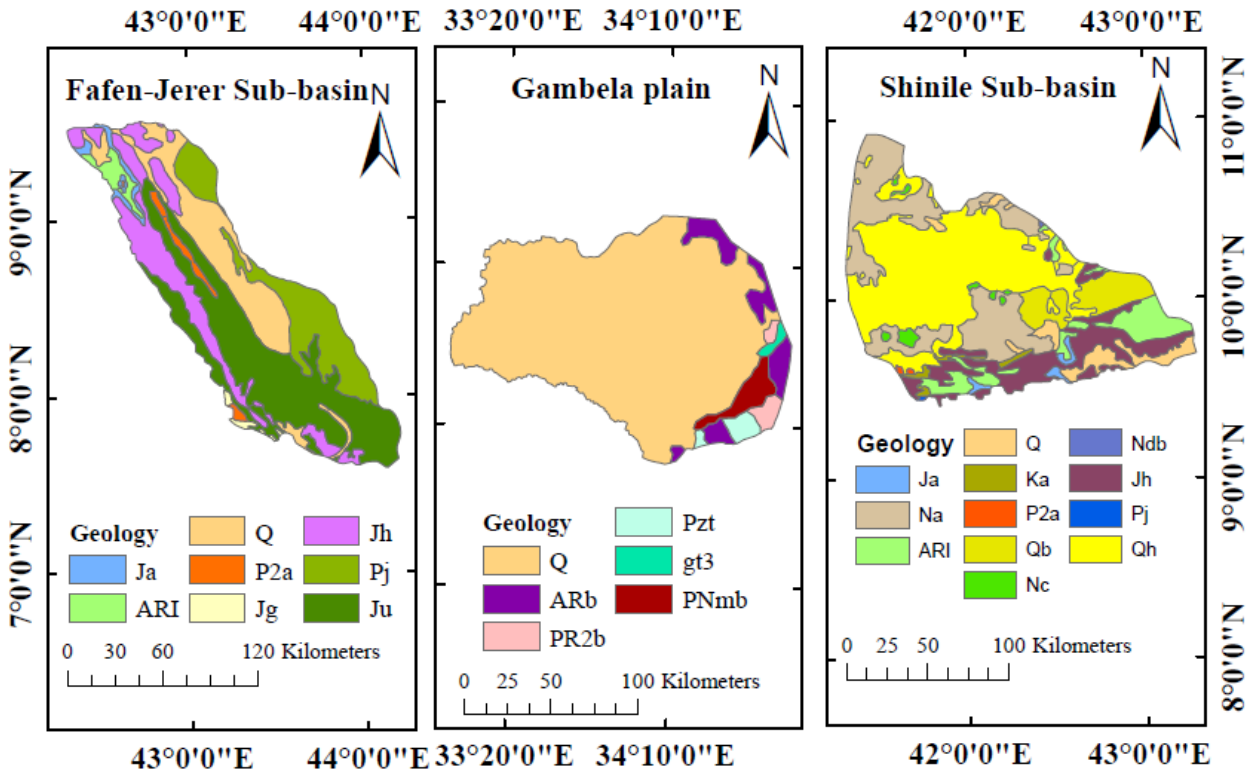

Figure 4. 1 Geological maps

Table 4. 1 The Descriptions of the geological features in the study areas

(Amer et al., 2013; Geological Survey of Ethiopia, 1996; Getnet Tsegaye et al., 2018)

Symbol	**Geologic units**	**Description**	**Period**	**Remarks**
Q	Alluvial and lacustrine deposits	Sand, silt, clay, diatomite, limestone, and beach sand.	quaternary undifferentiated	Present in all three regions
Qb	Basalt flows, spatter cones and hyaloclastite's	Transitional type between alkaline and tholeiitic.		Shinile
Qh	Undifferentiated alluvial, lacustrine and beach sediments		Holocene	Shinile
Nc	Chilalo Formation (Lower part)	Trachyte, trachy- basalt, peralkaline rhyolite with subordinate akaline. basalt.	Pliocene – Pleistocene	Shinile
Na	Afar Series	Alkaline basalt with subordinate alkaline and peralkaline silicics (rhyolitic dome and flows and ignimbrites)	Miocene - Pliocene	Shinile
Ndb	Dalaha Formation	Fissural basalts and hawaiites with some intercalated detrital and lacustrine sediments, with rhyolitic flows and ignimbrites in the upper part.	Late Miocene	Shinile
PNmb	Makonnen Basalts	Flood basalts, commonly directly overlaying the chrystalline basement.	Oligocene - Miocene	Gambela plain
P2a	Ashangi Formation:	Deeply weathered alkaline and trasitional basalt flows with rare intercalations of tuff, often tilted (includes Akobo Basalts of SW Ethiopia).	Eocene	Fafen-Jerer and Shinile

Continued Table 4. 1

Pj	Jessoma Formation	Late Cretaceous-Paleocene sandstone.	Eocene	Fafen-Jerer and Shinile
Ka	Amba Aradom Formation:	Sandstone, conglomerate and shale.	Cretaceous	Shinile
Jg	Gabredarre Formation	Kimmeridgia -Tithonian; (Jg2) Upper unit and (Jg1) Lower unit: Limestone with shaly and gypsiferous units.	Late Jurassic	Fafen-Jerer
Ju	Urandab Formation	Oxfordian-Kmmerdgian marl and shaly limestone		Fafen-Jerer
Jh	Hamanlei Formation	Oxfordian limestone and shale.	Early - Late Jurassic	Fafen-Jerer and Shinile
Ja	Adigrat Formation	Triassic-Middle Jurassic sandstone	Early - Late Jurassic	Fafen-Jerer
Pzt	Enticho Sandstone, Edaga Arbi Glacials, Gura and Gilo Formations	Sandstone, shale, conglomerate and tillite	Late Paleozoic – Triassic	Gambela
PR2b	Birbir Group	Meta basalt, metaan desite, metarhyolit, phyllite, graphiticschist, marble, quartzite, metaconglomerate, green schist, metasandstone, metachert and amphibolite.	Late Proterozoic	Gambela
ARb	Baro Group	Biotite, hornblende - biotite, garnet - amphibole, garnet - sillimarite, calc - silicate and muscovite gneisses.	Archean	Gambela
ARI	Alghe Group	Biotite and hornblende gneisses, granulite and migmatite with minor metasedimentary gneisses.	Archean	Fafen-Jerer and Shinile
gt3	Late to post-tectonic granite.		Precambrian and Phanerozoic Intrusive Rocks	Gambela

Geomorphology

The majority of the study areas are plain areas having gentle sloping. The ridge and mountains found in the headwater zones of the study regions. Relatively large rolling areas are found in the Fafen-Jerer and Shinile sub-basins. For each of the three zones, there is a distinct elevation difference between the lowest and highest points. For Fafen-Jerer, Gambela, and Shinile, the reliefs (height difference) are 2211 meters, 577 meters, and 2676 meters, respectively. Fafen-Jerer and Shinile often have the greatest elevation differences.

The geomorphological classification was performed with the topographic position index method. The topographic Position Index was first developed by Gallant and Wilson in 2000 (Weishampel et al., 2011; Chauniyal and Dutta, 2018). The topographic index measures the difference between the elevation of pixels and the average elevation of the neighboring pixels. The topographic index has several applications in geomorphological and landform analysis (Chauniyal & Dutta, 2018). The landforms in the study region are classified namely: valleys, plains, local hills, high ridges, mountains, etc (Figure 4.2). These geomorphological parameters were given ranks (1-5) according to their influences on groundwater potential.

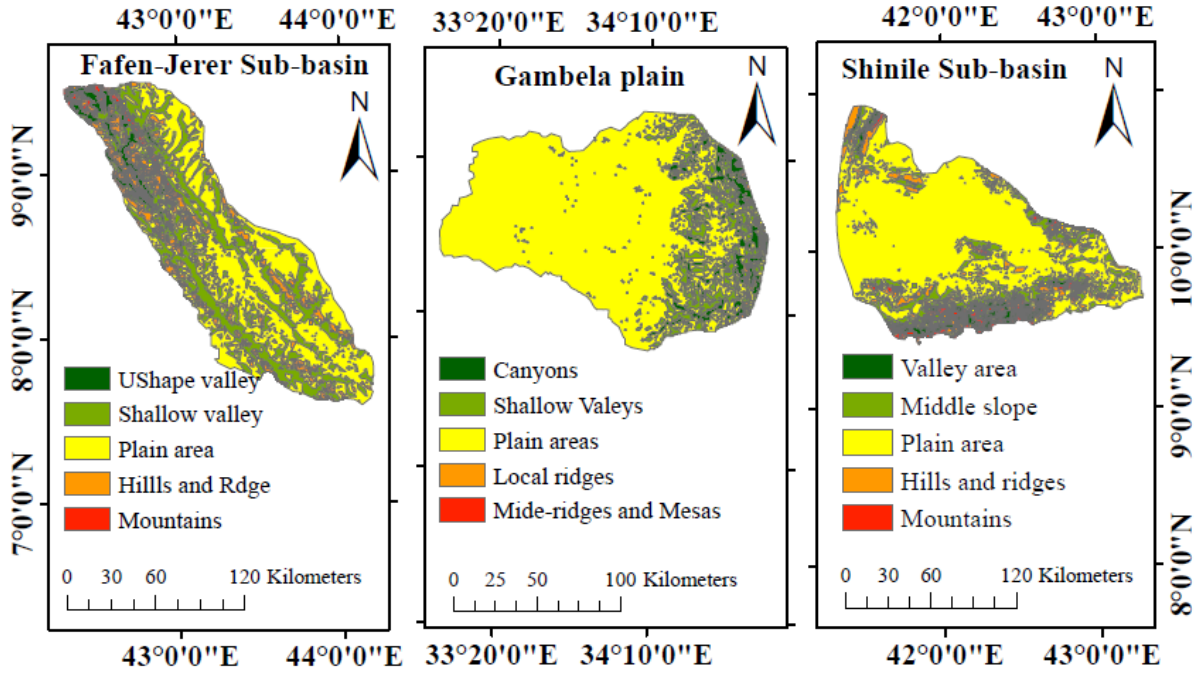

Figure 4. 2 Geomorphological maps

Slope

The slope of the surface alters runoff and infiltration which affect the groundwater recharge areas. Very little subsurface recharge occurs on steeper slopes due to higher runoff, and vice versa (Nag and Kundu, 2018). Groundwater potential zone related to the flat area having low runoff.

Table 4. 2 Slope characteristics

Study area		**Fafen-Jerer**		**Gambela**		**Shinile**	
Slope class	**Slope in Degree**	Area (sq. km)	Percent	Area (sq. km)	Percent	Area (sq. km)	Percent
Flat to very gentle slope	0-3	10223.89	58.22	14636.65	80.30	10541.88	52.79
Gentle sloping	3-10	6053.86	34.47	3470.74	19.04	7278.34	36.45
Strong slope	10-15	699.07	3.98	59.59	0.33	874.89	4.38
Moderate sloping	15-20	329.45	1.88	30.83	0.17	544.56	2.73
Steep sloping	>20	254.78	1.45	28.65	0.16	730.25	3.66
		17561.05	100.00	18226.46	100.00	19969.92	100.00

The slope map of the study was produced from the SRTM DEM data. The slope was then reclassified into five sub-classes and given weight according to their influence on groundwater zonation. The slope classes are: flat to very gentle sloping(0-3^{o}), gentle sloping (3^{o}-10^{o}), strong sloping(10^{o}-15^{o}), moderate sloping(15^{o}-20^{o}) and steep sloping(>20^{o}). The majority of the areas are gentle to the flat slope (0-3^{o}) which covers 58% of Fafen-Jerer, 80% of Gambela plain, and 53% of Shinile sub-basin area coverage (Table 4.2). Higher sloping ranges have been found in the Fafen-Jerer and Shinile sub-basins due to high relief. But the plain area of the Shinile sub-basin is relatively gently sloping than the Fafen-Jerer sub-basin. Flat and gently sloping surfaces have good infiltration capacity and give the highest value (Figure 4.3).

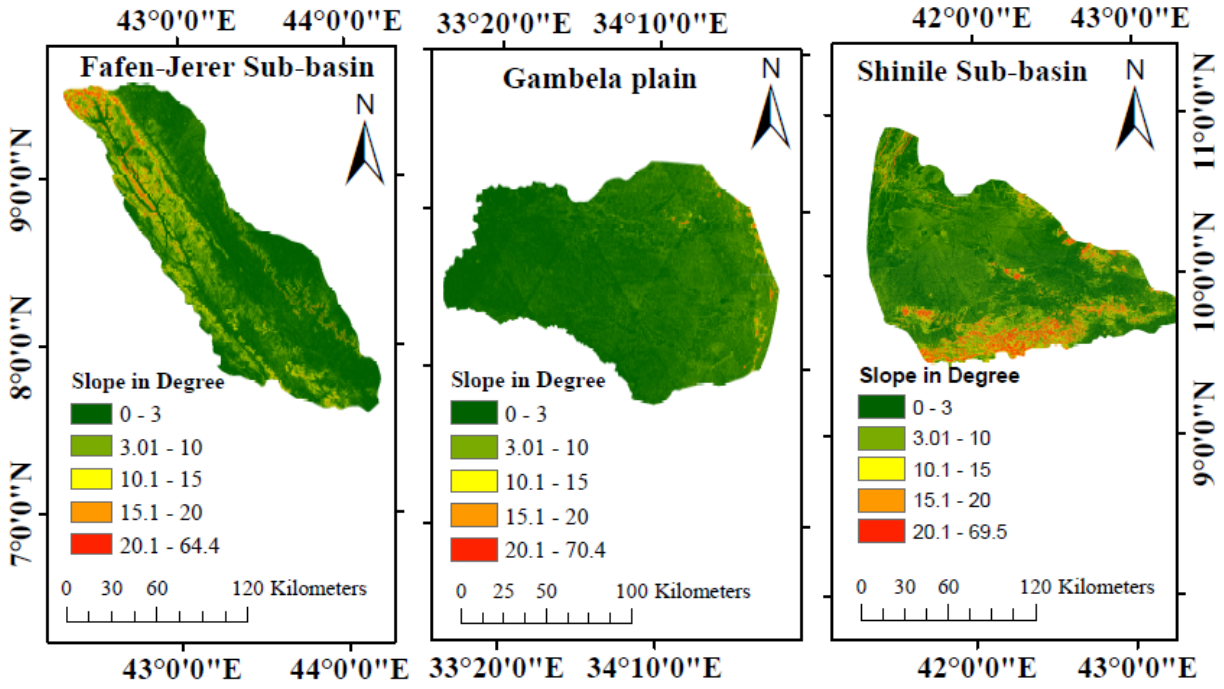

Figure 4. 3 Slope maps

Soil textures

Water transmission in the aquifer is largely dependent on the type, texture, permeability, and structure of the soil. The main characteristic of the soil is its infiltration capacity, which, depending on the characteristics of the soil particles, can influence the penetration of water droplets into the aquifer medium. High-infiltration soils are good groundwater recharge mediums; sandy soils have high infiltration, while clay soils become the least invasive (Juandi & Syahril, 2017).

The study areas contain various types of soil. According to the soil classification report by Berhanu, and others (2013): the predominant soil texture found in the study area includes clay, loam, loamy sand, and sandy loam. Clay soil has 60% coverage in Gambela plain and it has only 11% coverage at Shinile sub-basin. Sandy loam soil has 50% coverage at the Shinile sub-basin while not found in Gambela plain (Figure 4.4).

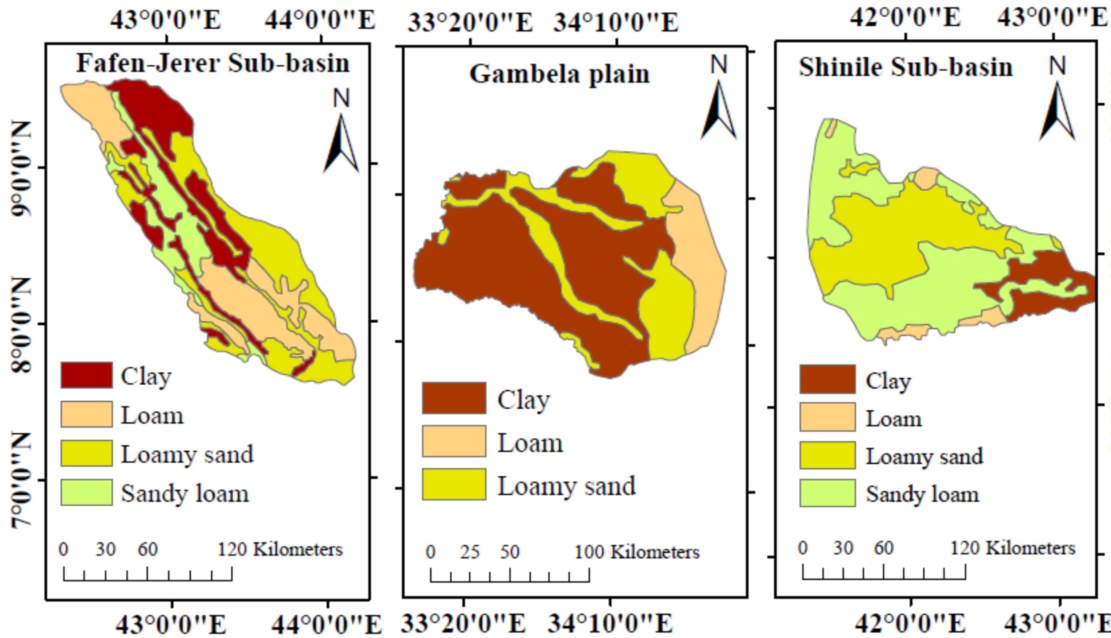

Figure 4. 4 Soil texture maps

Drainage Density

The drainage density of an area is defined as a measure of the total length of the stream in the area divided by the total area. The entire length of the stream in the region divided by the total area is the definition of the drainage density of that area. A high drainage density indicates the presence of a nearby stream in that region and vice versa. The groundwater zone and drainage density have an inverse relationship. Due to a lower infiltration rate, a high drainage density region becomes a low groundwater zone. The areas with the lowest drainage networks allow more water to seep into the subsurface, which is the groundwater's high potential zone (Magesh, et al, 2012; Nag and Kundu, 2018). Drainage density (D_d) of an area is calculated by using the formula:

$$D_d = \sum_{i=1}^{n} \left(\frac{D_i}{A}\right) \quad 4.1$$

where *Di* is the total length of all streams (km) and *A* is the watershed area (km^2).

The value of drainage density (km/km^2) is classified into five sub-classes: very low, low, medium, high, and very high) (Figure 4.5).

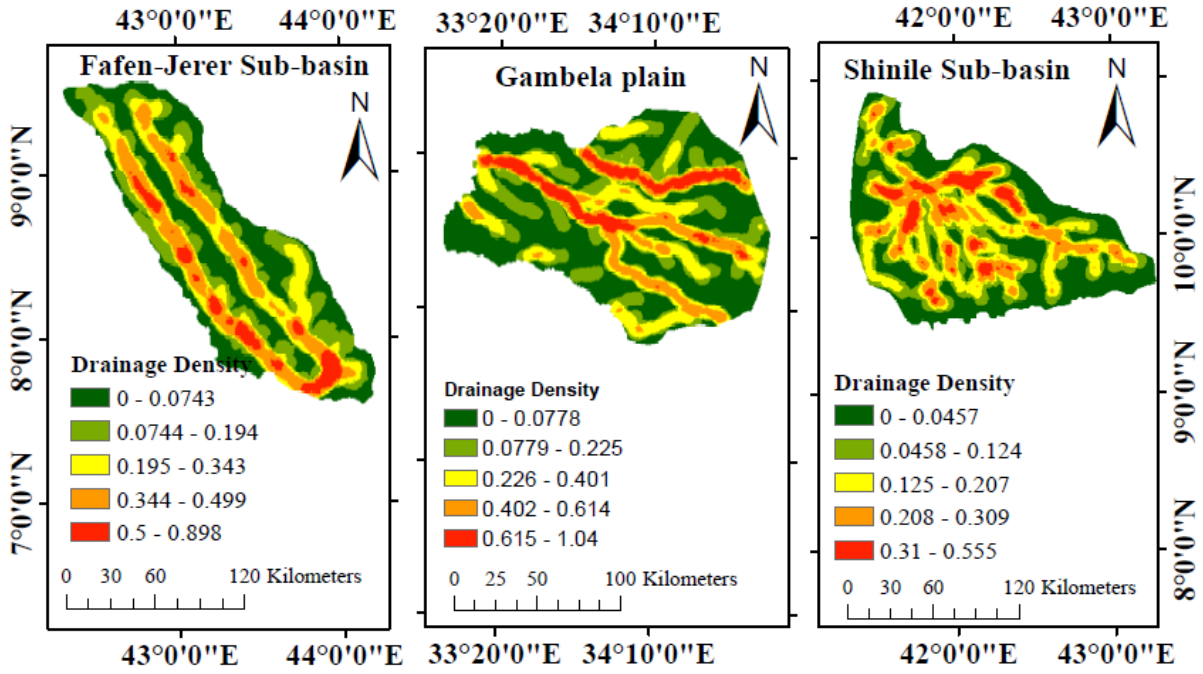

Figure 4. 5 Drainage density maps

Lineaments and Lineament Density

A lineament is a surface outcrop's contour feature, either straight or curved, that provides fundamental details about the underlying geological assemblage. Numerous lineaments in the region demonstrate the porosity of the terrain, which serves as a conduit for the circulation of groundwater (Mukherjee, et al 2012).

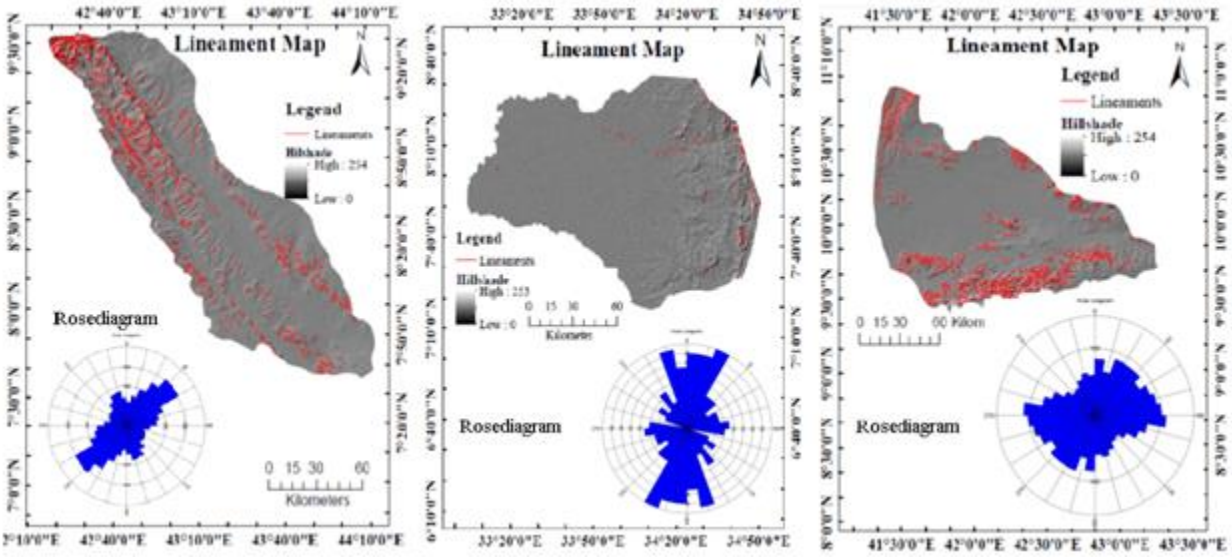

Figure 4. 6 Lineaments distributions and Rose diagram maps

A lineament map is a mapping of linear features using remotely sensed data which is key to understanding groundwater occurrence (Sander, 2007). The Lineament's density (L_d) of an area is defined as the ratio of the total length of the lineament structure to the area coverage.

$$L_d = \sum_{i=1}^{n} \left(\frac{L_i}{A}\right) \ldots \ldots \ldots \ldots \ldots \ldots \ldots \ldots \ldots \ldots \ldots \ldots \ldots \ldots \ldots \ldots \ldots \ldots \ldots \ldots 4.2$$

Where: *Li* the length of *i^th^* lineament (km), *A* area of the catchment (km^2)

The lineament density in km/km^2 was classified into five classes: very low, low, moderate, high, and very high. In the Fafen and Shinile sub-basins, the primary lineament direction is NNE-SSW, while in the Gambela plain region, it is NS (Figure 4.6).

In the Fafen sub-basin the lineaments are very high in the northwestern catchment areas (upper catchment of Fafen river) whereas very low lineaments are found in the eastern part. In general, the Gambela Plain has fewer lineaments than the other regions that spread the eastern boundary areas (Figure 4.6). In the Shinile sub-basin the upper catchments (highland area) have high distributions of lineaments. The lineament density is high in the area of dense distribution of lineaments (Figure 4.7).

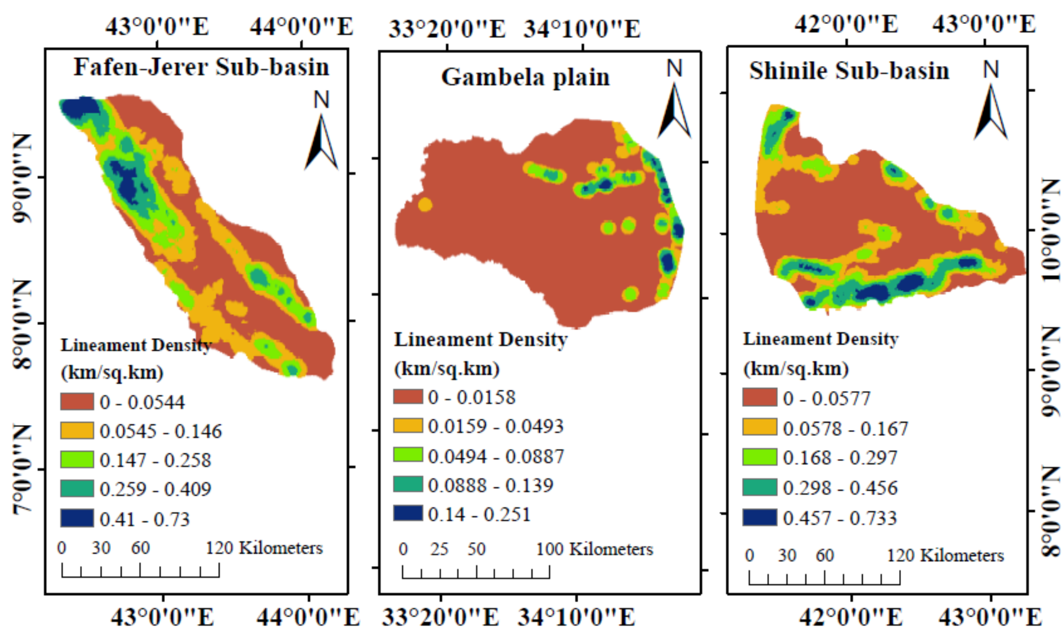

Figure 4. 7 Lineaments density maps

Land use and land cover (LULC)

One of the main parameters that influence the role of rainfall droplets on the surface is land use and land cover types. Land cover can facilitate the infiltration to the sub-surface on vegetated land and also it can aggravate the runoff in bare land areas (Chowdary et al., 2008). LULC maps were generated using the Sentinel 2 satellite imagery. The first procedure was collecting cloud-free sentinel 2 imagery of the specific region. Due to the size of the sentinel 2-pixel, there was more than 4-8 pixels were necessary to cover the specific region for specific temporal coverage. Mosaicking of multiple sentinel 2 imagery to the new raster dataset was performed with the ArcGIS tool. The satellite dataset was geometrically corrected to a common projection (Universal Transverse Mercator (UTM). Supervised classification using an inference supervised classifier technique was used to carry out to classify images with 10m compositions (bands 2, 3, 4, and 8) of sentinel 2.

The land use types identified include forest land, agricultural land (annual, perennial), shrub land, grassland, water body, bare land, rock outcrops, wetland, build-up area, etc. Shrubland and grassland cover large areas in the study regions (Figure 4.8). The value of weight for the sub-class of LULC was given based on the infiltration capacity of each LULC class. Build-up and bare land have less infiltration while waterbody and wetlands have greater infiltration capacity.

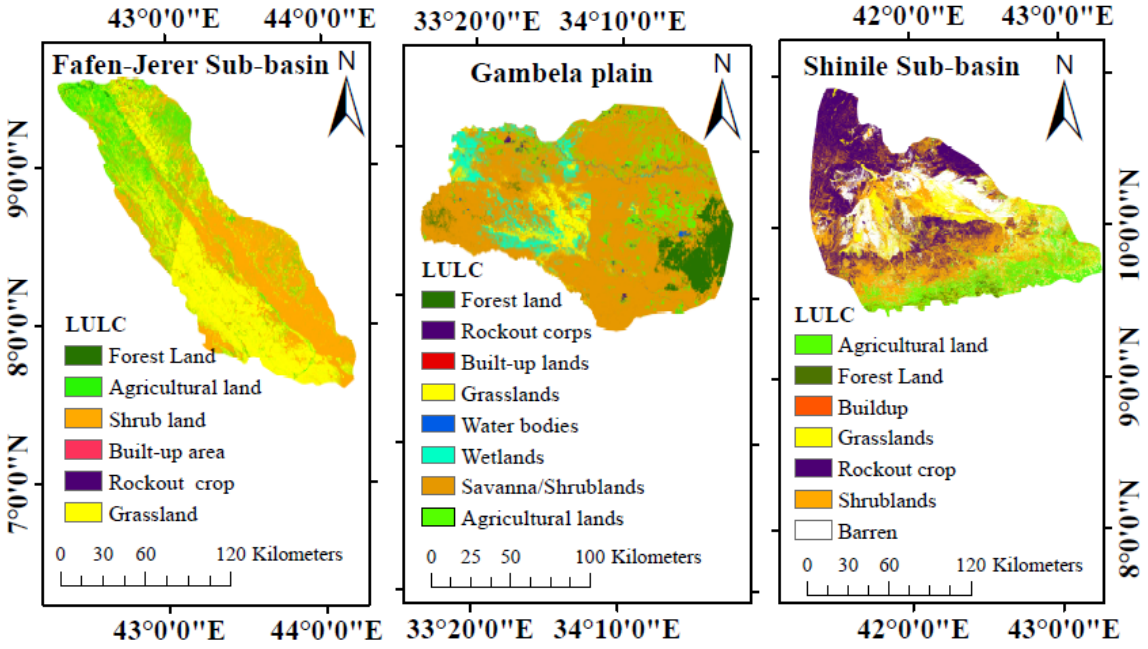

Figure 4. 8 LULC maps

Normalized Difference Vegetation Index (NDVI)

The Normalized Difference Vegetation Index (NDVI) is a numerical indicator that illustrates the behavior of vegetation and is used to measure vegetation cover in an area. NDVI uses the visible and near-infrared bands of the electromagnetic spectrum of the remotely sensed image to measure whether the target has green vegetation or not (Özyavuz et al., n.d.). Normalized Difference Vegetation Index (NDVI) is expressed using near-infrared (NIR) and visible red (R) light to measure the presence of vegetation index in plants.

$$Normalized\ Difference\ Vegetation\ Index = \frac{NIR - RED}{NIR + RED} = \frac{Band\ 8 - Band\ 4}{Band\ 8 + Band\ 4} \ldots\ldots\ldots\ldots 4.3$$

Where: NIR is near-infrared reflectance (strongly vegetation reflectance), and RED is red light (absorbs vegetation).

The groundwater storage capacity is strongly impacted by NDVI. A higher NDVI score indicates a higher concentration of vegetation, which helps replenish the groundwater table by reducing runoff. The values of NDVI range from a negative one (-1) to a positive one (1). The higher positive value of NDVI shows the vegetation cover, and the negative value indicates bare lands and water bodies, etc. (Gandhi et al., 2015). The NDVI value in the study areas ranges from (-0.451 to 0.994) in Fafen-Jerer, (-0.303 to0.731) for Gambela, and (-0.35 to 0.84) for the Shinile sub-basin. The deep blue in the figure (Figure 4.9) shows the vegetation cover which covers a larger area in southeastern Gambela plain.

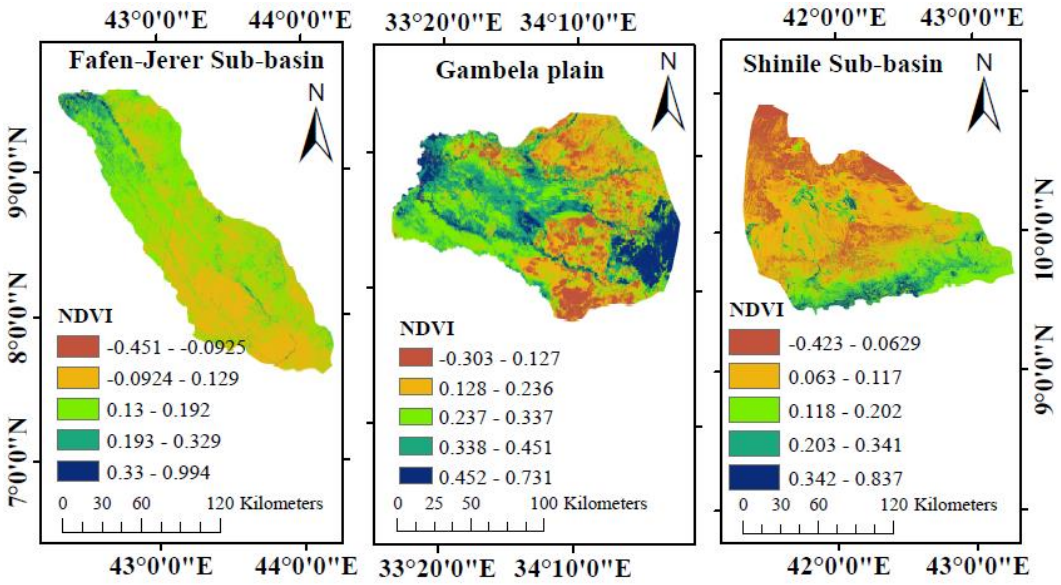

Figure 4. 9: Normalized difference vegetation index maps

Rainfall

Rainfall is one of the chief influencing parameters that govern the groundwater potential of an area. Precipitation has a direct impact on groundwater potential zone. The higher the precipitation the higher the water particles on the surface giving a casual increment in the infiltration to the sub-surface. As the study areas are semi-arid climates the average annual rainfall amount is much less particularly for the Fafen-Jerer. All the study areas are data-sparse regions having minimum numbers of meteorological stations compared to the other parts of the country.

The station's rainfall data was collected from the National Meteorological Agency (NMA). In collecting the rainfall point data neighboring stations bordering out of the study region were included. Rainfall observation stations in the study region as well as neighboring stations were used to map the distribution (Figure 4.10). The Fafen-Jerer sub-basin experiences lower yearly rainfall amounts and the Gambela experience higher.

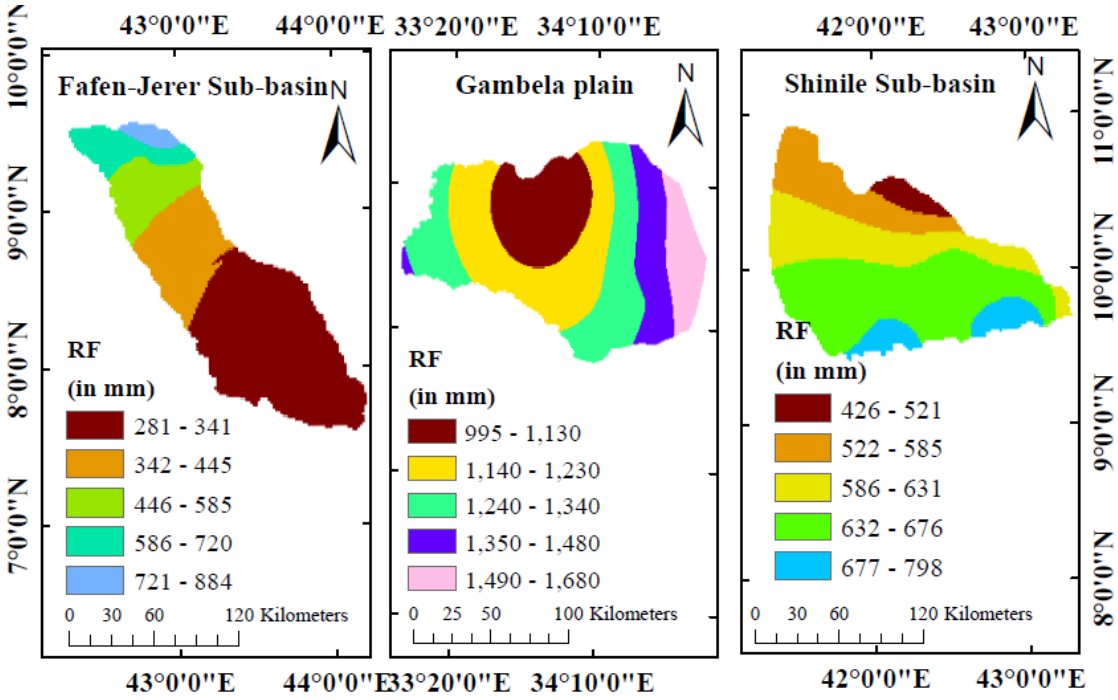

Figure 4. 10 Precipitation distribution maps

Topographic Wetness Index (TWI)

The topographic wetness index is a parameter that shows the terrain profile which can control the water accumulation. Topographic witness index was developed by Beven and Kirkby, (1979) with TOPMODEL. TWI shows the quantity of water that can flow within a specific site. TWI shows the control of topography on hydrological processes.

The topographic wetness index has a wide range of applications like as measuring soil moisture (Kopecký, Macek, and Wild, 2021) identifying hydrological flow paths (Robson, Beven, and Neal, 1992) biological processes (Besnard et al., 2013), and vegetation patterns (Kopecký & Čížková, 2010). The Topographic Wetness Index (TWI) is used to determine the groundwater potential infiltration due to topographic parameters. The topographic wetness index combines local upslope contributing area and slope gradient.(Beven, 1997; Beven & Kirkby, 1979) The TWI of an area calculated with:

$$TWI = \ln \frac{\alpha}{tan\beta} \quad \ldots\ldots 4.4$$

Where: $\alpha = upslope\ contributing\ area, \beta = topgraphic\ gradient(slope)$

The values TWI in the study area range from 2.41 to 25.5. Higher values are found in Shinile and the lower ones belong to the Gambela area. The value is classified into five classes giving ranks from "very low" for the lowest value to "very high" for the highest one. The figure below shows the value and classified maps of TWI in the study areas (Figure 4.11). The lower value of TWI indicates an area of low potential and vice versa.

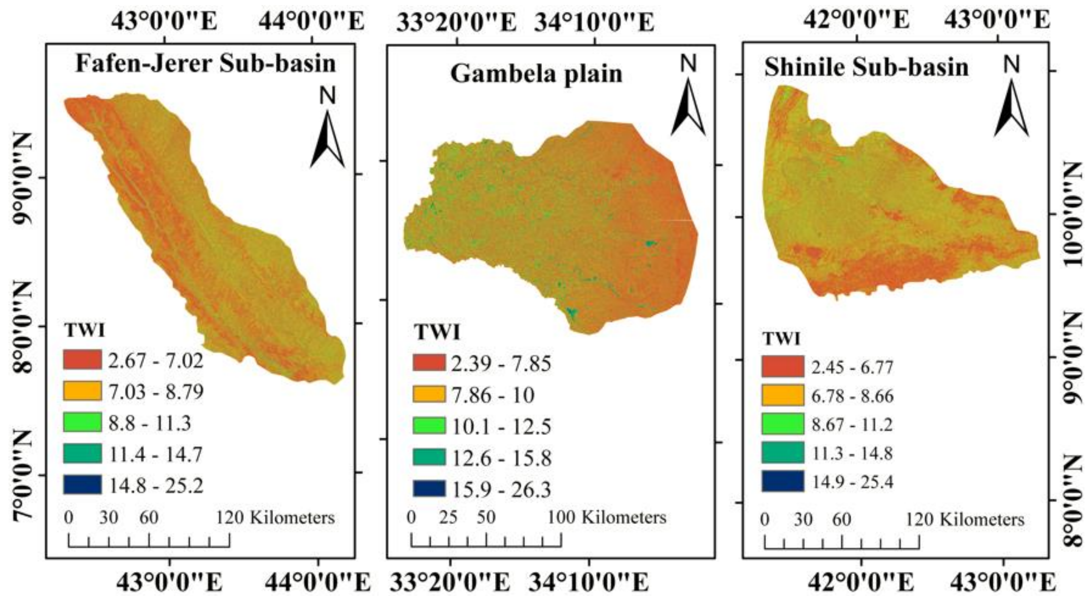

Figure 4. 11 Topographic wetness index maps

Topographic Roughness Index (TRI)

The Topographic Roughness Index is a topographic parameter that represents the local elevation variability of landforms. The texture of topography may vary from flat texture to uneven/irregular texture. The amount of this variability of land surface for a specific area is measured by the roughness index. The map of topographic roughness shows the ruggedness/irregularity of land surface parameters in the grid cell of DEM (Stambaugh and Guyette, 2008; Lindsay, 2019). The topographic roughness index (TRI) is given as:

$$Roghness = \frac{FS_{mean} - FS_{min}}{FS_{max} - FS_{mn}} \dots\dots\dots\dots\dots\dots\dots\dots\dots\dots 4.5$$

Where: FS_{mean} mean focal statistic, FS_{max} maximum focal statistics amd FS_{min} minimum focal statistic of a surface(Mukherjee & Singh, 2020).

The TRI of the study regions was used by classifying the into five class using natural brake method (Figure 4.12).

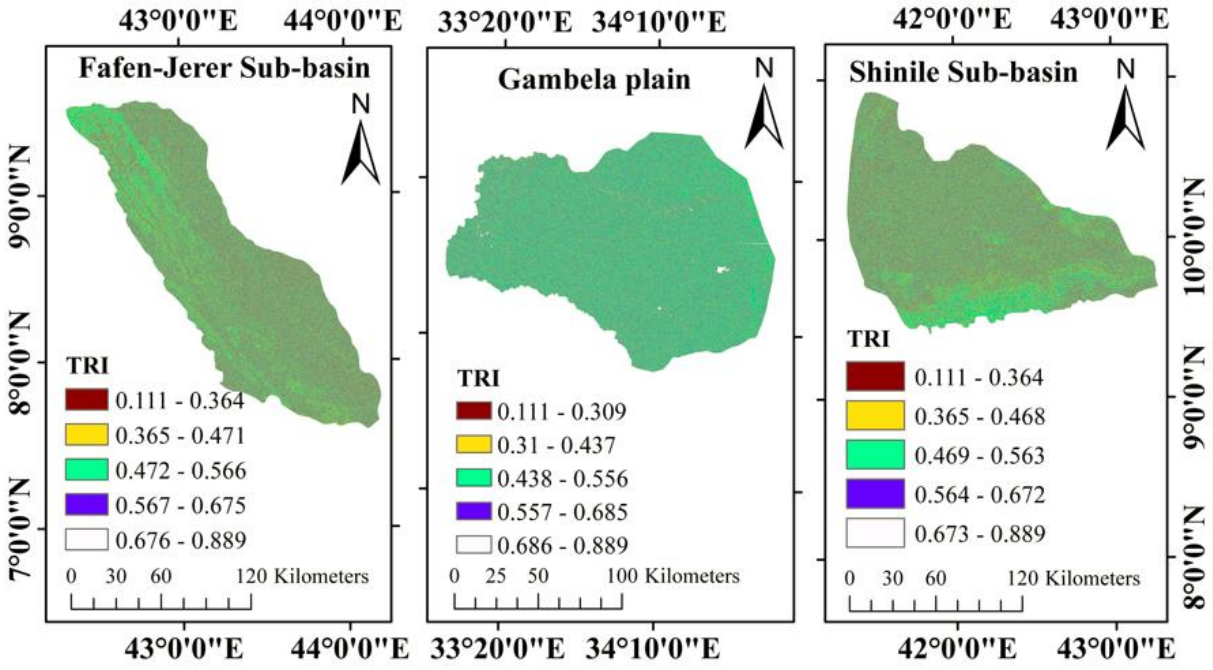

Figure 4. 12 Topographic roughness index maps

4.2.3. Assigning weight to the parameters

Saaty's analytical hierarchy method (AHP) was used to determine the relative importance of the parameters (Saaty & Katz, 1994). A nine-point scale, where '1' denotes equal significance between two criteria and '9' shows the extreme importance of one criterion over another, is suggested by Saaty (1980) for determining the relative relevance or 'intensity' of each pair of criteria (Table A4.1). The pairwise comparison matrix table of the relative importance of each parameter in the creation of the groundwater potential zone based on Saaty's scale was developed (Tables A4.2 to A4.4). The normalized comparison matrix was prepared by dividing each value in the pairwise comparison table by the sum of the weights assigned to each criterion. The average value of the row in the normalized comparison matrix table provides the weight of each criterion for GIS overlay analysis.

4.2.4. Checking the reliability of the analysis

The study uses consistency index and consistency ratio values to check the consistency rate in ranking and assigning weights for the thematic layer (Elubid et al., 2020; Mukherjee & Singh, 2020).

$$Consistency\ Ratio(CR) = \left(\frac{CI}{RCI}\right), Consistency\ Index(CI) = \left(\frac{\lambda_{max} - n}{n-1}\right) \ldots\ldots\ldots 4.6$$

Where λmax is the eigenvalue, RCI is the random consistency index (Table A4.5) and n is the matrix size (the number of criteria/thematic layers) (Tummala & Ling, 1996). The analysis was consistent, as indicated by the value consistency ratio (CR), which is CR<0.1 (Saaty, 2002).

4.2.5. Multicollinearity analysis

A method for determining the linearity of influencing factors and measuring data redundancy between components is called multicollinearity. The multicollinearity of the influencing elements must be examined as one of the prerequisites for model assessment. The multicollinearity of the components was investigated by doing a linear regression analysis with one factor as a dependent and the other as an independent variable. The multicollinearity of all components was ascertained using the variance inflation factor (VIF) and tolerance (TOL) of the model parameters.

$$TOL = 1 - R^2 \ldots\ldots\ldots\ldots\ldots\ldots\ldots\ldots\ldots\ldots\ldots\ldots\ldots\ldots\ldots\ldots\ldots\ldots\ldots 4.7$$

$$VIF = \frac{1}{Tollerance} \ldots\ldots\ldots\ldots\ldots\ldots\ldots\ldots\ldots\ldots\ldots\ldots\ldots\ldots\ldots\ldots\ldots\ldots\ldots 4.8$$

If a TOL < 0.10 or VIF ≥ 10 the analysis shows that the multicollinearity problem and the associated influencing factors should be removed from groundwater potential prediction models due to multicollinearity (Mukherjee & Singh, 2020).

4.2.6. GIS Overlay analysis

The weights were distributed according to the influence of each criterion on the zonation of groundwater potential. Each theme layer in ArcGIS was separated into subclasses according to the kind of layer. The weight calculation ratings 1 through 5 in the groundwater potential zone are allocated to the sub-classes of thematic layers based on their influence on groundwater recharge (Tables A4.6 to A4.8). The groundwater potential index (GWPI) was calculated as:

$$\begin{aligned} GWPI = {} & ((RF_w)(RF_{wi}) + (Ge_w)(Ge_{wi}) + (Gm_w)(Gm_{wi}) + (Sl_w)(Sl_{wi}) + (Dd_w)(Dd_{wi}) \\ & + (LULC_w)(LULC_{wi}) + (Ld_w)(Ld_{wi}) + (So_w)(So_{wi}) + +(TWI_w)(TWI_{wi}) \\ & + (TRI_w)(TRI_{wi}) \quad \ldots\ldots\ldots\ldots\ldots\ldots\ldots\ldots\ldots\ldots\ldots\ldots\ldots 4.9 \end{aligned}$$

Where: (RF) rainfall, (Ge) geology, (Gm) geomorphology, (Sl) slope, (Dd) drainage density, (LULC) land use land cover, (Ld) lineament density, (So) soil, (TWI) topographic wetness index and (TRI) topographic roughness index. While subscript *w* is normalized weight main criteria and subscript *wi* is normalized weight of sub criteria (Fashae et al., 2014; Rap & Briz-Kishore, 1991).

4.2.7. Machine learning technique

Random forest classifier (RFC)

Random forests are supervised MLAs that can be applied in majority voting for classification or averaging for regression. For classification tasks, the output of the random forest is the class selected by most trees. For regression tasks, the mean or average prediction of the individual trees is returned (Tyralis et al., 2019). Using ensemble learning, the random forest method combines numerous classifiers to offer solutions to challenging issues. The tendency of decision trees to overfit their training set is corrected by random decision forests. If C_b (x) is the class prediction of b^{th} random forest tree then:

$$C_{rf}^{B}(x) = majority\ vote\ \{C_b(x)_1^b \ldots\ldots\ldots\ldots\ldots\ldots\ldots\ldots\ldots\ldots\ldots\ldots\ldots\ldots\ldots\ldots\ldots\ldots\ldots\ldots\ldots\ldots\ldots\ldots 4.10$$

Gradient Boosting Classifier (GBC)

Gradient boosting is a functional gradient algorithm that iteratively selects a function pointer in the direction of the negative gradient, or a weak hypothesis, to minimize a loss function (Sachdeva & Kumar, 2021a). The gradient boaster model update equation is:

$$F_m(x) = F_{m-1}(x) + \sum_{j=1}^{Jm} \gamma_{jm} 1R_{jm}(x), \quad \gamma_{jm} = arg\min \sum_{zi\epsilon Rjm} L(y_i, F_{m-1}(x_i) + \gamma \ldots\ldots 4.11$$

Decision Tree Classifier (DTC)

A non-parametric supervised learning technique for classification and regression is called a decision tree. The objective is to learn straightforward decision rules derived from the data features in order to build a model that predicts the value of a target variable. A piecewise constant approximation of a tree can be thought of. The techniques known as decision tree inducers create a decision tree from a given dataset automatically. Typically, the best decision tree is found by reducing the generalization error (Tanimu et al., 2022).

K-Neighbor classifier (KNC)

An example of a nonparametric learning algorithm is the K-neighbor classifier. The algorithm determines the distance between the target point and the nearest points in the classification setting using the value supplied for K and the maximum number of votes from these adjacent points about the number of points that were selected. If we have data with certain qualities (X) and the value of the relationship, the algorithm K-Nearest Neighbor belongs to the class of algorithms that can categorize an unknown item (Y) (Avand et al., 2019). This approach uses the Euclidean distance function (D_{rt}) to determine how closely related (neighborhood) the real-time prediction value Xr = (X1n, X2n, X3n , ….., Xmr) is to the predictive value for each historical observation: Xt = (X1b, X2b, X3b , ….., Xmr)

$$D_{rt} = \sqrt{\sum_{i=1}^{m} W_i (X_{ir} - X_{it})^2}, t = 1,2, \dots, n \dots\dots\dots\dots\dots\dots\dots\dots\dots\dots\dots\dots\dots 4.12$$

Where W_i (i=1,2,...m) is the weight of predictors, whose sum is equal to one.

Dataset for MLAs

Using "spatial analyst tools," the dataset has been created in ArcGIS. Using centroid sample points throughout the raster dataset, a polygon grid has been created. All of the raster values, or independent variables, from the theme maps, were added to a point vector layer using the "extract multi values to point" tool. By using a spatial join, the well-data has also been added to it. Next, for training and testing the model, a dataset containing the current well data was exported separately.

The dataset was split into the train, validation, and test data, which were organized at 70%, 20%, and 10% correspondingly, to increase the performance of our MLA models (Figure 4.13). As a general rule, normalization and standardization are utilized in the next stage to increase the neural network's effectiveness. Data normalization ensures that each character contributes equally to the sum. This does not imply that all characteristics are equally significant when choosing a classifier, though. In several application domains, researchers have employed normalizing techniques to enhance classification performance (Thanh et al., 2022). In this study, we use Min-Max Scalar normalization (Deepa et al., 2022).

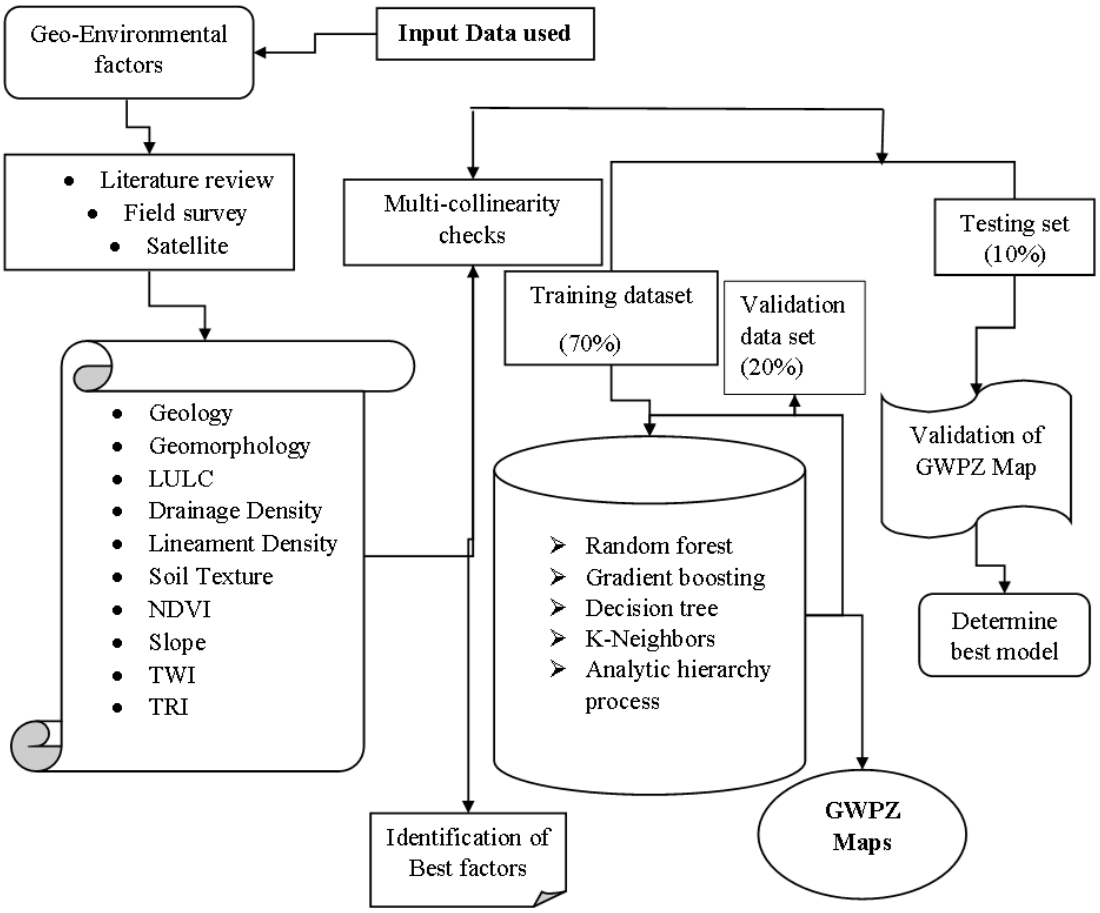

Figure 4. 13 Flow chart for MLAs

Random Search CV: The hyperparameter implementation "Randomized Search" goes by the name of the Randomized Search CV technique (Bergstra et al., 2012). Cross-validation, score, parameter distributions, estimators, and the number of iterations are only a few of the factors that the function considers. This method, in contrast to grid search, posits that not all hyperparameters are equally important. Each cycle generates a different random set of hyperparameters, which helps find more potent combinations. The probability of discovering beneficial combinations rises as a result of the random creation of a new set of hyperparameters with each cycle.

4.2.8. Model validation

A critical step in scientific inquiry is model validation. The accuracy of the groundwater potential zone concept was confirmed in several investigations using spring and borehole data (Mukherjee & Singh, 2020). To validate the model, receiver operating characteristic (ROC) analysis was

employed in this study. By employing the provided model approaches, the performance of GWPZ prediction has been assessed using the ROC curve and statistical measures of accuracy, precision, recall, fi-score, and kappa index (Table 4.3).

Table 4. 3 Accuracy indices calculated for each classifier

No	Parameters	Formulas
1	Accuracy	$\frac{TP+TN}{TP+FN+TN+FP}$
2	Precision	$\frac{TP}{TP+FP}$
3	Recall	$\frac{TP}{TP+FN}$
4	Fi-score	$\frac{2*precision*reall}{Precision+recall}$
5	Overall accuracy (OA)	$\frac{TP+TN}{TP+TN+FN+FP}$
6	Expected accuracy (EA)	$\frac{(TP+FP)*(TP+FN)*(FN+TN)*(FP+T}{(TP+TN+FN+FP)^2}$
7	Kappa	$\frac{OA-EA}{1-EA}$

Note: *TP is the number of truly classified (true positive), TN is the number of negatives classified as true negative, FP is the number of positives classified as false positive, FN is the number of negative classifieds as false negative, N is the total number of points, and EA is the expected accuracy.*

4.3. RESULTS AND DISCUSSION

4.3.1. Delineation of Groundwater Potential Zone

The current study's goals were to identify the study area's groundwater potential zones using GIS-based Multi-Criteria Decision Analysis (MCDA) techniques like AHP and MLAs. To make overlay analysis in ArcGIS all the thematic maps were converted into raster format (TIFF format). Additionally, the same coordinated projection (UTM, zone 37) should be given to each thematic map. For mapping the final output map of groundwater potential zones eleven thematic layers are used for each study region. The weights were given according to the influence of each criterion on groundwater potential. The overlay analysis of these thematic maps was performed in the ArcGIS weighted overlay tool. The groundwater potential indices raster map was created for each pixel in

the research region. Groundwater potential index in dimensionless quantity is used to show the possible groundwater zones of an area. The natural break (Jenks) approach was then used to reclassify and organize which is applied by many scholars as a standard approach. The higher index corresponds to high potential and the lower index corresponds to the lower potential area. The result of GIS overlay analysis for each area is shown in the figure (Figure 4.14).

Table 4. 4 The groundwater potential class in each study region

Value of GWPZ (codes)	**Study area**	**Fafen-Jerer**		**Gambela**		**Shinile**		**Geological units**
	GWPZ class	Area (sq. km)	%	Area (sq. km)	%	Area (sq.km)	%	
1	Very low	1810.34	10.3	118.01	0.65	143.11	0.72	Urandab Formation (Ju), Enticho Sandstone (Pzt), Alghe Group (ARI)
2	Low	12585.04	71.63	3954.7	21.7	3323.05	16.66	Urandab Formation (Ju),Jessoma Formation(Pj)
3	Moderate	2414.68	13.74	4033.13	22.13	3554.91	17.82	Alluvial and lacustrine deposits(Q), Hamanlei Formation (Jh), Adigrat Formation (Ja)
4	High	657.91	3.74	9813.84	53.86	4440.07	22.26	Alluvial and lacustrine deposits(Q), Hamanlei Formation (Jh)
5	Very high	101.26	0.58	301.93	1.66	8486.68	42.54	Alluvial and lacustrine deposits(Q)
	Total	17569.24	100	18221.61	100	19947.82	100	

The GWPZ map of the Fafen-Jerer sub-basin shows that 10.30% (1810.34 sq. km) is very low, 71.63% (12585.04 Sq.km) low, 13.75% (2414.68sq.km) moderate, 3.74% (657.91 sq. km) high and only 0.58% (101.26 sq. km) (Table 4.4) was found in the very high zone. The very high to moderate potential areas were concentrated on the upper catchment which has alluvial geology, lower depth groundwater, cultivation as main land use, clay and loam soil texture are dominant, and a high annual precipitation zone. The majority of the lower catchments of the Fafen-Jerer sub-basin have

a low and very low potential for groundwater. This area is characterized by low drainage density, lower mean annual precipitation, deep water table, and very sparse vegetation.

The GWPZ map of Gambela plain shows that 0.65% (181.01 sq. km) is very low, 21.70% (3954.7 sq. km) is low, 22.13% (4033.13 sq. km) is moderate, 53.86% (9813.84 sq. km) high and only 1.66% (301.93 sq. km) is found in the very high zone (Table 4.4). In Gambela plain, the high potential zone covers the majority of the northern parts of the region. The findings indicate that a small area near Gambela along the Baro River has a very high potential. This area is an area of accessible groundwater at a lower depth. The southern portion, which was dominated by an area of shrubland and had deep groundwater, was home to moderate and low potential zones. The characteristics that had the greatest influence on GWPZ mapping for the model were geomorphology and rainfall.

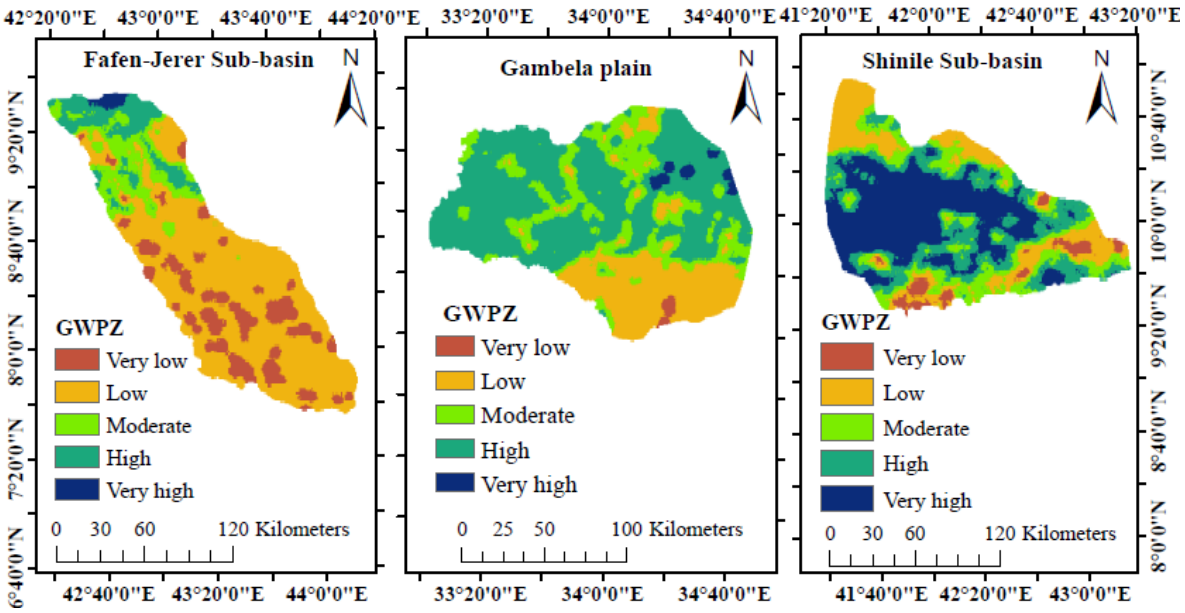

Figure 4. 14 Groundwater potential zone maps

The GWPZ map of the Shinile sub-basin show that 0.72% (143.11 sq. km) very low, 16.66% (3323.05 sq. km) low, 17.82% (3554.91 sq. km) moderate, 22.26% (4440.07 sq. km) high and about 42.54% (8486.68 sq. km) was found in the very high zone (Table 4.4). The results show that the majority of the central part of the Shinile sub-basin has a very high groundwater potential area. The very high potential zone is an area of alluvial geology, plain landform, and dominated by sandy loam soil texture. The low potential zones are distributed in the bordering area of the sub-basin and

the low vegetation area of the lower catchments. The very low potential zone was concentrated on the hilly and undulating surface of the upper catchment. Geology is the main parameter that influences the groundwater potential of the Shinile sub-basin.

4.3.2. Comparison of results with previous study

The results are comparable and similar to those of the previous study results of the British geological survey (Smedley, 2001) (Figure 4.15). The best aquifers with the most readily available groundwater resources are located in the study regions. The more permeable regions of alluvial sediment are the primary locations where groundwater is used for irrigation. Clusters of wells are occasionally used to increase access to water in places that use traditional dug wells and have limited water supplies, such as the low-lying plains of eastern Ethiopia.

Well-drilling investigation of groundwater provision is frequently unsuccessful due to low groundwater yields, unfavorable drilling conditions, or low water quality in eastern Ethiopia. Reports show that a combination of these factors has led to the abandonment numbers of drilled wells in eastern Ethiopia (UN, 1989).

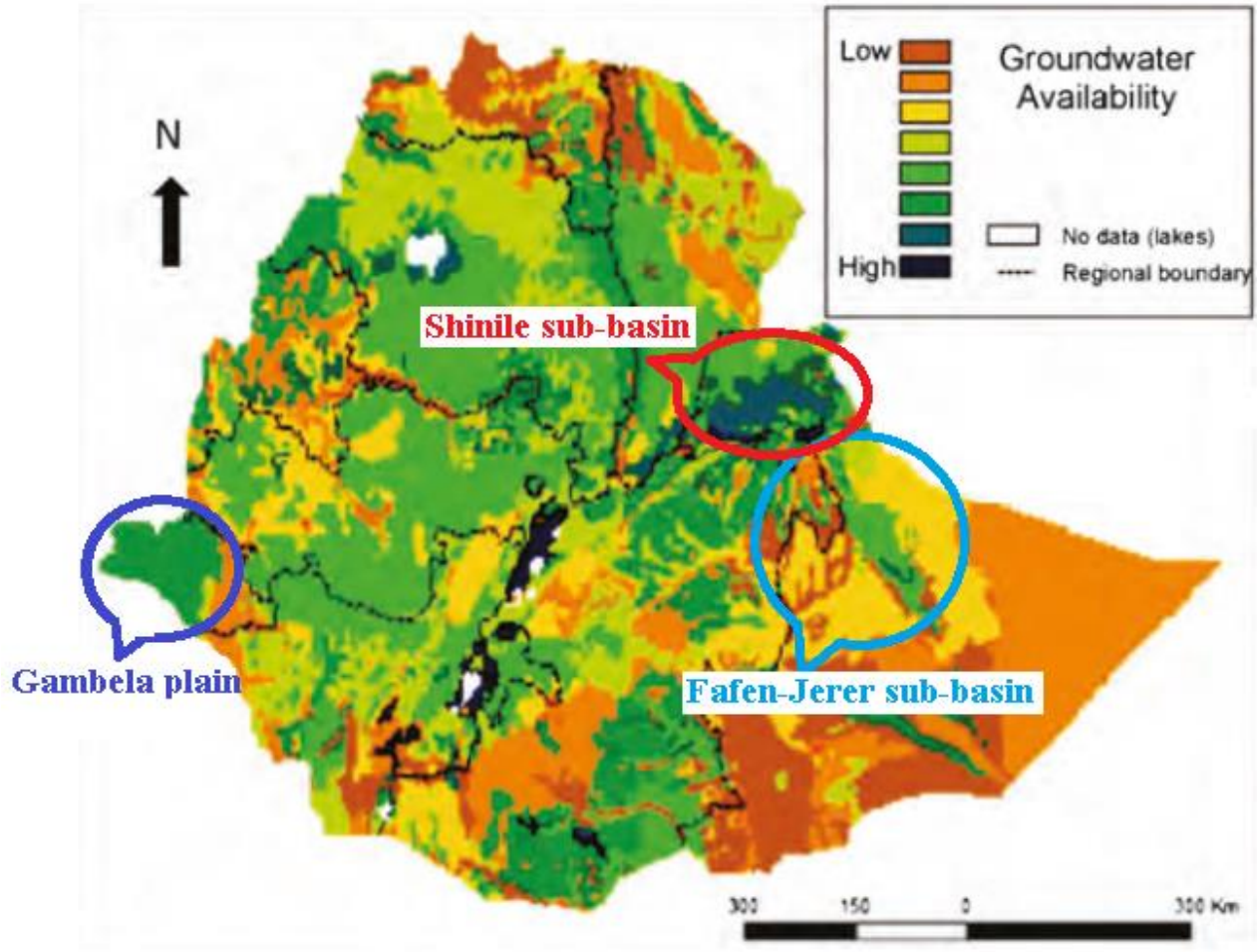

Figure 4. 15 Water availability map of Ethiopia (Smedley, 2001)

The eastern part of the Fafen-Jerer sub-basin (Jerer catchment) roughly estimated storage capacity of 2.7 to 30 billion m^3 (cubic meters/volumes) (Amer, et al.,2013). This area covers up to 35 km wide and 200 km long in the north-south direction, and it is located along the Jerer valley at a depth of 50 to 700 m below the surface.

The Gambela plain has quaternary alluvio lacustrine aquifers, primarily in the western sector. The range of well yield is 0.01 to 0.5 l/s. A previous estimate put the total groundwater recharge in the Gambela plain at 128.4 $*10^6$ m^3/year. An estimated 200 km^3 of groundwater is stored in the basin overall (Kebede, 2013).

It is estimated that the Shinile area has up to 150 billion m3 of groundwater stored overall, assuming a saturated thickness of 100 m and a 15% porosity (Kebede, 2013).

4.3.3. Results of Machine Learning Technique

A machine learning approach was used to map the groundwater potential of the Gambela plain. The figure (Figure 4.16) displays the groundwater potentiality's model-wise spatial variance. The results show, that there are differences in the spatial area coverage between the models' categories. In the majority of models, high and very high potential zones cover the largest areas whereas low classes only cover the tiniest sections. A region with very low potential is located on the research area's southern edge. The GWPZ map results in RFC show very high and very low-class coverage in larger areas of 44.9% and 20.6% respectively. The two extreme points cover a large area of the map (65.4%) for RFC. The GWPZ classification with GBC results 16.1%, 12.7%, 12.3%, 20.8%, and 38% area coverage for very low, low, moderate, high, and very high respectively (Figures 4.16). Large area coverage in the GBC model in a high and very high class of GWPZ (58.8%). In the DTC, high and very high potential classes make up the majority of the coverage (66.23%). The GWPZ class with K-Neighbors classifier (KNC) results in 16.2%, 7.9%,15.1%, 21.2%, and 39.6% area coverage for very low, low, moderate, high, and very high respectively (Figures 4.16).

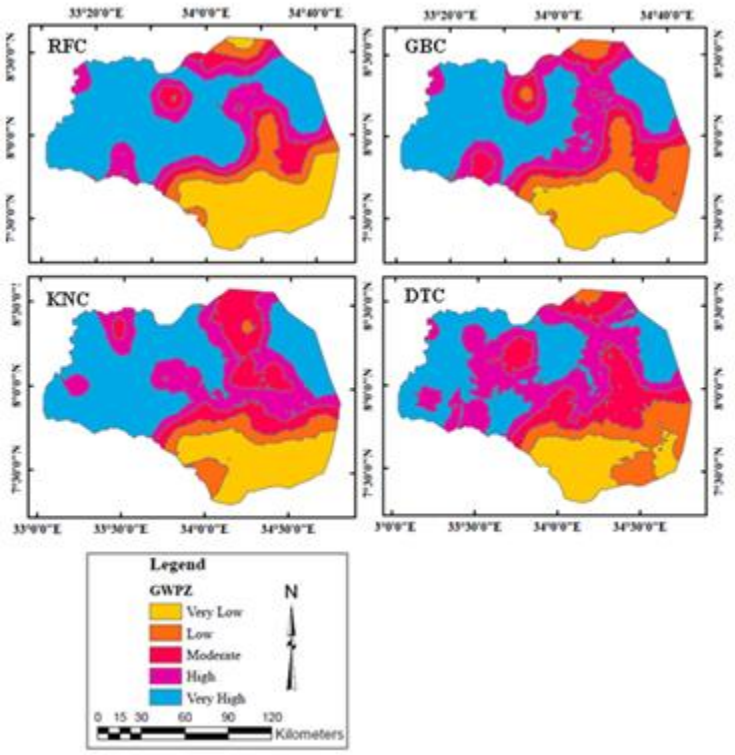

Figure 4. 16 Groundwater potential zone maps results of the machine learning models

4.3.4. Validation results

To validate the research water point (well/ borehole) data were collected and the distribution of the study areas to compared with the produced groundwater potential map. The map of water level in the study regions was correlated to the groundwater potential zone output map.

The validation was performed using the receiver operating curve (ROC). By mapping the effects of varied choice criteria, the ROC curve accounts for all possible combinations of correct and incorrect judgments. ROC is a well-known method of justification of groundwater potential zone mapping (Andualem & Demeke, 2019; Naghibi et al., 2017; Sameen et al., 2019). ROC is a graph of the connection between the true-positive rate (sensitivity) and the false-positive rate (1-specificity). According to ROC curve analysis, the area under the curve (AUC) demonstrates the accuracy of prediction. AUC values vary from 0 to 1, and values close to 1 indicate better model accuracy. The value of area under the ROC curve (AUC) is expressed as poor (0.5–0.6); average (0.6–0.7); good (0.7–0.8); very good (0.8–0.9); and excellent (0.9–1). According to the validation results, the AHP model's area under the ROC curve performs well (87.0%) for Fafen Jerer, better (78.2) for Gambela plain, and a very good (94.1%) in the Shinile sub-basin (Figure 4.17).

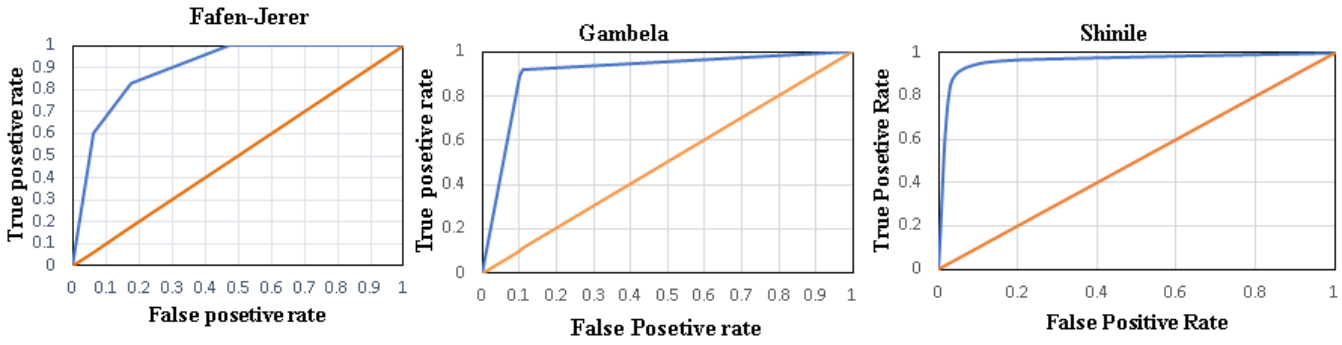

Figure 4. 17 ROC curve for AHP technique analysis

The analysis of the MLAs models shows that the area under the curve of RFC, GBT, KNC, and DTC respectively results in 93.4%, 92.5, 87.7%, and 72.4%. From the ROC curve results of each model, it is clear that RFC and GBC are the best models for GWPZ estimation. The models' performance has been assessed by employing five metrics: accuracy, precision, kappa, recall, and f1 score. The hyperparameters are fitted using the Randomized Search CV technique (Bergstra et al., 2012). It is crucial to specify the search space and provide a starting point. The estimator uses

a random state of 42 and performs three convolutions for every 100 candidates, resulting in 300 fits. Table 4.5 shows the search space used in the base and best scenarios.

Table 4. 5 Hyperparameter used for the baseline, best algorithms and search space

Hyperparamters	Search space	RFC		GBC		DTC		kNN	
		Baseline	Best parameters	Baseline	Best parameters	Baseline	Best parameters	Baseline	Best parameters
n_estimators	[200, 2000, num = 10]	['100']	['600']	['100']	['200']	_	_	_	_
max_features	['auto', 'sqrt','log2']	['auto']	['auto']	['auto']	['sqrt']	'None'	['auto']	_	_
max_depth	[10, 110, num = 11]	['None']	['60']	['None']	['50']	['10']	['80']	_	_
min_samples_split	[2, 5, 10]	['2']	['2']	['2']	['10']	['2']	['2']	_	_
min_samples_leaf	[1, 2, 4]	['1']	['2']	['1']	['2']	['1']	['2']	_	_
bootstrap	[True, False]	['True']	['False']	None	None	_	_	_	_
Metric	['euclidean','manhattan','minkowski']	_	_	_	_	_	_	['minkowski']	["manhattan']
N_Neighors	[3,5.11,19]	_	_	_	_	_	_	['5']	['19']
Weights	['uniform','distance']	_	_	_	_	_	_	['uniform']	['distance']
critrion	['gini'.'entropy']	_	_	_	_	['gini']	'entropy']		

The hyperparameters used in the two scenarios (baseline and random search) were applied as follows are given in the table (Table 4.6). The RFC model fared better than the other models in this experiment in terms of accuracy (96.42%), precision (89%), recall (89%), F1 score (88%), and kappa (0.76).

Table 4. 6 Performance analysis for algorithms

Model		Accuracy	precision	Recall	f1-score	Kappa	Improvement
GBC	Base Line	94.14%	80%	81%	81%	0.61	2.09%
	Random search CV	96.11%	88%	88%	87%	0.74	
RFC	Base Line	95.30%	85%	84%	84%	0.68	1.18%
	Random search CV	96.42%	89%	89%	88%	0.76	
DTC	Base Line	93.02%	78%	77%	77%	0.54	1.66%
	Random search CV	94.57%	82%	82%	82%	0.63	
K-NC	Base Line	92.09%	74%	74%	74%	0.46	1.01%
	Random search CV	93.02%	77%	77%	77%	0.52	

Following RFC, the GBC model measured measures including Accuracy (96.11%), Precision (88%), Recall (87%), F1 Score (88%), and Kappa (0.74). Since all of the top-performing models

have kappa values between 0.61 and 0.80, the interpretation demonstrates substantial performance (Czodrowski, 2014). The study makes use of weighted and macro averages. However, the weighted average produced respectable outcomes. Accordingly, the models exhibited a significant improvement once the Random search CV hyperparameters were optimized. GBC has the greatest improvement, followed by DTC, which displays improvements of 2.09% and 1.66%, respectively.

4.3.5. Feature importance for MALs

The features class characteristics are listed on the left side of the figure (Figure 4.18) in order of their relevance to model prediction. The horizontal axis displays the average absolute SHAP value of each feature. Geomorphology and rainfall are the most important, followed by drainage density and NDVI, while TRI and geology are the least important for GWPZ prediction. The right side of Figure 4.17 illustrates not only the significance of the characteristic but also whether it has a positive or negative influence on prediction. According to the test results, high precipitation, drainage density, NDVI, and TRI levels improve GBC forecast quality. The expected RFC quality is improved by high rainfall, NDVI, and geology factors. DTC prediction quality is enhanced due to high rainfall, geology, and lineament density. The presentation demonstrates that the average values of geomorphology produce a good forecast for all three models.

Feature importance results are different for different groundwater models (Arabameri, et al., 2019; Gómez-Escalonilla et al., 2021). Different studies report the feature importance parameters differently. Some researchers identify geology as an important parameter to influences groundwater potential (Singh et al., 2010; Chen et al. 2020). The report from Guru and others (2017) shows geology seemed less important for groundwater influence.

In this particular study, the geomorphology and rainfall were the main or very important parameters that influenced the groundwater potential mapping for the machine learning models. These findings coincided with findings from other writers in various geographic settings (Gómez-Escalonilla et al., 2021). In the AHP model case, the geology was the other main important parameter in addition to geomorphology and rainfall.

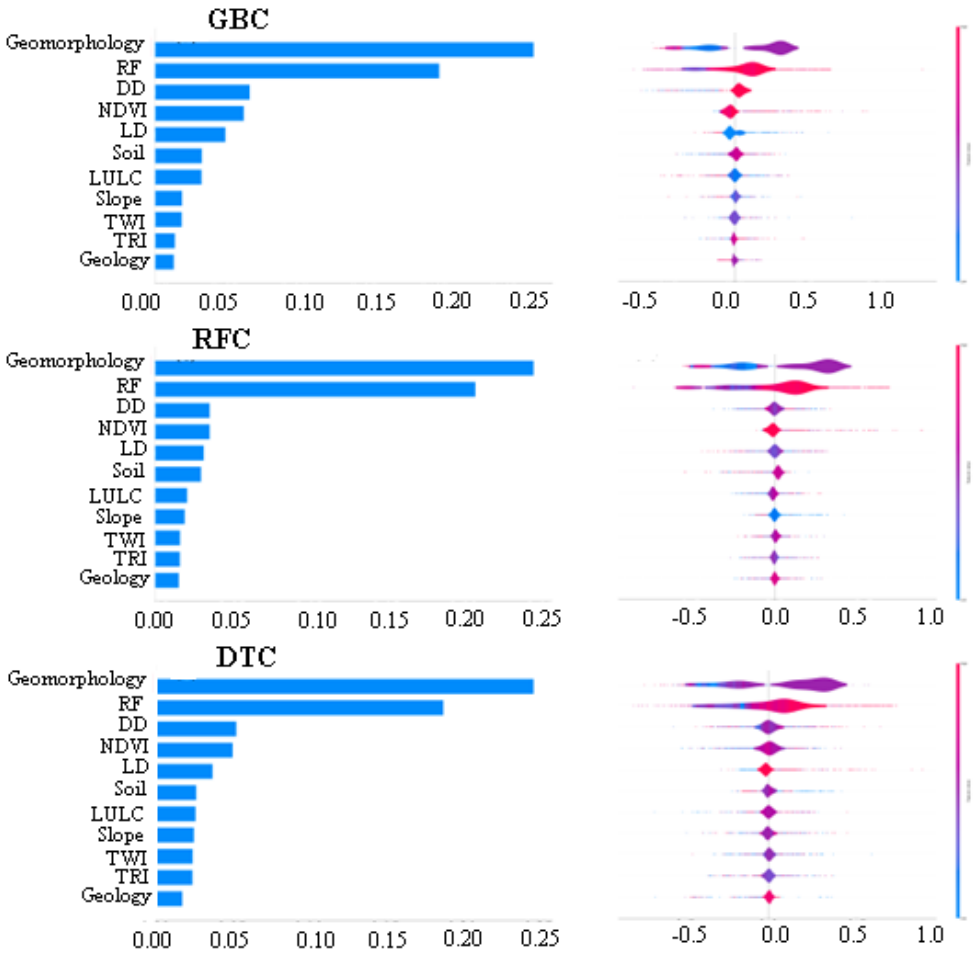

Figure 4. 18 The Summary bar (on the left) and global interpretability plot (on the right)

4.4. CONCLUSION

The current study used GIS-based Multi-Criteria Decision Analysis (MCDA) techniques, such as AHP and MLA approaches, to delineate groundwater potential zones in the study area. These areas are geologically covered by alluvial-lacustrine sediments of shallow-depth aquifers. The regions are different in geographical, hydrological, topographical, ecological, and agricultural parameters. The study region is generally classified as semi-arid climate having a mean annual rainfall range of 290 mm/year to 1113 mm/year. The research regions were distinguished, sparse meteorological stations, a low number of lineaments, lowland nature, and geological material of alluvial-lacustrine deposits. Eleven thematic maps were generated that influence the local groundwater. Groundwater potential zone was categorized into five classes from very low to very high potential zones. According to the GWPZ results, the majority of the Fafen-Jerer sub-basin has a low and very low potential zone. Both the Gambela (10115.7 sq. km) and the Shinile sub-basin (12926.7 sq. km) have

relatively large coverage for high and very high potential zones. The characteristics that had the greatest influence on GWPZ mapping for all of the models were geology, geomorphology, and rainfall. The validation results show that the area under the ROC curve for the AHP model shows good (87.0%) for Fafen Jerer, better (78.2) for Gambela plain, and a very good performance (94.1%) in the Shinile sub-basin. This study demonstrated the zoning for groundwater potential by considering a variety of influencing elements, which can increase the accuracy of the investigation. The results of machine learning algorithms reveal that RFC and GBC outperform GWPZ prediction. The results of the study show that GIS and remote sensing method of groundwater potential zone delineation works for semi-arid regions in Ethiopia. The method is a very cost-effective and efficient method for groundwater exploration in data-scarce regions. To effectively and economically evaluate groundwater conditions, remote sensing has produced valuable data on groundwater conditioning variables to supplement traditional intrusive field data. The strategies utilized also show how machine learning algorithms may be beneficial due to their great efficiency, particularly in groundwater management. Given the restricted availability of data, it would be beneficial to compare other models in addition to testing them to see which is better for prospective prediction.

CHAPTER 5

STABLE ISOTOPE AND GEOCHEMICAL ANALYSIS

Abstract

The use of tracers, particularly isotope geochemistry tracers, is the most efficient method for understanding and providing fresh perspectives on hydrologic processes. The purpose of this study is to determine the stable isotope and geochemical characteristics of groundwater alluvial aquifers in eastern Ethiopia. Samples of water from rainfall, surface water, and groundwater sources were gathered and analyzed. The research discovered that EC, pH, and TDS fluctuated from 871 to 6090 µS/cm, 6 to 8.2, and 558 to 3898 mg/L, correspondingly. In both regions major cation and anion concentrations fall in the order of $Ca^{2+} > Na^{+} > Mg^{2+} > K^{+}$ and $SO_4^{2-} > HCO_3^{-} > Cl^{-} > NO_3^{-}$ respectively. The most common water types are mixed Na-Mg-Ca, Ca-Cl, Na-Cl, and Ca- HCO3-. Hydrogeochemical experiments revealed that carbonate and silicate weathering and ionic exchanges primarily govern the supply of important ions in the waters and the geochemical history. The stable isotopic compositions vary from −2.772 to −0.418 ‰ with a mean value of −1.772 ‰, for oxygen and from −10.37 to 1.01 ‰ with a mean value of −4.306 ‰ for hydrogen. The results show precipitation has been found to have more enriched isotope compositions than groundwater. In other words, both the hydrogen and oxygen isotope of groundwater are depleted than the precipitation isotope composition. The findings contribute to our knowledge of the stable isotope and geochemistry and are useful in determining the primary compositions of groundwater, water type, and the hydrogeochemistry of semi-arid areas.

Keywords: Stable isotope; Geochemistry; Gibbs plot; Piper diagram, Groundwater; Alluvial aquifers

5.1. INTRODUCTION

The water cycle, which includes precipitation, surface, and groundwater, should be fully considered for integrated water resources management (Cosgrove & Loucks, 2015; Qadir et al., 2003). Globally, groundwater has emerged as the primary source of water supply (Element & Crisis, n.d.; Harter, 2003; Hossein et al., 2019; Kebede, 2013). Groundwater is the primary source of water supply in dry and semi-arid climates (Kassie et al., 2009; Priyan, 2021; Sreedevi et al., 2019). Studies showed that groundwater resources in a number of arid and semi-arid regions around the

world have declined dramatically in quality and quantity since the mid-twentieth century as a result of industrial and agricultural development, expanding urbanization, population growth, inadequate sanitation, pollutant risk, lack of adequate water quality monitoring, seasonal precipitation patterns, and anthropogenic constraints (Adimalla et al., 2019; Bagher et al., 2010; Sreedevi et al., 2019). The other main problems are the quality assurance of groundwater in semi-arid climatic zones due to groundwater being the primary supply and the widespread occurrence of inorganic pollutants and their health effects (Adimalla & Wu, 2019). In line with this, the alluvial aquifers are easily discovered and so utilized in such regions as a supply of drinking water (Dippong et al., 2022).

According to a study by Kebede (2013), quaternary aquifers cover nearly 25% of Ethiopia's landmass. Quaternary sediments make up the majority of the geologic material in the study area (Kebede, 2013). Alluvial aquifers are generally unconfined aquifers, and it is a composition of gravel, sand, silt, and clay, deposited by a river in a river channel, banks, or flood plain (Kassune et al., 2018). Alluvial aquifers, which are made of sediments deposited by rivers, have a high-water storage capacity and permeability, making them potentially very productive aquifers. These aquifers are valuable resources for a variety of water supply and irrigation uses because they are single-layer groundwater bodies with effective water storage and transmission capabilities (Di Lorenzo & Galassi, 2013; Owen & Dahlin, 2005). The overall groundwater trends in alluvial aquifers can be influenced by a variety of factors, including the climate, agricultural practices, land use, and land cover.

When compared to deep groundwater, groundwater in alluvial aquifer zones is relatively shallow, making it sensitive to pollutant incursion and rapidly impacted by natural water-rock interactions and anthropogenic activity. Groundwater pollution may be triggered by both natural and anthropogenic causes. In natural conditions, the aquifer minerals have the greatest effect on groundwater quality. When groundwater flows, geochemical processes such as weathering, dissolution, precipitation, ion exchange, and oxidation-reduction regulate the interaction between groundwater and aquifer minerals considerably (Bhatt et al., 2022). Alluvial aquifers are highly vulnerable to natural pollution caused by weathering, biologic, ion exchange processes, precipitation, and anthropogenic pollution caused by a wide range of industrial, mining, agricultural, and household activities (Dippong et al., 2022).

Several techniques, methods, and approaches have been undertaken by scholars to alleviate such problems. Groundwater chemistry characterization is critical for both surface and groundwater management. The hydrochemical research also discloses the water's quality, i.e., if it is good for drinking, agriculture, or industry. Groundwater chemistry based on hydrochemical data is valuable for giving early information on water kinds, categorizing water for various applications, identifying distinct groundwater aquifers, and studying various chemical processes (Iwmi et al., 2013). Water's stable isotopes provide us with an idea of the general distribution and flow patterns of water inside aquifers (J. Liu et al., 2014; Penna et al., 2018). The correlation between stable isotopes of hydrogen and oxygen in natural water was studied by Craig (1961). He developed an equation illustrating the relationship between the isotope composition of the oxygen and hydrogen in water ($\delta^2H = 8\ \delta^{18}O + 10$). The equation is referred to as the Global Meteoric Water Line (GMWL) which is used to trace natural waters.

The isotope composition of precipitation in Ethiopia was the focus of an outstanding study by Bedaso and Wu (Bedaso & Wu, 2021). They investigated how precipitation's isotopic composition varied across time and space. They chose four stations for precipitation sampling (Gondar, Debre Markos, Jimma, and Jigjiga) to represent the country's various physiographic and climatic regions. Another noticeable work was done by Kebede and Travi (Kebede & Travi, 2012) on the origin of the $\delta^{18}O$ and δ^2H in Ethiopia. They examined water samples gathered from various locations in Ethiopia, including underground water, reservoirs, streams, and rain, to establish a stable isotope of the water. Nevertheless, the extent of this investigation was extensive and thus does not reflect the specific characteristics of the studied region. The stable isotopes of precipitation and groundwater are not well characterized in the alluvial plains of eastern Ethiopia. Few studies have however focused on the hydrology of groundwater in semi-arid areas of eastern Ethiopia. There are several geochemical studies in Ethiopia (Ayenew, 2005; Gebeyehu et al., 2022; Hailu & Haftu, 2023) that show groundwater quality is the main challenge for water supply. There are no papers that describe the geochemical natures of Ethiopia's southeastern semi-arid areas.

The main objectives of this study were to use geochemical methods and stable isotopes (^{18}O and ^2H) to understand the properties of groundwater. The purpose of stable isotope analysis in this research is to understand groundwater flow dynamics around the alluvial aquifer and, subsequently, its potential recharge locations. It also aims to get the isotopic characterization of rainfall and

groundwater. It is feasible to determine potential locations for groundwater recharge by comparing the signatures. It is necessary to identify a local meteoric line since isotopic meteoric lines differ by location. Additionally, the study plans to assess surface water–groundwater interaction in the alluvial aquifer region and to determine the role of precipitation on aquifer recharging. The originality of the article lies in its ability to: 1) use the distribution of important physicochemical characteristics and geochemical processes to determine and evaluate the chemical composition 2) to ascertain the composition of stable isotopes by utilizing stable isotopes of hydrogen and oxygen 3) comparing hydro-chemical and isotopic studies of alluvial zones. The study's findings may assist in the selection of contaminated areas to apply appropriate mitigation strategies to restrict exposure. Understanding the chemical as well as isotope composition of groundwater is very essential and applicable technique in groundwater management. Therefore, to obtain basic information on the quality of groundwater in alluvial aquifers as well as its fundamental composition, this chapter is focused on these key issues.

5.2. MATERIALS AND METHODS

5.2.1. Sample collection and preparation

Several submersible pump-equipped sealed wells, ranging in depth from 40 to 400 meters, are utilized for residential purposes. From these operational water supply wells, water samples were obtained. For each sample, measurements were made on-site of the pH, electrical conductivity (EC), and water temperature. Groundwater samples were collected both in the Shinile area (around Dire Dawa) and the Fafen-Jerer sub-basin (Jerer catchment). The samples were collected in June 2022 using 60 mL sample collecting vials for analysis of stable isotopes. Those samples are collected and stored in a 60 mL bottle with a leak-proof seal that can tolerate frequent dynamic shaking. Samples for determination of stable isotopes were stored in 60 mL high-density polyethylene vials, the necks and caps of which were sealed with a paraffin film. After being packed into an insulated box, each sample was brought to the lab to be processed. The groundwater samples were collected from wells of variable depths (40–400 m) along the flow path of the surface flow system. From different locations, the water samples were collected with ranges of altitudes 1000–2500 meters. For this investigation, 65 groundwater samples were used. The precipitation samples were collected in two stations (Dire Dawa and Jigjiga) having different altitudes and temperatures. Only three surface water samples were taken for analysis due to the seasonal variation with no available surface water

at the time of sample collection. For the majority of samples, the field parameters that were measured were pH, temperature (T), and electrical conductivity. In addition to the lab reports different formats of geological data (text, jpg, raw data, maps) are also collected for hydrogeological studies of the regions.

5.2.2. Hydro-chemical measurement and lab analysis

The temperature, pH, and electrical conductivity (EC) are measured for each sample. OAKTON PCD 650 portable multiparameter instrument is used to measure the hydro-chemical parameters. Water samples were prepared for oxygen and hydrogen isotope ratio analyses reported in δ-notation relative to Vienna standard mean ocean water (VSMOW). The stable isotope contents ($\delta^{18}O$ and $\delta^{2}H$) were performed by McDonnell Hillslope Hydrology Lab on a Los Gatos Research liquid water Off-Axis Integrated-Cavity Output Spectroscopy (Off-Axis ICOS) unit and post-processed using LIMS for Lasers with an analytical error of ^{2}H, and ^{18}O analyses are 2 ‰, and 0.8 ‰, respectively. The analysis was performed at Saskatchewan University, Hillslope Hydrology Lab, Canada. For Dire Dawa city and the Shinile region, the Dire Dawa meteorological station's air temperature and precipitation data were used, whilst the Jigjiga and Deghabur stations' data were used for the Jerer catchment.

Water chemistry and quality are regulated by geochemical processes including ion exchange, silicate/carbonate weathering, and water-rock interaction. To understand the groundwater chemistry of the study area all parameters were analyzed. Most of the possible chemical anions and cations were analyzed and evaluated for this study.

5.2.3. The approach of the study

Stable isotopes of water were used in two distinct flow systems of alluvial aquifer areas of eastern Ethiopia to examine probable sources of groundwater and its flow paths. Relative to Vienna Standard Mean Ocean Water (V-SMOW), the stable isotopes of water are expressed using delta (δ) notation in unit part per thousand, (per mil, ‰). VSMOW is an internationally accepted standard for reporting the hydrogen and oxygen isotopic ratios of water. The stable isotope of water is expressed as the “difference” or delta (δ) notation of the rare to common isotope ratio as:

$$\delta(‰) = \left(\frac{R_{sample} - R\_standard}{R_{standard}}\right) \ldots\ldots\ldots\ldots\ldots\ldots\ldots\ldots\ldots\ldots\ldots\ldots\ldots\ldots\ldots\ldots\ldots\ldots 5.1$$

Where; R is the molar ratio of the heavy (rare) to the light (common) isotope of the sample and standard: R= $^{2}H/^{1}H$ or $^{18}O/^{16}O$. The isotope analysis of precipitation and non-evaporating water shows the relationship between $\delta^{2}H$ and $\delta^{18}O$ is called the global meteoric water line (GMWL). The global meteoric water line is typically defined by the following equation (Rozanski et al., 1993).

$$\delta^{2}H = 8\,\delta^{18}O + Y\ ‰ \quad \ldots\ldots\ldots\ldots\ldots\ldots\ldots\ldots\ldots\ldots 5.2$$

Where:

$\delta^{2}H$ is the concentration of hydrogen-2 relative to hydrogen in units per mill (%),

$\delta^{18}O$ is the concentration of oxygen-18 relative to oxygen in units per mill (%), and

y is the deuterium excess.

The number (8) is the slope determined by the physical properties of the isotopes. The value of Y is called deuterium excess. The term d-excess refers to the excess deuterium relative to heavy oxygen ($\delta^{18}O$) in the vapor that results from the diffusion of water molecules made up of various hydrogen and oxygen isotopes over a density gradient during evaporation processes. The relative proportions of $\delta^{18}O$ and $\delta^{2}H$ contained in water, which shows the intersection between the Y-axis and GMWL is known as Deuterium excess (d-excess). The amount of deuterium excess in meteoric water indicates the degree of evaporation for the water vapor source areas; the greater the degree of evaporation, the greater the y value; the stronger the re-evaporative fractionation under the cloud after a raindrop condenses (Cozma et al., 2017). According to Craig (1961), deuterium excess is calculated as:

$$d - excess = \delta^{2}H - 8 * \delta^{18}O \quad \ldots\ldots\ldots\ldots\ldots\ldots\ldots\ldots\ldots\ldots 5.3$$

The local value of d-excess ranges from 0 to +25. So, the local meteoric water line was developed for local conditions. In Ethiopia, the national meteoric water line is (Bedaso & Wu, 2021)

$$\delta^{2}H = 7.61\delta^{18}O + 13.32 \quad \ldots\ldots\ldots\ldots\ldots\ldots\ldots\ldots\ldots\ldots 5.4$$

5.2.4. Geochemical analysis

To understand the groundwater characteristics of the study area: geochemical analysis like piper plot, Gibbs plot, and combinations of scatter plots were done. The geochemical analysis and equations used for the groundwater samples are presented in the table below (Table 5.1). Sodium Percentage (%Na), sodium adsorption ratio (SAR), Residual sodium carbonate (RSC), electrical

conductivity (EC), and permeability index (PI), are the hydrochemical characteristics of groundwater used to assess irrigation appropriateness (Nazzal et al., 2014).

Table 5. 1 Parameters used in the geochemical analysis of groundwater

Parameters used	Equation	Remark
The sodium adsorption ratio (SAR)	$= \frac{Na}{\sqrt{\frac{(Ca+Mg)}{2}}} \ldots\ldots (5.5)$	meq/L
Sodium Percentage (Na%)	$= \frac{N_a^+}{N_a^+ + K^+ + C_a^{2+} + M_g^{2+}} * 100 \ldots (5.6)$	meq/L
Residual sodium carbonate (RSC)	$= CO_3^- + HCO_3^-) - \left(C_a^{2+} + M_g^{2+}\right) \ldots (5.7)$	meq/L
Total hardiness (TH)	$= 2.5 * C_a^{2+} + 4.1 * M_g^{2+} \ldots . (5.8)$	mg/L
Permeability Index (PI)	$= \frac{N_a^+ + \sqrt{HCO_3^-}}{N_a^+ + C_a^{2+} + M_g^{2+}} * 100 \ldots . (5.9)$	meq/L
Potential salinity (PS)	$= Cl^- + \frac{SO_4^{2-}}{2} \ldots . . (5.10)$	meq/L
Gibbs Ratio of cation (GRC)	$= \frac{N_a^+}{N_a^+ + C_a^{2+}} \ldots . . (5.11)$	meq/L
Gibbs Ratio of anion (GRA)	$= \frac{Cl^-}{Cl^- + HCO_3^-} \ldots . . (5.12)$	meq/L
Base-exchange index (r_1)	$= \frac{N_a^+ - Cl^-}{SO_4^{2-}} \left(\frac{meq}{L}\right) \ldots\ldots (5.13)$	meq/L
Meteoric genesis index (r_2)	$= \frac{(K^+ + N_a^+) - Cl^-}{SO_4^{2-}} \ldots (5.14)$	meq/L
Chloro-alkaline indice (CAI 1)	$= \frac{Cl - (N_a + K)}{Cl} \ldots . . (5.15)$	meq/L
Chloro-alkaline indice (CAI 2)	$= \frac{Cl^- - (K^+ + N_a^+)}{SO_4^{2-} + HCO_3^- + NO_3^-} \ldots . . (5.16)$	meq/L
Total Hardness	$= 2.5(Ca^{2+}) + 4.1\ (Mg^{2+}) \ldots . . (5.17)$	

Piper diagram

To facilitate comprehension of the origins of the dissolved component salts in water, Piper (1944) devised a pictorial approach known as a Piper diagram for presenting facts related to water chemistry. The idea behind this process is that the concentrations of cations and anions in water ensure the electroneutrality of the dissolved salts. The Piper diagram consists of a diamond and two triangles, in which the diamonds are divided into six regions. The diamond depicts the water sample's overall hydro-chemical properties, while the triangle depicts the relative amount of each ion (Singh et al., 2013).

Gibbs Diagram

The link between the lithological properties of an aquifer and the composition of its water is commonly established using the Gibbs diagram. The Gibbs plot was used to depict the mechanism influencing groundwater geochemistry in terms of atmospheric precipitation, rock-water interaction, and evaporation (Gibbs, 1970). Plotting TDS versus $Na^{+}/(Na^{+}+ Ca^{2+})$ and $Cl^{-}/(Cl^{-} + HCO_3^{-})$ yields the Gibbs diagram. The Gibbs diagram displays three different fields, such as the dominance regions of precipitation, evaporation, and rock-water interaction.

5.3. RESULTS AND DISCUSSION

5.3.1. Groundwater physicochemical characteristics

The electrical conductivity value in the research region (eastern catchment) ranged from 871.8 to 17223µs/cm. Electrical conductivity (EC) varies depending on the height and type of the subsurface deposit. Because dissolved salts supply electrical charges that interact as ions in motion, their presence in water impacts the value of its EC (Peinado-Guevara et al., 2012) (Table 5.2). The results of EC for boreholes in the eastern regions suggest that it does not follow a specific pattern but rather depends wholly on well depth and temperature conditions.

Table 5. 2 Permissible limits of EC for classes of irrigation water

EC (µs/cm)	**Classes of water based on permissibility for irrigation**
<250	Excellent
250-750	Good
750-2250	Permissible
2250-4000	Doubtful
>4000	Unsuitable

Specifically, a higher conductivity value was recorded in wells around Deghabur. This indicates that there are more ions or contaminants in the groundwater around Deghabur (Marandi et al., 2013). The lowest conductivity value recorded was at Shinile Town (811.4µs/cm).

Table 5. 3 Water class based on TDS values

TDS (mg/l)	**Water type/Quality**
0-1,000	Fresh
1,000-10,000	Brackish
10,000-100,000	Saline
>100,000	Brine

This might be because the alluvial soil at Shinile lacks ions that would contribute to the high electrical conductivity. The total dissolved solid (TDS) levels in all samples ranged from 390 to 3898 mg/L. TDS values of greater than 1000mg/L are found in more than 55% of the samples (Table 5.3). According to the TDS classification (Pradhan et al., 2011), 55% of the wells have brackish water and 44% have fresh (TDS <1,000mg/L) water. TDS values less than 1,000 mg/L are seen in the watershed's plateau and escarpment zones of Shinile. TDS levels in the Fafen-Jerer usually rise from northwest to southeast, with higher values to the east of Deghabur town. TDS levels are lower in the northwest, notably in the Fafen valley than in the Jerer valley. EC value in the Gambela plain ranges from 67 to 1078 µs/cm and the average value is 440 µs/cm. The EC value should not be higher than 400 µS/cm, according to WHO guidelines. 48% of the samples are above the standards and large value EC records for samples in the eastern area of the plain which exaggerate the mean value. The EC and TDS results show all the study regions have water quality problems due to dissolved solvents. The groundwater in the eastern catchment is basic, according to the pH readings, with a pH range from 6.00 to 8.2 and an average of 7.25. Only one sample falls outside of the permitted (6.5-8.5) range. The pH of 75% and 60% of samples in the Fafen-Jerer and Shinile sub-basins is more than 7, indicating an alkaline state. When rainwater travels through soil during the groundwater formation process, its contact with the soil adds alkalinity to the groundwater (Bhatt et al., 2022).

5.3.2. Geochemical composition of Groundwater

The geochemical parameters of the study region were summarized (Table 5.5) and different geochemical plots were presented to show the characteristics of groundwater samples. Calcium and

magnesium are the most prevalent components of groundwater. The concentration of dissolved Mg^{2+} in groundwater, however, is lower than that of Ca^{2+}. Calcium cation values range from 55 to 650 mg/L in the study region. According to WHO guidelines, however, the water in the study area exceeds the drinking water edge (75 mg/L). Magnesium values varied from 13 to 250 mg/L in all samples. More than 70% of the samples had Mg^{2+} levels higher than the WHO drinking water standard (50 mg/L). Calcium and magnesium account for approximately all of the hardness in ordinary water. The total hardness (TH) value ranges from 167 mg/L to 746 mg/L and 75 to 900 mg/L as $CaCO_3$ for Fafen and Shinile respectively.

Table 5. 4 Water quality based on Hardness

Hardness, mg/L of CaCO3)	**Water type**
0-60	soft
60-120	moderately soft
120-180	hard
>180	very hard

When calcium carbonate concentrations in waterfall below 60 mg/L, they are often categorized as soft, 60–120 mg/L as moderately hard, 120–180 mg/L as hard, and more than 180 mg/L as extremely hard (Rout et al., 2011) (Table 5.4). No sample was recorded in the soft water range in the research area. Few samples are found in moderately hard and hard classes. The majority of the samples were found in the very hard classification. So, hardness is the characteristic of the groundwater of the study regions. The basic cause of hardness in the study region is the calcium content of groundwater which is more than 82.5% of the samples show Ca^{2+} greater than 100 mg/L.

The bicarbonate concentration in water is present mainly in association with Ca^{2+} and Mg^{2+}. The concentration in the study region varies from 95 to 556 mg/L. All samples of groundwater much higher than the acceptable limit of HCO_3^- (30 mg/L). Water containing carbon dioxide (including additional CO_2 absorbed by soil organisms) dissolves some of the calcium carbonate when it travels through limestone or other calcium carbonate-bearing rocks, becoming richer in bicarbonate (Sidhu et al., 2013). In Shinile around Dire Dawa, Ca-Bicarbonate is found in the transitional on the escarpment, and basic on the rift shoulder. Mg-carbonate transitional around Dre dawa, and Ca-

Sulphate basic within Shinile plain. The Shinile plain often has 800-1000 mg/L of calcium bicarbonate basic.

Sodium (Na^{+}) and potassium (k^{+}) concentrations in all samples vary from 17 to 290 mg/L and 0.5 to 42.50 mg/L, respectively. High concentration was recorded at the Fafen catchment than that of the Shinile sub-basin. A higher Na^{+} ion content in drinking water may induce cardiac issues. Higher levels of Na^{+} ions in irrigation water may also create salt issues (Rout et al., 2011). A high concentration of Na^{+} ions in groundwater often reduces water palatability.

Table 5. 5 Summary statistics of geochemical data

	Min	**Max**	**Mean**	**Stad.dev**
TDS (mg/L)	558	3898	1549.05	851.31
EC (us/cm)	871.8	17223.4	2724.64	2665.74
pH	6	8.2	7.26	0.5
Na (mg/L)	17	290	110.84	66
K (mg/L)	0.5	42.5	5.46	8.78
Ca (mg/L)	55	650	257.76	182.54
Mg (mg/L)	13	250	62.18	50.13
HCO_3^{-} (mg/L)	95	556.32	371.62	108.05
CI (mg/L)	14	424.1	117.6	93.01
F (mg/L)	0.22	2.17	0.83	0.36
SO_4^{2-} (mg/L)	43	2590	660.28	649.61
NO3 (mg/L)	0.16	102	14.12	18.84
SAR (meq/L)	0.26	5.97	1.82	1.22
RSC (meq/L)	-50.35	2.29	-11.91	12.71
TH (mg/L)	215.6	2650	899.34	595.87
PI (meq/L)	10	78	38	18
PS (meq/L)	1.1	29.35	10.2	7.14
GRC (meq/L)	0.06	0.73	0.32	0.19
GRA (meq/L)	0.08	0.78	0.32	0.16
%Na	4.37	58.29	23.89	13.86

Note: *max: maximum, min: minimum, Stad.dev: standard deviation*

Chloride concentration in the study region varies from 14 to 424.1 mg/L. Higher concentration (over the permissible standard, 250 mg/L) is found in samples from the Fafen catchment. High levels of chloride can cause water to taste salty and damage pipes, pumps, and plumbing fixtures.

Groundwater chloride might come from a variety of sources, including household and municipal pollution, weathering, and leaching from sedimentary rocks. The major sources of chloride in the Fafen should include weathering and leaching from beneath the rocks, as well as numerous physicochemical interactions like as ion exchange (Rout et al., 2011; Singh et al., 2013). Sulphate concentration is in the studied samples varied from 43 to 2590 mg/L. Only 47.5% of the sample is lower than the standard WHO (400 mg/L). The whole Fafen Valley and the upper northwestern regions of Jerer valley had concentrations of < 400 mg/L and 400 - 483 mg/L, respectively. The northeastern and lower sections of Jerer valley, as well as the neighboring eastern escarpment regions, have 483 - 2000 mg/L and 2000 - 4000 mg/L levels, respectively. These amounts are higher than the Ethiopian drinking water quality guideline level (ECA, 2013), which might be produced by groundwater contact with shale and gypsum. The amount of Nitrate ions varied from 0.16 mg/L to 102 mg/L throughout the study area, with an average of 13.7 mg/L. The majority of the samples fall below the permitted nitrate concentration limit. There are signs of high nitrate concentration in the upper Fafen and Dire Dawa areas of the study region. Nitrates are the main plant nutrients, but excessive levels can create serious water quality issues. The concentration of nitrate is also a significant consideration in regulations managing groundwater quality for drinking purposes. The WHO recommended a fluoride level of 0.5 to 1.5 mg/L, depending on climate, local environment, and other fluoride sources. Fluoridation has little effect appearance, taste, or smell of drinking water. The results show that the concertation of Fluoride in groundwater samples ranged from 0.22 to 2.17 mg/L. Higher Fluoride concentrations (>1.5 mg/L) are found in the deepest wells of the Fafen-Jerer catchment and Dire Dawa samples. Fluoride levels beyond the permitted limit are harmful to public health because they promote bone and tooth decay.

5.3.3. Indices for groundwater characterization

Sodium adsorption ratio (SAR): The sodium adsorption ratio (SAR) is used to indicate the relative mobility of Na^+ ions in soil media exchange processes. The replacement of adsorbed calcium and magnesium ions with sodium ions has a deleterious impact on soil permeability and soil structure (Akakuru et al., 2021) (Table 5.6).

Table 5. 6 SAR limits

SAR values	Sodium hazard	Comments
1-10	Low	
10-18	Medium	Tolerable with soil treatment with lime
18 - 26	High	Generally unsuitable for continuous use
> 26	Very High	Generally unsuitable for use

SAR is a crucial aspect in determining soil permeability. In other words, higher SAR concentrations in water degrade soil's physical qualities, notably soil permeability. A higher sodium concentration reduces soil permeability. The SAR value varied from 0.26 to 5.9 meq/L with an average value of 1.8 meq/L. Every sample is contained within allowable bounds (< 10). Only 25% of the samples have a SAR value of 2.5 and above.

%Na^+: The Soluble Sodium Percentage (%Na^+) is another valuable measure for identifying groundwater suitability for agricultural applications. The parameter %Na^+ is defined as the sodium-to-total-cation ratio in meq/L (P. Li et al., 2014). Water with a %Na^+ value of more than 60% may induce salt accumulations, causing a breakdown in the physical qualities of the soil. The value of % Na^+ in the study ranges from 4.2 to 58.23. All the samples are in the excellent (<20) (50%) and permissible (40-60) (50%) classes for irrigation.

Residual sodium carbonate (RSC): The connection between feeble acids and alkaline earth can be depicted as far as RSC, which is utilized to assess the quality of irrigation water (Nagaraju et al., 2014). Water with an RSC value of 1.25 meq/L or less is often safe for irrigating. Water with an RSC value between 1.25 and 2.5 meq/L is considered marginal, whereas water with an RSC value more than 2.5 meq/L is of poor quality for irrigation. Except for one sample, the results reveal that the majority of the samples are safe for irrigation (<1.25 meq/L).

Permeability Index (PI): The vertical movement of water through the unsaturated zone from the ground surface is qualitatively categorized by the Permeability Index. Doneen (1964) established the permeability index (PI) to measure the appropriateness of water for irrigation. Doneen classified PI into three classes: class I (> 75%, suitable), class II (25-75%, good), and class III (25%, undesirable). Irrigation should be done with water from classes I and II. With a maximum

permeability of 25%, Class III waters are inappropriate (Nagaraju et al., 2014). In the study, the PI value ranges from 9.7 to 78.4 meq/L. According to PI classification, 25 % of the sample has a permeability of less than 25%, which is not suitable for irrigation. This sample area sample is from deep wells collected from the lower part of Jerer valley and deep wells of Boren and Tone station of Dire Dawa city.

Potential salinity (PS): Adding half the chloride concentration and the sulfate content gives the potential salinity. The potential salinity of the water samples varied from 1.1 to 29.3 meq/L.

5.3.4. Correlation matrix

The correlation matrix was used to demonstrate the contribution of individual minerals to the natural chemical components of groundwater (Islam et al., 2019).

When there is a strong connection between water quality metrics, it usually means that they are impacted by the same source (Singh et al., 2013).

For the Fafen sample TDS has an excellent positive correlation with, Ca, Mg, and SO_4^{2-}. EC has a positive correlation with Mg and SO_4^{2-} (Table 5.7). There is also a very good correlation between Ca -SO_4^{2-}, Mg-SO_4^{2-}, a positive correlation between, K-Cl, Mg-Cl, Na-F, and for Fafen samples.

TDS have also an excellent correlation with Ca, and SO_4, a very good correlation with Mg and a significant correlation with $F^-$and EC for Shinile samples (Table 5.8). There is also an excellent correlation between Ca and SO_4, a very good correlation between Mg-SO_4, Na-Cl, K-NO_3, a significant correlation between Ca-Mg, Na-F, pH- HCO_3, Na- HCO_3, and Cl- HCO_3 for Shinile samples (Table 5.8).

Fafen samples show a positive correlation between EC and Ca, Mg, and Cl suggesting the influence of human activities in providing these ions to the groundwater of the study area (Table 5.7) (Patel et al., 2016). Ca–Mg has a significant correlation (r = 0.56 in Fafen- and r = 0.66 in Shinile) depicting that dolomite is providing Ca and Mg in the groundwater. The positive relation between Mg and Na (r = 0.35) of Shinile samples demonstrates that the silicate weathering process provides both ions in groundwater. Correlation coefficients greater than 0.5 become significant to take into consideration in studies. In both areas there is a positive relationship coefficient between Na^+ and Cl^- was identified, indicating that halite dissolution (NaCl) was a possible source of Na^+ and Cl^- in groundwater (Xiao et al., 2021).

Table 5. 7 Correlation matrix table of Fafen geochemical parameters

	%Na	GRFA	GRFC	PS	PI	TH (mg/l)	RSC	SAR	No3	So4	F	CI	HCo3	Mg	Ca	K	Na	ph	EC	TDS
TDS	-0.40	0.76	-0.46	0.98	-0.61	0.95	-0.95	-0.09	-0.21	0.99	0.25	0.82	-0.56	0.55	0.95	0.94	0.43	0.52	1.00	1.00
EC	-0.38	0.76	-0.46	0.98	-0.60	0.95	-0.95	-0.08	-0.18	0.99	0.26	0.83	-0.55	0.54	0.95	0.93	0.44	0.53	1.00	
ph	0.25	0.56	0.14	0.54	0.06	0.28	-0.31	0.45	0.27	0.49	0.28	0.56	-0.48	-0.14	0.41	0.51	0.72	1.00		
Na	0.64	0.39	0.50	0.44	0.43	0.16	-0.17	0.84	0.31	0.39	0.67	0.47	-0.19	-0.07	0.23	0.31	1.00			
K	-0.45	0.60	-0.54	0.88	-0.63	0.89	-0.88	-0.17	-0.35	0.95	0.11	0.62	-0.48	0.39	0.94	1.00				
Ca	-0.57	0.65	-0.69	0.91	-0.74	0.95	-0.94	-0.28	-0.20	0.93	0.08	0.73	-0.47	0.44	1.00					
Mg	-0.50	0.54	-0.25	0.60	-0.60	0.69	-0.70	-0.38	-0.50	0.60	0.04	0.52	-0.48	1.00						
HCo3	0.18	-0.84	0.16	-0.62	0.36	-0.54	0.65	0.04	0.12	-0.55	-0.37	-0.64	1.00							
CI	0.57	0.47	0.42	0.32	0.43	0.08	-0.13	0.73	0.44	0.77	0.47	1.00								
F	-0.42	0.73	-0.44	0.97	-0.63	0.95	-0.95	-0.12	-0.32	1.00	0.21									
So4	0.46	0.14	0.21	-0.13	0.44	-0.32	0.31	0.49	1.00											
No3	0.95	0.05	0.81	-0.06	0.84	-0.36	0.33	1.00												
SAR	0.60	-0.77	0.60	-0.94	0.78	-0.99	1.00													
RSC	-0.63	0.71	-0.64	0.93	-0.80	1.00														
TH (mg/l)	0.96	-0.41	0.89	-0.59	1.00															
PI	-0.36	0.85	-0.40	1.00																
PS	0.91	-0.21	1.00																	
GRFC	-0.19	1.00																		
GRFA	1.00																			

Table 5. 8 Correlation matrix table of Shinile geochemical parameters

	%Na	GRFA	GRFC	PS	PI	TH	RSC	SAR	No3	So4	F	CI	HCo3	Mg	Ca	K	Na	ph	EC	TDS

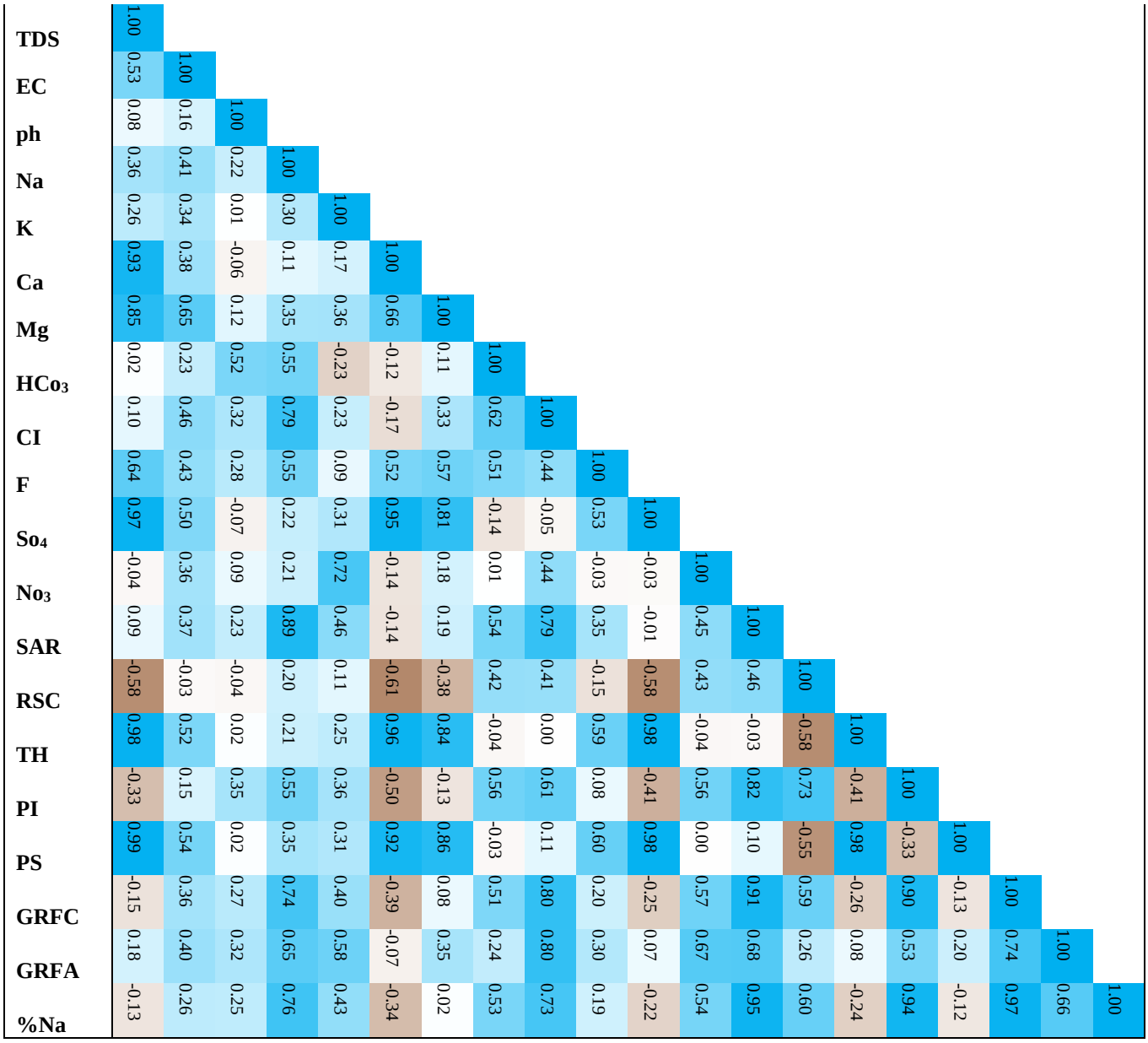

Note: *SAR-sodium adsorption ratio, RSC- Residual sodium carbonate, TH - total hardness (mg/L), PI -Permeability Index, PS-Potential salinity, GRC-Gibbs Ratio of cation, GRA -Gibbs Ratio of anion*

5.3.5. Hydro-geochemical process

Groundwater's hydrogeochemical components can come from a variety of sources and are influenced by a variety of activities. The basis of groundwater hydrochemical composition is laid by natural processes, which typically fall into three categories: precipitation, rock, and evaporation dominance. The chemical composition of natural waters, as well as the number of their ionic species, can be affected by the solvent's degree of weathering, the solubility of the mineral

components of rocks and soils, temperature, the extent and duration of groundwater contact with rocks and soils, and a variety of other environmental factors (Bhatt et al., 2022). Scatter plots and ionic ratios are frequently employed to establish the geochemical mechanism that produces groundwater's chemical signature (Nazzal et al., 2014; Singh et al., 2013).

The scatter plot of Ca^{2+} + Mg^{2+} vs HCO_3^- + SO_4^{2-} following equiline (1:1) signifies both silicate and carbonate weathering contribution in the study region mineral weathering actions (Figure 5.1a). The Ca^{2+} + Mg^{2+} data points reflect an overabundance of these ions and are generated from reverse ion exchange (Brindha et al., 2020; Zhang, et al., 2020). The plot also reveals that most samples are above the 1:1 line, indicating that the ion exchange process was taking place in the study region. To understand the source of these ions, the Ca/Mg ratio was employed. Dolomite and calcite are the principal sources of Ca^{2+} and Mg^{2+} in groundwater. If the dominant reactions in a system are calcite, dolomite, and gypsum dissolutions, the plot of (Ca^{2+}+Mg^{2+}) versus (SO_4^{2-} + HCO_3^-) be close to the 1:1 line.

Most of the aquifer samples fell between the 1:2 and 1:4 lines in the Ca versus HCO_3 plot (Figure 5.1c), which can be attributed to the weathering of calcite and dolomite. Few samples lie within the 1:1 equiline in the Ca^{2+} Vs. SO_4^{2-} scatter plot (Figure 5.1d). The majority of them are above equiline (excess sulphate) while a few are below equiline (excess calcium). Groundwater samples taken after the 1:1 equiline appear to be obtained by gypsum or anhydrite breakdown, but abundant calcium indicates another geochemical activity. The majority of samples exhibit an excess of sulphate over calcium, indicating that calcium was likely removed from the system via calcite precipitation (Das et al., 2015). The ratio of Na^+ + K^+ to total cations (TZ^+) can be used to understand silicate weathering (Subramani et al., 2010). The Na^+ + K^+ versus (TZ+) plot in the analysis demonstrates that the majority of the sample points lie above the (Na^++K^+) =0.5TZ^+ line (Figure 5.1e). This demonstrates how silicate weathering plays a role in geochemical processes, primarily supplying salt and potassium ions to groundwater (Das et al., 2015). This suggests that alkali metals have a smaller contribution than alkali earth metals, which is explained by the Ca-Na exchange process' enrichment of groundwater with Ca^{2+}.

The dominancy of Ca^{2+} and Mg^{2+} in the study region is reflected by comparing the plot of TZ^+ Vs. Na^+ + K^+ and Ca^{2+} + Mg^{2+} (Figures 5.1e & 5.1f). The plot of (Ca^{2+} + Mg^{2+}) versus TZ indicates that the majority of the samples follow the equiline (line 1:1) and fall within the 1:1 and the 1:1.5

line, indicating the abundance of Ca^{2+} and Mg^{2+} in the study region. Most samples below the 1:1.5 line may be the reverse ion exchange and carbonate minerals (Figure 5.1f).

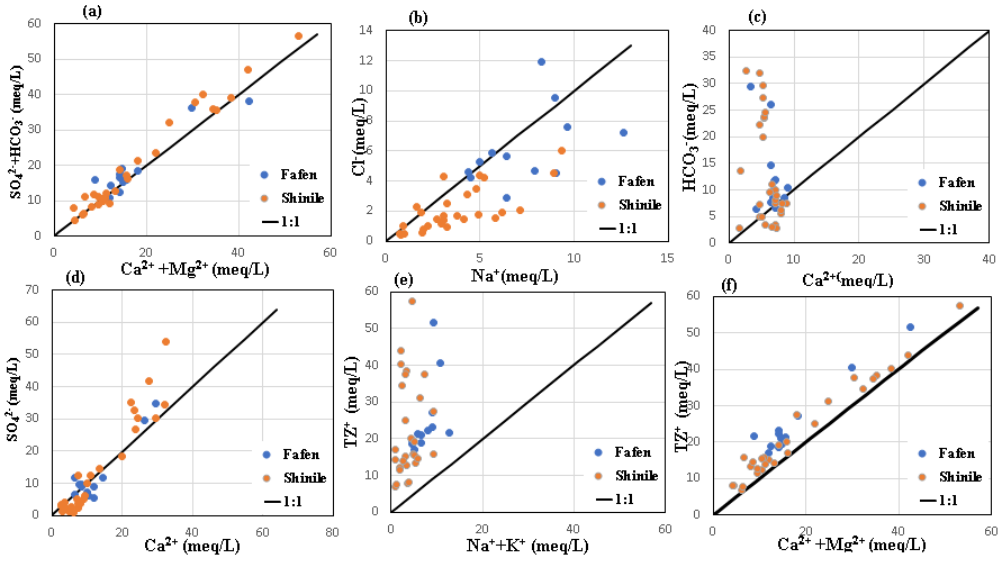

Figure 5. 1 Scatter plot hydrogeological analysis of samples

The ratio of Cl^- to Na^+ is proportional to 1.0 and can be used to estimate the source of Na^+ in groundwater. When the ratio is larger than 1.0, the Na^+ source in groundwater is due to alternating cation adsorption; when the ratio is less than one, the Na^+ source in groundwater originates from worn silicate minerals. When the ratio equals one, it shows that halo stone dissolution is the source of Na^+ in groundwater (Refat & Humayan, 2021; Zhang, et al., 2020). The majority of the samples in Figure (Figure 5.1b) are below the line 1:1 which indicates the ratio Cl^-/Na^+ <1, showing that the sodium sources from groundwater are weathered silicate minerals. Some samples above line one (Cl/Na >1) show that the Na^+ source in groundwater is also due to the alternating adsorption of cations. The weathering of silicate minerals also increases the Na^+ in the groundwater system (Wei et al., 2020). The scatter graph of SO_4^{2-} Vs. (Ca^{2+}+Mg^{2+}) (Figure 5.2b) shows that the majority of the dots fall above the 1:1 equiline, indicating that $MgSO_4$ and $CaSO_4$-rich rocks are the primary sulfate sources. A strong association (r=0.89, 0.96) between the Ca^{2+} + Mg^{2+} and SO_4^{2-} plots shows that they might have come from source rocks including dolomites and gypsum (Figure 5.2b).

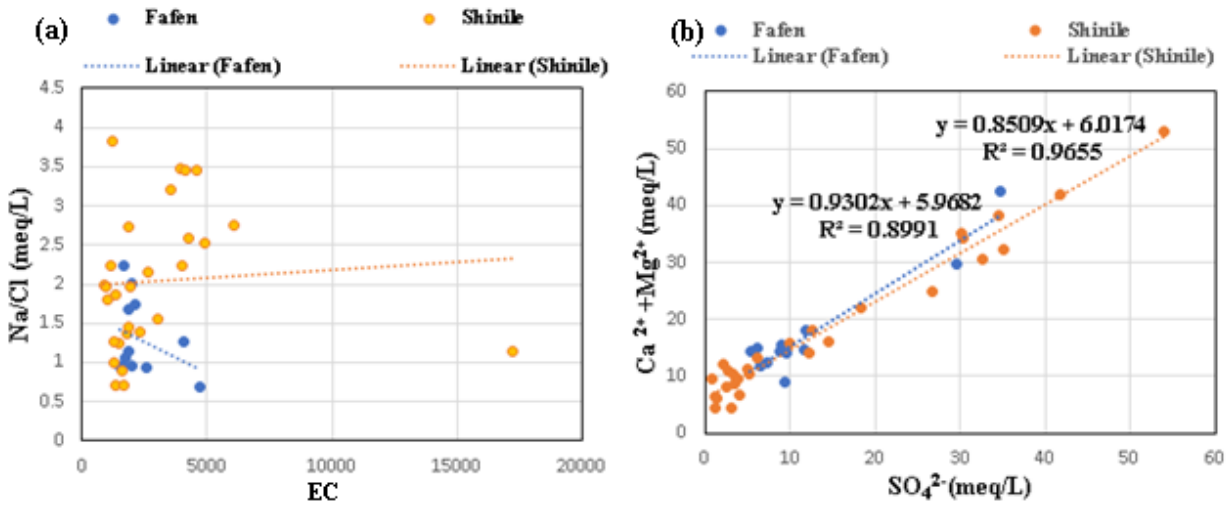

Figure 5. 2 Scatter plots of (a) EC versus NA/Cl, (b) SO_4^{2-} versus $Ca^{2+} + Mg^{2+}$

Silicate and carbonate weathering: The plot of Ca^{2+} vs HCO_3^- shows that the majority of the samples are below the equiline, showing the preponderance of ionic sources from silicate mineral weathering (Figure 5.3a).

The scatter plot of HCO_3^- Vs. Na^+ all samples are below the 1:1 line indicating the dominancy of silicate weathering (Figure 5.3b) (Kumar et al., 2009; Refat N. & Humayan A., 2021). The curve of Na/Cl versus EC, which shows a direct proportion, also confirms silicate weather. Silicate weathering is the main process if Na/Cl increases with EC (Das et al., 2015; M. Kumar et al., 2006). According to the graph of EC vs Na/Cl increasing for the Shinile samples and it is declining for the Fafen cases (Figure 5.2a).

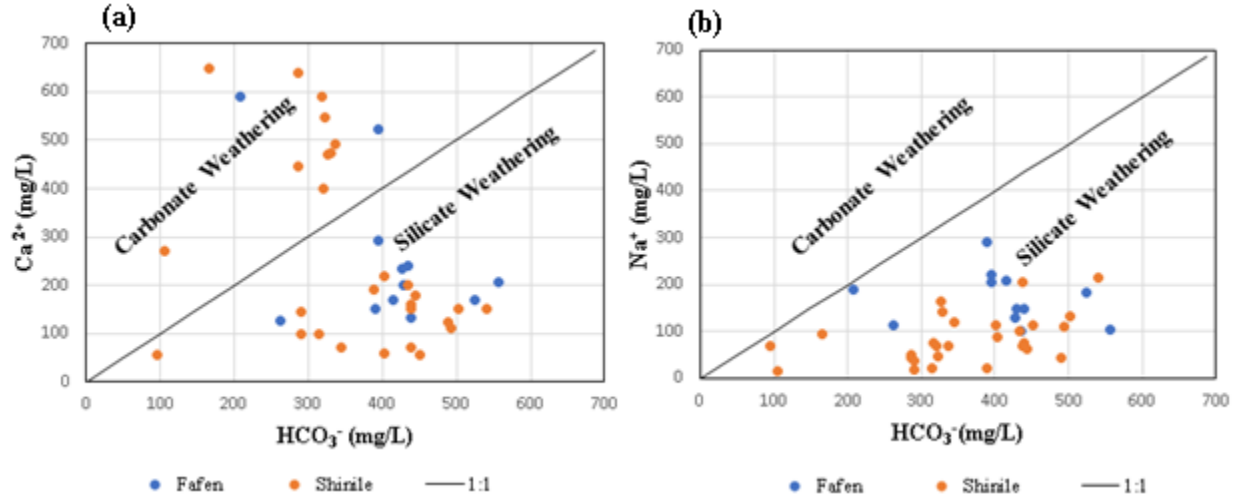

Figure 5. 3 Scatter plots showing the weathering process

5.3.6. Gibbs diagram

The figure (Figure 5.4a & b) depicts the plot of Gibbs ratios I and II (Eq.5.11 &5.12) versus the TDS graph. In the current investigation, the mean value of the ratio $Na^+/(Na^+ + Ca^{2+})$ and $Cl^-/(Cl^- + HCO_3^-)$ was 0.42 and 0.35 for Fafen, while the mean value of $Na^+/(Na^+ + Ca^{2+})$ and $Cl^-/(Cl^- + HCO_3^-)$ was 0.30 and 0.16 for Shinile respectively. However, the TDS value is relatively high (558-3900mg/L) and ratio findings move the Gibbs plot to the left-center corner area of which rock-water interaction is dominating.

The Gibbs diagram of the water samples demonstrates that the majority of the water samples are concentrated in the zone of rock-water interaction. The results confirm that rock-water interaction is the driving force in controlling groundwater chemistry in the study area, implying that the interaction between rock and water primarily controls the major ion chemistry of groundwater. Because the study region experiences dry and semiarid climatic conditions, evaporation may also contribute to water chemistry, which affects groundwater quality.

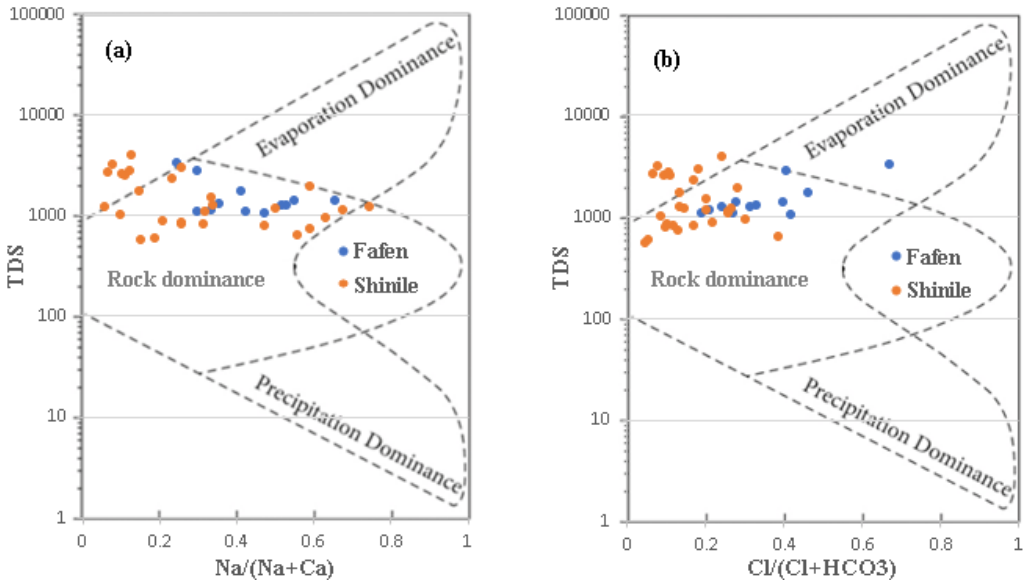

Figure 5. 4 Gibbs plot of samples

Precipitation has minimal impact on the hydro-geochemistry of the aquifers under investigation, as evidenced by the fact that none of the water sample locations were inside the rain dominance zone. Thus, Gibbs plots indicate that in the research site, groundwater quality is mostly influenced by rock water interaction (80%) and evaporation (20%).

5.3.7. The groundwater types

Most of the water samples belong to classes mixed type (Ca-Mg-Cl) and some samples are found in calcium chloride type in the Fafen catchment. In Shinile mixed type (Ca-Mg-Cl) is the dominant class followed by Mg-bicarbonate and Calcium chloride type. One sample is found in the sodium chloride type class. So, mixed ions of Ca-Mg-Cl types are the common hydro-chemical characteristics of the regions (Figure 5.5).

When the cation triangles of the two locations are compared, the Calcium type is the dominating cation in both, followed by no dominant class. The anions triangle shows that bicarbonate and sulfate are the dominating classes in the Shinile sample, but there is no dominance other than the negligible sulphate type in the Fafen sample. The water types in the study region include calcium type, bicarbonate type, sulphate type, Na-Cl type, Ca-Cl type, and mixed Ca-Mg-Cl type. So, the results indicate that Ca-Mg-Cl is the prevalent water type in the studied areas. The spatial variation of samples collected at Shinile varies more widely than the Fafen samples. However, the Fafen samples have greater vertical variability than Shinile. The depth of samples varies from 52.5 to 550 m.

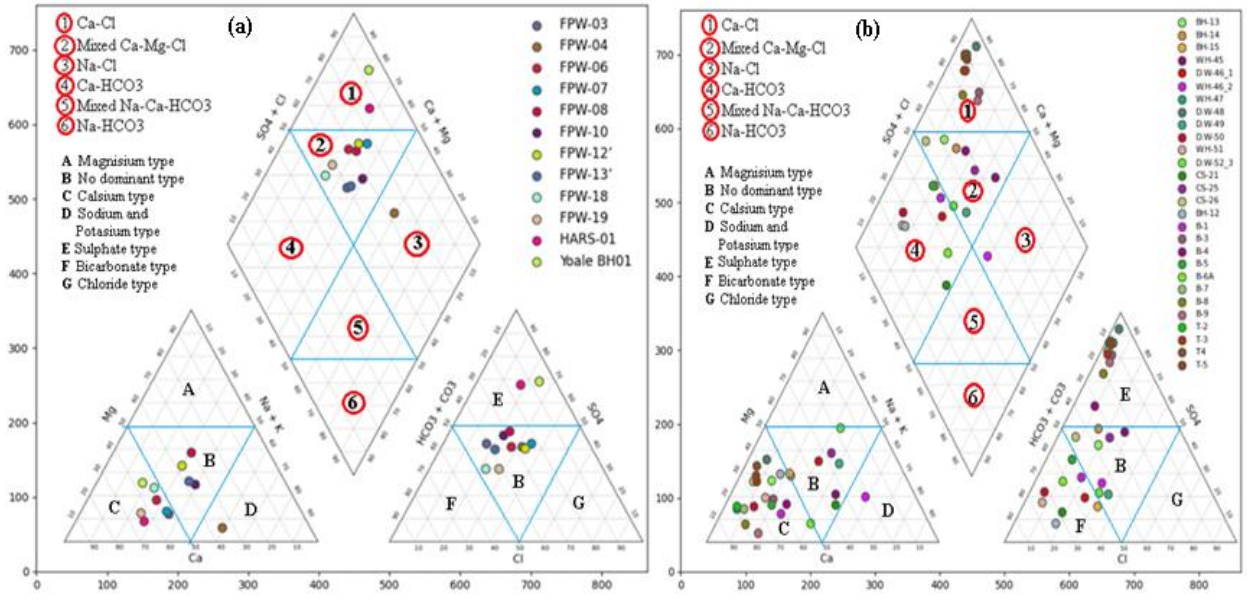

Figure 5. 5 Piper plots for samples a) Fafen and b) Shinile

Base-exchange Index

Groundwater samples were categorized using base-exchange indices value (Eq. 5.13 in Table 5.1). If r_1 is less than one, the groundwater sources are of Na^+ - SO_4^{2-} type, and if r_1 is more than one, the sources are Na^+ - HCO_3^- type (Eyankware et al., 2022; Shukla & Saxena, 2021). Only three samples (7.5%) have a base-exchange index greater than one, which means 7.5% of the samples are sourced from Na^+ - HCO_3^- type. These samples are from the Shinile area around west of Shinile town, Dire Dawa, Boren field. The majority (92.5%) of the groundwater samples in the study regions are Na^+ - SO_4^{2-} type.

Meteoric Genesis Index (r_2)

The value of r_2 stipulates the groundwater sources in a given area (Singh et al., 2013). If r_2 is less than one, the groundwater source is deep meteoric water percolation, whereas r_2 larger than one implies shallow meteoric water percolation (Eq. 5.14). The findings of meteoric genesis indices suggest that 92.5% of groundwater samples are shallow meteoric percolation water and just 7.5% are deep meteoric percolation water.

Chloro-alkaline indices (CAI)

Chloro-alkaline indices indicate the ion exchange between the groundwater and the environment (Eq. 5.15 & 5.16) (Nagaraju et al., 2014). When CAI > 0, Na^+ or K^+ are replaced by Ca^{2+} from the sediments; when CAI < 0, a reverse ion exchange occurs, and Ca^{2+} is replaced by Na^+ or K^+ from the sediments (Nsabimana et al., 2023). In the present study region, 80% of the groundwater sampling points show negative (-2.86 to -0.0006) and 20% are positive (0.003 to 0.28) values of CAI (Figure 5.5). These findings indicate that Ca^{2+} and Mg^{2+} in groundwater exchange for Na^+ and K^+ from aquifer material. As a result, Na^+ or K^+ appears to be the most frequent cation in the current research region (Rao et al., 2020). That means the chlor-alkali index CAI-1 and CAI-2 values of 80% of the samples were negative, suggesting that the cation exchange process in the research area was that Ca^{2+} or Mg^{2+} in the water exchanged Na^+ or K^+ in the aquifer minerals and that the region water Ca^{2+} or Mg^{2+} was depleted and Na^+ or K^+ was enriched.

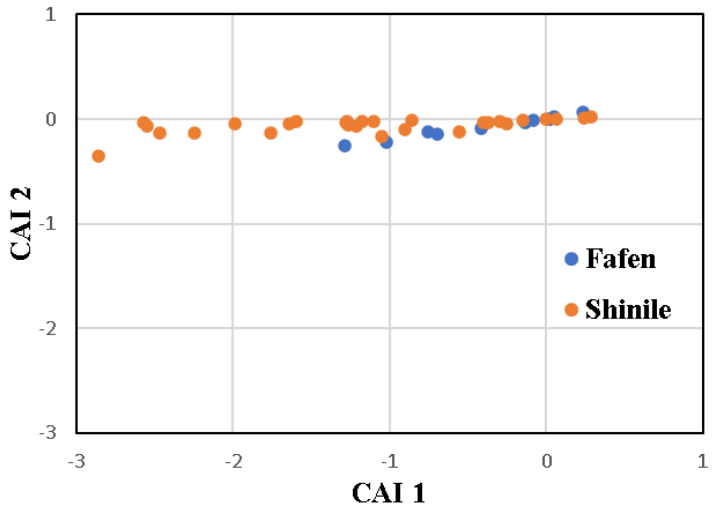

Figure 5. 6 Chloro-Alkaline Indices

5.3.8. Isotope compositions

The stable isotope composition of hydrogen and oxygen allows for the effective tracing of water as it moves through the critical zone. In Figure 5.8, the stable isotopic compositions ($\delta^{18}O$ and δD) of water samples in the research region were displayed. Overall, across the research region, the isotopic values of all water samples varied from -10.37‰ to 31.34‰ for δD and from -2.772‰ to 6.68‰ for δ18O. Plotting of all samples along the global (Craig, 1961) and local (Bedaso & Wu, 2021) meteoric water lines showed that the precipitation was the source of recharging the waters in the study regions.

Isotope composition of precipitation: The precipitation results range from 12.37 to 28.24‰ with a mean value of 20.30‰ for $\delta^{2}H$ and 0.76 to1.43‰ with a mean value of 1.09 ‰ for $\delta^{18}O$ at Jigjiga. The result at Dire-Dawa ranges from −0.09 to 25.33‰ with a mean value of 12.62 for $\delta^{2}H$ and −0.229 to 4.217‰ with a mean value of 1.994‰ for $\delta^{18}O$. The result shows that isotopically depleted water is found in Dire-Dawa than in Jigjiga city. Different kinds of water in the research sites displayed unique isotopic compositions. (i) Plotted on the top-right of the LMWL and GMWL is, a rainwater sample with an enriched isotopic composition that displayed unique features from other samples (Figure 5.7).

The isotope composition of hydrogen in the rainwater sample is relatively enriched in Jigjiga than in Dire Dawa. However, the oxygen composition of rainwater in Jigjiga was more depleted than in Dire Dawa. A single sample in Dire Dawa is most enriched in isotope composition. The results

demonstrate that a heavier isotope composition of oxygen and hydrogen is recorded in Jigjiga than in Dire Dawa. This is due to the lower altitude of Dire Dawa than that of Jigjiga. In other words, the results of the mean oxygen isotope ($\delta^{18}O$) at the higher temperature zone of Shinile (1.994‰) are higher than that of the Jigjiga (1.09 ‰). These results confirm that temperature variations also affect the $^{18}O/16O$ ratio. More ^{18}O evaporation occurs at higher temperatures, whereas less evaporation occurs at lower temperatures. The heavier isotope concentration rises with temperature, resulting in an abundance of it in the precipitation of warm times (Gourcy et al.,2005).

Previously reported that the isotope composition of precipitation at the Jigjiga station ranged from −12.6 to 6.4‰ for $\delta^{18}O$ and from −91.8 to 47.1‰ for $\delta^{2}H$ (Bedaso & Wu, 2021). This indicates the present result is within the range of the previous report of the stations. In the other study, the weighted mean value isotope composition for the Addis Ababa station was −1.56‰ for $\delta^{18}O$ and +1.48‰ for $\delta^{2}H$, which are broad in range (Kebede & Travi, 2012). These results indicate the isotope composition of precipitation in the study area was in good agreement with the previous studies.

The isotope composition of surface water: The isotope results of the surface water sample taken 10km southeast of Jigjiga become −1.073‰ for $\delta^{18}O$ and 5.87‰ for $\delta^{2}H$. The result at 95km south of Jigjiga, the stable isotope of surface water was 6.689‰ for $\delta^{18}O$ and 31.34‰ for $\delta^{2}H$. The surface water analysis shows that the most enriched isotope result occurred in the southern part of the study area near Deghabur town. It is well known that with increasing altitude, precipitation, and surface waters become increasingly depleted in $\delta^{18}O$ and $\delta^{2}H$ compositions (Poage & Chamberlain, 2001; Dansgaard, 1964). In both cases, the surface water isotope is enriched in both stable water isotope compositions than groundwater samples. The results at this point also show a good association between precipitation and surface water (Figure 5.7).

The isotope composition of groundwater

The groundwater recharge is greatly influenced by the signal of $\delta^{18}O$- δD from meteorites. The isotopic composition of groundwater is the combined average of the weights of the different sources of recharge, such as precipitation and river water. Therefore, it is anticipated that isotopic ratios in groundwater will differ from those in precipitation (Yeh, et al.,2011). The hydrogen and oxygen stable isotope ratio of groundwater for the Fafen-Jerer and Shinile catchment area is presented in the figure (Figure 5.7).

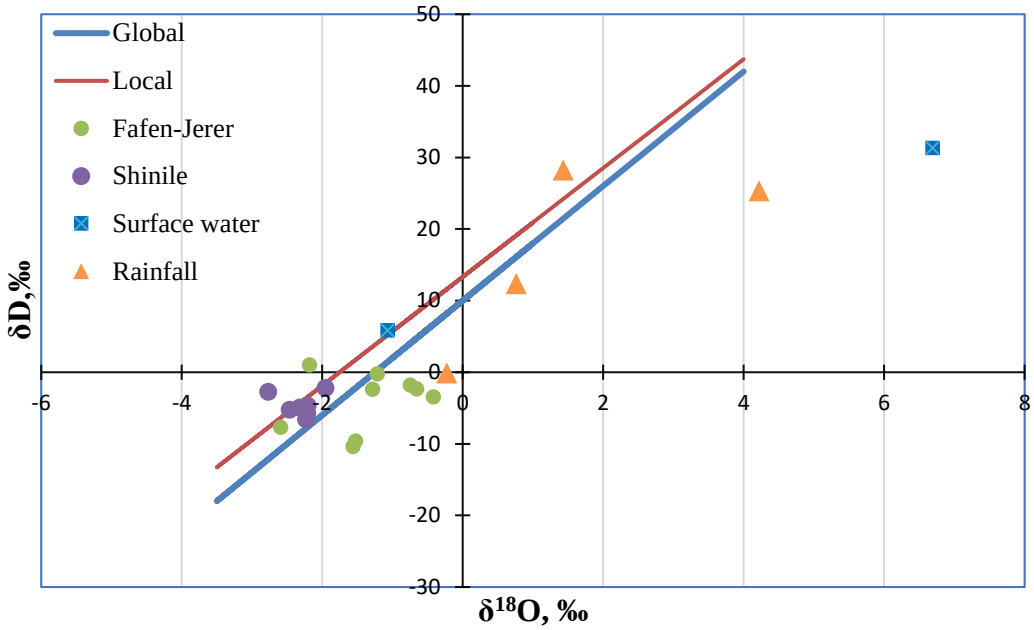

Figure 5. 7 Distribution of stable isotope composition around LMWL and GMWL.

The isotope composition of the Shinile and Dire Dawa region groundwaters ranges from -6.56 to -2.18 with a mean value of -4.57 for δ^2H and -2.772 to -1.956 with a mean value of -2.31 for $\delta^{18}O$. The stable isotope compositions varied from -10.37 to 1.01 with a mean value of 4.101 for δ^2H and from -2.691 to -0.418 with a mean value of -1.354 for $\delta^{18}O$ in the Fafen-Jerer. These results showed that both hydrogen and oxygen isotope composition are depleted than that of surcae water and precipitation.

The figure (Figure 5.7) illustrates that the Fafen-Jerer samples exhibit a significantly broader range of values in comparison to the Shinile groundwater samples. The reason for this is the Fafen-Jerer area's geological state and the depth of the groundwater. The Fafen-Jerer alluvial aquifer is surrounded by distinct geologic formations that provide diverse components to the groundwater. Most water samples of Shinile plot to the right of (below) the LMWL, with some surface water samples showing similar compositions to the LMWL (Figure 5.7). The distribution of most of the Fafen-Jerer groundwater samples plot to the right of (below) both the LMWL as well as GMWL graphs.

We applied the Pearson correlation coefficient stable Isotope results of the study area with the geographical location (UTM coordinate) of the samples and physicochemical parameters.

Correlation matrix demonstrates that $\delta^{18}O$ and δD have a positive association (0.23). The results show that EC and TDS have a stronger positive connection with $\delta^{18}O$ (0.44) than δD (0.11). A relatively high range of value of isotope composition ($\delta^{18}O$, δD, and d- excess) was recorded in the Fafen-Jerer catchment than that of the Shinile. This is due to the variable nature of geomorphology leading to variable water infiltration in the Fafen-Jerer catchment (Fynn et al., 2016). The mean isotope composition of groundwater results in most of the Jerer catchment being relatively enriched than that of the Shinile cases. More depleted isotope composition is due to high temperature and lower altitude conditions of the Shinile area. The precipitation isotope results in the Shinile area are relatively better associated with groundwater than the Jerer catchment. This is due to the relatively shallow depth conditions of Shinile wells. The isotope composition of hydrogen in the Shinile catchment shows a good association between precipitation and groundwater than in the Jerer case. On the other hand, the Jerer catchment has a stronger correlation with rainfall in terms of the oxygen isotope composition than the Shinile. In comparison to the Jerer examples ($\delta^{18}O = -1.354$), the oxygen isotope near the Shinile is comparatively lighter ($\delta^{18}O = -2.31$). The distribution of hydrogen and oxygen isotope composition aligns with the meteoric water line graph.

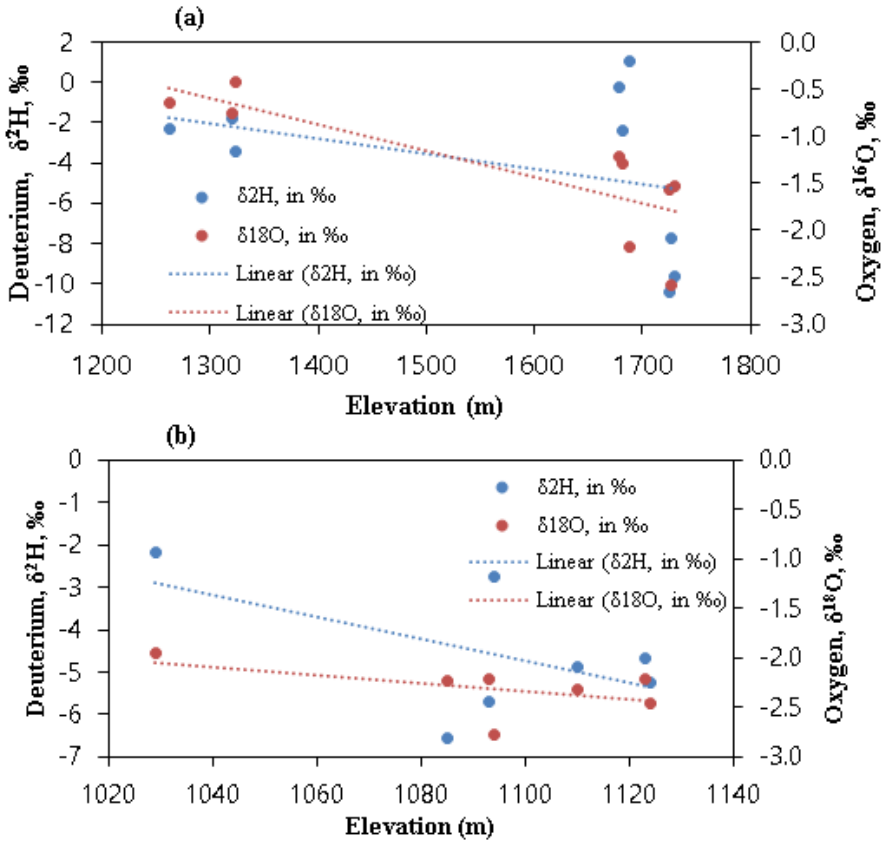

Figure 5. 8 Elevation vurses stable isotope (a) Fafen-Jerer and (b) Shinile

The isotope composition of hydrogen in the Shinile catchment shows a good association between precipitation and groundwater than in the Fafen-Jerer case. However, the oxygen isotope composition relationship shows more association was found in the Fafen-Jerer catchment than in the Shinile. The isotope of oxygen around Shinile is relatively heavier ($\delta^{18}O$ =−2.31) than in the Fafen-Jerer cases ($\delta^{18}O$ = −1.354). This is due to the higher temperature of the Shinile area than the Fafen-Jerer. The distribution of hydrogen and oxygen isotope composition aligns with the meteoric water line graph.

There is almost a similar relationship between isotope composition with topographic elevation. A higher range of elevation (1262-1730m) is noted in the Fafen-Jerer than (Figure 5.8a) the Shinile (1085-1124m) which resulted in a higher isotope variation in the Fafen-Jerer catchment (Figure 5.8). Results from previous studies and the present isotope ratio data for groundwater and precipitation were integrated (Ayenew et al., 2008; Bedaso & Wu, 2021). The $\delta^{18}O$ isotope composition of groundwater result of alluvial aquifer zone showed that within the previous study range for shallow groundwater (−4 to 0‰).

D-excess at Fafen-Jerer ranges from −0.106 to 18.46‰ with a mean value of 6.73‰. The d-excess value of the Shinile range was from 11.28 to 19.44 with a mean value of 13.91‰. The d-excess values of most of the samples are above the global average. The value of d-excess in the Shinile area was higher than that of the Fafen-Jerer catchment (Figure 5.9). The higher d-excess value recorded in Shinile is due to a relative depletion in oxygen isotope composition. In the Fafen-Jerer catchment larger-scale variation of d-excess was recorded than in the Shinile case. All the values of d-excess at the Shinile area are larger than the global meteoric water line value of 10‰. This is due to the dry climate condition of the Shinile area while local climate is one of the parameters that influence d-excess. The lower altitude (1094m) and the higher mean annual temperature (21.6 °C) of Shinile also influence the d-excess value (Bershaw, 2018). In the research region, the d-excess value rises from south to north. That means the result shows the d-excess value at higher latitudes becomes higher (>10‰) and vice versa. The difference between the southern part from the north is due to the moisture sources (Kern et al., 2020). Study shows that the Indian Ocean is the major source of moisture that influences the d-excess values in southern and eastern Ethiopia. This is due to the depleted oxygen isotope record of the region (S. Kebede & Travi, 2012b). Additionally, the

higher value of d-excess was due to the seasonal condition. The samples were taken in the Sahel rains (June, July, August, and September) season, where relative depletion of $\delta^{18}O$ isotope was recorded.

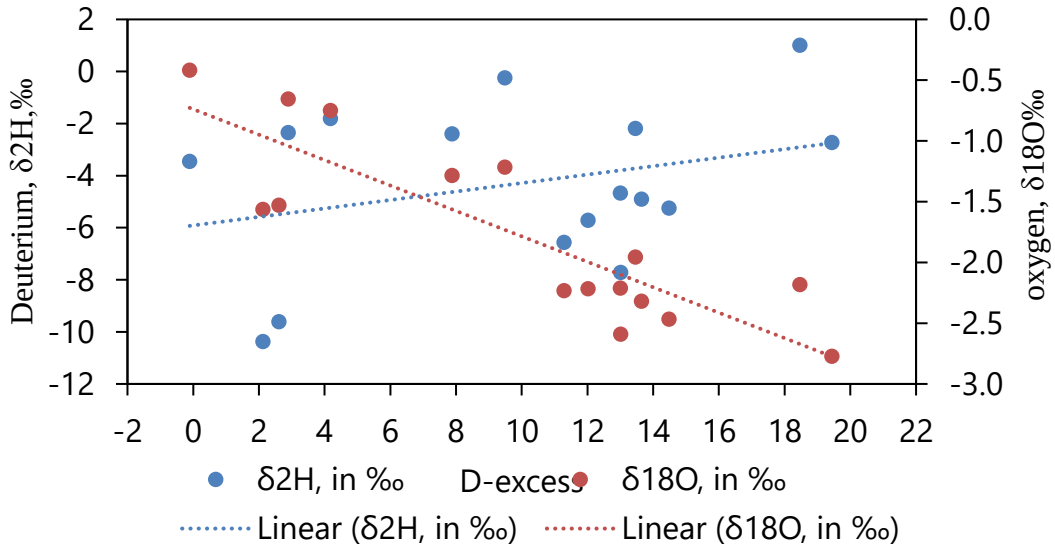

Figure 5. 9 D-excess verses $\delta^{18}O$ and δD isotope

The report from a previous study shows that the oxygen isotope composition of precipitation at Jigjiga station ranges in value from −12.6 to 6.4 ‰ with a mean of −0.1 ± 3.2 ‰. The hydrogen value raged from −91.8 to 47.1‰ with a mean of 7.6 ± 23.3‰ (Bedaso et al., 2020). This showed that the isotope composition of groundwater at the Fafen-Jerer catchment (around Jigjiga) was within the range of precipitation composition and a smaller amount of depletion for both D and $\delta^{18}O$ compared to the mean value.

Due to economic and time-bound, the stable isotope study was limited to areas around Dire Dawa city and Shinile town in the Shinile sub-basin and covers the eastern catchment of the Fafen-Jerer. The next study should consider these cases and cover the other portions of the sub-basins for integrated groundwater management. Therefore, the groundwater resources of the study area are very limited, and the sources of recharge should be studied. Further studies should incorporate methods like radioactive carbon dating and very detailed data to get precise results.

5.4. CONCLUSION

This work evaluated the stable isotope and geochemical composition of the alluvial districts of eastern Ethiopia. The groundwater chemistry was evaluated using multiple criteria for agricultural and drinking reasons. To understand the hydrogeochemical character of the groundwater, the research examined chemical indices such as SAR, Na%, PS, RSC, PI, and CAI of the study regions. The study area is characterized by hardness and high salinity. Conventional graphical plots and geochemical modeling are utilized to analyze groundwater chemistry and the processes governing groundwater change. The graphical plot suggests that silicate weathering and carbonate mineral dissolution are major factors influencing the groundwater quality in the studied region. The majority of water samples are suitable for agricultural usage. Groundwater of acceptable quality is widely distributed in the Fafen watershed, although groundwater of doubtful quality may be found in the Fafen-Jerer catchment and Shinile in the Dire Dawa area. The base-exchange index result shows that 92.5% of the groundwater samples in the study regions are Na^{+} - SO_4^{2-} type. According to the results of meteoric genesis indices, 92.5% of groundwater samples are shallow meteoric percolation water. According to the Piper diagram, the most prevalent water types in the research area were mixed (Ca-Mg-Cl), with calcium as the primary cation and bicarbonate as the dominant anion. The Gibbs diagram results show groundwater chemistry is largely governed by rock-water interaction, and evaporation crystallization is one of the causes of increased salinity and hence poor groundwater quality. A stable isotope signature studied in the alluvial aquifers of eastern Ethiopia unveils a homogeneous system in its lateral extent. The examination of the isotope composition of the Fafen-Jerer and Shinile areas brings about a substantially more comparable connection between precipitation and groundwater. In the two cases, the steady isotope results show a decent relationship between precipitation and groundwater. Generally, a higher range of values was kept in the Fafen-Jerer catchment than the Shinile region in both hydrogen and oxygen results. This is expected to more profound groundwater information and topographic variations of the Fafen-Jerer case. The author recommends groundwater quality be evaluated at the household level in the research location to determine groundwater quality and appropriateness for human use. The finding of this study has extensive importance for water resources management in the semi-arid climate zone and to cope with climate change.

CHAPTER 6

INTRINSIC VULNERABILITY ASSESSMENT

Abstract

Effective groundwater resource management is essential to preventing contamination and preserving quality in the semi-arid region, where the main concerns are changing land cover and climate change. The purpose of this study was to use the modified DRASTIC model to examine the intrinsic vulnerability of groundwater. The DRASTIC method applied seven hydrogeological parameters: depth to water (D), net recharge (R), aquifer media (A), soil media (S), topography (T), the impact of vadose zone (I), and hydraulic conductivity (C). Lineament and Land use land cover (LULC) were added to the DRASTIC parameters, and the impact of these parameters on the resulting vulnerability map was determined using sensitivity analysis. The results of the modified DRASTIC index are between 87-263 for Fafen, and, 11-254 for Gambela plain, and 92-252 for Shinile respectively. Based on these results, the study area was classified into five categories very low, low, moderate, high, and very high groundwater hazards. The distribution of the index map was different for each catchment. The sensitivity analysis shows that depth and impact on the vadose zone were the main parameters that influenced the vulnerability map. The study was validated using data on nitrate and electric conductivity (EC) concentrations in groundwater from the study areas. The validation result showed there is a positive correlation between the risk map and the nitrate and EC concentration map of the study regions. These results can serve as a guide for those responsible for making decisions regarding to prevention of groundwater pollution in such a sensitive area.

Keywords, Modified DRASTIC, aquifer vulnerability, sensitivity, nitrate concentration, Ethiopia

6.1. INTRODUCTION

Groundwater pollution is defined as the addition of unwanted substances to groundwater caused by human activities (Harter, 2003). There are several causes of contamination of groundwater, leachates from waste disposal sites (Singh et al., 2016), seepage from sewage (Pedley & Howard, 1997), human and animal wastes (Whaley-Martin et al., 2017), organic contaminants (Tu et al., 2023), natural sources (Krishan et al., 2023) and human influences (Schoeman et al., 2014; Wakejo et al.,2022) which cause microbial and nitrate (NO3) contamination of shallow groundwater are the

common sources (Han et al., 2016; Li et al., 2021; Subbarao et al., 1996). Groundwater contamination can also be caused by toxic substances found in soil or rock particles (Ismanto et al., 2023; Nigeria et al., 2016). The geological setting of the area affects groundwater vulnerability as well because it controls infiltration activity from the soil's upper surface to the deeper subsurface (Duvva et al., 2022; Economou-Eliopoulos et al., 2014; M. R. Islam et al., 2000). Water bodies may get contaminated by pollution from both point and nonpoint sources. Discharges from municipal sewage treatment plants, industrial facilities, factories, power plants, and underground coal mines, as well as specific sources like drain pipes, ditches, sewer outfalls, as well as oil wells, are examples of non-point sources, that lack specific source locations (Lapworth et al., 2012; Li et al., 2021).

To manage groundwater resources effectively, pollution prevention is essential, and groundwater hazard assessment is crucial for resource protection. Pollution is caused by physical, social, economic, and environmental factors or processes that make the resources (groundwater) more susceptible to the effects of hazards. The resources become vulnerable meaning that the quality or state of being exposed to the possibility of being attacked or harmed, either physically or emotionally. Groundwater vulnerability is a condition determined by physical, social, and natural variables or forms that increase the susceptibility of a resource to the impacts of hazards. In a broader sense, "groundwater vulnerability" refers to the possibility of an underlying aquifer becoming contaminated due to both natural and artificial occurrences (Metzger et al., 2006; Piscopo, 2001). There are two types of vulnerabilities recognized in the literature; intrinsic (or natural) and specific (or built-in) vulnerabilities. Intrinsic vulnerability considers the unique geological, hydrological, hydrogeological, and hydrogeochemical features of an area to assess the vulnerability of groundwater to pollutants caused by human activities. A term used to define specific vulnerability is used to define the vulnerability of groundwater to a particular contaminant considering the relationship between contaminant properties and various factors of inherent vulnerability (Lima et al., 2022; Rama et al., 2022).

Several works have been done throughout the globe to evaluate the groundwater pollution impact (Balaram et al., 2022; Fida et al., 2022; Kurwadkar, 2014; Zhao & Pei, 2012; Zohud & Alam, 2022). Many different approaches to assessing groundwater's vulnerability have been developed in recent years (Boufekane et al., 2022; Ekanem et al., 2022; Kirlas et al., 2022; Saranya & Saravanan, 2023; Taghavi et al., 2022; Umar et al., 2022). DRASTIC is a frequently used standard technique for

assessing groundwater vulnerability. The United States Environmental Protection Agency (USEPA) developed DRASIC as a technique to evaluate potential groundwater pollution (Aller et al., 1987). DRASTIC is an acronym used to state a comprehensive picture of all the main geohydrologic aspects that influence and regulate groundwater movement into, through, and out of a location (Aller et al., 1987). DRASTIC used seven hydrogeological parameters, depth, recharge, aquifer, soil media, topography (slope), the impact of the vadose zone, and conductivity of the aquifer. The methods weigh various criteria affecting vulnerability while considering the physical, chemical, and biological processes in the saturated zone (Goodarzi et al., 2022). Additionally, the DRASTIC method has been modified in recent years to consider the characteristics of the study area by adding new parameters to the existing ones (Khosravi et al., 2021; L et al., 2021; Singh et al., 2015).

Due to its lower initial cost, superior water quality, and year-round availability when compared to surface water sources, groundwater is an alternative source of domestic water supply for the major cities, towns, and villages in Ethiopia. In both rural and urban areas, Ethiopia has not yet fully enabled society's access to fresh water (Berhanu et al., 2014; Kebede, 2013.; Mengistu et al., 2019). The main groundwater quality difficulties include high fluoride concentrations in the central rift valley (Kloos & Tekle Haimanot, 1999), high salinity problems in the dry zone of the southeastern (Kebede, 2013; Mengistu et al., 2019), and high micro-biological and nitrate concentrations in shallow aquifers around large cities (Akale et al., 2018; Wakejo et al., 2022). Growing population density, scarcity, and pollution of surface waters are the main factors that influence drinking water quality. The country falls short of delivering the highest feasible degree of access to clean water, especially in rural areas (Rahm, 1999). The quality of domestic water is also very far apart from the recommended by international sectors (Mengistu et al., 2019; Reimann et al., 2003).

Located in the alluvial region the study area suffers from simultaneous drought, and variable rainfall, rising temperatures (Seifu et al., 2022). For the past period, there has been a high increment in average temperature and a reduction in annual rainfall. Grasslands and shrublands are the major land cover of the study region. According to the report, the study area's water quality has declined because of significant contaminants like dissolved solids, nitrate, sulfate, and chloride as well as electrical conductivity (Kebede, 2013; Li et al., 2021; Tadesse et al., 2008; Wakejo et al., 2022). Indeed, it is vital to create a vulnerability map that considers several hydrogeological criteria to restrict and prevent the dangers of pollution of these waters and maintain their quality. This was the

initial study in the area to use modified DRASTIC methods by including the lineament and LULC characteristics to measure groundwater vulnerability. We estimated groundwater hazard potential risk by producing a susceptibility map of an aquifer using a Geographic Information System (GIS) environment. This study provides direct information on aquifer vulnerability and helps decision-makers to manage groundwater resources more effectively and sustainably.

One area of interest that academics and stakeholders involved in groundwater management should be aware of is the study of groundwater vulnerability to natural causes. To achieve this, this particular topic discusses the problem of groundwater vulnerability to natural hazards and offers some fundamental advice.

6.2. MATERIALS AND METHODS

There has been a lot of progress in aquifer vulnerability assessments to establish accurate, precise, and workable methods. This has led to the creation of several vulnerability evaluation models, each with unique techniques, data requirements, and wider applicability. In general, the DRASTIC model is studied via the most widely used vulnerability assessment approach. The DRASTIC model has become one of the most popular techniques for determining how vulnerable groundwater is to pollution. The model's input variables (hydrogeological parameters) are adopted from those of the typical DRASTIC model (Aller, 1987). The modified DRASTIC includes the lineament and LULC parameters. The preparation of input parameters was the initial step of the research work. The second step was producing the thematic layers for each input parameter in the GIS environment. The complete structure of the analysis is presented in the methodology chart (Figure 3.5).

6.2.1. DRASTIC model

The study applied the DRASTIC method of groundwater vulnerability to intrinsic pollutants. DRASTIC was created by the US Environmental Protection Agency (Aller et al., 1987). The DRASTIC method applied seven parameters, depth, recharge, aquifer media, soil media, topographic (slope), impact vadose zone, and hydraulic conductivity. DRASTIC (Aller et al. 1987) is a weighting and rating method that assesses vulnerability using thematic parameters. The method utilizes weight for each parameter based on its relative importance contributing to the contamination potential and rating esteem between 1 and 10 for each parameter.

The DRASTIC index can be determined using equation:

$$Modified\ DRASTIC\ Index = W_D R_D + W_R R_R + W_A R_A + W_S R_S + W_T R_T + W_I R_I + W_C R_C + W_L R_L + W_{LULC} R_{LULC} \ldots \ldots \ldots \ldots \ldots \ldots \ldots \ldots \ldots \ldots \ldots \ldots \ldots \ldots \ldots \ldots \ldots \ldots \ldots \ldots \ldots \ldots \ldots \ldots \ldots \ldots \ldots \ldots \ldots \ldots 6.1$$

The seven effective hydro-geological parameters are denoted by the abbreviations D, R, A, S, T, I, and C in the equation (Eq 6.1). The modified model includes lineament (L) and LULC parameters. The subscripts "R" and "W" stand for the respective ratings and weights.

6.2.2. Sensitivity analysis

The impact of the evaluations and weights given to the parameters ought to be checked and assessed. The assessment was carried out using a sensitivity analysis method. In this particular case, there are essentially two types of sensitivity analysis: a single-parameter sensitivity analysis and a map-removal analysis.

Single-Parameter Sensitivity Analysis

The single-parameter sensitivity analysis (SPSA) was used to compare the theoretical and actual weight of individual polygons. The sensitivity assessment helped in examining the impact of a specific layer on the aquifer susceptibility index. It was developed by Lodwick and others (Lodwick et al., 2007) and several researchers in recently applied single sensitivity analysis in their work (Ourarhi et al., 2023; Saravanan et al., 2023; Şener, 2023). The effective weight of the polygons was obtained using Equation (Eq 6.2).

$$W = \frac{P_r P_w}{D_i} * 100 \ldots \ldots \ldots \ldots \ldots \ldots \ldots \ldots \ldots \ldots \ldots \ldots \ldots \ldots \ldots \ldots \ldots \ldots \ldots \ldots 6.2$$

Where:

W refers to the “effective” weight

Pr is the rating of each parameter

Pw is the weight of the respective parameter

Di is the overall vulnerability index

Map-Removal Analysis

The map-removal sensitivity analysis (MRSA) was developed by (Lodwick et al., 1990) and implemented by removing one or more influencing parameters. Map removal was used to check parameter relevance in assessing intrinsic vulnerabilities and deriving the most representative ones in applying the method. So, by removing a given parameter on the vulnerability index the degree of influence was evaluated in the overlay process (Djémin et al., 2016). This map removal index is calculated using Equation (Eq.6.3).

$$S = \left| \frac{V}{N} - \frac{V_{xi}}{n} \right| \ldots \ldots \ldots \ldots \ldots \ldots \ldots \ldots \ldots \ldots \ldots \ldots \ldots \ldots \ldots \ldots \ldots \ldots \ldots \ldots \ldots \ldots \ldots \ldots \ldots 6.3$$

Where:

S is the sensitivity index of the parameter;

V is the intrinsic vulnerability index of the method;

N is the total number of parameters used to calculate V;

Vxi represents the intrinsic vulnerability index obtained after the removal of the parameter X.

6.2.3. Model validation

One of the fundamental stages in modeling groundwater systems is validation. Data scarcity was the main challenge while evaluating the results of the DRASTIC model. Due to its excellent quality, groundwater has historically been the preferred source of drinking water in Ethiopia. However, inadequate waste management, agricultural practices such as chemical fertilizer application, poor sanitation, and lack of sanitary conditions threaten its quality today. The primary concept in the study of groundwater vulnerability is the concentration of pollutants in a particular area. Nitrate concentration is the key determinant of susceptibility when assessing the vulnerability of groundwater (Bera et al., 2022; Elzain et al., 2022; Lakshminarayanan et al., 2021). Ethiopian drinking water is primarily contaminated by nitrate concentration (Akale et al., 2018; Lewoyehu, 2021; Wakejo et al., 2022). Reports also showed that nearly all Ethiopian region's water resources (groundwater and surface water) have nitrate data exceeding the WHO standard limit, with varying degrees.

The study applied nitrate and EC data for validation of the model. Nitrate concentration is a well-known method used for DRASTIC model evaluation (Javadi et al., 2011). Several studies also used EC for vulnerability model evaluation (Sresto et al., 2022; Hasan, et al., 2019).

6.2.4. Generation of thematic layers

DRASTIC index method of vulnerability analysis involves (a) gathering geology and hydrogeologic data; (b) creating a GIS map of the region; (c) calculating the DRASTIC index; and (d) assessing the relative degree of contamination susceptibility. Table (Table 6.1) displays the normal weights and the DRASTIC parameter. Thematic layers of each hydrogeological parameter were created utilizing the ArcGIS program. Water resources and other related parameters are collected from the Ministry of Water and Energy (MoWE). The weather parameters were collected from the National Meteorological Agency (NMA). The geological and other aquifer parameters are collected from the Geological Survey Institute (GSI). To create vulnerability maps, hydro-geological data was eventually gathered, digitalized, and overlaid using GIS. This process creates a new layer known as the DRASTIC index. To determine the modified DRASTIC index, an additional parameter was added to the DRASTIC index, which was lineament and land use (Eq. 6.1). The higher the DRASTIC Index, the higher the vulnerability to groundwater pollution.

For the modified DRASTIC methodology, nine thematic maps were created for the study area's aquifer vulnerability assessment. These parameters were presented as follows:

Depth of water (D)

An area's susceptibility to contamination is mostly determined by its depth to the water table or the distance between the water table and the ground surface. Water depth affects the time available for contaminants to undergo chemical and biological reactions such as dispersion, oxidation, and natural decay. A deep-water table permits tainted waters to penetrate for a sufficient amount of time before attenuation mechanisms take over and effectively remove the pollution (Singh et al., 2015).

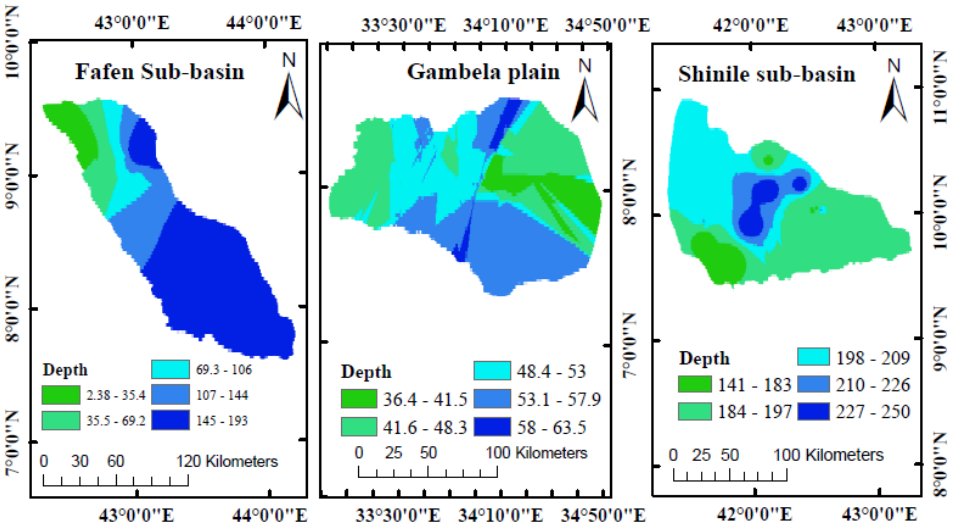

Figure 6. 1 Water depth maps

Depth to the water table is inversely proportional to vulnerability; the greater the depth, the less likely pollutants reach the water table and the greater the potential for contaminant mitigation (Lakshminarayanan et al., 2021). The water table depth in the study area was obtained from geological investigation reports of the water service (MoWE). Compared to the eastern catchments, the Gambela plain area has a narrower range of fluctuation and a shallower water table (Figure 6.1). The spatial distribution of water level produced using the ArcGIS program.

Net recharge (R)

Recharge is the amount of surface water that infiltrates the ground and reaches the water level. Net recharge value can be estimated using field experiments, hydrological precipitation-runoff models, or simply by multiplying the difference between the spatial distribution of evapotranspiration and the spatial distribution for mean annual rainfall by an infiltration coefficient (L et al., 2021). To determine the net recharge, we applied the Piscopo method (Piscopo, 2001):

$$Net\ recharge = Soil\ permeability + Rainfall\ (mm) + slope(\%) \dots\dots\dots\dots\dots\dots 6.4$$

The SRTM DEM data of USGS was used to determine the slope of the study area. The slope in percent was determined by spatial tool analysis of ArcGIS. The mean annual rainfall is determined from the past three decades' daily rainfall. Permeability of soil collected from the governmental organization (MoWR). The map of net recharge (Eq.6.4) was determined from the raster calculator tool of spatial analysis of ArcGIS. A high recharge zone is a zone of higher precipitation. The

recharge is directly proportional to the topographical elevation of the study areas (Figure 6.2). Reclassifying and giving weight were performed accordingly (Table 6.1).

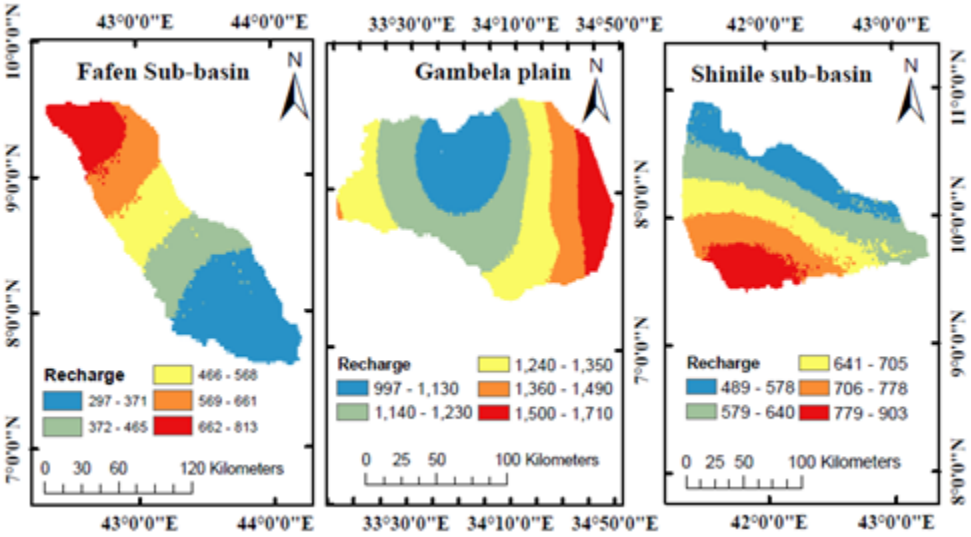

Figure 6. 2 Net recharge maps

Aquifer media (A)

Aquifer media is a sign of the saturate zone's material properties. Aquifer media considers the characteristics of the media within the immersed zone such as porosity, grain estimate, and porousness that control contaminant weakening forms (Khosravi et al., 2021).

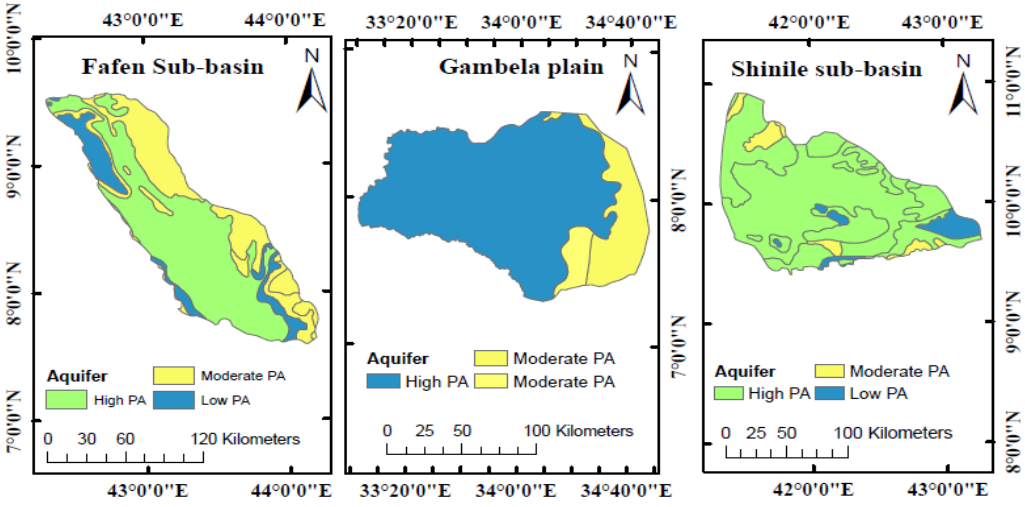

Figure 6. 3 Aquifer media maps

In this study, the aquifer media layer was prepared using the information gathered by Water and Energy. The majority of the area has high aquifer productivity (Figure 6.3). Productive aquifers are also susceptible to vulnerability and vice versa.

Soil media (S)

The upper part of the unsaturated zone that reaches the organic material and plant roots, the soil media, is active. The amount of recharge that can contaminate groundwater is controlled by a soil type (Singh et al., 2015). The study regions' soil maps, created from the latest soil map of Ethiopia (Figure 4.4)

Topography (T)

Topography is an indicator of land slope changes in the area. The time that water spends on the soil's surface is governed by topography, which also affects the rate of infiltration. Additionally, topography reveals where pollutants are concentrated. The SRTM DEM of the research region retrieved from the USGS website was used to prepare the surface's slope. The research region's topography distribution map is shown in the figure (Figure 4.3).

Impact of vadose zone (I)

The region between the soil cover and the aquifer is referred to as the unsaturated zone or vadose zone. The attenuation behavior of materials that are above the groundwater table and below the soil is demonstrated by the vadose zone characteristics. The geological data of the study region was used to prepare the vadose zone map of the study area (Singh et al., 2015; Patel et al., 2022). The impact of the vadose zone was obtained from the lithological cross-sections of core data. The vadose zone media in the study region includes sandstone, limestone, basalts, alluvial, shale, etc.

Hydraulic conductivity (C)

An aquifer's hydraulic conductivity is a characteristic that describes how easily water can flow through the aquifer. The amount of contamination depends on how quickly groundwater flows. Groundwater flow, which is the primary regulator of the flow rate of contaminants, is governed by hydraulic conductivity. That indicates that groundwater vulnerability is directly proportional to aquifer hydraulic conductivity (Omeje et al., 2023).

Lineaments (L)

Lineaments serve as important markers for groundwater exploration because they reveal how groundwater moves and is stored. Higher lineament density values could indicate greater potential for groundwater contamination because lineament refers to a variety of linear features of the land surface related to geological evolution and closely related to groundwater flow and contaminant migration. The lineament was produced from the SRTM DEM data with ArcGIS spatial tool analysis (Figure 4.7).

LULC

Land use practices, especially in agricultural areas have demonstrated the anthropogenic domain significantly affects the quality of groundwater. The MODIS satellite data was used to generate the land use of the study regions. A land-use map was created to assess the potential for groundwater contamination due to the pollutants that could be released from residential areas and agricultural activities. The main LULC in the study regions includes forests, shrublands, grasslands, and croplands (Figure 4.8). Grassland and shrublands are the major LULCs of the study area.

Table 6. 1 The assigned rates and weight given to the parameters

parameters	Class (sub-parameters)	Rating	weight
Depth	2.15-62.61	10	5
	62.6-116.8	9	
	116.8-136.4	5	
	136.4-152.5	3	
	152.5-204.35	1	
Recharge	Very high	10	4
	High	9	
	Moderate	5	
	Low	3	
	Very low	1	
Aquifer media	Low PA	4	3
	Moderate PA	7	
	Highly PA	10	

Table 6.1 Continued….

Soil media	Sandy loam	6	2
	Loamy sand	7	
	Loam	5	
	Clay	3	
Topography (slope in %)	0-2	10	1
	2-6	9	
	6-12	5	
	12-18	3	
	>18	1	
Impact of vadose zone	Sandstone	6	5
	Shale	3	
	Alluvial and lacustrine deposits(Q)	10	
	Alkaline and transitional basalt	9	
	Limestone	7	
	Gneisses	4	
Hydraulic conductivity	0.01-0.5	1	3
	0.5-2	3	
	2-5	5	
	5-15	9	
	15-28	10	
Lineament density	Very high	10	5
	High	9	
	Moderate	5	
	Low	3	
	Very low	1	
LULC	Closed Shrublands	5	3
	Open Shrublands	5	
	Woody Savannas	3	
	Grasslands	3	
	Croplands	8	
	Urban and Built-up lands	7	
	Barren	2	

6.3. RESULTS AND DISCUSSION

6.3.1. DRASTIC Index Map

This paper's primary goal is to determine the groundwater vulnerable zones in Ethiopian alluvial aquifers using a Geographic Information System (GIS) and the modified DRASTIC model. To perform DRASTIC analysis of groundwater vulnerability assessment, the hydrogeological parameters of the study area were used and evaluated. Each parameter was given a value ranging from 1 (least important) to 10 (most important), based on the level of susceptibility. The most significant and susceptible parameter was given a higher weight, while the least significant and resistant parameter received the lowest weight. Each of these factors was rated and given a weight according to how similar it was to all the areas in the table (Table 6.1). The overlay analysis and index calculation were performed in the raster calculator tool of ArcGIS.

Here, the research applied the modified DRASTIC method for the study regions by adding the two additional parameters (lineament and LULC). A modified DRASTIC vulnerability map of the watershed was developed using overlay analyses of water depth, net recharge, aquifer media, soil media, topography, vadose effects, hydraulic conductivity, line alignment, and land use land cover parameters. These rate and weight values, as well as the specifics of the DRASTIC parameters that were employed, were covered above.

The value of the DRASTIC index range is different for each study region. The results of the index range from 94 to 269 for the Fafen-Jerer, 111 to 254 for the Gambela, and 92 to 252 for the Shinile sub-basin (Figure 6.4 and Table 6.2). These index values were used to categorize the susceptible zones. A higher vulnerability value denotes a higher potential for surface pollution to enter an aquifer and spread. In other words, a zone with a low index value is seen to be less vulnerable, whereas one with a higher index value is thought to be more vulnerable.

Different studies show different index values for DRASTIC analysis (Awawdeh, et al.,2015; Malakootian & Nozari, 2020; Aboulouafa, et al., 2017, Ahmed, et al.,2017). The classification of high, medium, and low is also different from study to study. Similar results of values are also found in researchers' reports (Colins et al., 2016; Kirlas et al., 2023). The classification of the DRASTIC index value is based on ArcGIS tools. Most studies applied the natural breaks (Jenks) classification method of the ArcGIS tool (Kazakis & Voudouris, 2015; Arzu & Fatma, 2013).

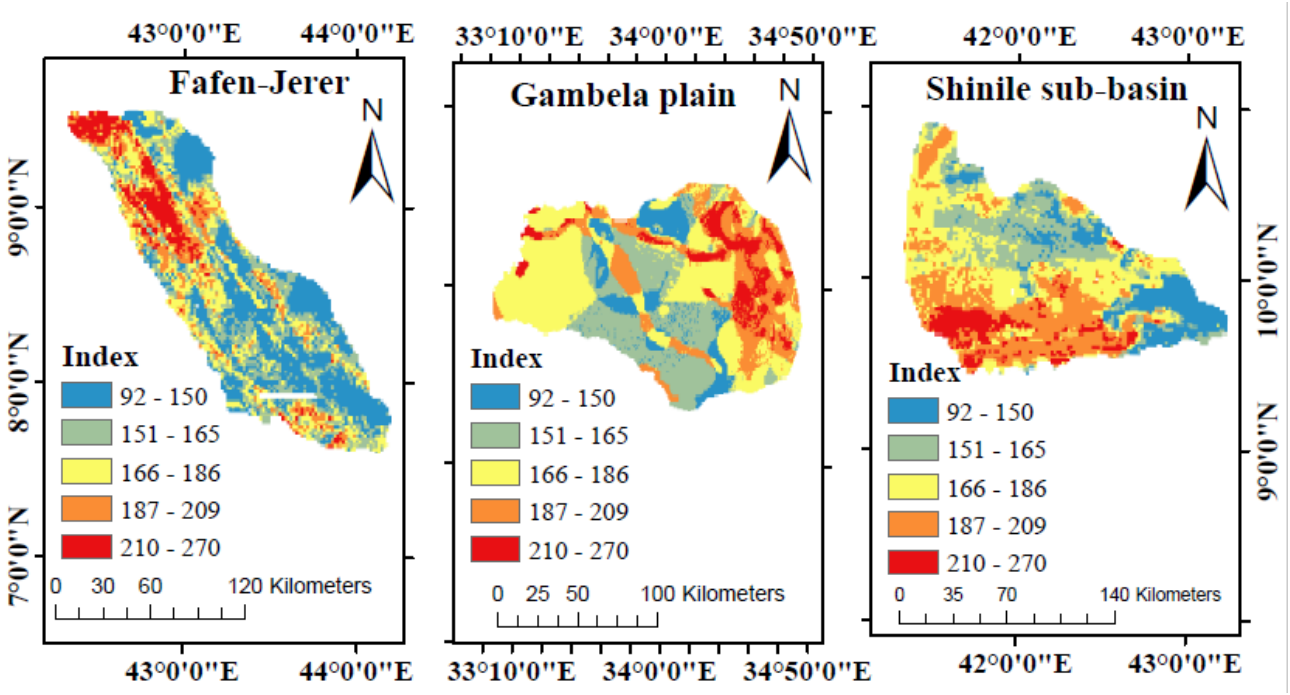

Figure 6. 4 Vulnerability map of the modified DRASTIC Index

Therefore, after calculating the vulnerability index in the raster calculator tool of ArcGIS, the result was reclassified into five classes (Malakootian & Nozari, 2020; Aboulouafa, et al., 2017, Ahmed, et al.,2017) (very low, low, medium, high, and very high) according to the natural breaks (Jenks) classification method.

The result shows that 21.4% (3621..5 sq. km) of the Fafen-Jerer, 28.7% (5146.7 sq. km) of the Gambela, and 33.8% (6496.5 sq. km) of the Shinile are grouped in the high and very high vulnerability zones (Table 6.2). The low and very low-risk zones are 55.7% (9428 sq. km) in the Fafen-Jerer, 34.8% (6256.9 sq. km) in the Gambela, and 34.6% (6640.8 sq. km) for the Shinile sub-basin. These show the high and very high-risk zones cover a larger area in all regions compared to lower-risk zones.

Table 6. 2 The classified DRASTIC index value with area coverage

	Model Value Range	Class	Percentage of Area coverage		
			Fafen-Jerer	Gambela	Shinile
Modified DRASTIC Index	<150	Very low	34.10	10.00	14.40
	151-165	Low	21.62	24.89	20.18
	166-186	Medium	22.88	36.42	31.59
	187-209	High	12.41	19.78	26.43
	>209	Very High	8.99	8.92	7.40

A similar study of groundwater vulnerability assessment by applying the original DRASTIC and modified DRASTIC model was found in several regions previously, especially in arid regions with similar agro-climatic and geological environments (Arya et al., 2020; Jmal et al., 2022; Khemiri et al., 2013; Taheri et al., 2021, 2023). The results show that the vulnerability index is higher than the previous study around Dire Dawa using the original DRASTIC index (Tilahun & Merkel, 2010). The modified index results of the previous studies at the Elalla-Aynalem catchment (Berhe et al., 2020), and Megech watershed (Asfaw & Mengistu, 2020) in northern Ethiopia also have a lower value of index compared to the present results. The value of the DRASTIC index varies depending on the study area. The changes in the index are determined by the values of the parameters and the area's vulnerability to pollution. According to various research findings, the area has a higher value of 200 and above (Abdullah, 2017; Gheisari, 2017; Ahmed, 2017).

6.3.2. Results of sensitivity analysis

Single parameters sensitivity analysis (SPSA)

Impact vadose zone, depth to water, and aquifer media are the most sensitive parameters, and they have a greater impact on the vulnerability of the study area. Recharge, lineaments, hydraulic conductivity, LULC, soil, and topography followed the order of influence on groundwater vulnerability. The impact vadose zone has the highest effective weight while topography lowest effective weight. The analysis shows the effective weight of the model parameters agrees with the theoretical weight.

Map removal Sensitivity analysis

Map removal sensitivity analysis revealed that the average partial vulnerability index for soil and topographic parameters was larger than the removal for other parameters (Tables A6.1, A6.3, & A6.5). The analysis shows that the vulnerability map is strongly influenced by the depth of the water table and the impact of the vadose zone parameters for the Fafen-Jerer and the Gambela plain (Tables A6.2 & A6.4). For the Shinile sub-basin topography and impact vadose zone were influencing parameters (Table A6.6). Land use and land cover (Fafen-Jerer and Gambela) and soil media (Shinile) have the least impact on the hazard map.

6.3.3. Validation of results

The nitrate and EC concentration were compared to the created vulnerability map to perform the validation. The findings of the correlation indicate a positive association between the concentration of pollutants and danger zones. The validation of both Fafen-Jerer and Shinile was performed using nitrate concentration. In the Fafen-Jerer sub basin higher nitrate concentration at the upper catchment around Fafen and lower catchment of Jerer river. There is a larger nitrate concentration in Shinile, the upper catchment around Dire Dawa city, up to 100 mg/L. The Gambela plain risk map was compared to the EC concentration map. The eastern and northeastern areas have relatively high EC concentrations.

The nitrate concentration and risk map for Fafen-Jerer and Shinile become $R^2 = 0.56$ and $R^2 = 0.71\%$ respectively (Figure 6.5). The verification result indicates that the risk map is directly related to concentration distribution in the study region. The study employed EC to validate the risk map for Gambela Plain, and the results indicate a favorable association between the EC distribution and the danger zone (Figure 6.6).

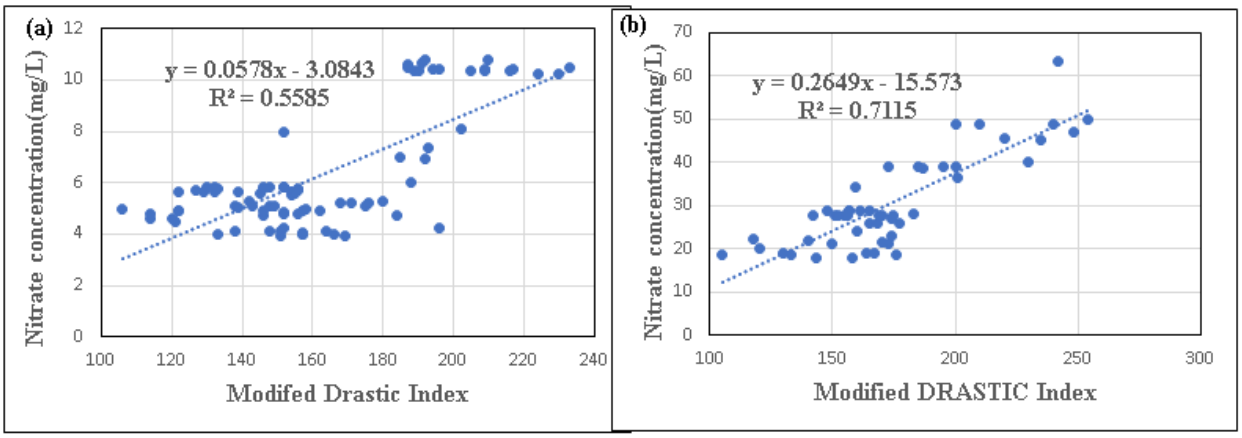

Figure 6. 5 DRASTIC index and nitrate concentration (a) Fafen-Jerer and (b) Shinile

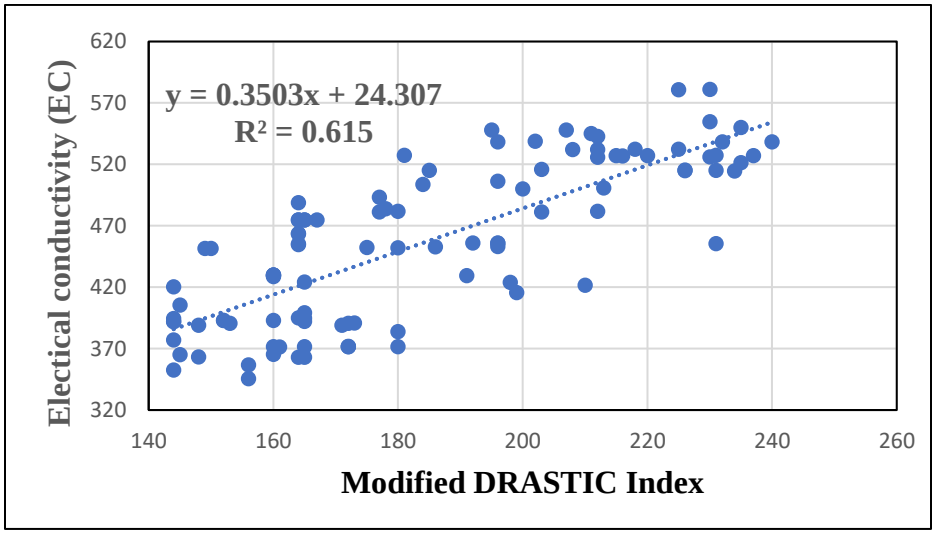

Figure 6. 6 DRASTIC indexes versus Electrical conductivity (EC) for Gambela plain

The depth of the water table and the impact of the vadose zone are the major parameters that influence the maps of groundwater vulnerability in the study area. Removing these parameters from the index calculation makes a big difference and significantly reduces the vulnerability index. These results justify the greater weighting of these two parameters when using the DRASTIC method. These results have similar output to the study on the Elalla-Aynalem catchment in northern Ethiopia (Berhe et al., 2020) and the Dabou region in southern Côte d'Ivoire (Djémin et al., 2016). The impact of parameters on the vulnerability index varies by region. The water table and land use (Goodarzi et al., 2022; Omeje et al., 2023), depth, recharge, and soil (Gupta & Kumari, 2023), and depth to water (Smail & Dişli, 2023) are some examples of different sensitivity parameters result of DRASTIC index analysis. The recharge and topography (slope) are the other parameters that

influence the aquifer vulnerability analysis of the region. LULC, soil, and hydraulic conductivity are the least influence on the vulnerability index.

6.4. CONCLUSION

Using the modified DRASTIC approach, an effort has been made to evaluate the aquifer susceptibility of alluvial groundwater to determine the impact of land use activities and lineaments on groundwater vulnerability. Five sensitive zones have been identified using the vulnerability index: very low, low, moderate, high, and very high. The result of the DRASTIC map analysis shows that 21.4%, of Fafen, 28.7%of Gambela, and 33.83% of Shinile are grouped in the high and very high-risk zones. While low and very low-risk area covers 55.72%, of Fafen, 34.89% of Gambela, and 34.58% of the Shinile area. The medium class covers a significant portion of the watersheds, in each study region. Gambela and Shinile have a high-risk area for intrinsic vulnerability to pollution compared to the Fafen-sub basin. High-risk zones are areas covered by grasslands, loam and loamy sand soil texture, high recharge zones, and lower water depth zones of the regions. The results also showed that deep water level depth, low hydraulic conductivity, and sparse population areas were less susceptible to groundwater risk. Nitrate and electric conductivity (EC) contamination was used to validate the model, which was found to be suitable for the watershed's current conditions. In the assessment of groundwater risk to contamination for intrinsic vulnerability in the study area, the modified models provided accurate results. The study's findings support the use of the DRASTIC model by policymakers to more accurately delineate aquifer zones that are susceptible to anthropogenic contamination, particularly in and around agricultural and industrial areas.

CHAPTER 7

CLIMATE AND LAND COVER CHANGES ANALYSIS

Abstract

Climate and land use land cover (LULC) change are the main challenges to present-day water resources management. The impact of climate and land cover change on groundwater resources was studied in alluvial regions (i.e. Western Catchment (WC) and Eastern Catchment (EC) catchments) in Ethiopia. The technique employs a deduction grid to merge the effective rainfall and De Martone aridity index (DMI) for evaluating the influence of climate effect on groundwater using spatial dimensions. The study applied a bias-corrected ensemble of three global climate models (GCM): (CMCC-ESM2, FGOALS-g3, and MIROC6) experiments of CMIP6 to perform high-resolution climate projections under SSP2-RCP4.5 and SSP5-RCP8.5. To find the changes in land cover, the historical land cover analysis was assessed. The climate results show an average annual temperature rise of ~0.95 and ~0.30 for the last three decades for WC and EC respectively. And an annual precipitation reduction of ~4.2 mm/year and ~1.2 mm/year over the period for WC and EC, respectively. The temperature forecast for the next time indicates that it will rise in both catchments. The potential evapotranspiration will increase for catchment by the end of 2070s following temperature increments. The climate effect on the groundwater was assessed for the historical and future periods. Five subcategories were created from the resultant values, ranging from very high effect to very low effect. Very low zones are not sensitive to climate change, whereas very high zones are sensitive. The results show the coming climate change will significantly affect the groundwater resources. The western section of WC and the northern and southern extremes of EC will be highly vulnerable to climate change. The impact of climate change analysis was supported by empirical estimation of the potential recharge technique. The results also show the future potential recharge will be reduced in both catchments. This research has implications for water resource management, agriculture, social and economic livelihoods of people in drought-prone areas and other similar regions.

Keywords: Climate impact, CMIP 6, Groundwater, Effective precipitation, Recharge, Ethiopia

7.1. INTRODUCTION

The lack of available water is a major problem in areas with a semi-arid environment (Aibaidula et al., 2023; Saade et al., 2021). One of the most ecological concerns for advancement is global warming as it has an impact on water security, especially in arid and semi-arid regions. In areas with little precipitation, global warming can improve the water cycle through higher temperatures, concentrated precipitation during short bursts, and longer dry spells (Gössling & Dolnicar, 2023; Lawrence et al., 2023). Climate change's impact on water resources in general (Asif et al., 2023, 2023; Papa et al., 2022; Sheikha-Bagem Ghaleh et al., 2023; Tanguy et al., 2023) and on groundwater resources in particular (Alghamdi et al., 2023; Eltarabily, et al., 2023; Patil et al., 2020) were studied in different regions with different methods. Because groundwater depends on temperature-dependent evapotranspiration rates and variations in precipitation patterns, it is especially susceptible to the effects of climate change (Eltarabily, et al., 2023). Several approaches have been employed in the past to demonstrate how groundwater is changing due to climate change. The water level variation (Fallahi et al., 2023; Nourani et al., 2023; Stelling et al., 2023), quality change (Yuan et al., 2023), and recharge variation (Dubois et al., 2023; Gumuła-Kawęcka et al., 2023), are the primary methods used to address how the impact of climate and land use change on groundwater.

According to a study, Ethiopia's agricultural and water sectors have already been impacted by the consequences of climate change (Urgessa, 2013; Mera, 2018; Teshome & Zhang, 2019; Chakilu et al., 2022; Adane, et al., 2023). Recently several researchers have confirmed that the climate impact on water resources is high in Ethiopia (Hailemariam, 1999; Setegn et al., 2011; Hussen et al., 2018; Roth et al., 2018). In every region of Ethiopia, there have been noticeable variations in precipitation and temperatures (Avhmed et al., 2023; Gedefaw, 2023; Palmer et al., 2023). Due to an excess of precipitation, certain places have experienced floods (Mitiku et al., 2023), while other regions have been affected by extended droughts due to insufficient rainfall (Mera, 2018). Frequent dry spells in Ethiopia's Somali, Afar, and Borana regions demonstrate the negative effects of climate change (Catley et al., 2014; Guye et al., 2022; Kamangira & Melaku, 2023).

However, very little study has been conducted on how Ethiopia's climate affects groundwater (Kahsay et al., 2018; Khadim et al., 2023; Telford & Lamb, 1999; Tigabu et al., 2021; Yifru et al., 2021). Comprehensive hydrometeorological datasets at several scales (including precipitation,

groundwater level readings, streamflow, and temperature) are crucial for evaluating the impact of climate change on groundwater resources. Obtaining hydrogeological records in a developing country such as Ethiopia is extremely difficult. Additionally, the other hydro-meteorological records often have equally constrained durations and monitoring intervals.

This study is conducted in a tropical region where various changes in water resources are occurring due to climate change (Lawrence et al., 2023). Over the past period, the rainfall has been reducing alarmingly while the temperature of the area has been rising. No previous study has explored and confirmed the effects of climate change on groundwater in the studied regions. Water resources research such as this is essential for the area since it is already heavily burdened by auxiliary farming practices and a lack of potable water, which impedes activities that rely on it.

With the advent of numerous climate model products that can assess and forecast future climatic conditions in a particular location, the study of climate change in the twenty-first century is becoming more and more digital. The primary climate model that accurately replicates the climate parameters and applicable globally is the General Circulation Model (GCM) simulation (Hamed et al., 2022; Iqbal et al., 2021; Try et al., 2022). The technique utilized in this specific investigation adopts a comparable methodology to the one employed by Nistor (2006), wherein a spatially diverse analysis of climate effects was modeled for both present and future epochs.

The objective of this research was to show the spatial and temporal distribution of climate change's effect on groundwater in western and eastern Ethiopia. The study focuses on three specific objectives: I) determining land cover and NDVI change; II) determining climate change; and III) investigating the effects of climate change on groundwater while accounting for changes in land cover. This analysis aimed to fill this gap and determine the effectiveness of the suggested method in terms of spatial distribution and temporal coverage. Hence, the uniqueness of this research was dual - firstly, the methodology utilized and secondly, the inclusion of both the spatial and temporal coverage. To ascertain the impact of the precipitation variation, the potential groundwater recharge was also computed using the results of the climate model. As a consequence, this research would provide a basic understanding of the state of groundwater resources under present and future climatic circumstances, which would aid in the development of mitigation techniques. The availability of water resources is impacted by climate change, which poses a challenge to the

development of water resources worldwide. Thus, the current chapter illustrates how LULC and climate change impact the groundwater resources of alluvial aquifers.

7.2. MATERIALS AND METHODS

The research applied global climate models (GCM) data to predict the future change effect on groundwater. The land cover parameters of the studied regions were also considered to regulate the land cover effect on the groundwater through crop evapotranspiration determination. The hydrological parameters of the catchments are presented in the figure (Figure 7.1).

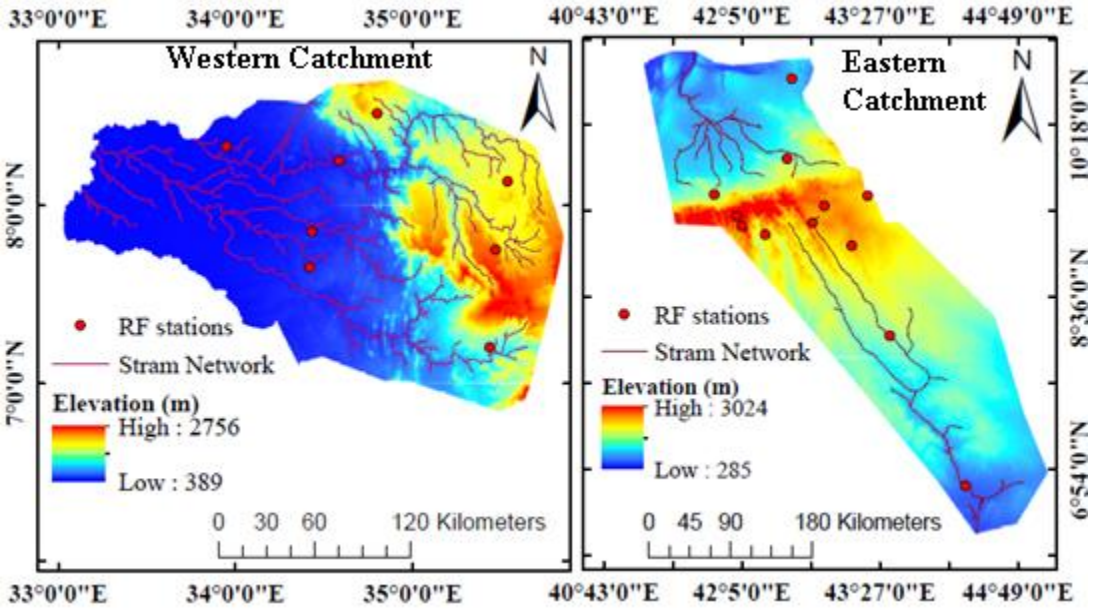

Figure 7. 1 Topographic map of the study area

7.2.1. Climate data model

The study applied the CMIP6 climate model product from the World Climate Research Program website / https://esgf-node.llnl.gov/projects/cmip6 /. The two-climate scenario of the representative concentration pathway (SSP2-RCP 4.5 and SSP5-RCP 8.5) was used. For the future climate change analysis, the research applied the projection of the climate model for the present (2011-2040) and future (2041-2070) cases. The weather data comes from the National Meteorological Agency of Ethiopia. Geographic Information System (GIS) software was used for climate data preparation and mapping. The general methodology of the investigation is shown in the framework (Figure 3.6).

7.2.2. Model Selection

The available GCM models were found and listed for the research regions based on the literature review. Seven GCM models were chosen from the available models to be assessed for the climatic forecast of two district catchments. Euro-Mediterranean Centre on Climate Change with Climate and Earth System Models (CMCC-ESM2), the Earth System Model EC-Earth3 with carbon cycle (EC-Earth3-CC), Flexible Global Ocean-Atmosphere-Land System Model Grid-Point Version 3 (FGOALS-g3), Model for Interdisciplinary Research on Climate version 6 (MIROC6), Max Planck Institute Earth System Model (MPI-ESM1-2-HR), Meteorological Research Institute Earth System Model Version 2.0 (MRI-ESM2-0) and NUIST Earth System Model (NESM) version 3 (NESM3) were evaluated models with meteor observations of 20 stations data. The parameters of the climate model are presented in the table (Table 7.1).

Table 7. 1 Descriptions of global climate models (GCM)

No	GCM	Institution	Resolution (Lon.* Lat., Deg)	References	Remark
1	CMCC-ESM2	Euro-Mediterranean Centre on Climate Change, Italy	1^o*1^o	(Lovato et al., 2022)	Selected
2	EC-Earth3-CC	European EC-Earth consortium	0.7^o*0.7^o	(Farhat et al., 2022)	
3	FGOALS-g3	Chinese Academy of Sciences, China	2^o * 2.3^o	(L. Li et al., 2020)	Selected
4	MIROC6	Japan Agency for Marine-Earth Science and Technology, Japan	1.4^o*1.4^o	(Tatebe et al., 2019)	Selected
5	MPI-ESM1-2-HR	Max Planck Institute for Meteorology, Germany	0.94^o * 0.94^o	(Müller et al., 2018)	
6	MRI-ESM2-0	Meteorological Research Institute, Tsukuba, J + C34apan	1.1^o*1.1^o	(Yukimoto et al., 2019)	
7	NESM3	Nanjing University of Information Science and Technology, China	1.9^o *1.9^o	(Yang et al., 2020)	

Note that "selected" in the remark is to state that the data from the three models were applied for the projected climate analysis.

The study employed model assessment criteria, including Root Mean Square Error (RMSE), Percent Bias (PBIAS), Nash-Sutcliffe Efficiency (NSE), and Correlation Coefficient (R^2), to evaluate the GCM model. The best-performing bias-corrected CMIP6 models were ultimately

chosen to forecast the future climatic extreme indices for the regions. The results showed that CMCC-ESM2, FGOALS-g3, and MIROC6 have the best agreements with the study region's meteorological observation (Table 7.2) for both precipitation and temperature datasets.

Table 7. 2 GCM models' authentication with ground observations

Climate Models	Correlation Coefficient	RMSE	R2	PBIAS	NSE
CMCC-ESM2	0.99	13.33	0.98	0	0.84
EC-Earth3-CC	0.94	13.86	0.88	0	0.69
FGOALS-g3	0.98	18.72	0.97	0	0.84
MIROC6	0.99	28.46	0.98	0	0.83
MPI-ESM1-2-HR	0.97	25.29	0.94	0	0.77
MRI-ESM2-0	0.99	14.58	0.97	0	0.83
NESM3	0.67	33.64	0.5	0.01	-0.18

7.2.3. LULC data

Environmental change is mostly caused by changes in land use and land cover (LULC), which is progressively of concern to the public because of its effects on the local, regional, and global environments. Currently, one popular tool for assessing LULC change in many parts of the world is remote sensing equipment (Verburg et al.,2011; Yang et al., 2014)

The data from the Moderate Resolution Imaging Spectroradiometer (MODIS) satellite was used for land cover change analysis. The land cover data of the study region was accessed from the United States Geological Survey (USGS) website. The MODIS instruments acquire information in 36 spectral ranges that span from 0.4 μm to 14.4 μm and exhibit diverse spatial resolutions (2 ranges at 250 m, 5 ranges at 500 m, and 29 ranges at 1 km) (Friedl et al., 2002; Safaei et al., 2021; Tian et al., 2023) (Table 7.3). The MODIS satellite data from 2001-2020 were determined and used for the LULC detection. The Kc was established for each type of land cover at a spatial scale using standard FAO data (Allen et al., 1998) on land cover classified.

For NDVI data, the MOD13Q1 MODIS study used NDVI data from the NASA website. MODIS satellite was launched and developed by NASA in 1999. The MODIS is a key instrument onboard the Terra (originally known as EOS AM-1) and Aqua (originally known as EOS PM-1) satellites

(Tian et al., 2023; Tran et al., 2023; Xiong & Ren, 2023). The character of the MODIS satellite product used for this analysis is presented in the table (Table 7.3).

Table 7. 3 The characteristics of MODIS LULC and NDVI data

	MODIS land cover type	**MODIS NDVI**
Instrument:	MCD12Q1	MOD13Q1
Processing Level:		Level-3
Spatial Resolution:	500m	250 m
Temporal Resolution:	yearly	16 days
Availability	2001, present	2001, present

7.2.4. Change detection

The technique of identifying changes in an object's state by viewing it at various times is known as "change detection" (Hu et al., 2023; Zhu et al., 2022). The change from one LULC class to another class between 2001 and 2020 was quantified. A change matrix plotting land cover changes from 2001 to 2020, assessing overall changes in LULC classes.

Accuracy assessment of LULC

The comparison between the classified image and the ground truth data can be verified by accuracy assessment. The accuracy assessment of a classified image is important for analyzing LULC changes and determining the acceptability of the classification process. 50 sites were chosen at random from the research regions, and Google Earth software was used to confirm the selections to assess the correctness of the LULC interpretation (Bie et al., 2022; Islami et al., 2022; Tasgara & Kumar, 2023). The producer's accuracy (PA), user's accuracy (UA), overall accuracy (OA), and kappa coefficient (K) are the parameters used to evaluate the LULC classification. The formula for each assessment is presented as:

$$Overall\ accuracy = \frac{total\ no\ of\ correct\ classifed\ pixel}{No\ referencce\ pixel} * 100 \dots\dots\dots\dots\dots\dots 7.1$$

$$User\ acuracy = \frac{no\ of\ correct\ classifed\ pixel\ in\ each\ class}{Total\ no\ classified\ \ pixel\ in\ that\ class} * 100 \dots\dots\dots\dots\dots 7.2$$

$$Procedur\ acuracy = \frac{no\ of\ correct\ classifed\ pixel\ in\ each\ class}{Total\ no\ refernced\ \ pixel\ in\ that\ class} * 100 \dots\dots\dots 7.3$$

$$Kappa\ coefficient = \frac{(TS * TCS) - \sum(column\ total * \ row\ total)}{TS^1 - \sum(column\ total * \ row\ total)} * 100 \ldots \ldots \ldots .7.4$$

7.2.5. Potential evapotranspiration (ET_0)

The ET_0 for the given periods was calculated using the Thornthwaite approach, which requires the use of average monthly air temperature information. Despite being a straightforward approach, it is still widely employed in hydrological and climatological research for diverse analyses, particularly for extended timeframes (Proutsos et al., 2021; Thornthwaite, 1948). The formula used to develop ET_0 from the Thornthwaite approach is presented in the equations (Eq.7.5 to 7.7).

$$ET_0 = 16\left(\frac{10T_i}{I}\right)^a \ldots \ldots \ldots \ldots \ldots \ldots .7.5$$

$$I = \sum_i^{12}\left(\frac{T_i}{5}\right)^{1.514} \ldots \ldots \ldots \ldots \ldots \ldots .7.6$$

$$a = 6.7 * 10^{-7}I^3 - 7.71 * 10^{-5}I^2 + 1.7912 * 10^{-2}I + 0.49239$$

where:

Ti = average air temperature

I = annual heat index

The potential evapotranspiration was adjusted using an adjustment factor due to the latitude of each station.

$$ET_{0_{Adjusted}} = ET_{0_{Unadjusted}} * Adjustment\ factor \ldots \ldots \ldots \ldots \ldots 7.7$$

7.2.6. Annul crop evapotranspiration

Using the temperature and precipitation records, the potential evapotranspiration (ET_0) as well as crop evapotranspiration (ETc) were computed. To ascertain the yearly ETc, the ET_0 was multiplied by the Kc of the respective land cover impact (Eq 7.8). Kc values are derived from the land cover standard coefficient (Allen et al., 1998). The calculations were carried out using raster grid data in the ArcGIS system.

$$Annual\ ETc = Annual\ ET0 * Annual\ Kc \ldots \ldots \ldots \ldots \ldots 7.8$$

The Budyko equation was applied to estimate the yearly AETc and effective precipitation(Abera et al., 2019; Budyko & Miller, 1974). The Budyko formula (Eq. 7.9) was applied to determine the yearly AETc using the yearly ETc and precipitation. The technique of AETc computation involves the determination of the aridity index φ as given in the equation (Eq. 7.10) using precipitation data. The Budyko approach has been utilized in numerous investigations of climatology, hydrology, and agricultural research (Tang & Wang 2017; Teng et al., 2012; Wang et al., 2016; Gan et al., 2021).

In the current study, we substituted the ET_0 with the ETc value in the Budyko equation as it was necessary to evaluate the water evapotranspiration while taking into account the land cover capacity for evapotranspiration. Equation (Eq 7.9) demonstrates the calculation of annual crop evapotranspiration (AETc) which includes of annual precipitation.

$$\frac{AETc}{P} = \left[\left(\varphi \tan\left(\frac{1}{\varphi}\right)\right)(1 - exp^{-\varphi})\right]^{0.5} \quad \ldots\ldots\ldots\ldots\ldots\ldots\ldots\ldots\ldots\ldots\ldots\ldots\ldots\ldots 7.9$$

$$Aridity\ index(\varphi) = \frac{ETc}{P} \quad \ldots\ldots\ldots\ldots\ldots\ldots\ldots\ldots\ldots\ldots\ldots\ldots\ldots\ldots\ldots\ldots\ldots\ldots\ldots\ldots 7.10$$

where:

AETc is actual land cover evapotranspiration [mm]

P is total annual precipitation [mm]

7.2.7. Effective precipitation

The quantity of water that may seep into the soil is known as effective precipitation. It is the quantity of water availability that is practically maintained as groundwater rather than being retained as runoff water. Effective precipitation is the portion of the total precipitation that falls on the cropped area during a given period that is used to meet the region's evapotranspiration. Relative to total rainfall, effective rainfall (or precipitation) is the difference between evapotranspiration and total rainfall. The meteorological factors and the usable ground reserves may be used to directly compute the amount of effective rainfall (Nistor et al., 2022). The computation of effective precipitation involved comparing the yearly precipitation with the yearly AETc (as shown in Eq. 7.11) (Sommer et al.,2016; Nistor, 2019;). These computations were carried out at a spatial scale for the past, present, and future time frames.

$$Effective\ precipiation = annula\ precipiation - annual\ AETc \quad \ldots\ldots\ldots\ldots 7.11$$

7.2.8. Aridity indices

De Martone Aridity Index (DMI)

The De Martone Index evaluates the annual levels of precipitation and temperature. Emmanuel De Martone, a French scientist, developed this index during the early 1900s (Pellicone et al., 2019). De Martone's index is determined from the ratio of the average annual rainfall (P) and temperature (T) increased by 10°C (Eq. 7.12)(De Martonne, 1926). The climate of an area characterized by the De Martone aridity index is shown in the table (Table 7.4).

$$DMI = \frac{P}{T + 10} \quad \ldots\ldots\ldots\ldots\ldots\ldots\ldots\ldots\ldots\ldots\ldots\ldots\ldots\ldots\ldots\ldots\ldots\ldots\ldots\ldots\ldots\ldots 7.12$$

UNEP Aridity Index (AI)

The aridity index (AI), was developed by the United Nations Environment Programme (UNEP) and used to classify climatic regimes and monitor drought events (Dave et al., 2019; Ganem et al., 2022). The UNEP aridity index is defined as:

$$AI = \frac{P}{PET} \quad \ldots\ldots\ldots\ldots\ldots\ldots\ldots\ldots\ldots\ldots\ldots\ldots\ldots\ldots\ldots\ldots\ldots\ldots\ldots\ldots\ldots\ldots 7.13$$

where P and PET are respectively the mean annual precipitation [mm] and the potential annual evapotranspiration [mm](UNEP. et al., 1997). The P/PET ratio is a better representation of climate change (Li et al., 2017). According to the UNEP aridity index, aridity is classified into five categories (climate classification) (Boschetto et al., 2010) (Table 7.4)

Table 7. 4 The climate classification according to aridity index value

(Baltas, 2007; UNEP (1992).)

Index	**Type of climate**	**Index Value**
De Martone Aridity Index	Arid	DMI<10
	Semi-arid	10≤DMI<20
	Mediterranean	20≤DMI<24
	Semi-humid	24≤DMI<28
	Humid	28≤DMI<35
	Very humid	35≤DMI≤55
	Extremely	DMI>55
UNEP Aridity Index	Hyper-arid	<0.05
	Arid	0.05_0.20
	Semi-arid	0.20_0.50
	Dry sub-humid	0.50_0.75
	Humid	>0.75

7.2.9. Climate Impact on Groundwater

The approach to evaluating the impact of climate on groundwater takes into account the effective rainfall and climate aridity. The method integrates effective precipitation with the De Martone aridity index, considering both spatial and temporal scales. This enables the identification and visualization of areas on the map that are more or less affected by climate changes in groundwater resources. The method was available for use in a study looking into how groundwater is affected by climate change (Haidu & Nistor, 2020; Nistor, 2019; Nistor & Cervi, 2021; Nistor & Mîndrescu, 2019).

7.2.10. Recharge Estimation

Using the empirical approach, the potential recharge estimation was applied to the precipitation outcomes of the three models. Natural rainfall is known to be one of the primary sources of groundwater recharge. The infiltrating precipitation replenishes the soil moisture deficit and/or percolates down to recharge the aquifer. Evaluation of rainfall recharging was carried out by

employing several empirical correlations between recharge and rainfall generated for different climate-related locations in different regions of the world (Chaturvedi, R.S., 1973; Kumar and Seethapathi, 2002; Krishna, 1970, Andualem et al., 2021)).

For areas of limited data, Krishna (1970) developed an empirical relationship between precipitation and groundwater recharge (Eq.7.14). He relates the precipitation with recharge with the following formula:

$$R = K(P - X) \ldots\ldots\ldots\ldots\ldots\ldots\ldots\ldots\ldots\ldots\ldots\ldots\ldots\ldots\ldots\ldots\ldots\ldots\ldots\ldots\ldots..7.14$$

Where:

R=groundwater recharge (mm)

P=annual precipitation (mm)

Krishna Rao established correlations for various levels of yearly rainfall (Table 7.5).

Table 7. 5 The class of recharge estimation according to Krishna Rao (1970)

No	Formula	Annual rainfall (P) in mm
1	R=0.20(P-400)	400-600
2	R=0.25(P-400)	600-1000
3	R=0.35(P-600)	Above 2000

This research applied Krishna Rao's (1970) technique and constructed an empirical relationship to calculate groundwater recharge. We interpolate values for yearly precipitation less than 400 mm and values between 1000 and 2000 mm, which are not included in the Krishna formula (Table 7.5). Therefore, for yearly precipitation less than 400mm we applied R=0.20(P-300), and for the range of annual rainfall between 1000 to 2000 we applied R=0.30(P-500) as implemented by Andualem (2021).

7.3. RESULTS

Using the methodology, it was possible to determine, at a spatial scale over two time shifts including the historical period analysis, how the climate affects groundwater resources in western and eastern Ethiopia. After the LULC analysis was finished, the annual ETc and annual AETc calculations were performed in the first step.

7.3.1. Results of LULC analysis

Croplands, forest, forests, grasslands, wetlands, water bodies, and urban are the LULC classes for the western catchment. Grasslands and forests cover about 75% of the area in WC. The western plains of the WC have been dominated by grassland land cover. The forests land cover represents the southeastern portion of the WC. However, built-up areas are land covers with the lowest coverage (Figure 7.4 a & b). The eastern catchment consists of five main LULC classes; bare lands, cropland, grasslands, shrubland, and urban land. Of these land cover classes; shrubland and grassland cover more than 88% of the EC. These land covers, dominate both the northern and southern parts of the eastern catchment (EC). Barren land cover type covers many areas in the northeastern part (around Aysha) and a small area in the southern part (northeast of Kebridehar) Urban and croplands have the lowest area coverage in the eastern catchment (Figure 7.4 c & d).

Land cover change (2001-2020)

The change in cover of the forest, and croplands is the largest change that occurred in the WC (Figure 7.2). The forest area coverage expanded by 513.4 sq. km of area while the cropland cover was reduced by 515.4sq.km. Wetlands, grasslands, and water bodies show a change of 3.7, 2.2, -0.9 sq. km respectively for the past two decades. There is no significant change for urban areas.

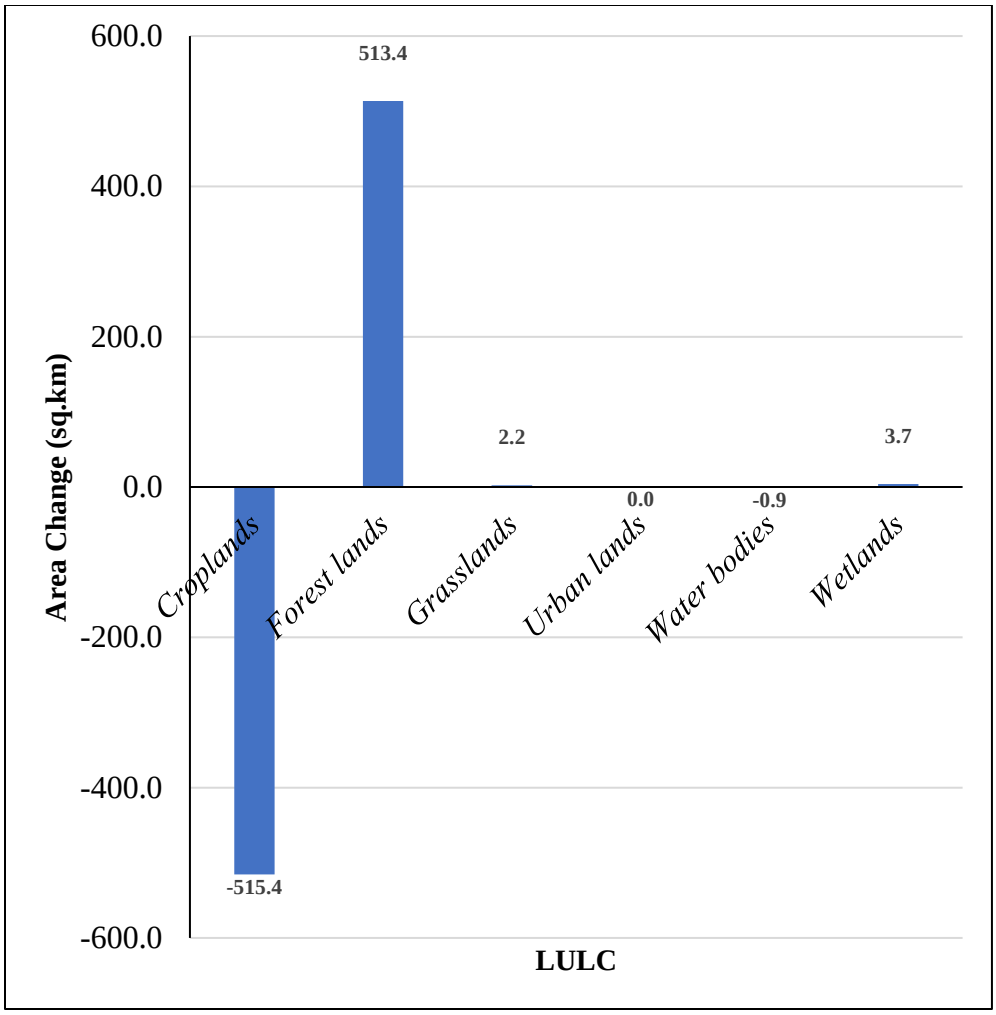

Figure 7. 2 The LULC change between 2001 and 2020 for the WC

The results of the land cover change analysis in EC showed that the grassland area was growing for the past two decades by 14454 sq. km (Figure 7.3). Similarly, croplands, and urban are the other land covers that have increments results in EC. However, shrublands and barren areas are reduced by 13686.2, and 1296.4 sq. km respectively.

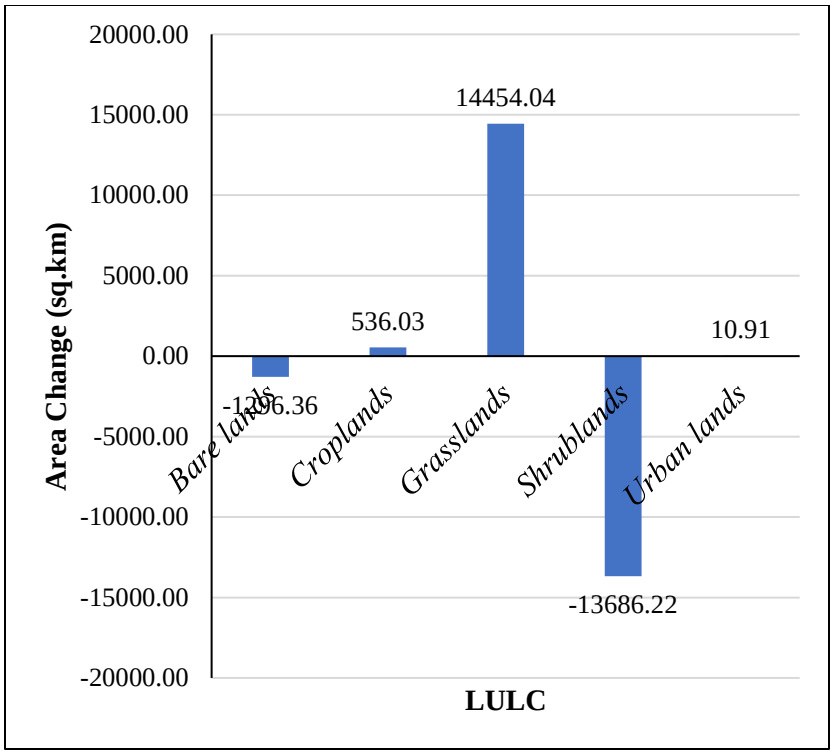

Figure 7. 3 The LULC change between 2001 and 2020 for the EC

According to the findings in WC, there has been growth in grassland in the western region along the rivers' flow paths. The results also indicate a decline in the density of the thick evergreen forest in the southeast (Figure 7.4 a & b). The EC land cover change shows that an extensive part of open shrubland in the central and southern parts of the region was replaced by grasslands (Figure 7.4 c & d).

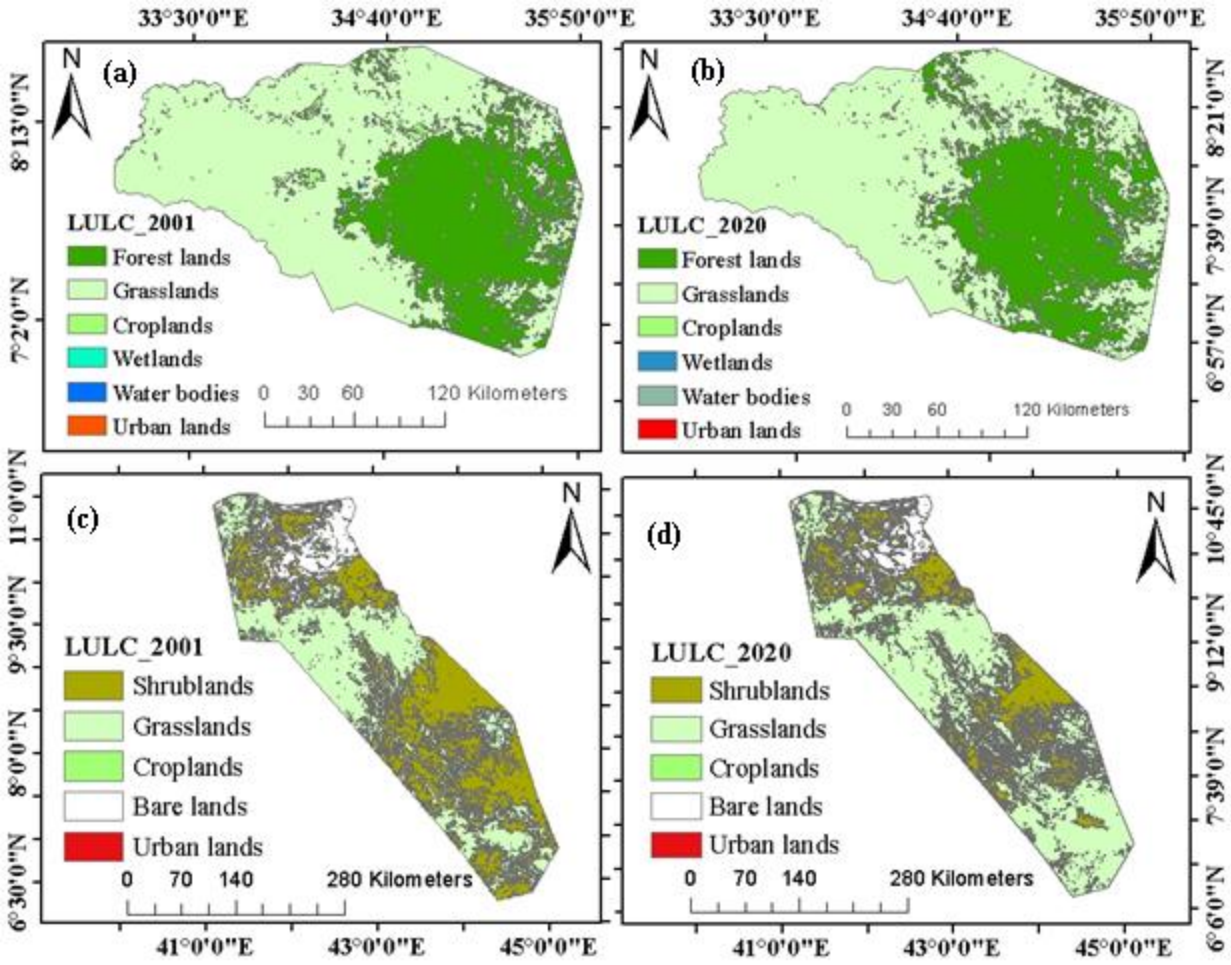

Figure 7. 4 LULC change for the WC (a & b) and EC (c & d)

Change detection between 2001_2020

The main change of LULC in WC is from grasslands to forests (2054.6sq.km). The change from grasslands to forests (1550.5 sq. km), croplands to grasslands (528.7sq.km), and grasslands to croplands (24.6sq.km) are the other changes that mainly occurred for the past periods. The other significant change in LULC is from cropland to grassland (Figure 7.5).

The LULC change detection of EC shows that there was a huge change of shrublands to grassland land covers (16868.7sq.km). The other major change is the change of grassland to shrublands (2099.5sq.km). Bare lands to shrublands (1494 sq. km), grasslands to croplands (641.8sq.km), and bare lands to grassland (287.9sq.km) are the other main changes between 2001 and 2020 (Figure 7.6).

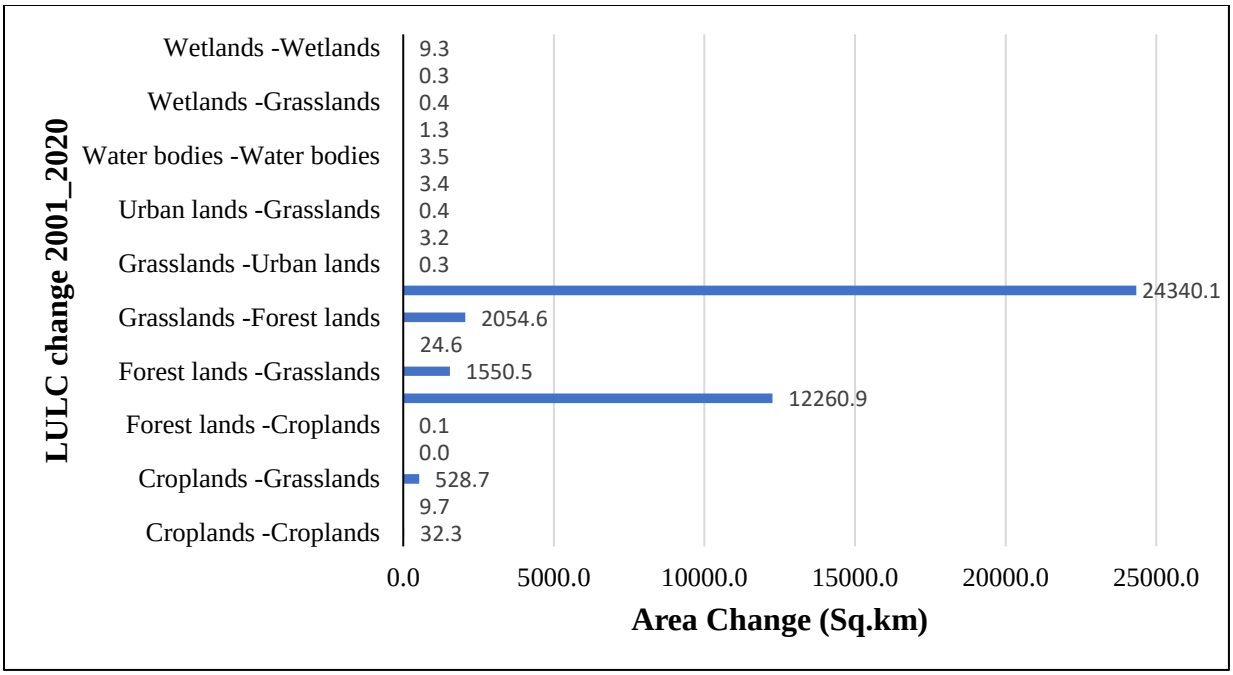

Figure 7. 5 LULC change detection for WC (2001_2020)

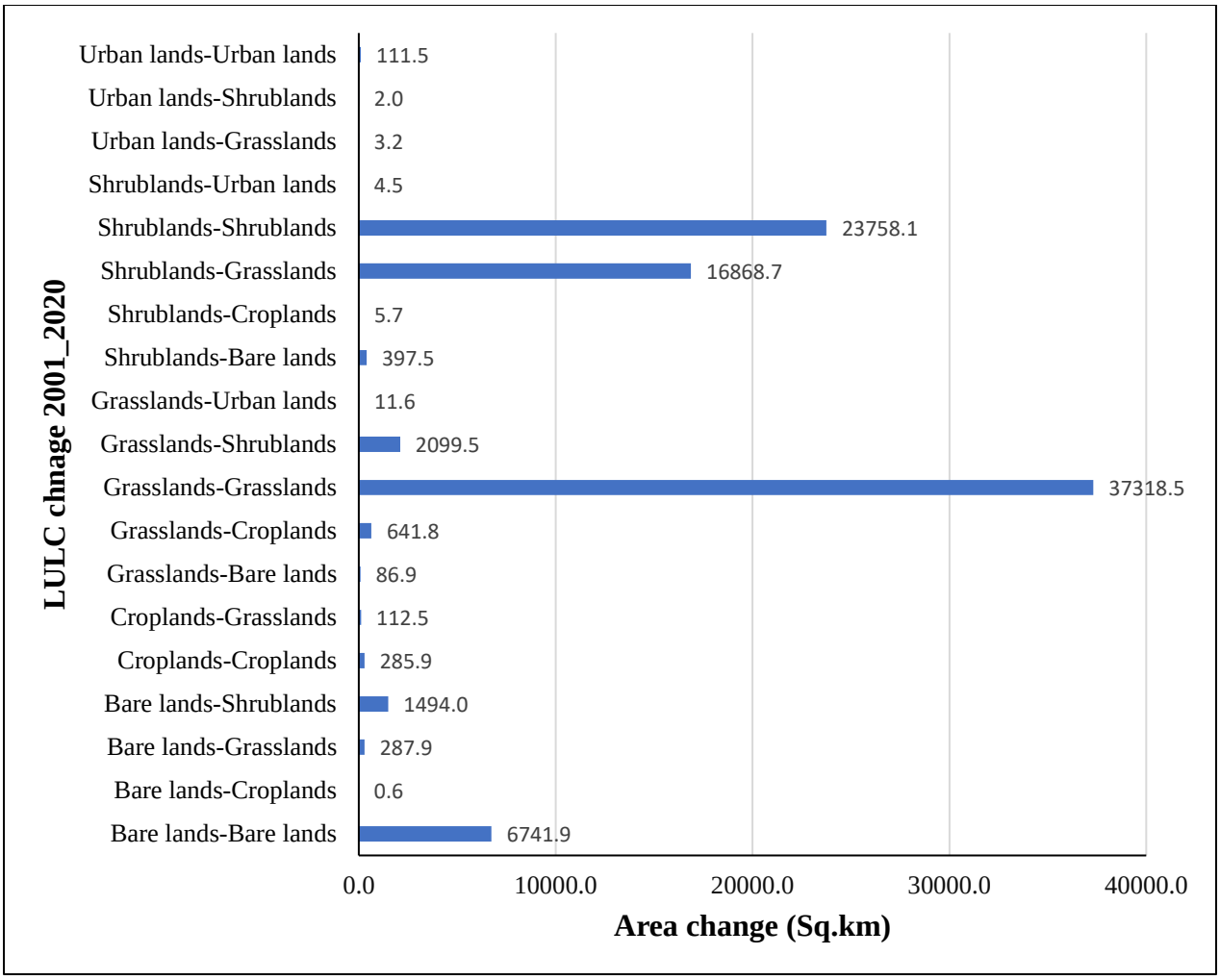

Figure 7. 6 LULC change detection for EC (2001_2020)

Accuracy assessment of LULC change

A comparison of the accuracy of the Google Pro data and the MODIS land cover data from randomly selected sites within the study area was conducted. The most often utilized evaluation technique, known as Kappa Accuracy, is used to verify accuracy. Overall classification accuracy for the classified image from 2001 to 2020 was found to be 85.4 % and 84% and the overall kappa statistics of 81.2 % and 80.1% for WC and EC respectively.t

7.3.2. NDVI Characteristics for the catchments

Western Catchment (WC)

Between 2001 and 2020, the NDVI's vegetation growth value grew on average. The value did, however, rise unevenly; it fell between 2001 and 2008, rose between 2008 and 2015, and then fell once more between 2015 and 2020. The classified value of NDVI showed a similar general trend for dense vegetation area coverage. The average value of NDVI for the dry period also increased between 2001 and 2020 with the highest increment between 2015 to 2020. Between 2001 and 2020, the NDVI during the dry season indicates that while bare land declined from 35% to 10% of coverage, dense vegetation covering increased from 27% to 44% of coverage (Figure 7.7).

Eastern catchment (EC)

The average dry season NDVI for the EC was 0.234, which is much lower than the western average of 0.403. The lowest minimum value is -0.113 and the highest maximum value becomes 0.666 for the dry month. More than 92% of the area is in the category of values between (0.015 to 0.18) for the whole period between 2001 and 2020 in dry months. The second main value range is from 0.18 to 0.27, which is 3.5% to 7 % covers of the area in the dry season. Compared to the dry season, the vegetation reflectance was somewhat higher during the rainy period and covers a wider region (Figure 7.8).

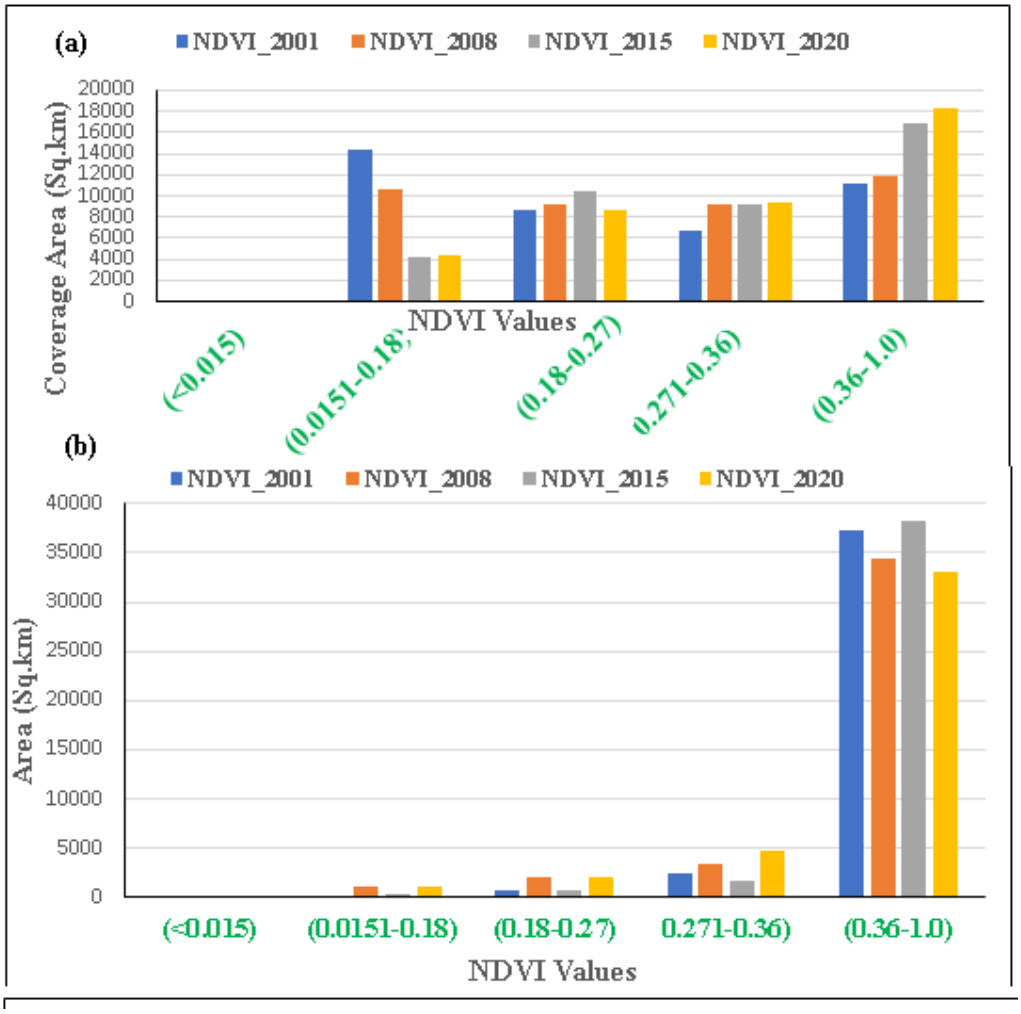

Figure 7. 7 NDVI trends of the WC (a) wet period and (b) dry period

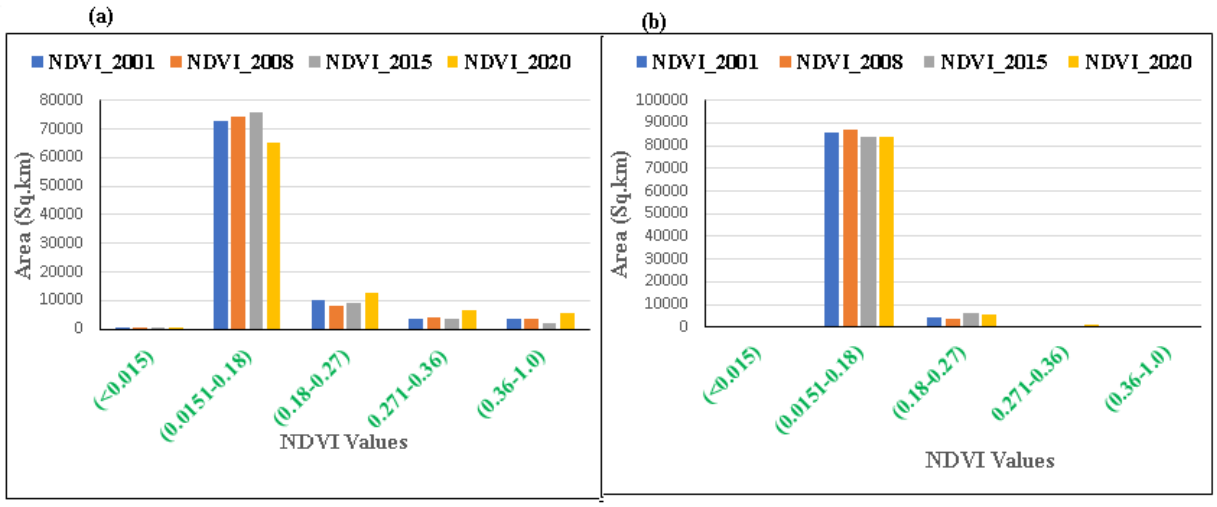

Figure 7. 8 NDVI trends of the EC (a) wet period and (b) dry period

Relationship between LULC and NDVI

The vegetation index results show that larger NDVI values occurred in forest and green vegetation areas, and the lowest value was found in barren and built-up uplands. Therefore, forest and other green vegetation are relatively more prominent in the WC than in the eastern catchment, which receives a higher NDVI value approaching 1.0. On the other hand, barren and related coverage, have the lowest NDVI value (<-0.0) pronounced in the EC.

7.3.3. Results of climate change analysis

This section presents climate change results based on baseline and future period analysis (scenarios: SSP2-RCP 4.5, and SSP5-RCP 8.5).

Temperature

Temperature, which depends on an area's latitude and height, is the main climatic component that influences evapotranspiration and aridity. For the western catchment, the mean annual temperature ranges from 18.1 ºC at the eastern borders to 28.7 ºC around Jikawo. The warmer temperature in this case was concentrated in the northern central part of the Gambela plain while the coldest one was in the eastern border areas (around Masha) (Figure 7.9a).

The mean annual temperature in the eastern catchment (EC) ranges from 18.2ºC to 27.6ºC (Figure 7.9b). The warmer temperature zone was in the southern (south of Deghabur) and northeastern extreme areas (Aysha). The coldest record was at the mountain areas of the upper catchment (Ahmar mountains). The temperature in the EC was increasing from the highland to the lowland which follows the topographic elevation of the region.

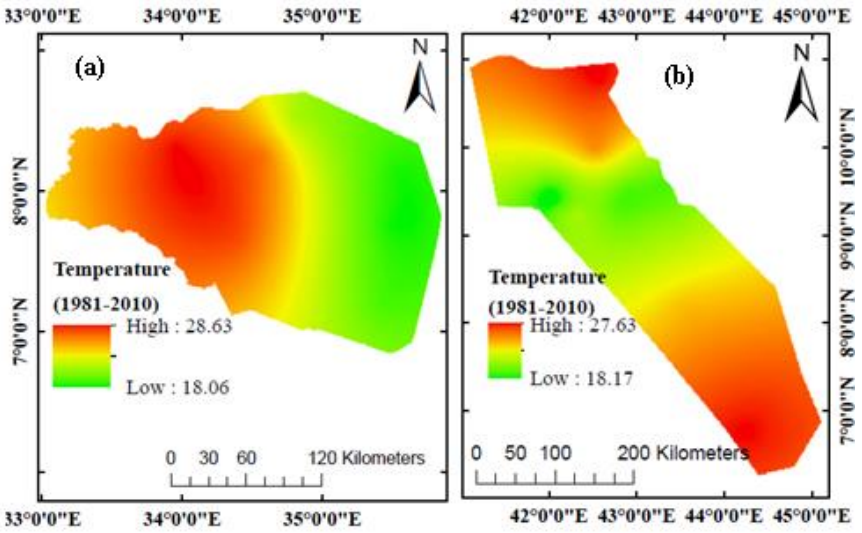

Figure 7. 9 Temperature distribution a) western, b) eastern catchment

Precipitation

Precipitation is the other major parameter that determines the evapotranspiration and aridity of a specific area. The minimum annual precipitation for the western catchment was 995 mm/year at Jikawo and the maximum was 2296mm/year at the eastern hills (Masha) (Figure 7.10a). The rainfall pattern in the western catchment is unimodal and maximum from June to August (Figure 7. 11). The lowest rainfall recorded was in the month of February (Figure 7.12). The annual precipitation of the eastern catchment ranges from 259-833mm. The area receives the lowest annual rainfall compared to the western catchment. The lowest rainfall occurs around Deghabur, and the highest record is in the mountain areas (Figure 7.10b). Taking the mountain as a locus point north and south of the mountain follow different rainfall patterns which are bimodal in both cases having two peak rainfall points (Figure 7.11).

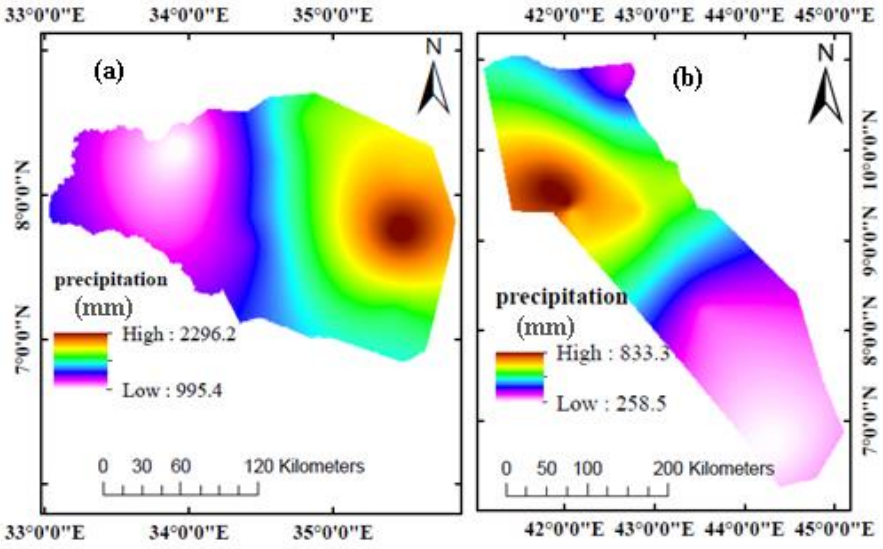

Figure 7. 10 The annual precipitation distribution a) western, b) eastern catchment

The peak period of the northern (Shinile) and the southern (Fafen-Jerer) occurred in a different month. In the southern (Fafen-Jerer) the two rainfall seasons are from March to May and from July to September. For northern (Shinile) the rainy seasons are from March to May and from June to August. The maximum annual rainfall record was in the month of July while the minimum is in January.

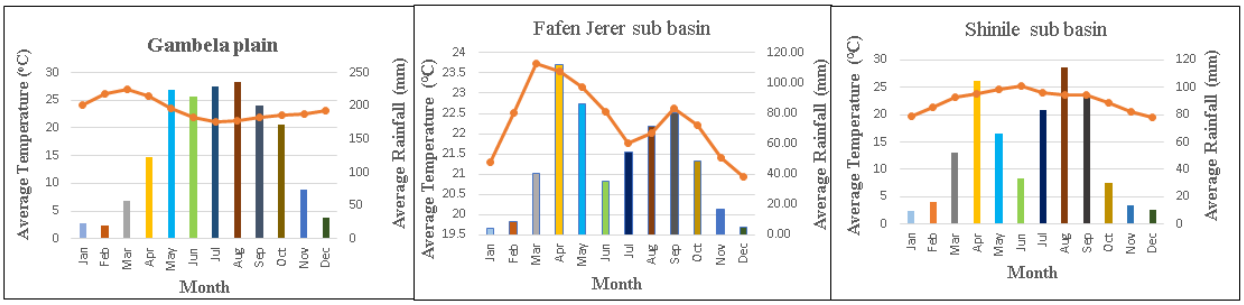

Figure 7. 11 Monthly mean temperature (°C) (line graph) and precipitation (mm) (bar graph)

According to the climatic trend results, the average yearly temperature increase for WC and EC over the previous three decades has been around 0.95 ºC and 0.30 ºC, respectively. Additionally, there was a drop in yearly precipitation of around 4.2 mm/year for WC and 1.2 mm/year for EC during the course of the period (Figure 7.12).

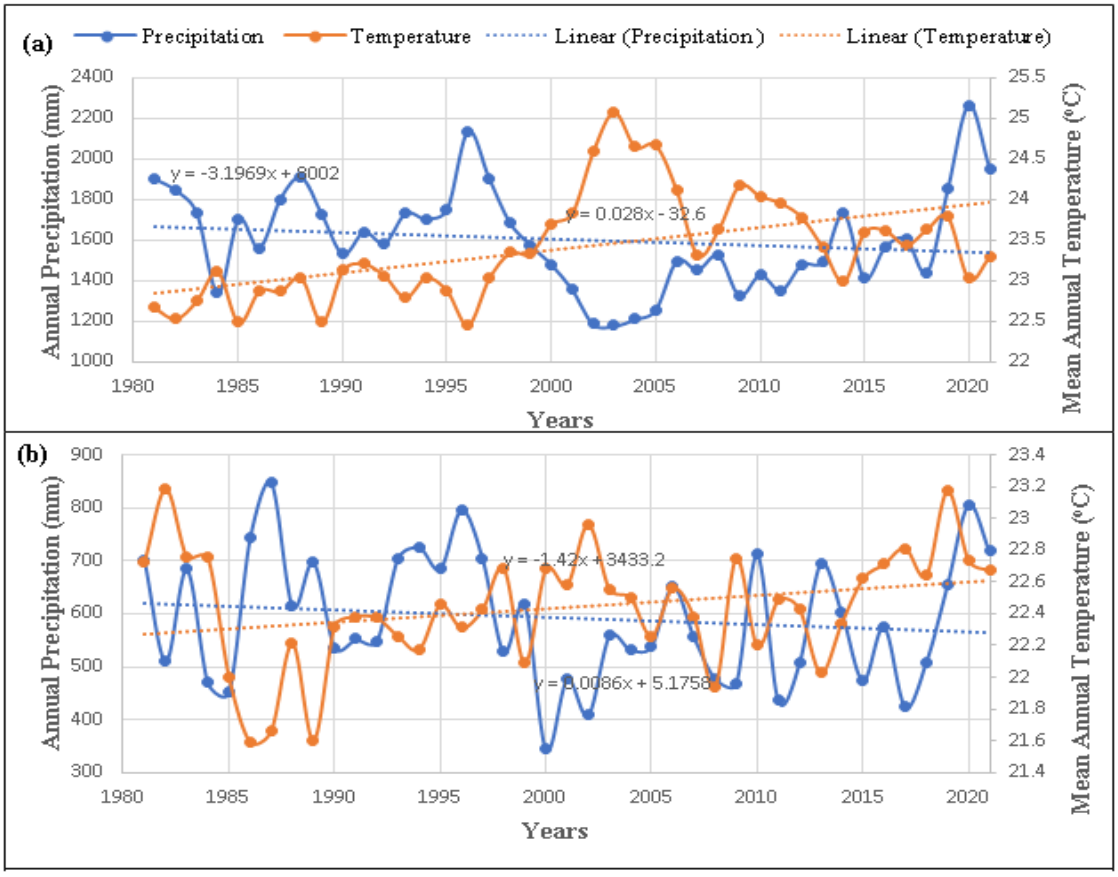

Figure 7.12 Precipitation and temperature trends a) western, and b) eastern catchment

Projected Temperature and Precipitation Trends

The western catchment will experience a significant rise in temperature with increases of 1.3 and 2.1 °C for SSP 2-RCP 4.5 and SSP 5-RCP 8.5, respectively by the end of 2070s. According to the precipitation trend, between 2015 and 2070, there will be a very slight increase for SSP 5-RCP 8.5 and a reduction for SSP 2-RCP 4.5 (Figure 7.13).

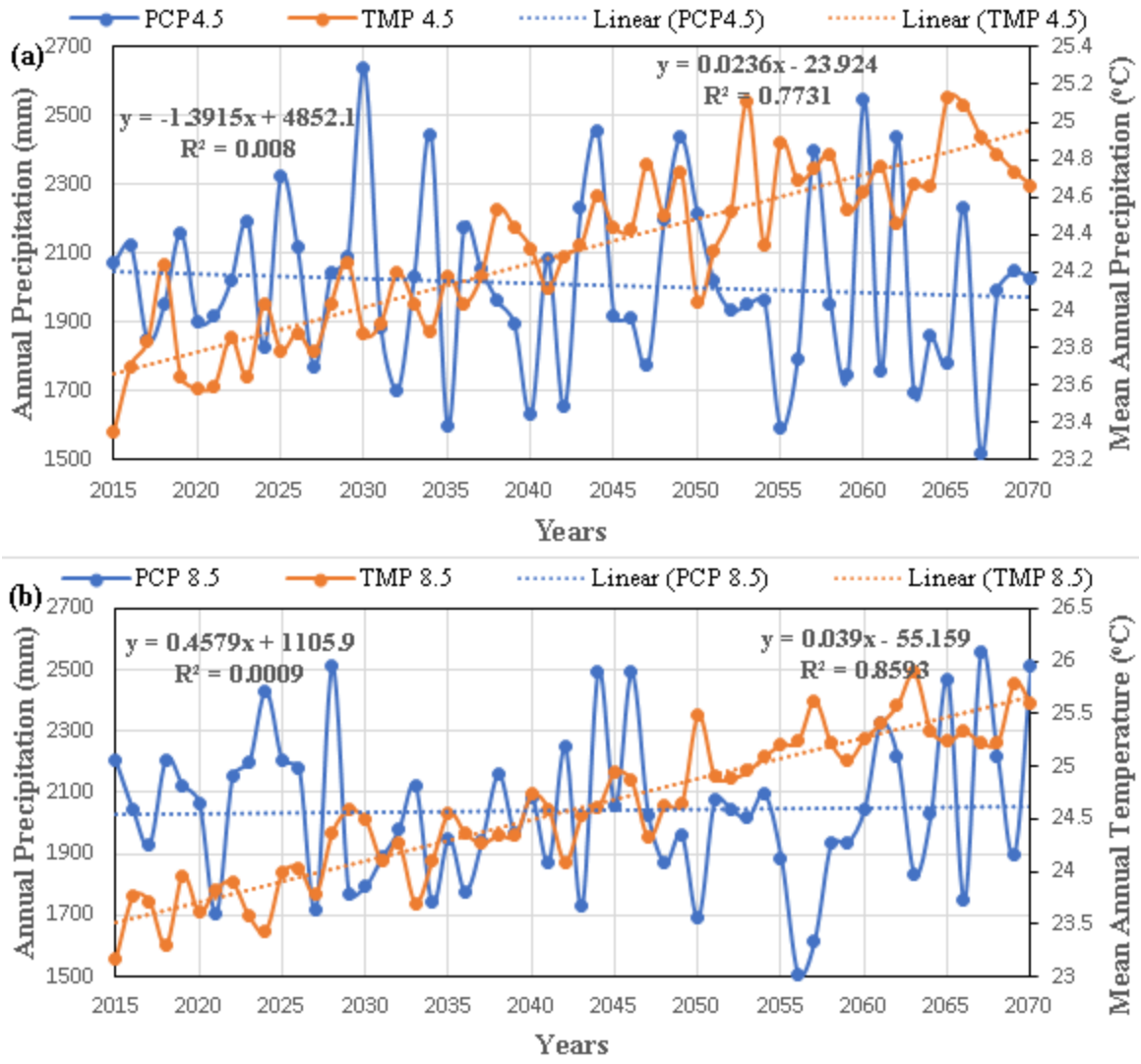

Figure 7. 13 Projected precipitation and temperature trend for WC a) SSP2-RCP4.5 and b) SSP5-RCP 8.5

The eastern catchment temperature will increase from 1.5 and 2.25 ºC for SSP 2-RCP 4.5 and SSP 5-RCP 8.5 respectively by the end of 2070s. The annual precipitation values have not changed significantly over the immediate near period (2015-2040), with some mean-period increases for both SSPs between 2041 and 2070) (Figure 7.14). The results show that both the temperature and precipitation percentage variations in both catchments for future instances. With no visible change over the years 2041–2070, the eastern catchment's southern and northeastern regions have experienced the driest conditions in recent decades, averaging 259–457 mm/year.

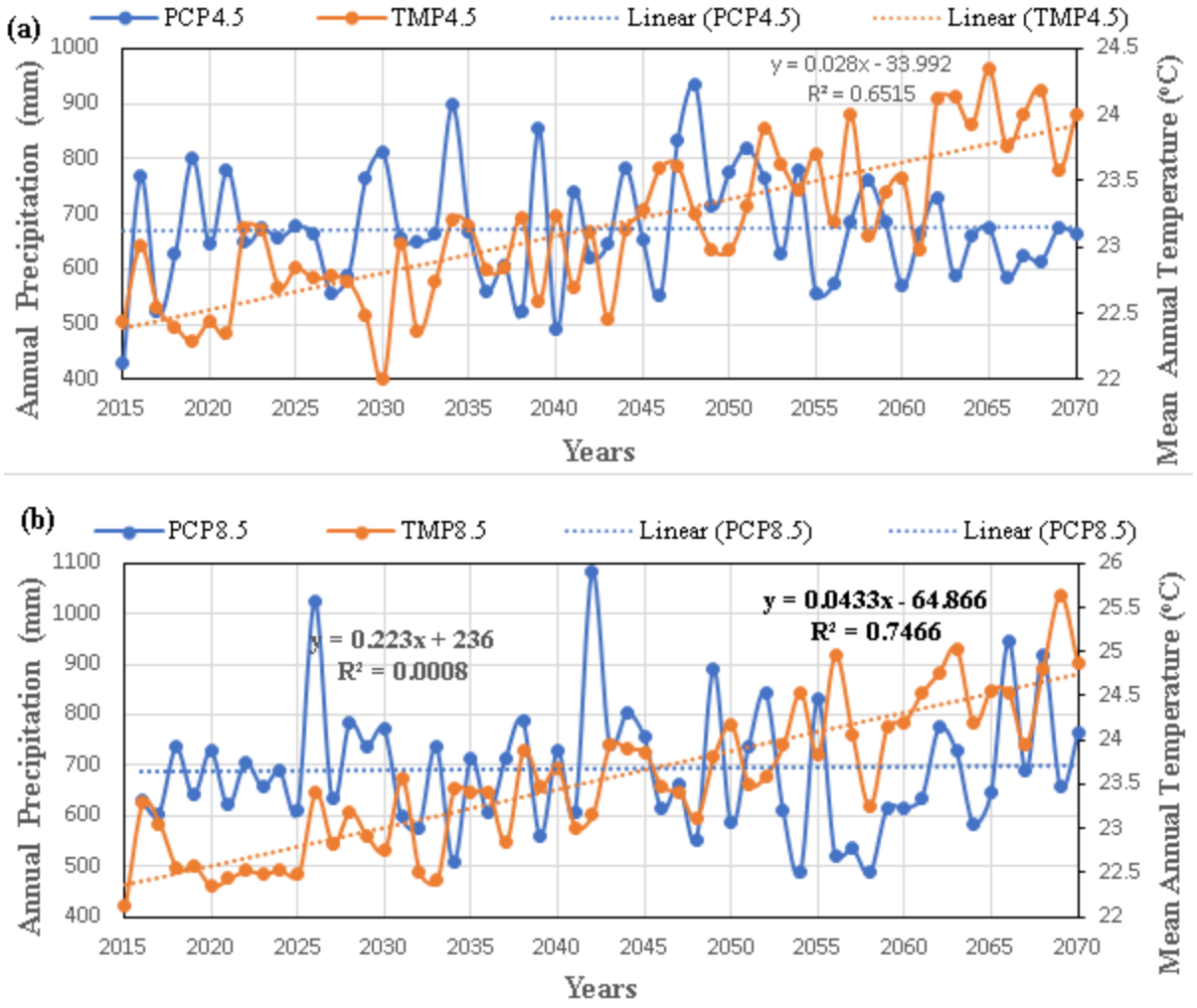

Figure 7. 14 Projected precipitation and temperature trend for EC a) SSP2-RCP4.5 and b) SSP5-RCP 8.5

7.3.4. Potential Evapotranspiration

In the study regions, the distribution of ET_0 follows a pattern resembling changes in temperature and precipitation. The warmer areas have a higher ET_0 content and vice versa. In the western catchment, the ET_0 value for the reference period ranged from 816 to 2328 mm/year (Figure 7.15a), which is a higher range of values compared to the eastern catchment. Particularly the plain area of Gambela region has higher ET_0 values. The ET_0 value of the eastern reference period ranged from 837 to 2093 mm/year (Figure 7.15b).

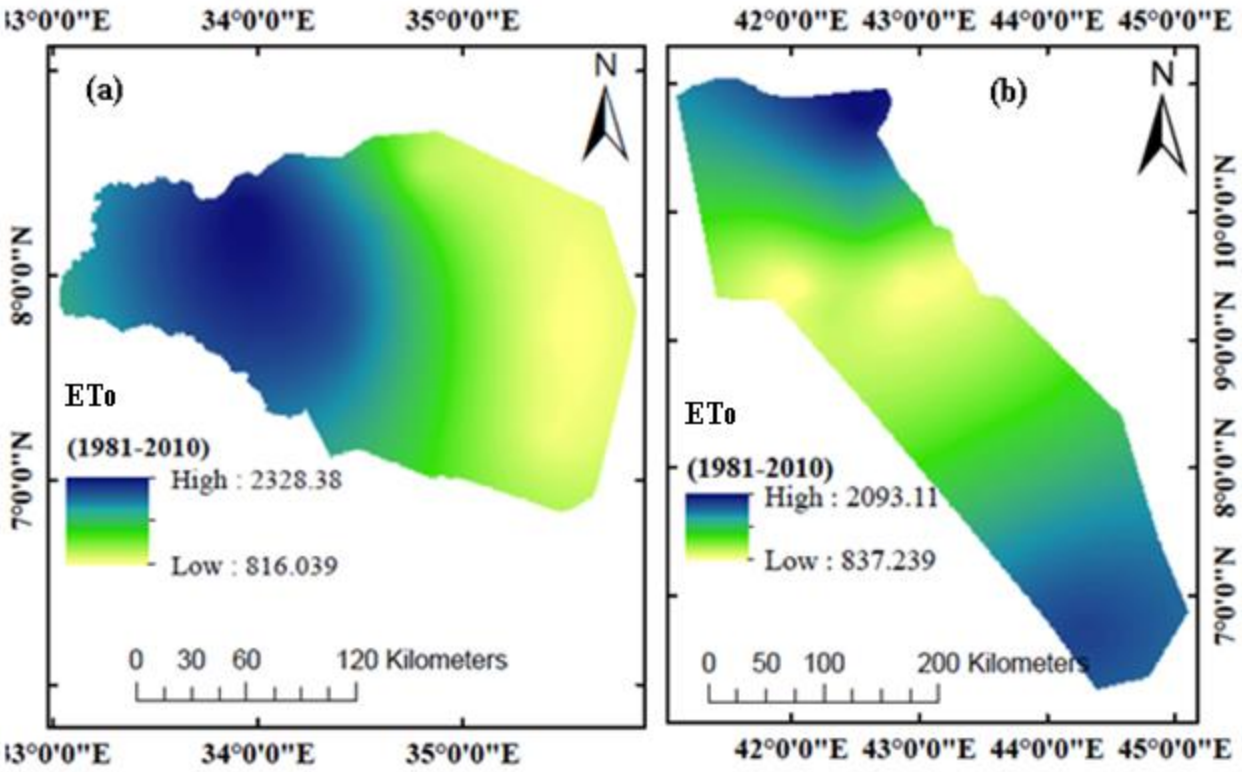

Figure 7. 15 Potential evapotranspiration (ETo) a) western and b) eastern catchment

Higher evapotranspiration for the eastern catchment is recorded at Aysha and south of Deghabur. The trend in evapotranspiration has increased by 10.15 and 1.05 mm/year for the western and eastern catchments, respectively, over the past decades (Figure 7.16).

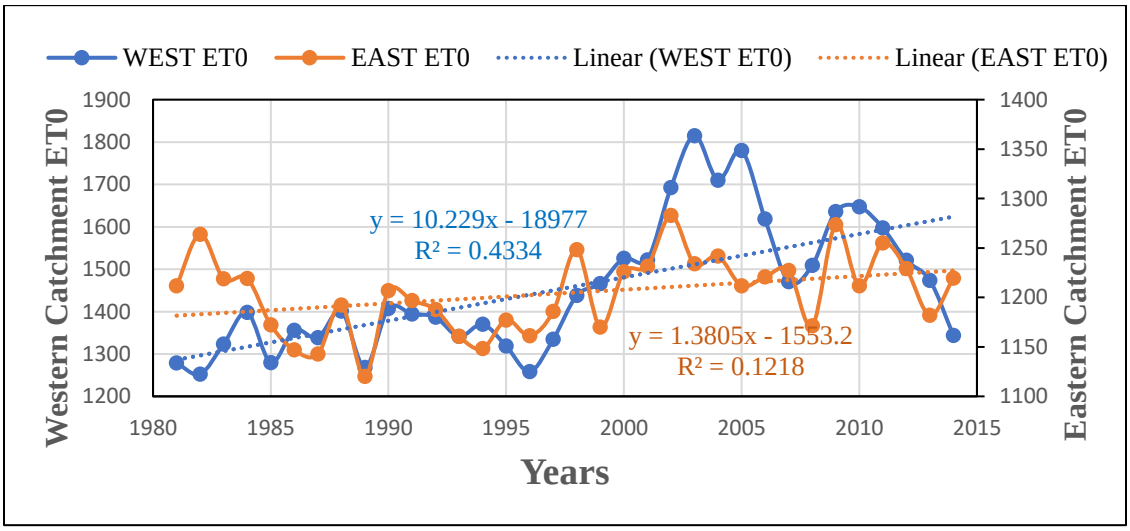

Figure 7. 16 The historical trend potential evapotranspiration

This change will continue to increase for the projected climate of both catchments. This shows that ET_0 will be one of the climate challenges of the 1970s.

7.3.5. Aridity indices

Different aridity /humidity conditions with a common number of climate classes were observed in the western and eastern catchments. The western catchment characteristic tilted to humidity while the easter tilted to aridity conditions. In other words, western catchments are wetter, and the easter catchments are frequently drier.

De Martone Aridity Index (DMI)

The climate classification using DMI is grouped into seven classes (Table 7.4)(Baltas, 2007). Based on the value of DMI the study areas were reclassified according to the stated climate classification. It is evident from the figure (Figure 7.17) that the eastern catchment is comparatively less humid than the western one. The lowest values of DMI, representing the highest dryness, were generally higher at the northeast (Aysha) and southern (around Deghabur) of the eastern catchment.

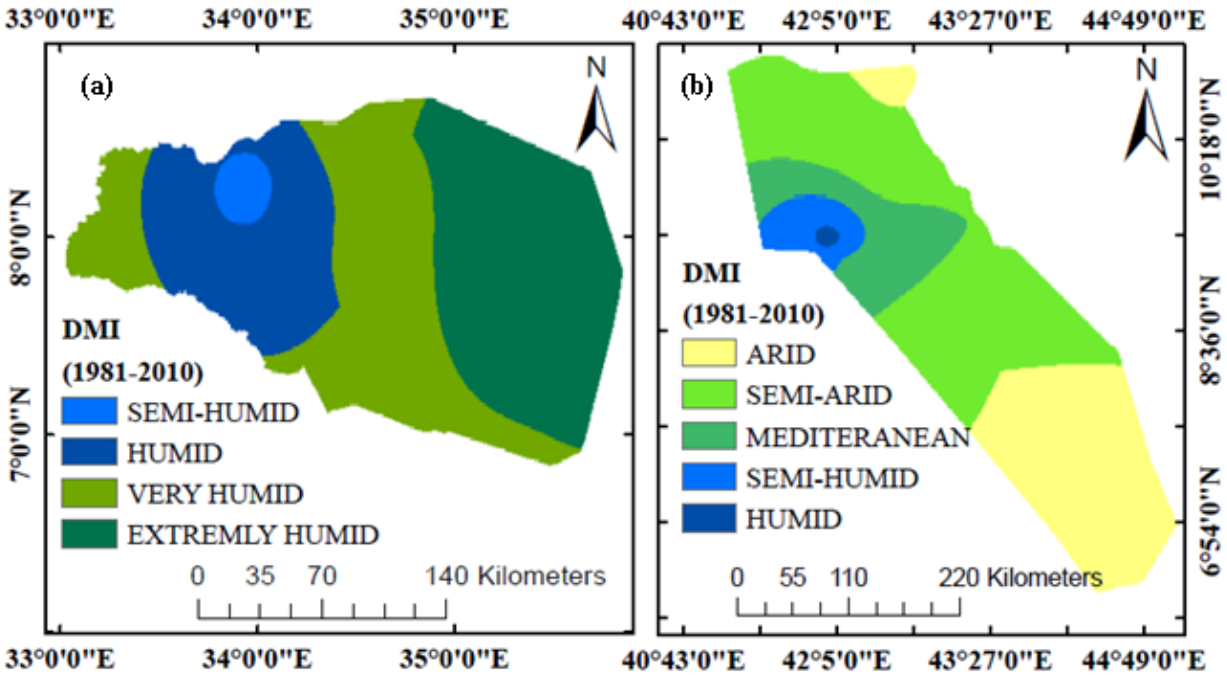

Figure 7. 17 The DMI distribution a) western and b) eastern catchment

A semi-arid climate class covers much of the eastern part (46.5%), while humidity was the feature of the western catchment (Table 7.6).

Table 7. 6 De Martone Aridity index for the historical period

DMI value	Climate class	West Catchment		East Catchment	
		Area (sq. km)	Percent	Area (sq. km)	Percent
DMI<10	Arid	–	–	30299.86	33.54
10<DMI<20	Semi-Arid	–	–	42003.9	46.49
20≤DMI<24	Mediterranean	–	–	12953.65	14.34
24≤DMI<28	Semi-humid	1022.94	2.5	4716.14	5.22
28≤DMI<35	Humid	9462.05	23.14	367.72	0.41
35≤DMI≤55	Very Humid	15237.95	37.27	–	–
DMI>55	Extremely Humid	15161.18	37.08	–	–

UNEP Aridity Index

The UNEP aridity classified the climate of an area into five classes (Table 7.4). The values of the aridity index and classification based on UNEP classification are shown in the figure (Figure 7.18). The classification of the climate in the west catchment ranges from semi-arid to humid, while in the east it ranges from arid to humid (Figure 7.18, Tables 7.6, & 7.7).

Table 7. 7 UNEP aridity index for the historical period

AI value	Climate class	West Catchment		East Catchment	
		Area (sq. km)	Percent	Area (sq. km)	Percent
AI<0.05	hyper-Arid	–	–	–	–
0.05-0.20	Arid	–	–	19429.75	21.51
0.20-0.50	Semi-Arid	1536.28	3.76	41651.57	46.12
0.5-0.75	Dry Sub-humid	8603.37	21.04	24305.72	26.91
AI>0.75	Humid	30746.46	75.2	4927.37	5.46

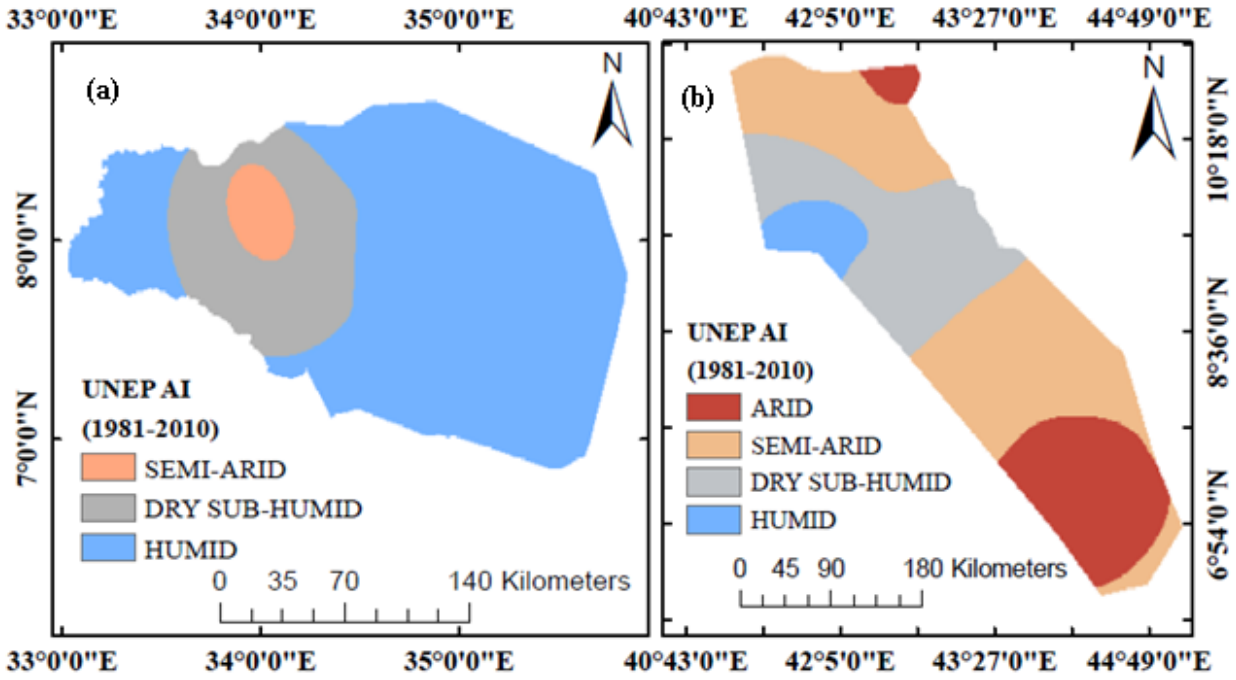

Figure 7. 18 UNEP AI distribution a) western and b) eastern catchment

Trends of Aridity Indices

Aridity in the western and eastern catchments has generally been declining for both aridity indices in past decades. The peak aridity value of the western catchment was recorded in the year 1996 with a value of 67.8 and 1.98 9 for DMI and UNEP AI respectively (Figure 7.19a). The minimum aridity value was recorded in 2003 with a value of 35.5 and 0.99 for DMI and UNEP AI respectively (Figure 7.19a). Relative to the western, the trend of aridity for the eastern catchment has a lot of peaks and valleys. The peak aridity in the eastern catchment value was recorded in the year 1987 with a value of 29.0 and 0.88 for DMI and UNEP AI respectively. The lowest aridity value was recorded in the year 2003 with a value of 10.9 and 0.32 for DMI and UNEP AI respectively (Figure 7.19b). The aridity nature has increased within the last decades which changes humidity conditions to a semi-humidity, semi-arid climate in the western catchment. The same is true for the eastern catchment with low intensity of change.

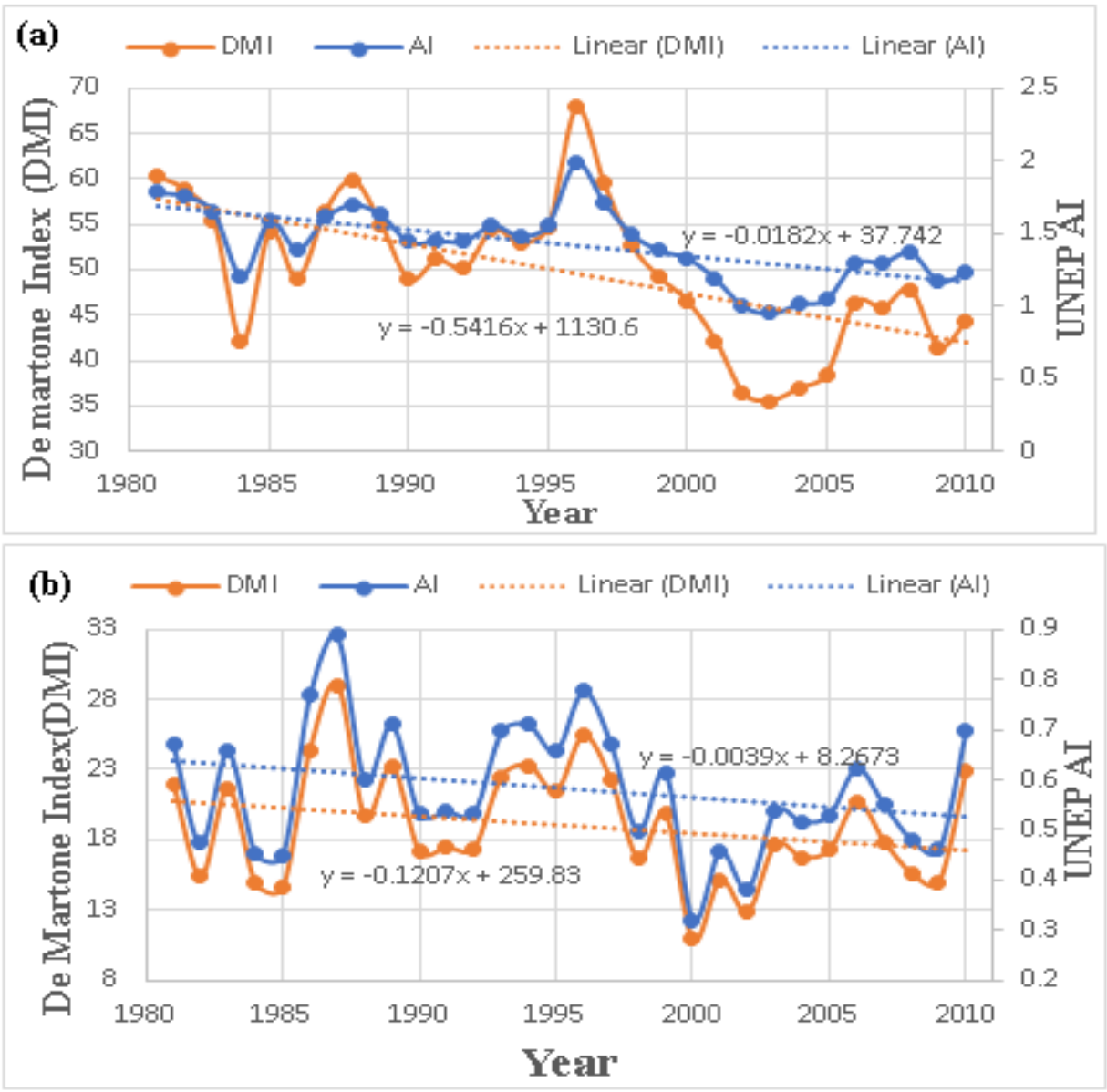

Figure 7. 19 Aridity indices (a) western and (b) eastern catchment.

Projected De Martone Aridity index

According to both climatic scenarios, the study regions' predicted aridity would reduction over the next several years for both catchments. The western catchment will have a higher rate of aridity declining than the eastern catchment (Figure 7.20).

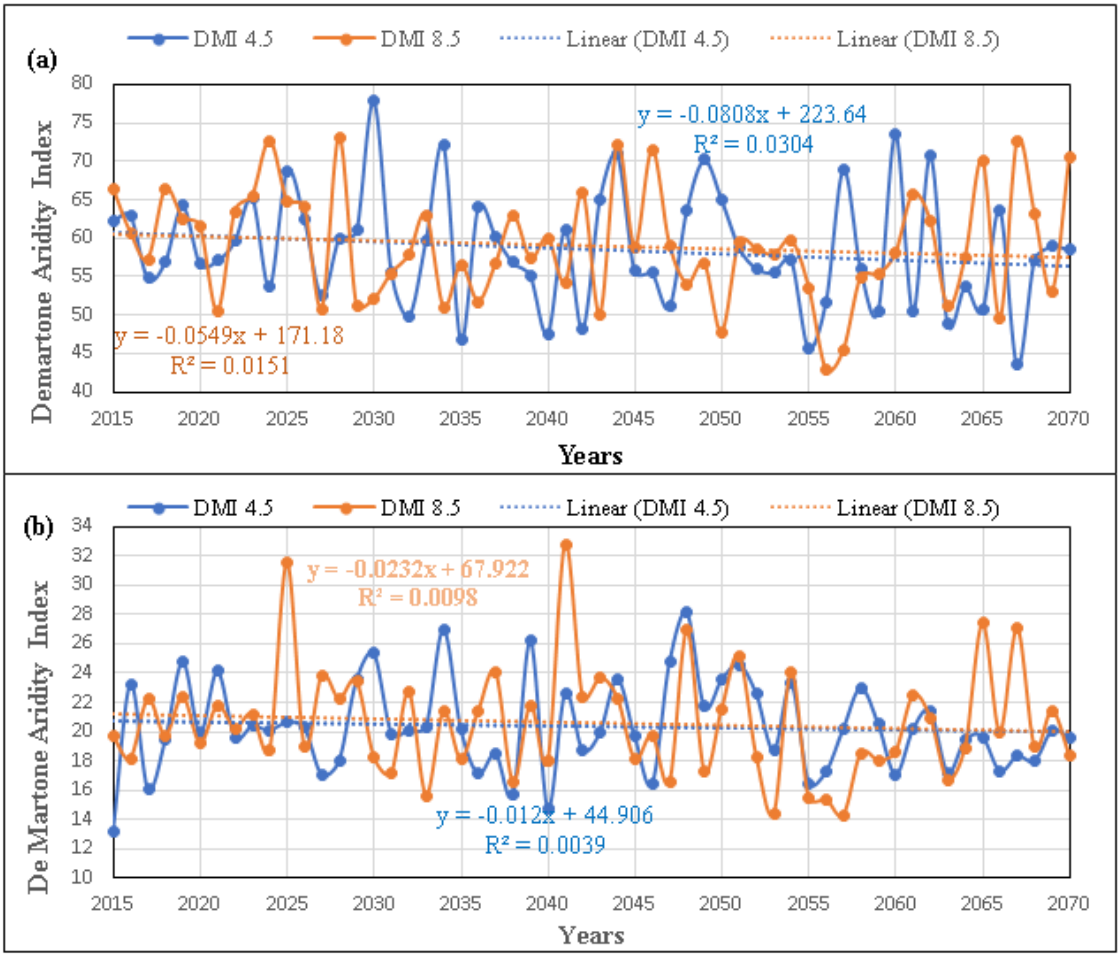

Figure 7. 20 De Martone aridity index (a) western, (b) eastern catchment

7.3.6. Results of crop evapotranspiration, and effective precipitation analysis

The potential evapotranspiration was computed for each station using the Thornthwaite technique (Eq. 7.5 &7.6), with adjustments made for the latitude factor of sunlight (Eq. 7.7). The spatial distribution of ET_0 for the study regions was prepared also for future cases. The results show areas with high ET_0 values are areas of high temperatures, and vice versa.

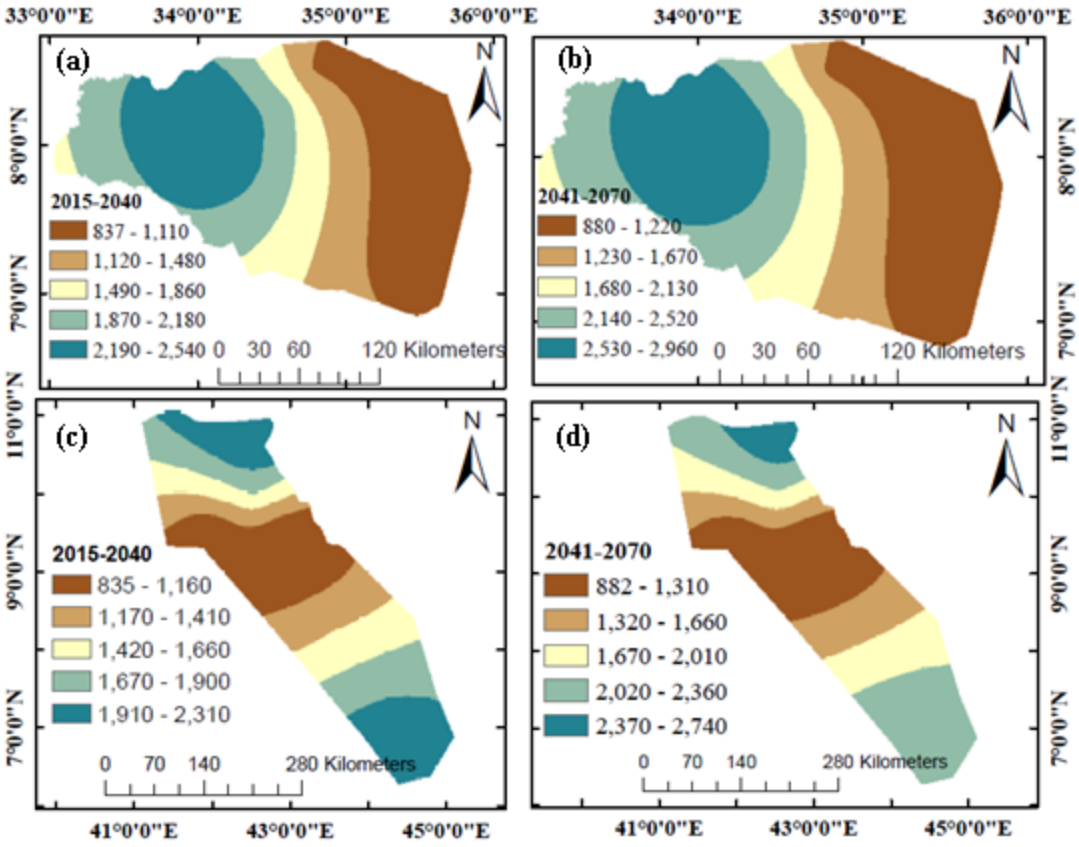

Figure 7. 21 Projected ET_0 (a & b) western and (c & d) eastern catchment

The high annual ET_0 value of WC spread mainly in the west-central region (Gambela plain), where the mean air temperature exceeds 25°C. The eastern part of WC has the lowest ET_0 than the other parts (Figure 7.21a & b). In EC the spatial variation of the ET_0 value follows the topographic elevation of the region. The higher value of ET_0 was found in the extreme northern and southern regions of EC (Figure 7.21 c & d). For crop evapotranspiration (ETc), the Kc value of the land cover parameter was applied for each region by assigning the Kc value for each land cover type (Figure 7.4) based on FAO crop coefficient (Figure 7.22) (Eq.7.8).

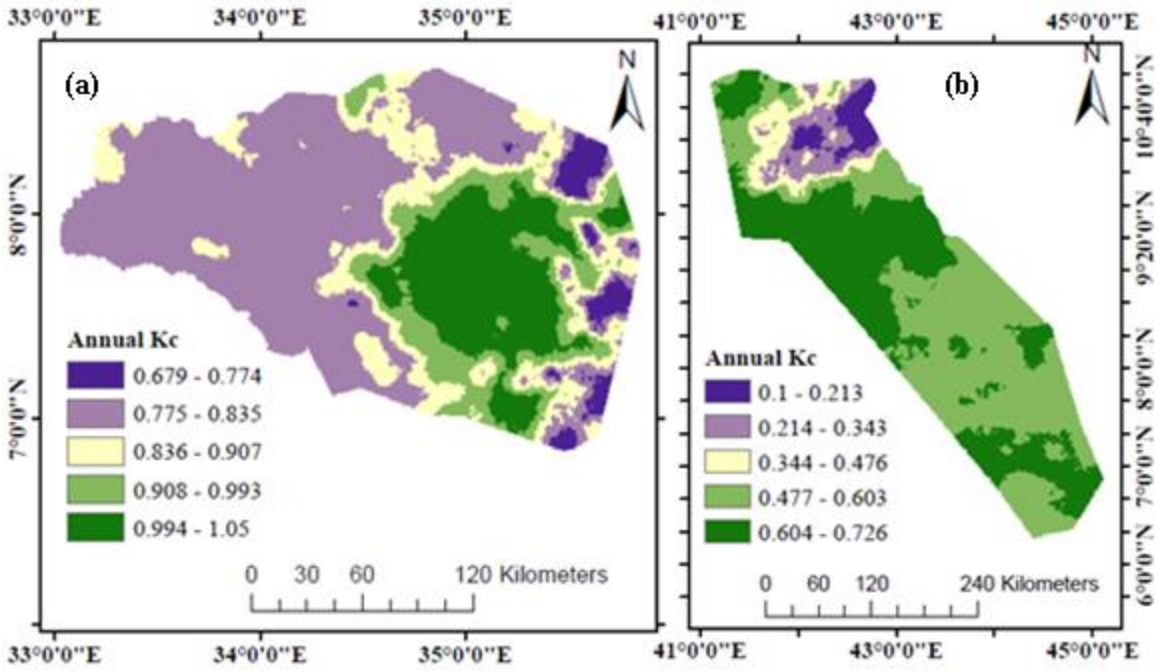

Figure 7. 22 Land cover coefficient (Kc) a) western and b) eastern catchment

Areas with the greatest ET_0 and Kc values also had the highest ETc values (Figure 7.23). The western region, namely the western central portion of the Gambela plain, will have the highest ETc values (over 1500 mm), especially in the Jikawo area (Figure 7.23a & b). For the EC, the ETc value follows an upward trend from higher elevation to lower elevation (Figure 7.23c & d). The lowest ETc of EC was found in the lower catchment of the region.

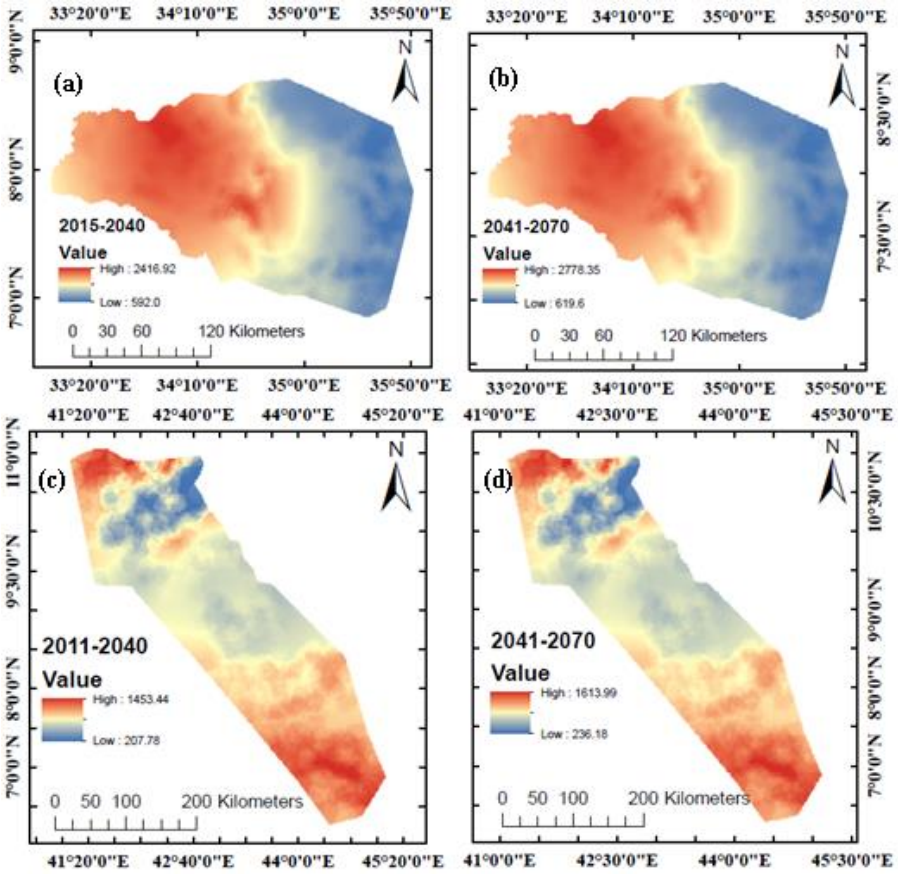

Figure 7. 23 Projected crop evapotranspiration (ETc) (a & b) western (c & d) eastern catchment

The value of actual crop evapotranspiration (AETc) is determined using the Budyko equation (Eq. 7.9). The highest levels of actual crop evapotranspiration (AETc) were found in the northwestern central region of the EC, whereas the value in the WC was centered on the highland and lowland margins. In EC, AETc will be lowest in northern and southern extreme areas of the region (Figure 7.24 c & d). On the other hand, the WC lowest values will be in the eastern part of the region, specifically around Masha and Gore (Figure 7.24 a & b).

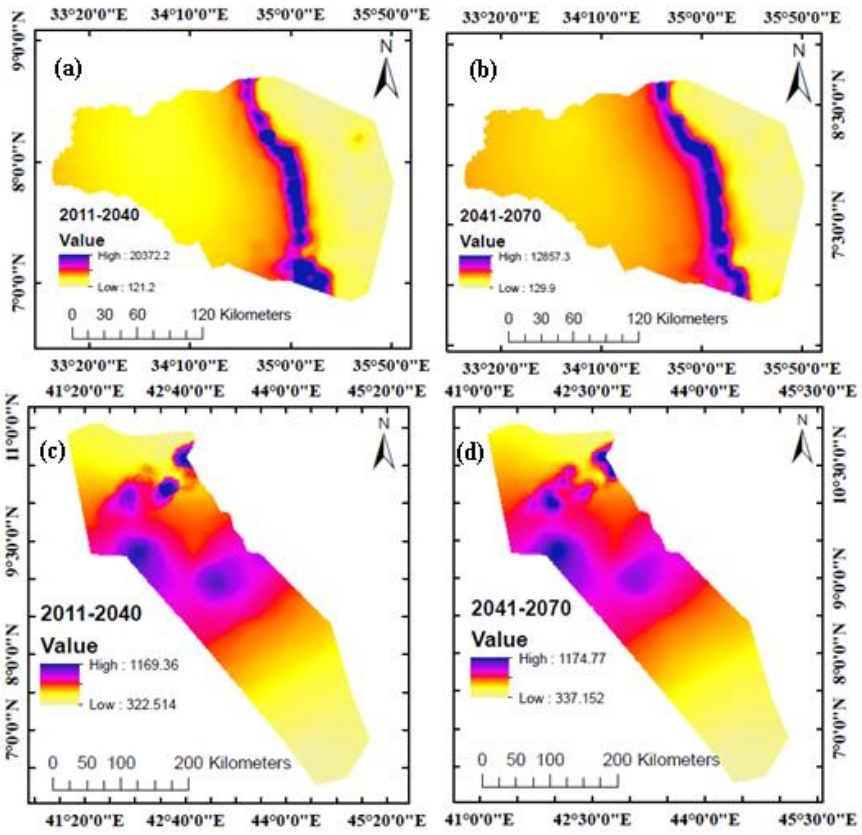

Figure 7. 24 Projected actual crop evapotranspiration (AETc) (a & b) western (c & d) eastern catchment

The equation (Eq. 7.11) was applied to determine the yearly value of effective precipitation. The effective precipitation value changes according to the quantity of rainfall in each region. The majority of the region (particularly the EC) receives less than 100mm of effective precipitation per year (Figure 7.25c & d). The area surrounding Masha in WC has the greatest effective precipitation record, while the lowest will be recorded in the western section around Jikawo (Figure 7.25a & b). There is a significant difference in the spatial distribution map comparing the two temporal periods of the regions.

The reddish color in the De Martone aridity index map (Figure 7.26) shows the highest value of the aridity index. The greater the aridity index, the more humid the climate. The analysis shows the WC has a DMI value ranging from 33.98 to 99.08 (Figure 7.26 a & b), whereas the EC has a DMI value ranging from 8.40 to 28.89. Moving from west to east, the moisture level in WC in increases and vice versa. The value of DMI in EC follows the pattern of elevation (Figure 7.1) which declines in the direction of lowlands (Figure 7.26 c & d).

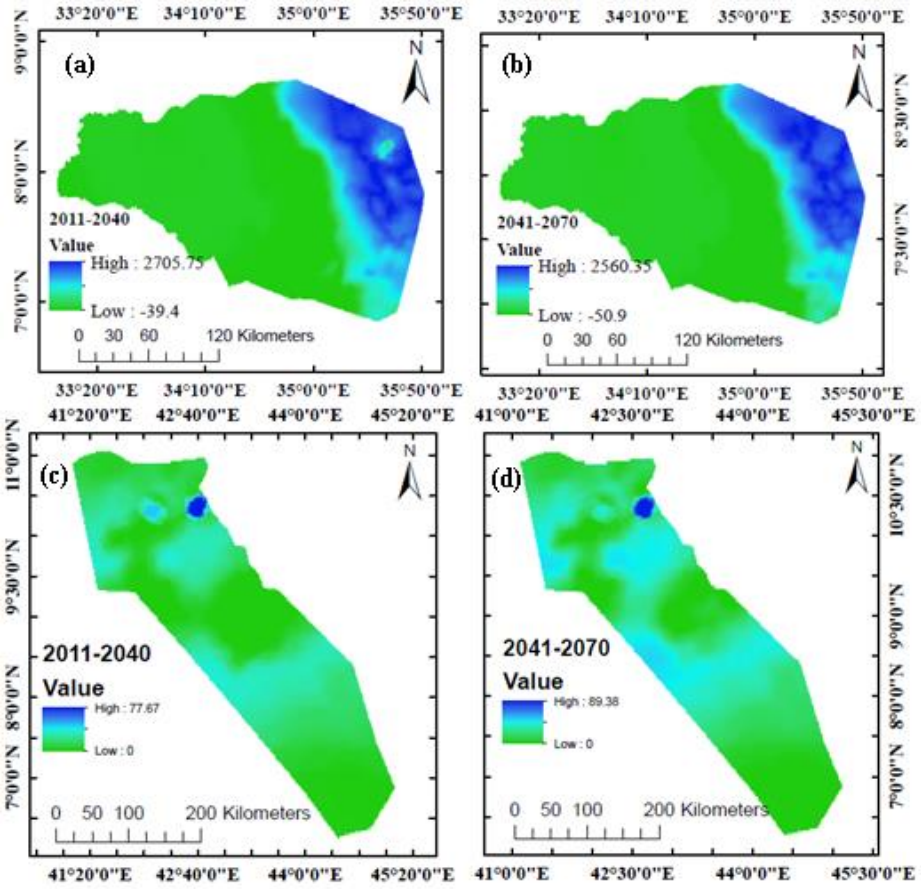

Figure 7. 25 Projected effective precipitation (a & b) western (c & d) eastern catchment

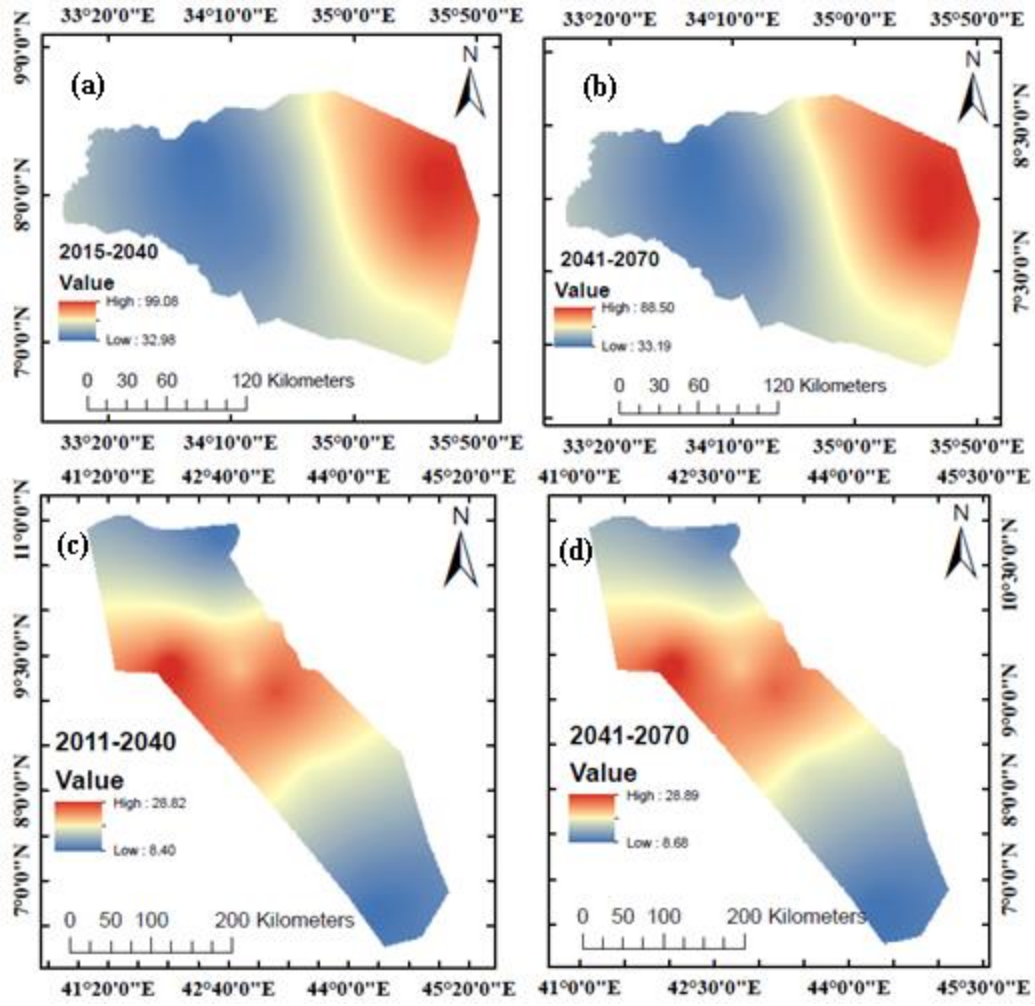

Figure 7. 26 Projected DMI (a & b) western (c & d) eastern catchment

7.3.7. Effect of climate change on groundwater

By utilizing the methodology, an assessment was conducted to ascertain the effect of climate on groundwater resources. The De Martone aridity index and effective precipitation were utilized in estimating the impact of climate on groundwater in this study. The spatial distribution of the aridity index and effective precipitation were produced for the total analysis.

The analysis of climate effect on groundwater was performed for present, and future periods considering the land cover change with the Kc value of each land cover. The analysis was done by assuming there will be no alterations in land cover during the upcoming period. Both the aridity index and effective precipitation were reclassified for the impact analysis to determine the climate effect on the groundwater. The reclassification of DMI was according to the De Martone (1926)

climatic classification (Table 7.4). The classification of DMI and the effective precipitation for each area are presented in the tables (Tables A7.1 & A7.2).

Using the ArcGIS raster calculator tool, the categorized DMI and effective precipitation were used for the climate effect analysis. Based on the results, the values were then divided into five subcategories, which ranged from very high effect to very low effect. The influence of climate change on groundwater (Figure 7.27) was rated from very high to very low. Very high zones have a significant sensitivity to climate change, but very low zones do not.

In WC the region with the very high impact was located in the northwest and western, specifically around Jikawo, and high effect is found margin area of highlands and lowlands in the central area around the escarpment. Notably, the medium effect zone will exhibit a significant increase in coverage from present to future periods (as shown in Figures 27a & b). In WC the accompanying climate effect map reveals that the western will be more vulnerable to climate effect than the eastern parts. In comparison to the current situation, the eastern section of the WC may have a higher spatial coverage for the extremely high-effect zone in the future (Figures 27a & b and A7.4a).

The spatial distribution of climate effect on groundwater in EC is clearly shown in the figure (Figures 7. 27 c & d and A7.4b). High and very high zones are located in the southern and northern regions of the EC. The findings suggest that groundwater in the northern portion (near the Shinile) may be significantly impacted by the climate. The spatial distribution of a very low effect may be substantially less than the current spatial distribution. In the future climate for WC, there could be a notable increase in the very high and low-effect classes. There may also be a significant increase in high and medium-effect areas in EC. This shows there will be climatic extremes in the study regions.

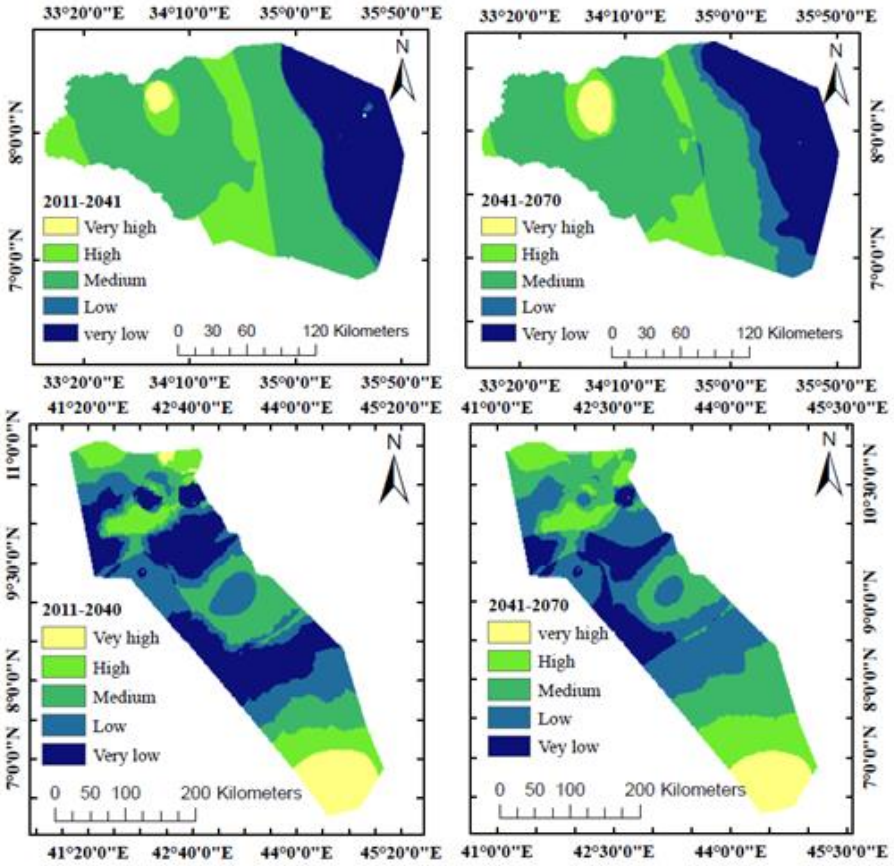

Figure 7. 27 Projected climate effect on groundwater ((a & b) western (c & d) eastern catchment

7.3.8. Climate impact on Potential Recharge from rainfall

For both catchments, the trend in rainfall over the previous few decades has been declining. Trends in precipitation have a direct impact on groundwater recharging. The recharge estimation results of the catchments have been diclining for the past decades (Figure 7.28). The slope of recharge to the time was steeper in the eastern catchment. As a result, the eastern catchment was experiencing a faster rate of recharge reduction than the western. The rate of decline of recharge follows a similar trend with a lower rate in both catchments for the coming periods (Figure 7.29).

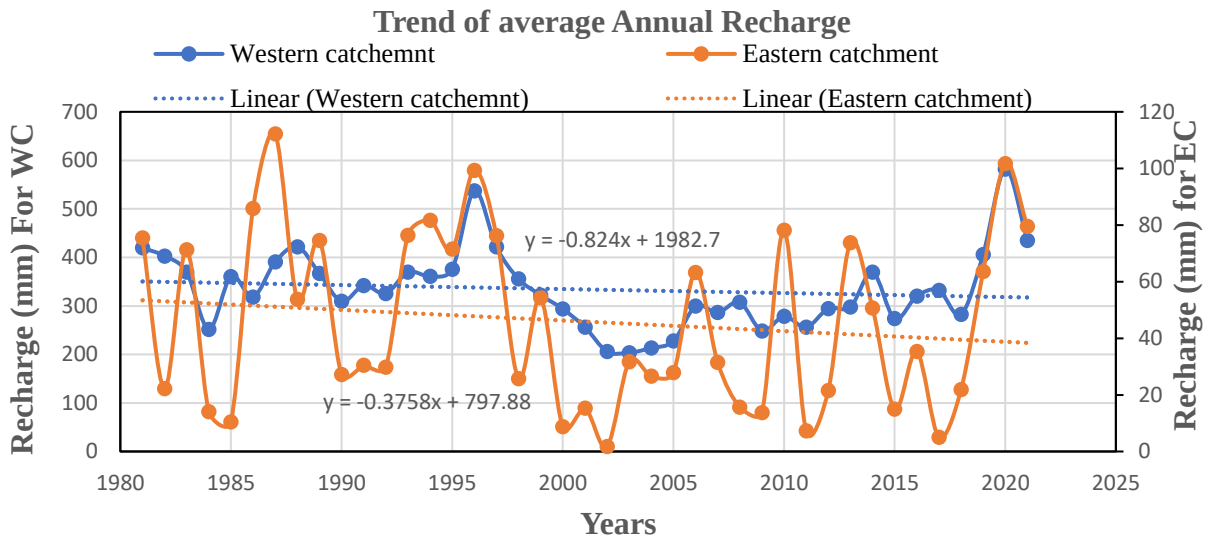

Figure 7. 28 The trend of historical annual potential recharge

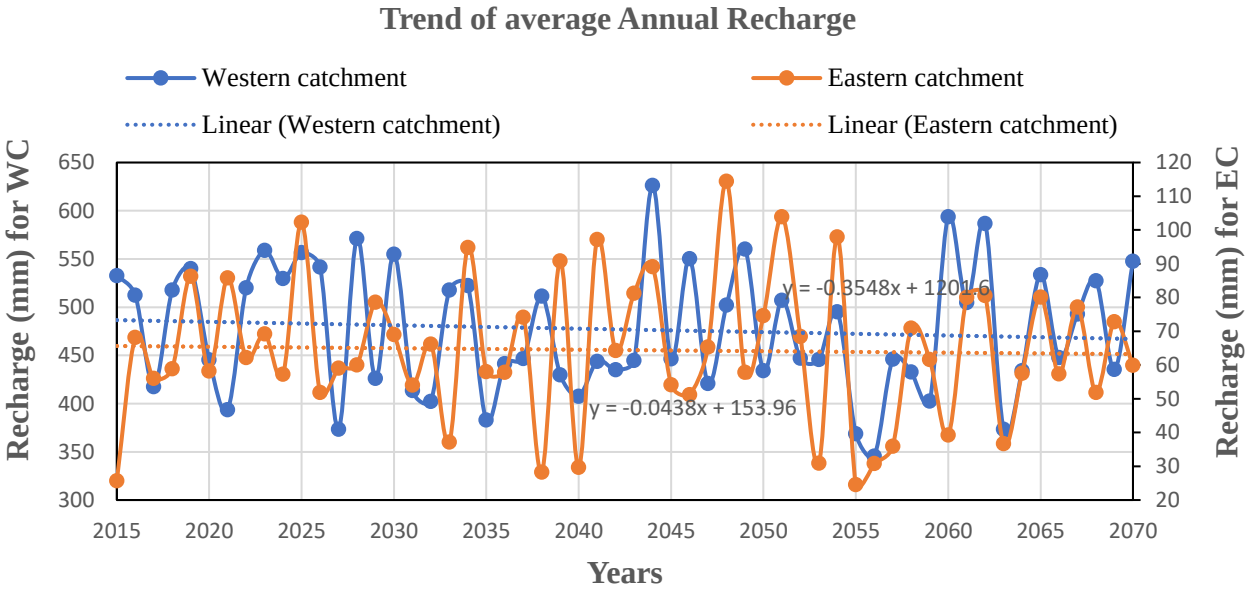

Figure 7. 29 The trend of projected annual potential recharge

7.4. DISCUSSION

The main goal of the study was to determine the impact of climate change on groundwater by representing the spatiality of the De Martonne Aridity Index and effective precipitation. For the crop evapotranspiration study, the type of land cover was directly correlated with the crop coefficient. In this research crop evapotranspiration was calculated to consider the impact of land

cover change on groundwater. It serves as the foundation for determining the actual crop evapotranspiration and effective precipitation. A greater crop coefficient is observed in regions with more green vegetation and higher NDVI values. Thus, variations in the NDVI affect evapotranspiration and regional variations in evapotranspiration impact groundwater conditions. The correlation between NDVI and groundwater resources of an area is seen by several researchers (Fu, B., & Burgher, I., 2015; Seeyan et al., 2014; White et al., 2016; Páscoa et al., 2020). So, the land cover effect on groundwater was considered in determining the evapotranspiration parameter.

The study applied a global climate model to project the climatic parameters for this research. The researchers attest to the CMIP6-GCM models' accuracy in predicting Ethiopia's future climate (Alaminie et al., 2021, 2023; Balcha et al., 2022). Based on the results of climate models used to estimate warming for the 2070s, a rise in the highest mean air temperature of 1.5 to 2.1 °C in the future will have a direct impact on increases in ET0, as well as on annual ETc and AETc. Because the study regions' land cover patterns are included in the ETc and AETc calculations, they have an impact on the effective precipitation calculation's spatial distribution.

Researchers show the way of techniques in different areas by applying the Thornthwaite evapotranspiration method (Yang et al., 2017; Dezsi et al., 218; Trajkovic, et al., 2019). Since Thornthwaite's formula requires less data than other approaches, it is the best option available for large-scale applications of potential evapotranspiration and aridity evaluation in varied climates and geographies.

The DMI indicator holds significant importance in determining and classifying climate types. Each climate type specifies whether the region has a moist or arid climate. In regions with the highest DMI, the quantity of precipitation is greater and the recharge of groundwater is expected to be more substantial. By combining the effective rainfall and the DMI, it is possible to accurately illustrate the impact of climate on groundwater (Nistor, 2018). The method is a useful tool to assess the aridity of a region and its potential impact on water resources. The crucial point to note is that reduced effective precipitation signifies an adverse climate impact on groundwater, resulting in a lower recharge rate of aquifers. Furthermore, the DMI is a valuable instrument for evaluating the aridity of a region and its potential ramifications on water resources. The initial phase of evaluating the climate impact involves identifying the categories of influence concerning the actual rainfall and the DMI. After calculating the effective precipitation and DMI of the region, the raster data are

reclassified accordingly to understand the distributions. Both were re-classified into sub-class for the next overlay analysis.

The high annual ET0 spread mainly in the South of the region, where the mean air temperature exceeds 16 °C. The regions with bare land and arable land cover the lowest values, according to the ETc spatial variation of EC. The low ETc values in the WC mountain regions are caused by relatively cold temperatures in the majority of the eastern regions. These conditions clarify why the climate parameters have a greater impact on ETc than land cover, even though broad-leaved forests are widespread in mountainous regions of eastern WC and have a significant Kc.

The increases in mean air temperature and annual ET0 over the future time are the cause of the yearly AETc rises for both catchments. Establishing a way to evaluate the effects of climate change on groundwater using the climatic aridity index and effective precipitation is one goal, and it makes a significant contribution to the existing literature-based approaches (Nistor et al. 2016; Nistor, 2018). Effective precipitation is one of the climate parameters that show the condition of water availability (Dezsi et al.,2018). The regions with the lowest DMI and effective precipitation have very high and high degrees of climatic influence on groundwater resources.

The effects of climate change on groundwater in the past (Figure A7.3) and the future (Figure 7.27) demonstrate that the two primary factors influencing the groundwater system in the next eras are the climate and land cover. Groundwater in shallow alluvial aquifers can refill more often and quickly than deep aquifers. These characteristics of the alluvial aquifer make it susceptible to climate and land cover change and any other environmental modification. Therefore, the groundwater in the research area's alluvial zones will be directly impacted by the impending climate change in one way or another.

7.5. CONCLUSION

Climate change affects the availability of water resources, which makes it difficult to develop and its management globally. Thus, the impact of both LULC and climate change on the groundwater resources of alluvial aquifers is demonstrated in this chapter. The purpose of this paper was to assess groundwater susceptibility to climate change while taking land cover change into account, using ArcGIS's spatial analysis feature. The effect of climate change on groundwater resources was assessed for historical and projected periods. To comprehend the impact of climate and land cover

change in the study regions, the De Martone climate classification and the effective precipitation-based analysis were utilized. Analysis was done on the effects of climate change on groundwater in terms of both time and space. The LULC result of this study reveals that the major land cover in the WC is grasslands to forest while shrublands to grasslands are the main land cover change for EC. According to the analysis, the climate models for the study region that best match ground observation data are CMCC-ESM2, FGOALS-g3, and MIROC6. The yearly precipitation declined while the mean annual temperature of the catchments had risen in the last decades. The aridity indices also followed a downward trend for the past periods. The potential evapotranspiration increased alarmingly in the western catchment for the last decades. This is due to an increase in temperature intensity. The results show that the climate in both study regions for the past decades was significantly warmer. The projected climate analysis showed that the temperature increment will be higher for the far future (2041-2070) than the present (near) future (2011-2040) period for both RCPs. The aridity analysis results showed that the overall spatial pattern of drought remains stable between 1981 and 2070, but important quantitative shifts toward more drought will occur in the western catchment and the northeastern and southern parts of the eastern catchment. The influence of climate change will be smaller in mountainous locations where yearly precipitation is higher and temperatures are lower than in other places. The study regions' lowlands would be more severely impacted by climate change than the other regions. Based on the effects of climate change, the WC catchment may be divided into two sections: the eastern portion, which is less affected by climate change, and the western lowland, which will be greatly affected. The lower elevation areas in EC are also impacted by climate effect, particularly around Aysha in the north and the area south of Deghabur in the south. The research region's potential recharge will be declining over the coming decades. The climatic effect of the future will be greater on the high recharge zone of both catchments than the lowest recharge area. The expansion of the very high impact zone on WC and the reduction of the very low effect zone on EC show that future climate change impacts on resources need to be carefully examined. This study's primary limitation is that it makes assumptions about the current LULC for the upcoming period. To obtain more accurate information about the effects, future research should concentrate on the similarities between LULC and climate change. The effects of climate change on water resources, and groundwater in particular, need to be further studied. The results of the present study will be helpful in future planning, assessment, and management of water resources to plan and act accordingly to the coming impacts of climate.

CHAPTER 8

SYNTHESIS, CONCLUSIONS, RECOMMENDATIONS AND FUTURE RESEARCH

8.1. SYNTHESIS

This study aims to explore the properties of Ethiopia's key alluvial aquifers and evaluate how sensitive they are to changes in land use land cover and the climate. The study used land cover detection, vulnerability to natural causes, vulnerability to climate change, and isotope geochemistry investigation to accomplish this essential goal.

The first part of the study concentrates on factors that largely influence an area's potential for groundwater. Numerous variables are considered in this method, including rainfall, topographic wetness index, topographic roughness index, drainage density, lineament density, soil, slope, LULC, NDVI, and geomorphology. At this point, the study ascertains (i) the main elements influencing the groundwater resources in each region, (ii) examines the prospective groundwater site in each region, and (iii) compares the effects of these criteria on the potential groundwater impact in each region.

The analysis moves on to the components of the resources after determining the variables influencing the resources and possible locations. The study made use of hydrogeochemical and stable isotope parameters to comprehend the features and composition of alluvial groundwater supplies. This section of the study identifies the main issues with water quality, the different types of water, the geochemical process, and the stable isotope signature of the regions under investigation. Owing to data unavailability and security issues, the study only addresses Shinile and Fafen-Jerer's situations in the eastern region.

Examining the likelihood of vulnerability owing to intrinsic (natural) factors was the next stage of the investigation. Using the DRASTIC vulnerability index approach, this investigative step finds vulnerabilities. This section examined the high-risk zone of pollution in the study areas.

Next, the paper provides an examination of land use and land cover change detection based on MODIS satellite data from 2001 to 2020, if any LULC influence was found. The analysis highlights the primary LULC shifts over the preceding 20 years. The findings indicate that LULC is one of

the primary variables influencing alluvial groundwater. Accordingly, using MODIS NDVI data from 2001–2022, the study examined the vegetation covering of the regions. It was observed that the amount of green vegetation had changed.

Following the LULC analysis, the research is devoted to the climate change investigation with historical and forecast climate features. Apart from the fundamental climate variables (temperature and precipitation), the research assessed the evapotranspiration and aridity indices for both the historical and the anticipated scenarios. At this stage, the study shows the temporal and spatial variability of climatic factors in the alluvial zones, including the aridity index.

Ultimately, the final section of the dissertation addressed how the study examines the combined effects of both climate change and LULC on the alluvial region. In this part, the effect of climate change considering the land cover on groundwater was investigated with spatial and temporal scales. Using a complex ArcGIS software calculation process, the research examines the spatiotemporal impact of climate conditions on the groundwater of the studied locations. Mapping demonstrated both the time and spatial spread of the climate influence.

8.2. CONCLUSIONS

This document's goal was to evaluate groundwater availability, composition, sensitivity to natural causes, and climate change while accounting for changes in land cover changes in the major alluvial aquifer zones. The geospatial techniques of the potential of groundwater resources with AHP and machine learning, stable isotope-geochemistry, inherent vulnerability using DRASTIC, and climate and land use change analysis with complex procedures were taken into consideration in this research. Groundwater resources were then evaluated for both historical and projected periods concerning the impact of climate change. The results of the study highlight the hydro-geoclimatic parameters and their impact on groundwater resources.

Based on the findings of the research work, the following conclusions have been drawn.

Data challenges exist in all studied regions for both surface and subsurface data. Geographical, hydrological, topographical, and agroecological characteristics vary among the regions. The three regions also differ in terms of water availability and use. The western region is characterized by humidity, while the eastern regions are prone to an arid climate. Level to gently sloping plain areas

make up more than two-thirds of the study regions. The three primary factors influencing the groundwater potentials in the study regions are rainfall, geology, and geomorphology.

The geochemical analysis results show that water quality is the other issue facing the region's water supply. Calcium is the dominant cation and SO_4 is the dominant anion. Salinity and hardness are the main characteristic of groundwater in the regions. Because of the depth and local geology, the depleted stable isotope composition of the groundwater in the eastern catchment indicates how long it will take for groundwater to replenish.

The upper watershed of each research region contains high and very high-risk zones, according to intrinsic vulnerability analysis. The medium class covers a significant portion of the watersheds in each research region. Grassland is the major LULC in the study regions. The result of LULC also reveals that the other major LULC in the WC forest while shrublands is the main LULC for EC next to grasslands. The most notable change in terms of LULC in WC was the change from grasslands to other land use classes such as forests. For the EC case, the change from shrubland to grassland is the most important.

The climate analysis results of this study conclude that CMCC-ESM2, FGOALS-g3, and MIROC6 are in better agreement with ground observation data (1981-2010). The most important climatic parameters (precipitation) have reduced in the last decades for both catchments. While the temperature is significantly warming for the past periods. This temperature gradient indicates that the areas are experiencing issues related to climate change. The reduction in precipitation and rise in temperature is of high intensity in the western catchment compared to the eastern catchment. The aridity indices followed a similar downward trend with higher intensity in the western catchment. The potential evapotranspiration also increased alarmingly due to an increase in temperature in recent decades. The findings of the predicted climate analysis also indicate that both research locations' futures will probably have much greater temperatures than they do now. The overall spatial pattern of drought remains stable between 1981 and 2070. However, important quantitative shifts toward more drought will occur in the western catchment and the northeastern and southern parts of the eastern catchment.

The findings indicate the western portion of the WC and the northern and southern extremes of the EC are the study regions most vulnerable to climate change. The influence of future climate change on resources should be carefully considered, as evidenced by the increase in the very high impact

zone on WC and the decline in the very low impact zone on EC. The climate model analysis also indicates that the potential recharge in the study region will decline for the next decades. The recharge data also imply that the two catchments' high recharge zones have a bigger climatic influence than their lowest recharge zones.

Lastly, the researcher hopes that the current study's findings will be useful in the future for the assessment, planning, and management of water resources in the regions.

8.3. RECOMMENDATION

- In any place where water resources are becoming more susceptible to variations in climate and land cover, an optimal policy and practice for managing water resources is necessary.
- To take into consideration the potential water supply deficit in the eastern area, a thorough quantitative assessment is required.
- Since water supply quality is the primary necessity, researchers should concentrate on thoroughly examining water contamination in the eastern watershed in particular.
- Since groundwater is the study area's main source of drinkable water, research should focus on helping to manage the region's water resources.
- Due to their high climatic unpredictability and propensity for drought, researchers should focus their efforts on examining the study location, as this might greatly improve the likelihood of the resident.

8.4. FUTURE RESEARCH

- This study mainly focuses on a few key points within the main alluvial zones; further research is needed to fully understand the hydrogeological conditions of the regions.
- Future scholars should also concentrate more on geochemical and isotopic analysis.
- Each research region's aquifer's susceptibility to natural causes defines a high-risk area. Thus, the next study should focused on anthropogenically generated detail and other particular vulnerabilities in the locations.
- Given the distinct climatic variations in these locations, the effects of climate change are an imminent concern that demands consideration

REFERENCES

Abdullah, T. (2017). Groundwater Vulnerability Using DRASTIC model Applied to Halabja Saidsadiq Basin, IRAQ (Doctoral dissertation, Luleå tekniska universitet). DOI 10.1007/s12517-015-2264-y.

Abebe, A., & Foerch, G. (2006). Catchment characteristics as predictors of base flow index (BFI) in Wabi Shebele river basin, east Africa. In proceedings of conference on international agricultural research for development (pp. 1-8).

Abera, K. A., Gebreyohannes, T., Abrha, B., Hagos, M., Berhane, G., Hussien, A., Belay, A. S., Van Camp, M., & Walraevens, K. (2022). Vulnerability Mapping of Groundwater Resources of Mekelle City and Surroundings, Tigray Region, Ethiopia. Water 2022, Vol. 14, Page 2577, 14(16), 2577. https://doi.org/10.3390/W14162577

Abera, W., Tamene, L., Abegaz, A., & Solomon, D. (2019). Understanding climate and land surface changes impact on water resources using Budyko framework and remote sensing data in Ethiopia. Journal of Arid Environments, 167, 56–64. https://doi.org/10.1016/j.jaridenv.2019.04.017

Aboulouafa, M., Taouil, H., Ahmed, S. I., Tairi, A., Arouya, K., & Hsaissoune, M. (2017). SINTACS and DRASTIC models for groundwater vulnerability assessment and mapping using a GIS and remote sensing techniques: a Case study on Berrechid plain. *IOSR Journal Eng*, *7*(5), 23-30.

Abrha, H., & Hagos, H. (2019). Future drought and aridity monitoring using multi-model approach under climate change in Hintalo Wejerat district, Ethiopia. Sustainable Water Resources Management, 5(4), 1963–1972. https://doi.org/10.1007/s40899-019-00350-1

Adelodun, B., Odey, G., Cho, H., Lee, S., Adeyemi, K. A., & Choi, K. S. (2022). Spatial-temporal variability of climate indices in Chungcheong provinces of Korea: Application of graphical innovative methods for trend analysis. Atmospheric Research, 280, 106420. https://doi.org/10.1016/J.ATMOSRES.2022.106420

Adimalla, N., & Wu, J. (2019). Groundwater quality and associated health risks in a semi-arid region of south India: Implication to sustainable groundwater management. Human and Ecological Risk Assessment, 25(1–2), 191–216. https://doi.org/10.1080/10807039.2018.1546550

Ahmed, M. S., Tanko, A. I., Eduvie, M. O., & Ahmed, M. (2017). Assessment of groundwater vulnerability in Kaduna metropolis, northwest Nigeria. Journal of Geoscience and Environment Protection, 5(06), 97. https://doi.org/10.4236/gep.2017.56011

Ahmed, N., Wang, G., Booij, M. J., Xiangyang, S., Hussain, F., & Nabi, G. (2022). Separation of the Impact of Landuse/Landcover Change and Climate Change on Runoff in the Upstream Area of the Yangtze River, China. Water Resources Management, 36(1), 181–201. https://doi.org/10.1007/S11269-021-03021-Z/FIGURES/9

Aibaidula, D., Ates, N., & Dadaser-Celik, F. (2023). Modelling climate change impacts at a drinking water reservoir in Turkey and implications for reservoir management in semi-arid regions. Environmental Science and Pollution Research, 30(5), 13582–13604. https://doi.org/10.1007/S11356-022-23141-2/FIGURES/2

Akakuru, O. C., Akudinobi, B. E., Nwankwoala, H. O., Akakuru, O. U., & Onyekuru, S. O. (2021). Compendious evaluation of groundwater in parts of Asaba, Nigeria for agricultural sustainability. Springer, 25(6), 915–927. https://doi.org/10.1007/s12303-021-0010-x

Akale, A. T., Moges, M. A., Dagnew, D. C., Tilahun, S. A., & Steenhuis, T. S. (2018). Assessment of Nitrate in Wells and Springs in the North Central Ethiopian Highlands. Water 2018, Vol. 10, Page 476, 10(4), 476. https://doi.org/10.3390/W10040476

Alaminie, A. A., Amarnath, G., Padhee, S. K., Ghosh, S., Tilahun, S. A., Mekonnen, M. A., Assefa, G., Seid, A., Zimale, F. A., & Jury, M. R. (2023). Nested hydrological modeling for flood prediction using CMIP6 inputs around Lake Tana, Ethiopia. Journal of Hydrology: Regional Studies, 46, 101343. https://doi.org/10.1016/J.EJRH.2023.101343

Alaminie, A. A., Tilahun, S. A., Legesse, S. A., Zimale, F. A., Tarkegn, G. B., & Jury, M. R. (2021). Evaluation of Past and Future Climate Trends under CMIP6 Scenarios for the UBNB (Abay), Ethiopia. Water 2021, Vol. 13, Page 2110, 13(15), 2110. https://doi.org/10.3390/W13152110

Alemayehu, T., Kebede, S., Liu, L., & Nedaw, D. (2016). Groundwater Recharge under Changing Landuses and Climate Variability : The Case of Baro-Akobo River Basin , Ethiopia. Journal of Environment and Earth Science, 6(1), 78–95.

Al-Kalbani, M. S., Price, M. F., Abahussain, A., Ahmed, M., & O'Higgins, T. (2014). Vulnerability Assessment of Environmental and Climate Change Impacts on Water Resources in Al Jabal Al Akhdar, Sultanate of Oman. Water 2014, Vol. 6, Pages 3118-3135, 6(10), 3118–3135. https://doi.org/10.3390/W6103118

Allen, R. G., Pereira, L. S., Raes, D., Smith, M., & Ab, W. (1998). Crop evapotranspiration - Guidelines for computing crop water requirements - FAO Irrigation and drainage paper 56 By. 1–15.

Aller, L., Bennet, T., Lehr, J. H., Petty, R. J., Hackett, G., Applications, J. T., Branch, A., & Kerr, R. S. (1987). EPA!600!2-87!035 Hay 1987 DRASTIC: A STANDARDIZED SYSTEM FOR EVALUATING GROUND WATER POLLUTION POTENTIAL USING HYDROGEOLOGIC SETTINGS.

AL-Washali, T., Sharma, S., & Kennedy, M. (2016). Methods of Assessment of Water Losses in Water Supply Systems: a Review. Water Resources Management, 30(14), 4985–5001. https://doi.org/10.1007/S11269-016-1503-7/TABLES/1

Alghamdi, A. G., Aly, A. A., Majrashi, M. A., & Ibrahim, H. M. (2023). Impact of climate change on hydrochemical properties and quality of groundwater for domestic and irrigation purposes in arid environment: a case study of Al-Baha region, Saudi Arabia. Environmental Earth Sciences, 82(1), 1–17. https://doi.org/10.1007/S12665-022-10731-Z/FIGURES/12

Ambalam, K. (2014). Challenges of compliance with multilateral environmental agreements: the case of the United Nations Convention to Combat Desertification in Africa. Journal of Sustainable Development Studies, 5(2).

Amer, S., Gachet, A., Belcher, W. R., Bartolino, J. R., & Hopkins, C. B. (2013). United State Geological Survey. Groundwater exploration and assessment in the Eastern Lowlands and associated Highlands of the Ogaden Basin Area, Eastern Ethiopia: Phase 1 final technical Report.

Andualem, T. G., & Demeke, G. G. (2019). Groundwater potential assessment using GIS and remote sensing: A case study of Guna tana landscape, upper blue Nile Basin, Ethiopia. Journal of Hydrology: Regional Studies, 24. https://doi.org/10.1016/j.ejrh.2019.100610

Andualem, T. G., Demeke, G. G., Ahmed, I., Dar, M. A., & Yibeltal, M. (2021). Groundwater recharge estimation using empirical methods from rainfall and streamflow records. *Journal of Hydrology: Regional Studies, 37*, 100917. https://doi.org/10.1016/j.ejrh.2021.100917

Arabameri, A., Rezaei, K., Cerda, A., Lombardo, L., & Rodrigo-Comino, J. (2019). GIS-based groundwater potential mapping in Shahroud plain, Iran. A comparison among statistical (bivariate and

multivariate), data mining and MCDM approaches. Science of the Total Environment, 658, 160–177. https://doi.org/10.1016/j.scitotenv.2018.12.115

Arya, S., Subramani, T., Vennila, G., & Roy, P. D. (2020). Groundwater vulnerability to pollution in the semi-arid Vattamalaikarai River Basin of south India thorough DRASTIC index evaluation. Geochemistry, 80(4), 125635. https://doi.org/10.1016/J.CHEMER.2020.125635

Arzu Firat, E., & Fatma, G. (2013). DRASTIC-based methodology for assessing groundwater vulnerability in the Gümüshaciköy and Merzifon basin (Amasya, Turkey). Earth sciences research journal, 17(1), 33-40.

Asfaw, D., & Mengistu, D. (2020). Modeling megech watershed aquifer vulnerability to pollution using modified DRASTIC model for sustainable groundwater management, Northwestern Ethiopia. Groundwater for Sustainable Development, 11, 100375. https://doi.org/10.1016/J.GSD.2020.100375

Asif, Z., Chen, Z., Sadiq, R., & Zhu, Y. (2023). Climate Change Impacts on Water Resources and Sustainable Water Management Strategies in North America. Water Resources Management, 37(6), 2771–2786. https://doi.org/10.1007/S11269-023-03474-4/FIGURES/1

Avand, M., Janizadeh, S., Naghibi, S. A., Pourghasemi, H. R., Bozchaloei, S. K., & Blaschke, T. (2019). A comparative assessment of Random Forest and k-Nearest Neighbor classifiers for gully erosion susceptibility mapping. Water (Switzerland), 11(10). https://doi.org/10.3390/w11102076

Awawdeh, M., Obeidat, M., & Zaiter, G. (2015). Groundwater vulnerability assessment in the vicinity of Ramtha wastewater treatment plant, North Jordan. *Applied Water Science, 5,* 321-334.

Awulachew, S. B., Yilma, A. D., Loulseged, M., Loiskandl, W., Ayana, M., & Alamirew, T. (2007). Wp123.

Ayad, A., & Saeid, A. (2022). Remote Sensing in Water Quality and Water Resources Management. International Journal for Research in Applied Sciences and Biotechnology, 9(1), 163–170. https://doi.org/10.31033/IJRASB.9.1.19

Ayenew, T. (2005). Major ions composition of the groundwater and surface water systems and their geological and geochemical controls in the Ethiopian volcanic terrain. SINET: Ethiopian Journal of Science, 28(2), 171–188. https://doi.org/10.4314/SINET.V28I2.18253

Ayenew, T. (2006). Major ions composition of the groundwater and surface water systems and their geological and geochemical controls in the Ethiopian volcanic terrain. SINET: Ethiopian Journal of Science, 28(2), 171–188. https://doi.org/10.4314/sinet.v28i2.18253

Ayenew, T., Kebede, S., & Alemyahu, T. (2008). Environmental isotopes and hydrochemical study applied to surface water and groundwater interaction in the Awash River basin. Hydrological Processes, 22(10), 1548–1563. https://doi.org/10.1002/hyp.6716

Ayenew, T., GebreEgziabher, M., Kebede, S., & Mamo, S. (2013). Integrated assessment of hydrogeology and water quality for groundwater-based irrigation development in the Raya Valley, northern Ethiopia. Water International, 38(4), 480–492. https://doi.org/10.1080/02508060.2013.821640

Ayenew, T., Demlie, M., & Wohnlich, S. (2008). Hydrogeological framework and occurrence of groundwater in the Ethiopian aquifers. *Journal of African Earth Sciences*, *52*(3), 97–113. https://doi.org/10.1016/j. jafrearsci.2008.06.006

Azma, A., Narreie, E., Shojaaddini, A., Kianfar, N., Kiyanfar, R., Alizadeh, S. M. S. & Davarpanah, A. (2021). Statistical modeling for spatial groundwater potential map based on gis technique. *Sustainability (Switzerland)*, 13. https://doi.org/10.3390/su13073788

Bahiru, E. A. (2011). INTER-RELATIONSHIP BETWEEN LITHOLOGY AND STRUCTURE AND ITS CONTROL ON GOLD MINERALIZATION IN BUHWEJU AREA , SW OF UGANDA Inter-Relationship between Lithology and Structure and its Control on Gold Mineralization in Buhweju area , SW OF UGANDA. 73.

Balakrishnan, M. (2019). Groundwater Potential Zone Mapping using Geospatial Techniques in Walayar Watershed. International Journal of Engineering and Advanced Technology, 9(1), 1157–1161. https://doi.org/10.35940/ijeat.a9511.109119

Balcha, Y., Malcherek, A., & Alamirew, T. (2022). Selection of CMIP6 Climate Models Using Statistical and Data Mining Approaches, Case of Upper Awash Sub-Basin (UASB), Ethiopia. https://doi.org/10.20944/preprints202209.0108.v1

Baye, T. G. (2017). Poverty, peasantry and agriculture in Ethiopia. Annals of Agrarian Science, 15(3), 420–430. https://doi.org/10.1016/j.aasci.2017.04.002

Baltas, E. (2007). Spatial distribution of climatic indices in northern Greece. 78, 69–78. https://doi.org/10.1002/met

Baltodano, A., Agramont, A., Reusen, I., & van Griensven, A. (2022). Land Cover Change and Water Quality: How Remote Sensing Can Help Understand Driver–Impact Relations in the Lake Titicaca Basin. Water (Switzerland), 14(7), 1021. https://doi.org/10.3390/W14071021/S1

Bedaso, Z., & Wu, S. Y. (2021). Linking precipitation and groundwater isotopes in Ethiopia - Implications from local meteoric water lines and isoscapes. Journal of Hydrology, 596(February), 126074. https://doi.org/10.1016/j.jhydrol.2021.126074

Bedaso, Z. K., DeLuca, N. M., Levin, N. E., Zaitchik, B. F., Waugh, D. W., Wu, S. Y., Harman, C. J., & Shanko, D. (2020). Spatial and temporal variation in the isotopic composition of Ethiopian precipitation. Journal of Hydrology, 585. https://doi.org/10.1016/j.jhydrol.2019.124364

Begashaw, G., & NT., T. (2017). Characteristics and Productivity of the Sediments and Volcanic Rocks Aquifers in. 4(1), 46–57. https://doi.org/10.20448/journal.506.2017.41.46.57

Beillouin, D., Cardinael, R., Berre, D., Boyer, A., Corbeels, M., Fallot, A., Feder, F., & Demenois, J. (2022). A global overview of studies about land management, land-use change, and climate change effects on soil organic carbon. Global Change Biology, 28(4), 1690–1702. https://doi.org/10.1111/GCB.15998

Bera, A., Mukhopadhyay, B. P., & Das, S. (2022). Groundwater vulnerability and contamination risk mapping of semi-arid Totko river basin, India using GIS-based DRASTIC model and AHP techniques. Chemosphere, 307, 135831. https://doi.org/10.1016/J.CHEMOSPHERE.2022.135831

Bera, A., Mukhopadhyay, B. P., & Barua, S. (2020). Delineation of groundwater potential zones in Karha river basin, Maharashtra, India, using AHP and geospatial techniques. Arabian Journal of Geosciences, 13(15). Retrieved from https://doi.org/ 10.1007/s12517 020 057022

Berehanu, B., Ayenew, T., & Azagegn, T. (2017). Challenges of groundwater flow model calibration using MODFLOW in Ethiopia: With particular emphasis to the upper awash river basin. *Journal of Geoscience and Environment Protection*, *5*(3), 50–66. https://doi.org/10. 4236/gep.2017.53005

Berhail, S. (2019). The impact of climate change on groundwater resources in northwestern Algeria.

Berhanu, B., Melesse, A. M., & Seleshi, Y. (2013). GIS based hydrological zones and soil geo database of Ethiopia. Catena, 104, 21–31. Retrieved from https://doi.org/10.1016/j.catena.2012.12.007

Berhanu, B., Seleshi, Y., & Melesse, A. M. (2014). Surface water and groundwater resources of Ethiopia: Potentials and challenges of water resources development. Nile River Basin: Ecohydrological Challenges, Climate Change and Hydropolitics (Vol. 9783319027203, pp. 97–117). Belin, Germany: Springer. Retrieved from https://doi.org/ 10.1007/978 3 319 02720 3_6

Bershaw, J. (2018). Controls on deuterium excess across Asia. Geosciences (Switzerland), 8(7). https://doi.org/10.3390/geosciences8070257

Berhe Zenebe, G., Hussien, A., Girmay, A., & Hailu, G. (2020). Spatial analysis of groundwater vulnerability to contamination and human activity impact using a modified DRASTIC model in Elalla-Aynalem Catchment, Northern Ethiopia. Sustainable Water Resources Management, 6(3), 1–16. https://doi.org/10.1007/S40899-020-00406-7/FIGURES/13

Bergstra, J., Ca, J. B., & Ca, Y. B. (2012). Random Search for Hyper-Parameter Optimization Yoshua Bengio. In Journal of Machine Learning Research (Vol. 13). http://scikit-learn.sourceforge.net.

Bešťáková, Z., Strnad, F., Vargas Godoy, M. R., Singh, U., Markonis, Y., Hanel, M., Máca, P., & Kyselý, J. (2023). Changes of the aridity index in Europe from 1950 to 2019. Theoretical and Applied Climatology, 151(1–2), 587–601. https://doi.org/10.1007/S00704-022-04266-3/FIGURES/7

Berhane, M. (2013). Estimation of monthly flow for ungauged catchment (case study baro. *Akobo Basin)*. http://edt.aau.edu.et/handle/123456789/9849

Beven, K., Kirkby, M., E. Freer, J., & Lamb, R. (2021). A history of TOPMODEL. Hydrology and Earth System Sciences, 25(2), 527–549. https://doi.org/10.5194/HESS-25-527-2021

Beven, K. (1997). Topmodel: A critique . *Hydrological Process*, 11. http://doi.org/10.1002/(SICI)169-1085(199707)11:9<1069

Bhan, S. K., & Krishnanunni, K. (1983). Applications of remote sensing techniques to geology. Proceedings of the Indian Academy of Sciences Section C: Engineering Sciences, 6(4), 297–311. https://doi.org/10.1007/BF02881136

Bhat, N. A., & Jeelani, G. (2018). Quantification of groundwater–surface water interactions using environmental isotopes: A case study of Bringi Watershed, Kashmir Himalayas, India. Journal of Earth System Science, 127(5), 1–11. https://doi.org/10.1007/s12040-018-0964-x

Bhatt, A. G., Kumar, A., & Singh, S. K. (2022). Hydro-geochemical evolution of groundwater and associated human health risk in River Sone subbasin of Middle-Gangetic floodplain, Bihar, India. *Arabian Journal of Geosciences*, *15*(5), 405. https://doi.org/10.1007/s12517-021-09269-4

Birhanu, A., Masih, I., van der Zaag, P., Nyssen, J., & Cai, X. (2019). Impacts of land use and land cover changes on hydrology of the Gumara catchment, Ethiopia. Physics and Chemistry of the Earth, 112(July 2018), 165–174. https://doi.org/10.1016/j.pce.2019.01.006

Bogale, G. A., & Erena, Z. B. (2022). Drought vulnerability and impacts of climate change on livestock production and productivity in different agro-Ecological zones of Ethiopia. Http://Www.Tandfonline.Com/Action/JournalInformation?Show=aimsScope&journalCode=taar20#.VsXoziCLRhE, 50(1), 471–489. https://doi.org/10.1080/09712119.2022.2103563

Brierley, G. J., Han, M., Li, X., Li, Z., & Huang, H. Q. (2022). Geo-eco-hydrology of the Upper Yellow River. Wiley Interdisciplinary Reviews: Water, 9(3), e1587. https://doi.org/10.1002/WAT2.1587

Bie, Q., Shi, Y., Li, X., & Wang, Y. (2022). Contrastive Analysis and Accuracy Assessment of Three Global 30 m Land Cover Maps Circa 2020 in Arid Land. *Sustainability 2023, Vol. 15, Page 741*, *15*(1), 741. https://doi.org/10.3390/SU15010741

Boschetto, R., Mohamed, R., Agronomy, J. A.-I. J. of, & 2010. (2010). Vulnerability to desertification in a Sub-Saharan region: a first local assessment in five villages of southern region of Malawi. Agronomy.It. https://www.agronomy.it/index.php/agro/article/view/72

Boufekane, A., Maizi, D., Madene, E., Busico, G., & Zghibi, A. (2022). Hybridization of GALDIT method to assess actual and future coastal vulnerability to seawater intrusion. Journal of Environmental Management, 318, 115580. https://doi.org/10.1016/J.JENVMAN.2022.115580

Budyko, M. I. (Mikhail I., & Miller, D. H. (1974). Climate and life. 508.

Campo, B., Bohacs, K. M., & Amorosi, A. (2020). Late Quaternary sequence stratigraphy as a tool for groundwater exploration: Lessons from the Po River Basin (northern Italy). *AAPG Bulletin*, *104*, 681–710. https:// doi.org/10.1306/06121918116

Chávez García Silva, R., Grönwall, J., van der Kwast, J., Danert, K., & Foppen, J. W. (2020, 15). Estimating domestic self-supply groundwater use in urban continental Africa. *Environmental Research Letters*, *15*(10), 1040b2. https://doi.org/10.1088/1748-9326/ab9af9

Campo, B., Bohacs, K. M., & Amorosi, A. (2020). Late Quaternary sequence stratigraphy as a tool for groundwater exploration: Lessons from the Po River Basin (northern Italy). AAPG Bulletin, 104(3), 681–710. https://doi.org/10.1306/06121918116

Caran, C., Jr, C. W., & Thompson, E. (1981). Lineament analysis and inference of geologic structure examples from the Balcones/Ouachita trend of Texas (1). Retrieved from https://archives.data pages.com/data/gcags/data/031/031001/0059.htm

Catley, A., Admassu, B., Bekele, G., & Abebe, D. (2014). Livestock mortality in pastoralist herds in Ethiopia and implications for drought response. Disasters, 38(3), 500–516. https://doi.org/10.1111/DISA.12060

Chakilu, G. G., Sándor, S., Zoltán, T., & Phinzi, K. (2022). Climate change and the response of streamflow of watersheds under the high emission scenario in Lake Tana sub-basin, upper Blue Nile basin, Ethiopia. Journal of Hydrology: Regional Studies, 42, 101175. https://doi.org/10.1016/J.EJRH.2022.101175

Chen, X., Yu, L., Cao, Y., Xu, Y., Zhao, Z., Zhuang, Y., Liu, X., Du, Z., Liu, T., Yang, B., He, L., Wu, H., Yang, R., & Gong, P. (2023). Habitat quality dynamics in China's first group of national parks in recent four decades: Evidence from land use and land cover changes. *Journal of Environmental Management*, *325*, 116505. https://doi.org/10.1016/J.JENVMAN.2022.116505

Chernet, T., Hart, W. K., Aronson, J. L., & Walter, R. C. (1998). New age constraints on the timing of volcanism and tectonism in the northern Main Ethiopian Rift - southern Afar transition zone (Ethiopia). Journal of Volcanology and Geothermal Research, 80(3–4), 267–280. https://doi.org/10.1016/S0377-0273(97)00035-8

Chimdessa, K., Quraishi, S., Kebede, A., & Alamirew, T. (2019). Effect of land use land cover and climate change on river flow and soil loss in Didessa River Basin, South West Blue Nile, Ethiopia. Hydrology, 6(1). https://doi.org/10.3390/hydrology6010002

Chishugi, D. U., Sonwa, D. J., Kahindo, J. M., Itunda, D., Chishugi, J. B., Félix, F. L., & Sahani, M. (2021). How Climate Change and Land Use/Land Cover Change Affect Domestic Water Vulnerability in Yangambi Watersheds (D. R. Congo). Land 2021, Vol. 10, Page 165, 10(2), 165. https://doi.org/10.3390/LAND10020165

Choto, M., & Fetene, A. (2019). Impacts of land use/land cover change on stream flow and sediment yield of Gojeb watershed, Omo-Gibe basin, Ethiopia. Remote Sensing Applications: Society and Environment, 14(January), 84–99. https://doi.org/10.1016/j.rsase.2019.01.003

Clarke, B., Otto, F., Stuart-Smith, R., & Harrington, L. (2022). Extreme weather impacts of climate change: an attribution perspective. Environmental Research: Climate, 1(1), 012001. https://doi.org/10.1088/2752-5295/AC6E7D

Coplen, T. B. (1996). New guidelines for reporting stable hydrogen, carbon, and oxygen isotope-ratio data. Geochimica et Cosmochimica Acta, 60(17), 3359–3360. https://doi.org/10.1016/0016-7037(96)00263-3

Craig, H. (1961). Isotopic Variations in Meteoric Waters. Science, 133(3465), 1702–1703. https://doi.org/10.1126/SCIENCE.133.3465.1702

Cosgrove, W. J., & Loucks, D. P. (2015). Water management: Current and future challenges and research directions. Water Resources Research, 51(6), 4823–4839. https://doi.org/10.1002/2014WR016869

Colins, J., Sashikkumar, M. C., Anas, P. A., & Kirubakaran, M. (2016). GIS-based assessment of aquifer vulnerability using DRASTIC Model: A case study on Kodaganar basin. *Earth Sciences Research Journal*, *20*(1), 1-8.

Croitoru, A. E., Piticar, A., Imbroane, A. M., & Burada, D. C. (2013a). Spatiotemporal distribution of aridity indices based on temperature and precipitation in the extra-Carpathian regions of Romania. Theoretical and Applied Climatology, 112(3–4), 597–607. https://doi.org/10.1007/S00704-012-0755-2

Czodrowski, P. (2014). Count on kappa. Journal of Computer-Aided Molecular Design, 28(11), 1049–1055. https://doi.org/10.1007/s10822-014-9759-6

Dandge, K. P., & Patil, S. S. (2022). Spatial distribution of ground water quality index using remote sensing and GIS techniques. Applied Water Science, 12(1), 1–18. https://doi.org/10.1007/s13201-021-01546-7

Dansgaard, W. (1964). Stable isotopes in precipitation. tellus, 16(4), 436-468. https://doi.org/10.3402/tellusa.v16i4.8993

Dargo, F., Madalcho, A., Dargo Girmay, F., Gebreselassie, G., & Bajigo, A. (2018). Climate change risk management and coping strategies for sustainable camel production in the case of Somali Region, Ethiopia. Researchgate.Net, 4(9), 66–75. Retrieved from https://doi.org/10.32861/jbr.49.66.75

Das, B., & Pal, S. C. (2020). Assessment of groundwater recharge and its potential zone identification in groundwater-stressed Goghat-I block of Hugli District, West Bengal, India. *Environment, Development and Sustainability*, *22*(6), 5905–5923. https://doi.org/10. 1007/s10668-019-00457-7

Das, S., Gupta, A., & Ghosh, S. (2017). Exploring ground water potential zones using MIF technique in semi arid region: A case study of Hingoli district, Maharashtra. Spatial Information Research, 25(6), 749–756. Retrieved from https://doi.org/10.1007/ s41324 017 0144 0

Das, N., Patel, A., Deka, G., Das, A., … K. S.-G. for, & 2015, undefined. (2015). Geochemical controls and future perspective of arsenic mobilization for sustainable groundwater management: a study from Northeast India. Elsevier. https://www.sciencedirect.com/science/article/pii/S2352801X15300060

Dave, V., Pandya, M., Zone, R. G.-Ann. A., & 2019, undefined. (2019). Identification of desertification hot spot using aridity index. Researchgate.Net.

Deepa, B., Sci, K. R.-Int. J. H., & 2022, undefined. (2022). Epileptic seizure detection using deep learning through min max scaler normalization. Media.Neliti.Com, 6(S1), 10981–10996. https://doi.org/10.53730/ijhs.v6nS1.7801

Degife, A. W., Zabel, F., & Mauser, W. (2018). Assessing land use and land cover changes and agricultural farmland expansions in Gambella Region, Ethiopia, using Landsat 5 and Sentinel 2a multispectral data. Heliyon, 4(11), e00919. https://doi.org/10.1016/j.heliyon.2018.e00919

Dehnavi, A. G., Sarikhani, R., & Nagaraju, D. (2011). Hydro geochemical and rock water interaction studies in East of Kurdistan, NW of Iran. Int J Environ Sci Res, 1(1), 16-22.

Deidda, R., Marrocu, M., Caroletti, G., Pusceddu, G., Langousis, A., Lucarini, V., Puliga, M., & Speranza, A. (2013). Regional climate models' performance in representing precipitation and temperature over selected Mediterranean areas. Hydrology and Earth System Sciences, 17(12), 5041–5059. https://doi.org/10.5194/hess-17-5041-2013

Demissie, T. A. (2022). Land use and land cover change dynamics and its impact on watershed hydrological parameters: the case of Awetu watershed, Ethiopia. *Journal of Sedimentary Environments 2021 7:1*, *7*(1), 79–94. https://doi.org/10.1007/S43217-021-00084-1

Deneke, F., Shetty, A., & Fufa, F. (2023). Land cover change and its implications to hydrological variables and soil erodibility in Lower Baro watershed, Ethiopia: a systematic review. *Sustainable Water Resources Management*, *9*(2), 1–13. https://doi.org/10.1007/S40899-023-00843-0/FIGURES/7

Deniz, A., Toros, H., & Incecik, S. (2011). Spatial variations of climate indices in Turkey. September 2018. https://doi.org/10.1002/joc.2081

Devereux, S. (2010). Better marginalised than incorporated? Pastoralist livelihoods in Somali Region, Ethiopia. European Journal of Development Research, 22(5), 678–695. Retrieved from https://doi.org/10.1057/ EJDR.2010.29/FIGURES/1

Devereux, S. (2006). Vulnerable livelihoods in Somali region, Ethiopia. Retrieved from https://dlci hoa.org/assets/ upload/combined documents/20200804033942909. Pdf

De Martonne, E. (1926). De Martonne, E. (1926) Une nouvelle function climatologique L'indice d'aridité [A New Climatological Function The Aridity Index]. La Meteorologie, 2, 449-458. - References - Scientific Research Publishing. https://www.scirp.org/(S(czeh2tfqw2orz553k1w0r45))/ reference/referencespapers.aspx? referenceid=3103106

Djémin, J. É., Kouamé, J. K., Deh, K. S., Abinan, A. T., Jourda, J. P., Djémin, J. É., Kouamé, J. K., Deh, K. S., Abinan, A. T., & Jourda, J. P. (2016). Contribution of the Sensitivity Analysis in Groundwater Vulnerability Assessing Using the DRASTIC Method: Application to Groundwater in Dabou Region (Southern of Côte d'Ivoire). Journal of Environmental Protection, 7(1), 129–143. https://doi.org/10.4236/JEP.2016.71012

Dippong, T., Hoaghia, M. A., & Senila, M. (2022). Appraisal of heavy metal pollution in alluvial aquifers. Study case on the protected area of Ronișoara Forest, Romania. Ecological Indicators, 143, 109347. https://doi.org/10.1016/J.ECOLIND.2022.109347

Dhar, A., Sahoo, S., & Sahoo, M. (2015). Identification of groundwater potential zones considering water quality aspect. Environmental Earth Sciences, 74(7), 5663–5675. Retrieved from https://doi.org/10.1007/ s12665 015 4580 7

Di Lorenzo, T., & Galassi, D. M. P. (2013). Agricultural impact on Mediterranean alluvial aquifers: Do groundwater communities respond? Fundamental and Applied Limnology, 182(4), 271–282. https://doi.org/10.1127/1863-9135/2013/0398

Dimkić, D., Anđelković, A., & Babalj, M. (2022). Droughts in Serbia through the analyses of De Martonne and Ped indices. Environmental Monitoring and Assessment, 194(4), 1–16. https://doi.org/10.1007/S10661-022-09911-Y/FIGURES/15

dos Santos, J. C., Lyra, G. B., Abreu, M. C., de Oliveira-Júnior, J. F., Bohn, L., Cunha-Zeri, G., & Zeri, M. (2022). Aridity indices to assess desertification susceptibility: a methodological approach using gridded climate data and cartographic modeling. Natural Hazards, 111(3), 2531–2558. https://doi.org/10.1007/S11069-021-05147-0/FIGURES/12

Duan, W., Maskey, S., Chaffe, P. L. B., Luo, P., He, B., Wu, Y., & Hou, J. (2021). Recent Advancement in Remote Sensing Technology for Hydrology Analysis and Water Resources Management. Remote Sensing 2021, Vol. 13, Page 1097, 13(6), 1097. https://doi.org/10.3390/RS13061097

Duan, X., Chen, Y., Wang, L., Zheng, G., & Liang, T. (2023). The impact of land use and land cover changes on the landscape pattern and ecosystem service value in Sanjiangyuan region of the Qinghai-Tibet Plateau. *Journal of Environmental Management*, *325*, 116539. https://doi.org/10.1016/J.JENVMAN.2022.116539

Dubois, E., Larocque, M., & Brunner, P. (2023). Impact of land cover changes on Long-Term Regional-Scale groundwater recharge simulation in cold and humid climates. Hydrological Processes, 37(2), e14810. https://doi.org/10.1002/HYP.14810

Duvva, L. K., Panga, K. K., Dhakate, R., & Himabindu, V. (2022). Health risk assessment of nitrate and fluoride toxicity in groundwater contamination in the semi-arid area of Medchal, South India. Applied Water Science, 12(1), 1–21. https://doi.org/10.1007/S13201-021-01557-4/FIGURES/15

Ebrahimi-Khusfi, Z., Mirakbari, M., & Soleimani-Sardo, M. (2021). Aridity Index Variations and Dust Events in Iran from 1990 to 2018. Https://Doi.Org/10.1080/24694452.2021.1896355, 112(1), 123–140. https://doi.org/10.1080/24694452.2021.1896355

Economou-Eliopoulos, M., Frei, R., & Atsarou, C. (2014). Application of chromium stable isotopes to the evaluation of Cr(VI) contamination in groundwater and rock leachates from central Euboea and the Assopos basin (Greece). CATENA, 122, 216–228. https://doi.org/10.1016/J.CATENA.2014.06.013

ECA. (2013). Ethiopian Drinking Water Quality Standard 2013 - CMP CoWASH Ethiopia. https://www.cmpethiopia.org/media/ethiopian_drinking_water_quality_standard_2013

Edossa, D. C., Babel, M. S., & Gupta, A. Das. (2010). Drought analysis in the Awash River Basin, Ethiopia. Water Resources Management, 24(7), 1441–1460. https://doi.org/10.1007/S11269-009-9508-0/METRICS

Edwards, P. N. (2011). History of climate modeling. Wiley Interdisciplinary Reviews: Climate Change, 2(1), 128–139. https://doi.org/10.1002/WCC.95

Ekanem, A. M., Ikpe, E. O., George, N. J., & Thomas, J. E. (2022). Integrating geoelectrical and geological techniques in GIS-based DRASTIC model of groundwater vulnerability potential in the raffia city of Ikot Ekpene and its environs, southern Nigeria. International Journal of Energy and Water Resources 2022, 1–20. https://doi.org/10.1007/S42108-022-00202-3

Eltarabily, M. G., Abd-Elaty, I., Elbeltagi, A., Zeleňáková, M., & Fathy, I. (2023). Investigating Climate Change Effects on Evapotranspiration and Groundwater Recharge of the Nile Delta Aquifer, Egypt. Water 2023, Vol. 15, Page 572, 15(3), 572. https://doi.org/10.3390/W15030572

Elias, E., Seifu, W., Tesfaye, B., & Girmay, W. (2018). Land Use Land Cover Changes and their impact on the lake ecosystem of the Central Rift Valley of Ethiopia. Preprints (Www.Preprints.Org), December, 1–17. https://doi.org/10.20944/preprints201812.0320.v1

El-Magd, S. A. A., Ahmed, H., Pham, Q. B., Linh, N. T. T., Anh, D. T., Elkhrachy, I., & Masoud, A. M. (2022). Possible Factors Driving Groundwater Quality and Its Vulnerability to Land Use, Floods, and Droughts Using Hydrochemical Analysis and GIS Approaches. Water 2022, Vol. 14, Page 4073, 14(24), 4073. https://doi.org/10.3390/W14244073

Elubid, B. A., Huang, T., Peng, D. P., Ahmed, E. H., & Babiker, M. M. (2020). Delineation of groundwater potential zones using integrated remote sensing, gis and multi-criteria decision making (Mcdm). *DESALINATION AND WATER Treatment*, *192*, 248–258. https://doi.org/10.5004/dwt.2020.25761

Elzain, H. E., Chung, S. Y., Senapathi, V., Sekar, S., Lee, S. Y., Roy, P. D., Hassan, A., & Sabarathinam, C. (2022). Comparative study of machine learning models for evaluating groundwater vulnerability to nitrate contamination. Ecotoxicology and Environmental Safety, 229, 113061. https://doi.org/10.1016/J.ECOENV.2021.113061

Esfandeh, S., Danehkar, A., Salmanmahiny, A., Sadeghi, S. M. M., & Marcu, M. V. (2022). Climate change risk of urban growth and land use/land cover conversion: An in-depth review of the recent research in Iran. *Sustainability (Switzerland)*, *14*(1), 338. https://doi.org/10.3390/SU14010338/S1

Espinosa, L. A., Portela, M. M., Matos, J. P., & Gharbia, S. (2022). Climate Change Trends in a European Coastal Metropolitan Area: Rainfall, Temperature, and Extreme Events (1864–2021). Atmosphere 2022, Vol. 13, Page 1995, 13(12), 1995. https://doi.org/10.3390/ATMOS13121995

Eze, J. N., & Onokala, P. C. (2022). Pattern of household vulnerability to desertification in Yobe state, Nigeria. GeoJournal, 87(4), 2699–2717. https://doi.org/10.1007/S10708-021-10395-5/FIGURES/3

Fallahi, M. M., Shabanlou, S., Rajabi, A., Yosefvand, F., & IzadBakhsh, M. A. (2023). Effects of climate change on groundwater level variations affected by uncertainty (case study: Razan aquifer). Applied Water Science, 13(6), 1–16. https://doi.org/10.1007/S13201-023-01949-8/TABLES/2

Farhat, F., Kashifi, M. T., Jamal, A., & Saba, I. (2022). Spatiotemporal projections of precipitation and temperature over Afghanistan based on CMIP6 global climate models. Modeling Earth Systems and Environment, 8(3), 4229–4242. https://doi.org/10.1007/S40808-022-01361-2/FIGURES/7

Franek, J., & Kresta, A. (2014). Judgment Scales and Consistency Measure in AHP. Procedia Economics and Finance, 12, 164–173. https://doi.org/10.1016/S2212-5671(14)00332-3

Farzin, M., Avand, M., Ahmadzadeh, H., Zelenakova, M., & Tiefenbacher, J. P. (2021). Assessment of ensemble models for groundwater potential modeling and prediction in a karst *water*shed. *Water*, *13*, 2540. https://doi.org/10. 3390/W13182540

Fashae, O. A., Tijani, M. N., Talabi, A. O., & Adedeji, O. I. (2014). Delineation of groundwater potential zones in the crystalline basement terrain of SW Nigeria: an integrated GIS and remote sensing approach. Applied Water Science, 4(1), 19–38. Retrieved from https://doi.org/10.1007/s13201 013 0127 9

Frederick, K. D., & Major, D. C. (1997). Climate change and water resources. Climatic Change, 37(1), 7–23. https://doi.org/10.1023/A:1005336924908/METRICS

Friedl, M. A., McIver, D. K., Hodges, J. C. F., Zhang, X. Y., Muchoney, D., Strahler, A. H., Woodcock, C. E., Gopal, S., Schneider, A., Cooper, A., Baccini, A., Gao, F., & Schaaf, C. (2002). Global land cover mapping from MODIS: algorithms and early results. Remote Sensing of Environment, 83(1–2), 287–302. https://doi.org/10.1016/S0034-4257(02)00078-0

Funk, C., Rowland, J., Eilerts, G., … E. K.-U. G. S., & 2012, undefined. (2012). A climate trend analysis of Ethiopia. Pubs.Usgs.Gov. https://pubs.usgs.gov/fs/2012/3053/FS12-3053_ethiopia.pdf

Fynn, O. F., Yidana, S. M., Chegbeleh, L. P., & Yiran, G. B. (2016). Evaluating groundwater recharge processes using stable isotope signatures—the Nabogo catchment of the White Volta, Ghana. Arabian Journal of Geosciences, 9(4), 1–15. https://doi.org/10.1007/S12517-015-2299-0/FIGURES/9

Galal Eltarabily, M., Abd-Elaty, I., Elbeltagi, A., Zelě Náková, M., & Fathy, I. (2023). Investigating Climate Change Effects on Evapotranspiration and Groundwater Recharge of the Nile Delta Aquifer, Egypt. https://doi.org/10.3390/w15030572

Gandhi, G. M., Parthiban, S., Thummalu, N., & Christy, A. (2015). Ndvi: Vegetation Change Detection Using Remote Sensing and Gis - A Case Study of Vellore District. Procedia Computer Science, 57, 1199–1210. https://doi.org/10.1016/j.procs.2015.07.415

Ganem, K. A., Xue, Y., Rodrigues, A. de A., Franca-Rocha, W., de Oliveira, M. T., de Carvalho, N. S., Cayo, E. Y. T., Rosa, M. R., Dutra, A. C., & Shimabukuro, Y. E. (2022). Mapping South America’s Drylands through Remote Sensing—A Review of the Methodological Trends and Current Challenges. Remote Sensing 2022, Vol. 14, Page 736, 14(3), 736. https://doi.org/10.3390/RS14030736

Gao, T., Liu, J., Zhang, T., Hu, Y., Shang, J., Wang, S., Xiao, X., Liu, C., Kang, S., Sillanpää, M., & Zhang, Y. (2017). Estimating interaction between surface water and groundwater in a permafrost region using heat tracing methods. The Cryosphere, September, 1–24. https://doi.org/10.5194/tc-2017-176

Gashaw, T., Tulu, T., Argaw, M., & Worqlul, A. W. (2018). Modeling the hydrological impacts of land use/land cover changes in the Andassa watershed, Blue Nile Basin, Ethiopia. Science of the Total Environment, 619(620), 1394–1408. https://doi.org/10.1016/j.scitotenv.2017.11.191

Gavrilov, M., An, W., Xu, C., Radaković, M., Atmosphere, Q. H.-, & 2019. (2019). Independent aridity and drought pieces of evidence based on meteorological data and tree ring data in Southeast Banat, Vojvodina, Serbia. Mdpi.Com. https://www.mdpi.com/542856

Gebrechorkos, S. H., Hülsmann, S., & Bernhofer, C. (2020). Analysis of climate variability and droughts in East Africa using high- resolution climate data products. Global and Planetary Change, 186(January), 103130. https://doi.org/10.1016/j.gloplacha.2020.103130

Gebremedhin, M. A., Kahsay, G. H., & Fanta, H. G. (2019). Assessment of spatial distribution of aridity indices in Raya valley , northern Ethiopia. Applied Water Science, January. https://doi.org/10.1007/s13201-018-0868-6

Gebrewahid, M., KASA, A., & K. E. J. (2017). Analyzing drought conditions, interventions and mapping of vulnerable areas using NDVI and SPI indices in Eastern Ethiopia, Somali region. Ejesm.Org, 10(9), 1998–0507. Retrieved from http://ejesm.

Gebremedhin, M. A., Abraha, A. Z., & Fenta, A. A. (2018). Changes in future climate indices using Statistical Downscaling Model in the upper Baro basin of Ethiopia. Theoretical and Applied Climatology, 133(1–2), 39–46. https://doi.org/10.1007/S00704-017-2151-4/FIGURES/4

Gebremedhin, M. A., Kahsay, G. H., & Fanta, H. G. (2018). Assessment of spatial distribution of aridity indices in Raya valley, northern Ethiopia. Applied Water Science, 8(8), 1–8. https://doi.org/10.1007/S13201-018-0868-6/FIGURES/4

Gebeyehu, A., Ayenew, T., & Asrat, A. (2022). Hydrogeochemistry of the groundwater system of the transboundary basement and volcanic aquifers of the Bulal catchment, Southern Ethiopia. Journal of African Earth Sciences, 194, 104622. https://doi.org/10.1016/J.JAFREARSCI.2022.104622

Gedefaw, M. (2023). Assessment of changes in climate extremes of temperature over Ethiopia. Http://Www. Editorialmanager.Com/Cogenteng, 10(1). https://doi.org/10.1080/23311916.2023.2178117

Gelete, G., Gokcekus, H., & Gichamo, T. (2020). Impact of climate change on the hydrology of Blue Nile basin, Ethiopia: A review. Journal of Water and Climate Change, 11(4), 1539–1550. https://doi.org/10.2166/wcc.2019.014

Gerrits, A. M. J., Savenije, H. H. G., Veling, E. J. M., & Pfister, L. (2009). Analytical derivation of the Budyko curve based on rainfall characteristics and a simple evaporation model. Water Resources Research, 45(4). https://doi.org/10.1029/2008WR007308

Geris, J., Comte, J. C., Franchi, F., Petros, A. K., Tirivarombo, S., Selepeng, A. T., & Villholth, K. G. (2022). Surface water-groundwater interactions and local land use control water quality impacts of extreme rainfall and flooding in a vulnerable semi-arid region of Sub-Saharan Africa. Journal of Hydrology, 609, 127834. https://doi.org/10.1016/J.JHYDROL.2022.127834

Gerlak, A. K., & Mukhtarov, F. (2015). 'Ways of knowing' water: integrated water resources management and water security as complementary discourses. International Environmental Agreements: Politics, Law and Economics, 15(3), 257–272. https://doi.org/10.1007/S10784-015-9278-5/TABLES/2

Gezie, M. (2019). Farmer's response to climate change and variability in Ethiopia: A review. Cogent Food & Agriculture, 5(1), 1613770. https://doi.org/10.1080/23311932.2019.1613770

Gheisari, N. (2017). *Groundwater vulnerability assessment using a GIS-based modified DRASTIC model in agricultural areas* (Doctoral dissertation, Université d'Ottawa/University of Ottawa). http://dx.doi.org/10.20381/ruor-20356

Gibbs, R. J. (1970). Mechanisms controlling world water chemistry. Science, 170(3962), 1088–1090. https://doi.org/10.1126/SCIENCE.170.3962.1088

Gintamo, T. T. (2017). Ground Water Potential Evaluation Based on Integrated GIS and Remote Sensing Techniques , in Bilate River Catchment : South Rift Valley of Ethiopia. January, 85–120.

Godfrey, S., Hailemichael, G., & Serele, C. (2019). Deep groundwater as an alternative source of water in the Ogaden Jesoma sandstone aquifers of Somali region, Ethiopia. Water (Switzerland), 11(8). https://doi.org/10.3390/w11081735

Golkarian, A., Naghibi, S. A., Kalantar, B., & Pradhan, B. (2018). Groundwater potential mapping using C5.0, random forest, and multivariate adaptive regression spline models in GIS. Environmental Monitoring and Assessment, 190(3). https://doi.org/10.1007/s10661-018-6507-8

Gomaa, M. M. (2020). Salinity and water effect on electrical properties of fragile clayey sandstone. Applied Water Science, 10(5), 1–9. https://doi.org/10.1007/s13201-020-01189-0

Gómez-Escalonilla, V., Vogt, M. L., Destro, E., Isseini, M., Origgi, G., Djoret, D., ... & Holecz, F. (2022). Delineation of groundwater potential zones by means of ensemble tree supervised classification methods in the Eastern Lake Chad basin. Geocarto International, 37(25), 8924-8951. https://doi.org/10.1080/10106049.2021.2007298

Gössling, S., & Dolnicar, S. (2023). A review of air travel behavior and climate change. Wiley Interdisciplinary Reviews: Climate Change, 14(1), e802. https://doi.org/10.1002/WCC.802

Gomroki, M., Hasanlou, M., & Reinartz, P. (2023). STCD-EffV2T Unet: Semi Transfer Learning EfficientNetV2 T-Unet Network for Urban/Land Cover Change Detection Using Sentinel-2 Satellite Images. *Remote Sensing 2023, Vol. 15, Page 1232*, *15*(5), 1232. https://doi.org/10.3390/RS15051232

Goodarzi, M. R., Niknam, A. R. R., Jamali, V., & Pourghasemi, H. R. (2022). Aquifer vulnerability identification using DRASTIC-LU model modification by fuzzy analytic hierarchy process. Modeling Earth Systems and Environment, 8(4), 5365–5380. https://doi.org/10.1007/S40808-022-01408-4/TABLES/5

Gourcy, L. L., Groening, M., & Aggarwal, P. K. (2005). Stable oxygen and hydrogen isotopes in precipitation. In Isotopes in the water cycle: past, present and future of a developing science (pp. 39-51). Dordrecht: Springer Netherlands.

Gumuła-Kawęcka, A., Jaworska-Szulc, B., Szymkiewicz, A., Gorczewska-Langner, W., Angulo-Jaramillo, R., & Šimůnek, J. (2023). Impact of climate change on groundwater recharge in shallow young glacial aquifers in northern Poland. Science of The Total Environment, 877, 162904. https://doi.org/10.1016/J.SCITOTENV.2023.162904

Gupta, T., & Kumari, R. (2023). Assessment of groundwater nitrate vulnerability using DRASTIC and modified DRASTIC in upper catchment of Sabarmati basin. Environmental Earth Sciences, 82(9), 1–17. https://doi.org/10.1007/S12665-023-10880-9/FIGURES/7

Guye, M., Legesse, A., & Mohammed, Y. (2022). Pastoralists under threat continuum: quantifying vulnerabilities of pastoralists to climate variability in southern Ethiopia. GeoJournal, 88(2), 1785–1806. https://doi.org/10.1007/S10708-022-10710-8/FIGURES/4

Guzha, A. C., Rufino, M. C., Okoth, S., Jacobs, S., & Nóbrega, R. L. B. (2018). Impacts of land use and land cover change on surface runoff, discharge and low flows: Evidence from East Africa. Journal of Hydrology: Regional Studies, 15, 49–67. Retrieved from https://doi.org/10.1016/j.ejrh.2017.11.005

Hagos, F., Jayasinghe, G., Awulachew, S. B., Loulseged, M., & Yilma, A. D. (2012). Agricultural water management and poverty in Ethiopia. Agricultural Economics, 43, 99-111.

Hák, T., Janoušková, S., & Moldan, B. (2016). Sustainable Development Goals: A need for relevant indicators. Ecological indicators, 60, 565-573.

Haidu, I., & Nistor, M. M. (2020). Long-term effect of climate change on groundwater recharge in the Grand Est region of France. Meteorological Applications, 27(1), e1796. https://doi.org/10.1002/MET.1796

Hailemariam, K. (1999). Impact of climate change on the water resources of Awash River Basin, Ethiopia. Climate Research, 12(2–3), 91–96. Retrieved from https://doi.org/10.3354/CR012091

Haile, B. T., Bekitie, K. T., Zeleke, T. T., Ayal, D. Y., Feyisa, G. L., & Anose, F. A. (2022). Drought Analysis Using Standardized Evapotranspiration and Aridity Index at Bilate Watershed: Sub-Basins of Ethiopian Rift Valley. Scientific World Journal, 2022. https://doi.org/10.1155/2022/1181198

Hailu, H., & Haftu, S. (2023). Hydrogeochemical studies of groundwater in semi-arid areas of northern Ethiopia using geospatial methods and multivariate statistical analysis techniques. Applied Water Science, 13(3), 1–17. https://doi.org/10.1007/S13201-023-01890-W/FIGURES/7

Hamza, S. M., Ahsan, A., Imteaz, M. A., Rahman, A., Mohammad, T. A., & Ghazali, A. H. (2015). Accomplishment and subjectivity of GIS-based DRASTIC groundwater vulnerability assessment method: a review. Environmental Earth Sciences, 73(7), 3063–3076. https://doi.org/10.1007/S12665-014-3601-2/TABLES/9

Hanifehlou, A., Hosseini, S. A., Javadi, S., & Sharafati, A. (2022). Sustainable exploitation of groundwater resources considering the effects of climate change and land use to provide adaptation solutions (case study of the Hashtgerd plain). Acta Geophysica, 70(4), 1829–1846. https://doi.org/10.1007/S11600-022-00843-2/FIGURES/15

Hasan, S. S., Zhen, L., Miah, M. G., Ahamed, T., & Samie, A. (2020). Impact of land use change on ecosystem services: A review. Environmental Development, 34(April). https://doi.org/10.1016/j.envdev.2020.100527

Hasan, M. H., Newton, I. H., Chowdhury, M. A., Esha, A. A., Razzaque, S., & Hossain, M. J. (2023). Land Use Land Cover Change and Related Drivers have Livelihood Consequences in Coastal Bangladesh. *Earth Systems and Environment*, *1*, 1–19. https://doi.org/10.1007/S41748-023-00339-Z/FIGURES/9

Hasan, E., Tarhule, A., Kirstetter, P. E., Clark, R., & Hong, Y. (2018). Runoff sensitivity to climate change in the Nile River Basin. Journal of Hydrology, 561, 312–321. https://doi.org/10.1016/j.jhydrol.2018.04.004Hashemi, H., Uvo, C. B., & Berndtsson, R. (2015). Coupled modeling approach to assess climate change impacts on groundwater recharge and adaptation in arid areas. 4165–4181. https://doi.org/10.5194/hess-19-4165-2015

Hata, S., Sugiyama, S., & Heki, K. (2022). Abrupt drainage of Lago Greve, a large proglacial lake in Chilean Patagonia, observed by satellite in 2020. Communications Earth & Environment 2022 3:1, 3(1), 1–8. https://doi.org/10.1038/s43247-022-00531-5

Harter, T. (2003). Groundwater Quality and Groundwater Pollution. In Groundwater Quality and Groundwater Pollution. University of California, Agriculture and Natural Resources. https://doi.org/10.3733/ucanr.8084

Hendrix, M. (2012). Water in Ethiopia: Drought, disease and death. Global Majority E-Journal, 3(2), 110-120.

Hordofa, A. T., Leta, O. T., Alamirew, T., & Chukalla, A. D. (2021). Spatiotemporal Trend Analysis of Temperature and Rainfall over Ziway Lake Basin, Ethiopia. Hydrology 2022, Vol. 9, Page 2, 9(1), 2. https://doi.org/10.3390/HYDROLOGY9010002

Hoogesteger, J. (2022). Regulating agricultural groundwater use in arid and semi-arid regions of the Global South: Challenges and socio-environmental impacts. *Curr Opin Environ Sci Health*, 27. https://doi.org/10.1016/j.coesh. 2022.100341

Hrnjak, I., Lukić, T., Gavrilov, M. B., Marković, S. B., Unkašević, M., & Tošić, I. (2014). Aridity in Vojvodina, Serbia. Theoretical and Applied Climatology, 115(1–2), 323–332. https://doi.org/10.1007/S00704-013-0893-1/FIGURES/7

Hu, Y., Raza, A., Syed, N. R., Acharki, S., Ray, R. L., Hussain, S., Dehghanisanij, H., Zubair, M., & Elbeltagi, A. (2023). Land Use/Land Cover Change Detection and NDVI Estimation in Pakistan’s Southern Punjab Province. *Sustainability 2023, Vol. 15, Page 3572*, *15*(4), 3572. https://doi.org/10.3390/SU15043572

Idrissou, M., Diekkrüger, B., Tischbein, B., de Hipt, F. O., Näschen, K., Poméon, T., Yira, Y., & Ibrahim, B. (2022). Modeling the Impact of Climate and Land Use/Land Cover Change on Water Availability in an Inland Valley Catchment in Burkina Faso. *Hydrology 2022, Vol. 9, Page 12*, *9*(1), 12. https://doi.org/10.3390/HYDROLOGY9010012

Ifediegwu, S. I. (2022). Assessment of groundwater potential zones using GIS and AHP techniques: a case study of the Lafia district, Nasarawa State, Nigeria. Applied Water Science, 12(1), 1–17. https://doi.org/10.1007/S13201-021-01556-5/FIGURES/13

Imbrenda, V., Coluzzi, R., Di Stefano, V., Egidi, G., Salvati, L., Samela, C., Simoniello, T., & Lanfredi, M. (2022). Modeling Spatio-Temporal Divergence in Land Vulnerability to Desertification with Local Regressions. Sustainability (Switzerland), 14(17). https://doi.org/10.3390/su141710906

Ioana-Toroimac, G., Zaharia, L., Moroșanu, G. A., Grecu, F., & Hachemi, K. (2022). Assessment of Restoration Effects in Riparian Wetlands using Satellite Imagery. Case Study on the Lower Danube River. Wetlands, 42(4), 1–14. https://doi.org/10.1007/S13157-022-01543-9/TABLES/2

IPCC. (2019). Climate Change and Land: an IPCC special report. Climate Change and Land: An IPCC Special Report on Climate Change, Desertification, Land Degradation, Sustainable Land Management, Food Security, and Greenhouse Gas Fluxes in Terrestrial Ecosystems, 1–864.

Islami, F. A., Tarigan, S. D., Wahjunie, E. D., & Dasanto, B. D. (2022). Accuracy Assessment of Land Use Change Analysis Using Google Earth in Sadar Watershed Mojokerto Regency. *IOP Conference Series: Earth and Environmental Science*, *950*(1), 012091. https://doi.org/10.1088/1755-1315/950/1/012091

Islam, M. R., Salminen, R., & Lahermo, P. W. (2000). Arsenic and other toxic elemental contamination of groundwater, surface water and soil in Bangladesh and its possible effects on human health. Environmental Geochemistry and Health, 22(1), 33–53. https://doi.org/10.1023/A:1006787405626/METRICS

Islam, M. J., Mosharof Hossain, A., Rahman, S., Khandoker, M. H., & Zahan, M. N. (2019). Hydrogeochemistry and Usability of Groundwater at the Tista River Basin in Northern Bangladesh. Academia.Edu, 12(47). https://doi.org/10.17485/ijst/2019/v12i47/147961

Ismanto, A., Hadibarata, T., Widada, S., Indrayanti, E., Ismunarti, D. H., Safinatunnajah, N., Kusumastuti, W., Dwiningsih, Y., & Alkahtani, J. (2023). Groundwater contamination status in Malaysia: level of heavy metal, source, health impact, and remediation technologies. Bioprocess and Biosystems Engineering, 46(3), 467–482. https://doi.org/10.1007/S00449-022-02826-5/FIGURES/4

Ismail, E. H., & Abdelsalam, M. G. (2012). Morpho-tectonic analysis of the Tekeze River and the Blue Nile drainage systems on the Northwestern Plateau, Ethiopia. Journal of African Earth Sciences, 69, 34-47. https://doi.org/10.1016/j.jafrearsci.2012.04.005

Ivkovic, K. M., Letcher, R. A., & Croke, B. F. W. (2009). Use of a simple surface-groundwater interaction model to inform water management. Australian Journal of Earth Sciences, 56(1), 71–80. https://doi.org/10.1080/08120090802541945

Iwmi, G., Lagudu, S., Jampani, M., & Bevara, M. (2013). Assessment of geochemical processes occurring in groundwaters in the coastal alluvial aquifer. Article in Environmental Monitoring and Assessment, 185(10), 8259–8272. https://doi.org/10.1007/s10661-013-3171-x

Jahangir, M. H., & Danehkar, S. (2022). A comparative drought assessment in Gilan, Iran using Pálfai drought index, de Martonne aridity index, and Pinna combinative index. Arabian Journal of Geosciences 2021 15:1, 15(1), 1–21. https://doi.org/10.1007/S12517-021-09107-7

Jannis, E., Adrien, M., Annette, A., & Peter, H. (2021). Climate change effects on groundwater recharge and temperatures in Swiss alluvial aquifers. Journal of Hydrology X, 11, 100071. https://doi.org/10.1016/J.HYDROA.2020.100071

Jmal, I., Ayed, B., Bahloul, M., Boughariou, E., & Bouri, S. (2022). Contribution of GIS tools and statistical approaches to optimize the DRASTIC model for groundwater vulnerability assessment in arid and semi-arid regions: the case of Sidi Bouzid shallow aquifer. Arabian Journal of Geosciences 2022 15:10, 15(10), 1–22. https://doi.org/10.1007/S12517-022-10149-8

John Henry Fieth. (1973). Water Facts and Figures for Planners and Managers - John Henry Feth - Google Books.https://books.google.com.et/books?hl=en&lr=&id=VE7PdFwgKVsC&oi=fnd&pg=PA3&d

q=water+facts+&ots=m1AR8nr5Wg&sig=PQzJmilJyMxlUFbNVcWLy2Q7x0&redir_esc=y#v=onepage&q=water%20facts&f=false

Johnson, T., Versteeg, R., Thomle, J., Hammond, G., Chen, X., & Zachara, J. (2015). Four-dimensional electrical conductivity monitoring of stage-driven river water intrusion: Accounting for water table effects using a transient mesh boundary and conditional inversion constraints. Water Resources Research, 51(8), 6177–6196. https://doi.org/10.1002/2014WR016129

Jothimani, M., Abebe, A., & Duraisamy, R. (2021). Groundwater potential zones identification in Arba Minch town, Rift Valley, Ethiopia, using geospatial and AHP tools. IOP Conference Series: Earth and Environmental Science, 822(1). https://doi.org/10.1088/1755-1315/822/1/012048

Juandi, M., & Syahril, S. (2017). Empirical relationship between soil permeability and resistivity, and its application for determining the groundwater gross recharge in Marpoyan Damai, Pekanbaru, Indonesia. Water Practice and Technology, 12(3), 660–666. https://doi.org/10.2166/wpt.2017.069

Jung, Y., Koh, D., Yoon, Y., Kwon, H., & Heo, J. (2019). Using stable isotopes and tritium to delineate groundwater fl ow systems and their relationship to streams in the Geum River basin , Korea. Journal of Hydrology, 573(March), 267–280. https://doi.org/10.1016/j.jhydrol.2019.03.084

Jury, M. R., & Funk, C. (2012). Climatic trends over Ethiopia : regional signals and drivers. https://doi.org/10.1002/joc.3560

Kabite, G., Muleta, M. K., & Gessesse, B. (2018). Assessing and Quantifying Impacts of Land Use and Climate Changes on Hydrological Processes: Review. 8(3), 10–18.

Kabeto, J., Adeba, D., Regasa, M. S., & Leta, M. K. (2022). Groundwater potential assessment using gis and remote sensing techniques: Case study of west Arsi zone, Ethiopia. Water (Switzerland), 14(12). Retrieved from https://doi.org/10.3390/w14121838

Kahsay, K. D., Pingale, S. M., & Hatiye, S. D. (2018). Impact of climate change on groundwater recharge and base flow in the sub-catchment of Tekeze basin, Ethiopia. Groundwater for Sustainable Development, 6, 121–133. https://doi.org/10.1016/j.gsd.2017.12.002

Kalantar, B., Al Najjar, H. A. H., Pradhan, B., Saeidi, V., Halin, A. A., Ueda, N., & Naghibi, S. A. (2019). Optimized conditioning factors using machine learning techniques for groundwater potential mapping. Water (Switzerland), 11(9). Retrieved from https://doi.org/10.3390/w11091909

Kalbus, E., Reinstorf, F., & Schirmer, M. (2006). Hess-10-873-2006. 873–887.

Kamangira, B., & Melaku, K. (2023). Prevalence and Determinants of Under-Five Malnutrition in Borana Zone of Oromia Region, Ethiopia: Effects of a Prolonged Drought. https://doi.org/10.21203/RS.3.RS-2825595/V1

Kana, J. D., Ahmad Diab, D., Hervé, D. G., N'kaya, G. D. M., Meli'i, J. L., Browdon, S. N. lionel, & Lebogo, S. P. K. N. (2022). A combined GIS-based remote sensing and wireline log data analysis for water resource management in the economic capital district of Cameroon. Sustainable Water Resources Management, 8(5), 1–14. https://doi.org/10.1007/S40899-022-00714-0/TABLES/4

Kassaye, A. Y., Shao, G., Wang, X., & Wu, S. (2021). Quantification of drought severity change in Ethiopia during 1952–2017. Environment, Development and Sustainability, 23(4), 5096–5121. https://doi.org/10.1007/S10668-020-00805-Y

Kassune, M., T. Tafesse, N., & Hagos, M. (2018). Characteristics and Productivity of Volcanic Rock Aquifers in Kola Diba Well Field, North-central Ethiopia. Universal Journal of Geoscience, 6(4), 103–113. https://doi.org/10.13189/ujg.2018.060401

Kattsov, V., Federation, R., Reason, C., Africa, S., Uk, A. A., Uk, T. A., Baehr, J., Uk, A. B., Catto, J., Canada, J. S., & Uk, A. S. (2013). Evaluation of climate models. Climate Change 2013 the Physical Science Basis: Working Group I Contribution to the Fifth Assessment Report of the Intergovernmental Panel on Climate Change, 9781107057, 741–866. https://doi.org/10.1017/CBO9781107415324.020

Kazakis, N., & Voudouris, K. S. (2015). Groundwater vulnerability and pollution risk assessment of porous aquifers to nitrate: Modifying the DRASTIC method using quantitative parameters. *Journal of Hydrology*, *525*, 13-25.

Kebede, S. (2013). Groundwater in Ethiopia: Features, numbers and opportunities. Groundwater in Ethiopia: Features, Numbers and Opportunities. Berlin, Heidelberg, Germany: Springer. Retrieved from https://doi.org/10.1007/978 3 642 30391 3

Kebede, H., Alemu, A., & Nedaw, D. (2020). Mapping Geologic Structures from Gravity and Digital Elevation Model in the Ziway-Shala Lakes Basin; central Main Ethiopian Rift. 1, 1–22.

Kebede, S. (2013). Functions of Groundwater. springer berlin heidelberg.

Kebede, S., Hailu, A., Crane, E., Dochartaigh, Ó., & Bellwood-Howard, B. É. and. (2018). Hydrogeology of Ethiopia. Africa Groundwater Atlas, 1–9.

Kebede, S., & Travi, Y. (2012). Origin of the δ 18O and δ 2H composition of meteoric waters in Ethiopia. Quaternary International, 257, 4–12. https://doi.org/10.1016/j.quaint.2011.09.032

Kebede, S., Travi, Y., Alemayehu, T., & Ayenew, T. (2005). Groundwater recharge, circulation and geochemical evolution in the source region of the Blue Nile River, Ethiopia. Applied Geochemistry, 20(9), 1658–1676. https://doi.org/10.1016/j.apgeochem.2005.04.016

Kebede, S., Travi, Y., Asrat, A., Alemayehu, T., Ayenew, T., & Tessema, Z. (2008). Groundwater origin and flow along selected transects in Ethiopian rift volcanic aquifers. Hydrogeology Journal, 16(1), 55–73. https://doi.org/10.1007/s10040-007-0210-0

Kebede, S., & Zewdu, S. (2019). Use of 222Rn and δ18O-δ2H isotopes in detecting the origin of water and in quantifying groundwater inflow rates in an alarmingly growing lake, Ethiopia. Water (Switzerland), 11(12). https://doi.org/10.3390/w11122591

Kebede, A., Meko, T., Hussein, A., & Tamiru, Y. (2017). Review on opportunities and constraints of fishery in Ethiopia. *International Journal of Poultry and Fisheries Sciences*, *1*(1), 1–4. https://doi.org/10.15226/2578-1898/1/1/00104

Keesari, T., Roy, A., Mohokar, H., Pant, D., & Sinha, U. K. (2020). Characterization of Mechanisms and Processes Controlling Groundwater Recharge and its Quality in Drought-Prone Region of Central India (Buldhana, Maharashtra) Using Isotope Hydrochemical and End-Member Mixing Modeling. Natural Resources Research, 29(3), 1951–1973. https://doi.org/10.1007/S11053-019-09550-0/FIGURES/15

Kern, Z., Hatvani, I. G., Czuppon, G., Fórizs, I., Erdélyi, D., Kanduč, T., Palcsu, L., & Vreča, P. (2020). Isotopic "altitude" and "continental" effects in modern precipitation across the Adriatic-Pannonian region. Water (Switzerland), 12(6). https://doi.org/10.3390/w12061797

Ketema, A., Lemecha, G., Schucknecht, A., & Kayitakire, F. (2016). Hydrogeological study in drought affected areas of Afar, Somali, Oromia and SNNP regions in Ethiopia (Issue November). https://doi.org/10.2788/050278

Ketema, D. K., Emanna, B., & Tesfay, G. (2022). Impact of land acquisition for large-scale agricultural investments on vulnerability of displaced households to climate change shocks in Ethiopia.

Https://Doi.Org/10.1080/26395916.2022.2143572, 18(1), 643–660. https://doi.org/10.1080/26395916.2022.2143572

Khadim, F. K., Dokou, Z., Lazin, R., Bagtzoglou, A. C., & Anagnostou, E. (2023). Groundwater Modeling to Assess Climate Change Impacts and Sustainability in the Tana Basin, Upper Blue Nile, Ethiopia. Sustainability 2023, Vol. 15, Page 6284, 15(7), 6284. https://doi.org/10.3390/SU15076284

Khemiri, S., Khnissi, A., Alaya, M. Ben, Saidi, S., & Zargouni, F. (2013). Using GIS for the Comparison of Intrinsic Parametric Methods Assessment of Groundwater Vulnerability to Pollution in Scenarios of Semi Arid Climate. The Case of Foussana Groundwater in the Central of Tunisia. Journal of Water Resource and Protection, 2013(08), 835–845. https://doi.org/10.4236/JWARP.2013.58084

Khosravi, K., Sartaj, M., Karimi, M., Levison, J., & Lotfi, A. (2021). A GIS-based groundwater pollution potential using DRASTIC, modified DRASTIC, and bivariate statistical models. Environmental Science and Pollution Research, 28(36), 50525–50541. https://doi.org/10.1007/S11356-021-13706-Y/FIGURES/6

Kidd, C., Levizzani, V., Turk, J., & Ferraro, R. (2009). Satellite precipitation measurements for water resource monitoring. Journal of the American Water Resources Association, 45(3), 567–579. https://doi.org/10.1111/j.1752-1688.2009.00326.x

Kirlas, M. C., Karpouzos, D., Georgiou, P. E., & Katsifarakis, K. L. (2022). A comparative study of groundwater vulnerability methods in a porous aquifer in Greece. Applied Water Science, 12(6), 1–21. https://doi.org/10.1007/S13201-022-01651-1/TABLES/10

Kirlas, M. C., Karpouzos, D. K., Georgiou, P. E., & Theodossiou, N. (2023). A GIS-based comparative groundwater vulnerability assessment using modified-DRASTIC, modified-SINTACS and NV index in a porous aquifer, Greece. *Environments*, *10*(6), 95.

Kloos, H., & Tekle Haimanot, R. (1999). Distribution of fluoride and fluorosis in Ethiopia and prospects for control. Tropical Medicine & International Health, 4(5), 355–364. https://doi.org/10.1046/J.1365-3156.1999.00405.X

Krause, S., Jacobs, J., & Bronstert, A. (2007). Modelling the impacts of land use and drainage density on the water balance of a lowland floodplain landscape in northeast Germany. Ecological Modelling, 200(3–4), 475–492. Retrieved from Retrieved from https://doi.org/10.1016/j.ecolmodel.2006.08.015

Krishan, G., Bhagwat, A., Sejwal, P., Yadav, B. K., Kansal, M. L., Bradley, A., Singh, S., Kumar, M., Sharma, L. M., & Muste, M. (2023). Assessment of groundwater salinity using principal component analysis (PCA): a case study from Mewat (Nuh), Haryana, India. Environmental Monitoring and Assessment, 195(1), 1–15. https://doi.org/10.1007/S10661-022-10555-1/FIGURES/7

Kumar, P., Herath, S., Avtar, R., & Takeuchi, K. (2016). Mapping of groundwater potential zones in Killinochi area, Sri Lanka, using GIS and remote sensing techniques. Sustainable Water Resources Management, 2(4), 419–430. Retrieved from https://doi.org/10.1007/S40899 016 0072 5

Knoche, M., Fischer, C., Pohl, E., Krause, P., & Merz, R. (2014). Combined uncertainty of hydrological model complexity and satellite-based forcing data evaluated in two data-scarce semi-arid catchments in Ethiopia. Journal of Hydrology, 519(PB), 2049–2066. https://doi.org/10.1016/j.jhydrol.2014.10.003

Koncagül, E. (2015). Facing the challenges: case studies and indicators: UNESCO's contributions to the United Nations world water development report 2015 (Vol. 2). UNESCO Publishing

Koop, S. H. A., & van Leeuwen, C. J. (2015). Assessment of the Sustainability of Water Resources Management: A Critical Review of the City Blueprint Approach. Water Resources Management, 29(15), 5649–5670. https://doi.org/10.1007/S11269-015-1139-Z/FIGURES/4

Kourtis, I. M., Nalbantis, I., Tsakiris, G., Psiloglou, B., & Tsihrintzis, V. A. (2022). Updating IDF Curves Under Climate Change: Impact on Rainfall-Induced Runoff in Urban Basins. Water Resources Management, 1–26. https://doi.org/10.1007/S11269-022-03252-8/FIGURES/8

Kumar, C. P. (2015). Impact of Climate Change on Groundwater Resources. 247667, 196–221. https://doi.org/10.4018/978-1-4666-8814-8.ch010

Kumar, M., Ramanathan, A., Rao, M. S., & Kumar, B. (2006). Identification and evaluation of hydrogeochemical processes in the groundwater environment of Delhi, India. Environmental Geology, 50(7), 1025–1039. https://doi.org/10.1007/S00254-006-0275-4/FIGURES/16

Lakshminarayanan, B., Ramasamy, S., Anuthaman, S. N., & Karuppanan, S. (2021). New DRASTIC framework for groundwater vulnerability assessment: bivariate and multi-criteria decision-making approach coupled with metaheuristic algorithm. Environmental Science and Pollution Research 2021 29:3, 29(3), 4474–4496. https://doi.org/10.1007/S11356-021-15966-0

Latha, P. S. (2022). Evaluation of groundwater quality for domestic and irrigation purposes in a coastal alluvial aquifer using multivariate statistics and entropy water quality index approach: a case study from West Godavari Delta, Andhra Pradesh (India). Environmental Earth Sciences, 81(10), 1–20. https://doi.org/10.1007/S12665-022-10387-9/TABLES/10

Lapworth, D. J., Baran, N., Stuart, M. E., & Ward, R. S. (2012). Emerging organic contaminants in groundwater: A review of sources, fate and occurrence. Environmental Pollution, 163, 287–303. https://doi.org/10.1016/J.ENVPOL.2011.12.034

Lautze, S., Aklilu, Y., Raven-Roberts, A., Young, H., Kebede, G., & Leaning, J. (2003). Risk and vulnerability in Ethiopia: Learning from the past, responding to the present, preparing for the future. Pdf.Usaid.Gov. https://pdf.usaid.gov/pdf_docs/pnacu497.pdf

Lawrence, T. J., Vilbig, J. M., Kangogo, G., Fèvre, E. M., Deem, S. L., Gluecks, I., Sagan, V., & Shacham, E. (2023). Shifting climate zones and expanding tropical and arid climate regions across Kenya (1980–2020). Regional Environmental Change, 23(2), 1–13. https://doi.org/10.1007/S10113-023-02055-W/FIGURES/5

Lewoyehu, M. (2021). Evaluation of Drinking Water Quality in Rural Area of Amhara Region, Ethiopia: The Case of Mecha District. Journal of Chemistry, 2021. https://doi.org/10.1155/2021/9911838

Leavesley, G. H. (1994). Modeling the Effects of Climate Change on Water resources — A Review. Assessing the Impacts of Climate Change on Natural Resource Systems, 159–177. https://doi.org/10.1007/978-94-011-0207-0_8

Legesse, S. A., Rao, P. V. V. P., & Rao, M. M. N. (2013). Statistical Downscaling of Daily Temperature and Rainfall Data From Global Circulation Models : in South Wollo Zone , North Central Ethiopia. National Monthly Referred Journal of Research in Science & Technology, 2(7), 27–39.

Levin, N. E., Zipser, E. J., & Ceding, T. E. (2009). Isotopic composition of waters from Ethiopia and Kenya: Insights into moisture sources for eastern Africa. Journal of Geophysical Research Atmospheres, 114(23), 1–13. https://doi.org/10.1029/2009JD012166

Li, L., Yu, Y., Tang, Y., Lin, P., Xie, J., Song, M., Dong, L., Zhou, T., Liu, L., Wang, L., Pu, Y., Chen, X., Chen, L., Xie, Z., Liu, H., Zhang, L., Huang, X., Feng, T., Zheng, W., … Wei, J. (2020). The Flexible Global Ocean-Atmosphere-Land System Model Grid-Point Version 3 (FGOALS-g3): Description

and Evaluation. Journal of Advances in Modeling Earth Systems, 12(9), e2019MS002012. https://doi.org/10.1029/2019MS002012

Li, Y., Feng, A., Liu, W., Ma, X., Water, G. D.-, & 2017. (2017). Variation of aridity index and the role of climate variables in the Southwest China. Mdpi.Com. https://doi.org/10.3390/w9100743

Li, Z., Research, S. Q.-W. R., & 2021, undefined. (2021). Identifying the dominant drivers of hydrological change in the contiguous United States. Wiley Online Library, 57(5). https://doi.org/10.1029/2021WR029738

Li, P., Wu, J., & Qian, H. (2014). Hydrogeochemistry and Quality Assessment of Shallow Groundwater in the Southern Part of the Yellow River Alluvial Plain (Zhongwei Section), Northwest China. Earth Sciences Research Journal, 18(1), 27–38. https://doi.org/10.15446/ESRJ.V18N1.34048

Li, P., Karunanidhi, D., Subramani, T., & Srinivasamoorthy, K. (2021). Sources and Consequences of Groundwater Contamination. Archives of Environmental Contamination and Toxicology, 80(1), 1–10. https://doi.org/10.1007/S00244-020-00805-Z/FIGURES/2

Library, W. O., Zeleke, T. T., Giorgi, F., Diro, G. T., & Zaitchik, B. F. (2017). Trend and periodicity of drought over Ethiopia. Wiley Online Library, 37(13), 4733–4748. https://doi.org/10.1002/joc.5122

Lk, G., Em, M., Pc, K., & Waita, J. (2019). Integration of Remote Sensing and Geological Mapping for Economic Mineralization Mapping in Mwitika-Makongo Area , Kitui Country. 1–5.

Lindsay, J. B., Newman, D. R., & Francioni, A. (2019). Scale- optimized surface roughness for topographic analysis. *Geosciences (Switzerland)*, *9*. https://doi.org/10.3390/ geosciences9070322

Lilay, M. Y., & Taye, G. D. (2023). Semantic segmentation model for land cover classification from satellite images in Gambella National Park, Ethiopia. *SN Applied Sciences*, *5*(3), 1–15. https://doi.org/10.1007/S42452-023-05280-4/FIGURES/7

L, B., R, S., K, S., & N A, S. (2021). Groundwater vulnerability mapping using the modified DRASTIC model: the metaheuristic algorithm approach. Environmental Monitoring and Assessment, 193(1), 25. https://doi.org/10.1007/S10661-020-08787-0/FIGURES/7

Lima, G. F. C., Ferreira, V. G., Lima, J. S. D., Duarte, J. C. M., Dufilho, A. C., & de Carvalho Filho, C. A. (2022). Intrinsic and specific groundwater vulnerability determination as a pre-operational baseline assessment of an unconventional hydrocarbon industry. International Journal of Environmental Science and Technology, 1–16. https://doi.org/10.1007/S13762-022-04551-8/FIGURES/9

Liu, J., Song, X., Yuan, G., Sun, X., Yang, L., & Jianrong Liu, B. (2014). Stable isotopic compositions of precipitation in China. Taylor & Francis, 66(1). https://doi.org/10.3402/tellusb.v66.22567

Liu, J., Gao, Z., Wang, Z., Xu, X., Su, Q., Wang, S., & Xing, T. (2020). Hydrogeochemical processes and suitability assessment of groundwater in the Jiaodong Peninsula, China. *Environ Monit Assess*, *192*(3), 192. https://doi. org/10.1007/s10661-020-08356-5

Liu, J., Zhang, C., Kou, L., & Zhou, Q. (2017). Effects of Climate and Land Use Changes on Water Resources in the Taoer River. Advances in Meteorology, 2017. https://doi.org/10.1155/2017/1031854

Liu, X., Xia, J., Song, X., Yu, J., Tang, C., & Zhan, C. (2006). A study of surface water and ground water using isotopes in Huaishahe basin in Beijing, China. IAHS-AISH Publication, 302, 106–114.

Lodwick, W. A., Monson, W., & Svoboda, L. (1990). Attribute error and sensitivity analysis of map operations in geographical informations systems: Suitability analysis. International Journal of Geographical Information Systems, 4(4), 413–428. https://doi.org/10.1080/02693799008941556

Lodwick, W. A., Monson, W., & Svoboda, L. (2007). Attribute error and sensitivity analysis of map operations in geographical informations systems: suitability analysis. Http://Dx.Doi.Org/10.1080/02693799008941556, 4(4), 413–428. https://doi.org/10.1080/02693799008941556

Lovato, T., Peano, D., Butenschön, M., Materia, S., Iovino, D., Scoccimarro, E., Fogli, P. G., Cherchi, A., Bellucci, A., Gualdi, S., Masina, S., & Navarra, A. (2022). CMIP6 Simulations With the CMCC Earth System Model (CMCC-ESM2). Journal of Advances in Modeling Earth Systems, 14(3), e2021MS002814. https://doi.org/10.1029/2021MS002814

Ludwig, P., Gavrilov, M. B., Radaković, M. G., & Marković, S. B. (2021). Malaco temperature reconstructions and numerical simulation of environmental conditions in the southeastern Carpathian Basin during the Last Glacial Maximum. Journal of Quaternary Science, 36(8), 1426–1435. https://doi.org/10.1002/JQS.3318

MacDonald, A. M., Bonsor, H. C., Dochartaigh, B. É. Ó., & Taylor, R. G. (2012). Quantitative maps of groundwater resources in Africa. Environmental Research Letters, 7(2). https://doi.org/10.1088/1748-9326/7/2/024009

Ma, W., Zhang, X., Zhen, Q., & Zhang, Y. (2016). Effect of soil texture on water infiltration in semiarid reclaimed land. Water Quality Research Journal of Canada, 51(1), 33–41. Retrieved from https://doi.org/10.2166/wqrjc.2015.02

Magesh, N. S., Chandrasekar, N., & Soundranayagam, J. P. (2012). Delineation of groundwater potential zones in Theni district, Tamil Nadu, using remote sensing, GIS and MIF techniques. Geoscience Frontiers, 3(2), 189–196. https://doi.org/10.1016/j.gsf.2011.10.007

Maja, M. M., Idiris, A. A., Terefe, A. T., & Fashe, M. M. (2023). Gendered Vulnerability, Perception and Adaptation Options of Smallholder Farmers to Climate Change in Eastern Ethiopia. Earth Systems and Environment, 7(1), 189–209. https://doi.org/10.1007/S41748-022-00324-Y/TABLES/12

Majeed, M., Tariq, A., Anwar, M. M., Khan, A. M., Arshad, F., Mumtaz, F., Farhan, M., Zhang, L., Zafar, A., Aziz, M., Abbasi, S., Rahman, G., Hussain, S., Waheed, M., Fatima, K., & Shaukat, S. (2021). Monitoring of Land Use–Land Cover Change and Potential Causal Factors of Climate Change in Jhelum District, Punjab, Pakistan, through GIS and Multi-Temporal Satellite Data. *Land 2021, Vol. 10, Page 1026*, *10*(10), 1026. https://doi.org/10.3390/LAND10101026

Malakootian, M., & Nozari, M. (2020). GIS-based DRASTIC and composite DRASTIC indices for assessing groundwater vulnerability in the Baghin aquifer, Kerman, Iran. *Natural Hazards and Earth System Sciences*, *20*(8), 2351-2363.

Malede, D. A., Alamirew, T., Kosgie, J. R., & Andualem, T. G. (2023). Analysis of land use/land cover change trends over Birr River Watershed, Abbay Basin, Ethiopia. *Environmental and Sustainability Indicators*, *17*, 100222. https://doi.org/10.1016/J.INDIC.2022.100222

Maliva, R., & Missimer, T. (2012). Aquifer concepts in arid lands. Environmental Science and Engineering (Subseries: Environmental Science), 9783642291036, 95–115. https://doi.org/10.1007/978-3-642-29104-3_4

Mallick, J., Singh, C. K., Al wadi, H., Ahmed, M., Rahman, A., Shashtri, S., & Mukherjee, S. (2014). Geospatial and geostatistical approach for groundwater potential zone delineation. Retrieved from https://doi.org/10.1002/hyp.10153

Manap, M. A., Sulaiman, W. N. A., Ramli, M. F., Pradhan, B., & Surip, N. (2013). A knowledge driven GIS modeling technique for groundwater potential mapping at the Upper Langat Basin, Malaysia.

Arabian Journal of Geosciences, 6(5), 1621–1637. Retrieved from https://doi.org/10.1007/S12517 0110469 2

Manna, F., Allocca, V., De Vita, P., Medici, G., & Langman, J. B. (2022). Pathways and Estimate of Aquifer Recharge in a Flood Basalt Terrain; A Review from the South Fork Palouse River Basin (Columbia River Plateau, USA). Sustainability 2022, Vol. 14, Page 11349, 14(18), 11349. https://doi.org/10.3390/SU141811349

Mansour, M. M., Hughes, A. G., Robins, N. S., Ball, D., & Okoronkwo, C. (2012). The role of numerical modelling in understanding groundwater flow in Scottish alluvial aquifers. Geological Society Special Publication, 364(1), 85–98. https://doi.org/10.1144/SP364.7

Marandi, A., Polikarpus, M., & Jõeleht, A. (2013). A new approach for describing the relationship between electrical conductivity and major anion concentration in natural waters. Applied Geochemistry, 38, 103–109. https://doi.org/10.1016/j.apgeochem.2013.09.003

Maskooni, E. K., Naghibi, S. A., Hashemi, H., & Berndtsson, R. (2020). Application of Advanced Machine Learning Algorithms to Assess Groundwater Potential Using Remote Sensing-Derived Data. Remote Sensing 2020, Vol. 12, Page 2742, 12(17), 2742. https://doi.org/10.3390/RS12172742

Masih, I., Maskey, S., … F. M.-H. and E., & 2014, undefined. (2014). A review of droughts on the African continent: a geospatial and long-term perspective. Hess.Copernicus.Org, 18, 3635–3649. https://doi.org/10.5194/hess-18-3635-2014

Meaza, H., Abera, W., & Nyssen, J. (2022). Impacts of catchment restoration on water availability and drought resilience in Ethiopia: A meta-analysis. Land Degradation & Development, 33(4), 547–564. https://doi.org/10.1002/LDR.4125

Mengistu, H. A., Demlie, M. B., & Abiye, T. A. (2019a). Review: Groundwater resource potential and status of groundwater resource development in Ethiopia. Hydrogeology Journal, 27(3), 1051–1065. https://doi.org/10.1007/S10040-019-01928-X

Mengistu, H. A., Demlie, M. B., & Abiye, T. A. (2019b). Review: Groundwater resource potential and status of groundwater resource development in Ethiopia. Hydrogeology Journal, 27(3), 1051–1065. https://doi.org/10.1007/S10040-019-01928-X

Medici, G., Lorenzi, V., Sbarbati, C., Manetta, M., & Petitta, M. (2023). Structural Classification, Discharge Statistics, and Recession Analysis from the Springs of the Gran Sasso (Italy) Carbonate Aquifer; Comparison with Selected Analogues Worldwide. Sustainability 2023, Vol. 15, Page 10125, 15(13), 10125. https://doi.org/10.3390/SU151310125

Mechal, A., Birk, S., Dietzel, M., Leis, A., Winkler, G., Mogessie, A., & Kebede, S. (2017). Dynamique de l'écoulement des eaux souterraines dans le système aquifère complexe du bassin de la Rivière Gidabo (Rift éthiopien): une approche multi-proxy. Hydrogeology Journal, 25(2), 519–538. https://doi.org/10.1007/s10040-016-1489-5

Mengesha T., Tadiwos C., & Workineh H. (1996). Geological Survey of Ethiopia.

Mengistu, H. A., Demlie, M. B., & Abiye, T. A. (2019). Review: Groundwater resource potential and status of groundwater resource development in Ethiopia. Hydrogeology Journal, 27(3), 1051–1065. Retrieved from https://doi.org/10.1007/s10040 01901928x

Mengistu, T. D., Chung, I. M., Chang, S. W., Yifru, B. A., Kim, M. G., Lee, J., ... & Kim, I. H. (2021). Challenges and prospects of advancing groundwater research in Ethiopian aquifers: A review. Sustainability, 13(20), 11500.

Merga, B. B., Moisa, M. B., Negash, D. A., Ahmed, Z., & Gemeda, D. O. (2022). Land Surface Temperature Variation in Response to Land-Use and Land-Cover Dynamics: A Case of Didessa River Sub-basin in Western Ethiopia. *Earth Systems and Environment*, *6*(4), 803–815. https://doi.org/10.1007/S41748-022-00303-3/FIGURES/7

Metzger, M. J., Rounsevell, M. D. A., Acosta-Michlik, L., Leemans, R., & Schröter, D. (2006). The vulnerability of ecosystem services to land use change. Agriculture, Ecosystems & Environment, 114(1), 69–85. https://doi.org/10.1016/J.AGEE.2005.11.025

Mihi, A., Ghazela, R., & wissal, D. (2022). Mapping potential desertification-prone areas in North-Eastern Algeria using logistic regression model, GIS, and remote sensing techniques. Environmental Earth Sciences, 81(15), 1–14. https://doi.org/10.1007/S12665-022-10513-7/FIGURES/5

Milly, P. C. D., & Dunne, K. A. (2016). Potential evapotranspiration and continental drying. Nature Climate Change, 6(10), 946–949. https://doi.org/10.1038/nclimate3046

Mitiku, A. B., Meresa, G. A., Mulu, T., & Woldemichael, A. T. (2023). Examining the impacts of climate variabilities and land use change on hydrological responses of Awash River basin, Ethiopia. HydroResearch, 6, 16–28. https://doi.org/10.1016/J.HYDRES.2022.12.002

Mohamed, M. T. A. M., Al Naimi, L. S., Mgbeojedo, T. I., & Agoha, C. C. (2021). Geological mapping and mineral prospectivity using remote sensing and GIS in parts of Hamissana, Northeast Sudan. Journal of Petroleum Exploration and Production, 11(3), 1123–1138. Retrieved from https://doi.org/10.1007/ s1320202101115_3

Mogaji, K. A., Aboyeji, O. S., & Omosuyi, G. O. (2011). Mapping of lineaments for groundwater targeting in the basement complex region of Ondo State , Nigeria , using remote sensing and geographic information system (GIS) techniques. 3(August), 150–160.

Mohamed, M. T. A. M., Al-Naimi, L. S., Mgbeojedo, T. I., & Agoha, C. C. (2021). Geological mapping and mineral prospectivity using remote sensing and GIS in parts of Hamissana, Northeast Sudan. Journal of Petroleum Exploration and Production, 11(3), 1123–1138. https://doi.org/10.1007/s13202-021-01115-3

Moisa, M. B., Dejene, I. N., Roba, Z. R., & Gemeda, D. O. (2022). Impact of urban land use and land cover change on urban heat island and urban thermal comfort level: a case study of Addis Ababa City, Ethiopia. *Environmental Monitoring and Assessment*, *194*(10), 1–20. https://doi.org/10.1007/S10661-022-10414-Z/FIGURES/11

Moral, F. J., Rebollo, F. J., Paniagua, L. L., García-Martín, A., & Honorio, F. (2016). Spatial distribution and comparison of aridity indices in Extremadura, southwestern Spain. Theoretical and Applied Climatology, 126(3–4), 801–814. https://doi.org/10.1007/S00704-015-1615-7/TABLES/11

Morán-Ramírez, J., Ledesma-Ruiz, R., Mahlknecht, J., & Ramos-Leal, J. A. (2016). Rock–water interactions and pollution processes in the volcanic aquifer system of Guadalajara, Mexico, using inverse geochemical modeling. Applied geochemistry, 68, 79-94.

MoWR. (2002). FEDERAL DEMOCRATIC REPUBLIC OF ETHIOPIA MINISTRY OF WATER RESOURCES WATER SECTOR DEVELOPMENT PROGRAM MAIN REPORT VOLUME II OCTOBER 2002. II(October).

Morbidelli, R., Saltalippi, C., Flammini, A., & Govindaraju, R. S. (2018). Role of slope on infiltration: A review. Journal of Hydrology, 557, 878–886. Retrieved from https://doi.org/10.1016/j.jhydrol.2018.01.019

Mukherjee, I., & Singh, U. K. (2020). Delineation of groundwater potential zones in a drought-prone semi-arid region of east India using GIS and analytical hierarchical process techniques. Catena, 194. https://doi.org/10.1016/j.catena.2020.104681

Mukherjee, P., Singh, C. K., & Mukherjee, S. (2012). Delineation of Groundwater Potential Zones in Arid Region of India-A Remote Sensing and GIS Approach. Water Resources Management, 26(9), 2643–2672. https://doi.org/10.1007/s11269-012-0038-9

Mukherjee, I., & Singh, U. K. (2020). Delineation of groundwater potential zones in a drought-prone semi-arid region of East India using GIS and analytical hierarchical process techniques. *Catena (Amst)*, 194. https://doi.org/ 10.1016/j.catena.2020.104681

Müller, W. A., Jungclaus, J. H., Mauritsen, T., Baehr, J., Bittner, M., Budich, R., Bunzel, F., Esch, M., Ghosh, R., Haak, H., Ilyina, T., Kleine, T., Kornblueh, L., Li, H., Modali, K., Notz, D., Pohlmann, H., Roeckner, E., Stemmler, I., … Marotzke, J. (2018). A Higher-resolution Version of the Max Planck Institute Earth System Model (MPI-ESM1.2-HR). Journal of Advances in Modeling Earth Systems, 10(7), 1383–1413. https://doi.org/10.1029/2017MS001217

Nag, S. K., & Kundu, A. (2018). Application of remote sensing, GIS and MCA techniques for delineating groundwater prospect zones in Kashipur block, Purulia district, West Bengal. Applied Water Science, 8(1). https://doi.org/10.1007/s13201-018-0679-9

Nagaraju, A., Sunil Kumar, K., & Thejaswi, A. (2014). Assessment of groundwater quality for irrigation: A case study from bandalamottu lead mining area, Guntur district, Andhra Pradesh, south India. Applied Water Science, 4(4), 385–396. https://doi.org/10.1007/S13201-014-0154-1/FIGURES/5

Naghibi, S. A., Ahmadi, K., & Daneshi, A. (2017). Application of Support Vector Machine, Random Forest, and Genetic Algorithm Optimized Random Forest Models in Groundwater Potential Mapping. Water Resources Management, 31(9), 2761–2775. https://doi.org/10.1007/s11269-017-1660-3

Naghibi, S. A., Pourghasemi, H. R., & Dixon, B. (2016). GIS-based groundwater potential mapping using boosted regression tree, classification and regression tree, and random forest machine learning models in Iran. Environmental Monitoring and Assessment, 188(1), 1–27. https://doi.org/10.1007/S10661-015-5049-6/FIGURES/18

Naghibi, S. A., Dolatkordestani, M., Rezaei, A., Amouzegari, P., Heravi, M. T., Kalantar, B., & Pradhan, B. (2019). Application of rotation forest with decision trees as base classifier and a novel ensemble model in spatial modeling of groundwater potential. Environmental Monitoring and Assessment, 191(4), 1–20. https://doi.org/10.1007/S10661-019-7362-Y/TABLES/5

Naghibi, S. A., Hashemi, H., Berndtsson, R., & Lee, S. (2020). Application of extreme gradient boosting and parallel random forest algorithms for assessing groundwater spring potential using DEM-derived factors. Journal of Hydrology, 589, 125197. https://doi.org/10.1016/J.JHYDROL.2020.125197

Nagy, M., & Lăzăroiu, G. (2022). Computer Vision Algorithms, Remote Sensing Data Fusion Techniques, and Mapping and Navigation Tools in the Industry 4.0-Based Slovak Automotive Sector. Mathematics 2022, Vol. 10, Page 3543, 10(19), 3543. https://doi.org/10.3390/MATH10193543

Nazzal, Y., Ahmed, I., Al-Arifi, N. S. N., Ghrefat, H., Zaidi, F. K., El-Waheidi, M. M., Batayneh, A., & Zumlot, T. (2014). A pragmatic approach to study the groundwater quality suitability for domestic and agricultural usage, Saq aquifer, northwest of Saudi Arabia. Environmental Monitoring and Assessment, 186(8), 4655–4667. https://doi.org/10.1007/S10661-014-3728-3/TABLES/4

Naz, S., Fatima, Z., Iqbal, P., Khan, A., Zakir, I., Ullah, H., Abbas, G., Ahmed, M., Mubeen, M., Hussain, S., & Ahmad, S. (2022). An Introduction to Climate Change Phenomenon. Building Climate Resilience in Agriculture, 3–16. https://doi.org/10.1007/978-3-030-79408-8_1/COVER

Negese, A. (2021). Impacts of Land Use and Land Cover Change on Soil Erosion and Hydrological Responses in Ethiopia. Applied and Environmental Soil Science, 2021, 15–17. https://doi.org/10.1155/2021/6669438

Nigeria, Nnaji, & Sk, O. (2016). Risk of toxic metal contamination in gold mining and processing areas of Borgu and Mashegu local government areas of Niger state, Nigeria IRJCCS Risk of toxic metal contamination in gold mining and processing areas of Borgu and Mashegu local government areas of Niger state. www.premierpublishers.org.

Nguyen, P. T., Ha, D. H., Nguyen, H. D., Phong, T. Van, Trinh, P. T., Al-Ansari, N., Van Le, H., Pham, B. T., Ho, L. S., & Prakash, I. (2020). Improvement of credal decision trees using ensemble frameworks for groundwater potential modeling. Sustainability (Switzerland), 12(7). https://doi.org/10.3390/su12072622

Nika, C. E., Gusmaroli, L., Ghafourian, M., Atanasova, N., Buttiglieri, G., & Katsou, E. (2020). Nature-based solutions as enablers of circularity in water systems: A review on assessment methodologies, tools and indicators. Water Research, 183, 115988. https://doi.org/10.1016/J.WATRES.2020.115988

Nistor, M. M., Dezsi, Ş., Cheval, S., & Baciu, M. (2016). Climate change effects on groundwater resources: a new assessment method through climate indices and effective precipitation in Beliş district, Western Carpathians. Meteorological Applications, 23(3), 554–561. https://doi.org/10.1002/met.1578

Nistor, M. M., Ronchetti, F., Corsini, A., Cheval, S., Dumitrescu, A., Rai, P. K., Petrea, D., & Dezsi, Ş. (2017). Crop evapotranspiration variation under climate change in South East Europe during 1991-2050. Carpathian Journal of Earth and Environmental Sciences, 12(2), 571–582.

Nistor, M. M. (2019). Climate change effect on groundwater resources in South East Europe during 21st century. Quaternary International, 504, 171–180. https://doi.org/10.1016/J.QUAINT.2018.05.019

Nistor, M. M., & Cervi, F. (2021). An area facing climate change: monthly water availability in the Emilia-Romagna region during 1961–2015. Climate and Land Use Impacts on Natural and Artificial Systems: Mitigation and Adaptation, 135–152. https://doi.org/10.1016/B978-0-12-822184-6.00011-9

Nistor, M. M., & Mîndrescu, M. (2019). Climate change effect on groundwater resources in Emilia-Romagna region: An improved assessment through NISTOR-CEGW method. Quaternary International, 504, 214–228. https://doi.org/10.1016/J.QUAINT.2017.11.018

Nistor, M. M., Satyanaga, A., Dezsi, Ş., & Haidu, I. (2022). European grid dataset of actual evapotranspiration, water availability and effective precipitation. Atmosphere, 13(5), 772.

Nourani, V., Ghareh Tapeh, A. H., Khodkar, K., & Huang, J. J. (2023). Assessing long-term climate change impact on spatiotemporal changes of groundwater level using autoregressive-based and ensemble machine learning models. Journal of Environmental Management, 336, 117653. https://doi.org/10.1016/J.JENVMAN.2023.117653

O'Callaghan, J. (1980). Remote sensing: principles and interpretation F.F. Sabins, Jr., W.H. Freeman and Co., San Francisco, 1978. 22 x 295 mm., xl and 426 pages (with index), 42 tables, 248 fig., 8 colour plates. $31.25.Cartography, 11(4), 251–252. https://doi.org/10.1080/00690805.1980.10438124

O'Geen, A. T., McDaniel, P. A., Boll, J., & Keller, C. K. (2005). Paleosols as deep regolith: implications for ground-water recharge across a loessial climosequence. Geoderma, 126(1–2), 85–99. https://doi.org/10.1016/J.GEODERMA.2004.11.008

Omeje, E. T., Obiora, D. N., Okeke, F. N., Ibuot, J. C., Ugbor, D. O., & Omeje, V. D. (2023). Investigation of aquifer vulnerability and sensitivity analysis of modified drastic and sintacs models: a case study of Ovogovo Area, Eastern Nigeria. Acta Geophysica, 1, 1–26. https://doi.org/10.1007/S11600-022-00992-4/FIGURES/6

Onačillová, K., Gallay, M., Paluba, D., Péliová, A., Tokarčík, O., & Laubertová, D. (2022). Combining Landsat 8 and Sentinel-2 Data in Google Earth Engine to Derive Higher Resolution Land Surface Temperature Maps in Urban Environment. Remote Sensing 2022, Vol. 14, Page 4076, 14(16), 4076. https://doi.org/10.3390/RS14164076

Ostad-Ali-Askari, Kaveh., Shayannejad, Mohammad., & Ghorbanizadeh-Kharazi, Hossein. (2017). Artificial neural network for modeling nitrate pollution of groundwater in marginal area of Zayandeh-rood River, Isfahan, Iran. KSCE Journal of Civil Engineering, 21(1), 134–140. https://doi.org/10.1007/s12205-016-0572-8

Ourarhi, S., Barkaoui, A. E., & Zarhloule, Y. (2023). Mapping groundwater's susceptibility to pollution in the Triffa Plain (Eastern Morocco) using a modified method based on the DRASTIC, RIVA, and AHP models. Environment, Development and Sustainability, 1–21. https://doi.org/10.1007/S10668-023-03262-5/FIGURES/15

Owen, R., & Dahlin, T. (2005). Alluvial aquifers at geological boundaries : Geophysical investigations and groundwater resources. Groundwater and Human Development: International Association of Hydrogeologists Selected Papers on Hydrogeology Volume 6, 233–246

Ozyavuz, M., Bilgili, B. C., & Salici, A. (2015). DETERMINATION OF VEGETATION CHANGES WITH NDVI METHOD. In Journal of Environmental Protection and Ecology (Vol. 16, Issue 1).

Pacheco Quevedo, R., Velastegui-Montoya, A., Montalván-Burbano, N., Morante-Carballo, F., Korup, O., & Daleles Rennó, C. (2023). Land use and land cover as a conditioning factor in landslide susceptibility: a literature review. *Landslides 2023*, 1–16. https://doi.org/10.1007/S10346-022-02020-4

Palmer, P. I., Wainwright, C. M., Dong, B., Maidment, R. I., Wheeler, K. G., Gedney, N., Hickman, J. E., Madani, N., Folwell, S. S., Abdo, G., Allan, R. P., Black, E. C. L., Feng, L., Gudoshava, M., Haines, K., Huntingford, C., Kilavi, M., Lunt, M. F., Shaaban, A., & Turner, A. G. (2023). Drivers and impacts of Eastern African rainfall variability. Nature Reviews Earth & Environment 2023 4:4, 4(4), 254–270. https://doi.org/10.1038/s43017-023-00397-x

Papa, F., Crétaux, J. F., Grippa, M., Robert, E., Trigg, M., Tshimanga, R. M., Kitambo, B., Paris, A., Carr, A., Fleischmann, A. S., de Fleury, M., Gbetkom, P. G., Calmettes, B., & Calmant, S. (2022). Water Resources in Africa under Global Change: Monitoring Surface Waters from Space. Surveys in Geophysics 2022 44:1, 44(1), 43–93. https://doi.org/10.1007/S10712-022-09700-9

Paper, O. (2013). Investigation of temporal and spatial climate variability and aridity of Iran. https://doi.org/10.1007/s00704-013-1040-8

Panahi, G., Hassanzadeh Eskaa, M., Faridhosseini, A., Reza Khodashenas, S., Rohani, A., & Hassanzadeh Eskafi, M. (2022). Projection of Groundwater Level Fluctuations Using Different Machine Learning Algorithms under Climate Change in the Mashhad Aquifer, Iran. https://doi.org/10.21203/rs.3.rs-2319553/v1

Pandey, H. K., Singh, V. K., & Singh, S. K. (2022). Multi-criteria decision making and Dempster-Shafer model–based delineation of groundwater prospect zones from a semi-arid environment. Environmental Science and Pollution Research, 29(31), 47740–47758. https://doi.org/10.1007/S11356-022-19211-0/TABLES/6

Panigrahi, B., Nayak, A. K., & Sharma, S. D. (1995). Application of remote sensing technology for groundwater potential evaluation. Water Resources Management, 9(3), 161–173. Retrieved from https://doi.org/10.1007/BF00872127

Paniagua, L. L., García-Martín, A., Moral, F. J., & Rebollo, F. J. (2019). Aridity in the Iberian Peninsula (1960–2017): distribution, tendencies, and changes. Theoretical and Applied Climatology, 138(1–2), 811–830. https://doi.org/10.1007/s00704-019-02866-0

Patel, P., Raju, N. J., Reddy, B. C. S. R., Suresh, U., Gossel, W., & Wycisk, P. (2016). Geochemical processes and multivariate statistical analysis for the assessment of groundwater quality in the Swarnamukhi River basin, Andhra Pradesh, India. Environmental Earth Sciences, 75(7). https://doi.org/10.1007/S12665-015-5108-X

Patel, P., Mehta, D., & Sharma, N. (2022). A review on the application of the DRASTIC method in the assessment of groundwater vulnerability. Water Supply, 22(5), 5190-5205.https://doi.org/10.2166/ws.2022.126

Patil, N. S., Chetan, N. L., Nataraja, M., & Suthar, S. (2020). Climate change scenarios and its effect on groundwater level in the Hiranyakeshi watershed. Groundwater for Sustainable Development, 10, 100323. https://doi.org/10.1016/J.GSD.2019.100323

Pavelic, P. Groundwater Availability and Use in Sub-Saharan Africa: A Review of 15 Countries; International Water Management Institute (IWMI): Colombo, Sri Lanka, 2012; ISBN 9789290907589

Peinado-Guevara, H., Green-Ruíz, C., Herrera-Barrientos, J., Escolero-Fuentes, O., Delgado-Rodríguez, O., Belmonte-Jiménez, S., & de Guevara, M. L. (2012). Relationship between chloride concentration and electrical conductivity in groundwater and its estimation from vertical electrical soundings (VESs) in Guasave, Sinaloa, Mexico. Ciencia e Investigación Agraria, 39(1), 229–239. https://doi.org/10.4067/S0718-16202012000100020

Penna, D., Hopp, L., Scandellari, F., Allen, S. T., Benettin, P., Beyer, M., Geris, J., Klaus, J., Marshall, J. D., Schwendenmann, L., Volkmann, T. H. M., Von Freyberg, J., Amin, A., Ceperley, N., Engel, M., Frentress, J., Giambastiani, Y., Mcdonnell, J. J., Zuecco, G., … Kirchner, J. W. (2018). Ideas and perspectives: Tracing terrestrial ecosystem water fluxes using hydrogen and oxygen stable isotopes–challenges and opportunities from an interdisciplinary. Bg. Copernicus.Org, 15, 6399–6415. https://doi.org/10.5194/bg-15-6399-2018

Pedley, S., & Howard, G. (1997). The public health implications of microbiological contamination of groundwater. Quarterly Journal of Engineering Geology, 30(2), 179–188. https://doi.org/10.1144/GSL.QJEGH.1997.030.P2.10

Pellicone, G., Caloiero, T., & Guagliardi, I. (2019). The De Martonne aridity index in Calabria (Southern Italy). Journal of Maps, 15(2), 788–796. https://doi.org/10.1080/17445647.2019.1673840

Pellicone, G., Caloiero, T., & Guagliardi, I. (2019). The De Martonne aridity index in Calabria (Southern Italy). Journal of Maps, 15(2), 788–796. https://doi.org/10.1080/17445647.2019.1673840

Peng, Y., Hirwa, H., Zhang, Q., Wang, G., & Li, F. (2021). Dryland Food Security in Ethiopia: Current Status, Opportunities, and a Roadmap for the Future. Sustainability 2021, Vol. 13, Page 6503, 13(11), 6503. https://doi.org/10.3390/SU13116503

Pham, B. T., Jaafari, A., Prakash, I., Singh, S. K., Quoc, N. K., & Bui, D. T. (2019). Hybrid computational intelligence models for groundwater potential mapping. Catena, 182. Retrieved from https://doi.org/10.1016/j.catena.2019.104101

Pinsri, P., Shrestha, S., KC, S., Mohanasundaram, S., Virdis, S. G. P., Nguyen, T. P. L., & Chaowiwat, W. (2022). Assessing the future climate change, land use change, and abstraction impacts on groundwater resources in the Tak Special Economic Zone, Thailand. Environmental Research, 211, 113026. https://doi.org/10.1016/J.ENVRES.2022.113026

Piper, A. M. (1944). A graphic procedure in the geochemical interpretation of water-analyses. Eos, Transactions American Geophysical Union, 25(6), 914–928. https://doi.org/10.1029/TR025I006P00914

Piscopo, G. (n.d.). Groundwater vulnerability map explanatory notes - Castlereagh.

Poage, M. A., & Chamberlain, C. P. (2001). Empirical relationships between elevation and the stable isotope composition of precipitation and surface waters: considerations for studies of paleoelevation change. *American Journal of Science*, *301*(1), 1-15.

Proutsos, N. D., Tsiros, I. X., Nastos, P., & Tsaousidis, A. (2021). A note on some uncertainties associated with Thornthwaite's aridity index introduced by using different potential evapotranspiration methods. Atmospheric Research, 260. https://doi.org/10.1016/j.atmosres.2021.105727

Pourghasemi, H. R., Pradhan, B., & Gokceoglu, C. (2012). Application of fuzzy logic and analytical hierarchy process (AHP) to landslide susceptibility mapping at Haraz watershed, Iran. *Natural Hazards*, *63*(2), 965–996. https://doi.org/10.1007/s11069-012-0217-2

Prasad, P., Loveson, V. J., Kotha, M., & Yadav, R. (2020). Application of machine learning techniques in groundwater potential mapping along the west coast of India. *GIScience & Remote Sensing*, *57*(6), 735–752. https://doi. org/10.1080/15481603.2020.1794104

Pradhan, B., Journal, S. P.-T. O. H., & 2011, undefined. (2011). Hydro-chemical analysis of the ground water of the basaltic catchments: upper Bhatsai region, Maharastra. Benthamopen.Com, 5, 51–57. https://benthamopen.com/ABSTRACT/TOHYDJ-5-51

Qadir, M., Boers, T. M., Schubert, S., Ghafoor, A., & Murtaza, G. (2003). Agricultural water management in water-starved countries: challenges and opportunities. Agricultural Water Management, 62(3), 165–185. https://doi.org/10.1016/S0378-3774(03)00146-X

Radaideh, O. M. A., Grasemann, B., Melichar, R., & Mosar, J. (2016). Detection and analysis of morphotectonic features utilizing satellite remote sensing and GIS: An example in SW Jordan. Geomorphology, 275, 58–79. https://doi.org/10.1016/j.geomorph.2016.09.033

Radaković, M. G., Tošić, I., Bačević, N., Mladjan, D., Gavrilov, M. B., & Marković, S. B. (2018). The analysis of aridity in Central Serbia from 1949 to 2015. Theoretical and Applied Climatology, 133(3–4), 887–898. https://doi.org/10.1007/S00704-017-2220-8/TABLES/4

Rahmati, O., Pourghasemi, H. R., & Melesse, A. M. (2016). Application of GIS-based data driven random forest and maximum entropy models for groundwater potential mapping: A case study at Mehran Region, Iran. CATENA, 137, 360–372. https://doi.org/10.1016/J.CATENA.2015.10.010

Rahm, D. (1999). WATER RESOURCE DEVELOPMENT IN ETHIOPIA: Issues of Sustainability and Participation.

Rajaveni, S. P., Brindha, K., & Elango, L. (2017). Geological and geomorphological controls on groundwater occurrence in a hard rock region. Applied Water Science, 7(3), 1377–1389. https://doi.org/10.1007/s13201-015-0327-6

Rama, F., Busico, G., Arumi, J. L., Kazakis, N., Colombani, N., Marfella, L., Hirata, R., Kruse, E. E., Sweeney, P., & Mastrocicco, M. (2022). Assessment of intrinsic aquifer vulnerability at continental scale through a critical application of the drastic framework: The case of South America. Science of The Total Environment, 823, 153748. https://doi.org/10.1016/J.SCITOTENV.2022.153748

Ranghetti, L., & Boschetti, M. (2021). Updated trends of water management practice in the Italian rice paddies from remotely sensed imagery. Https://Doi.Org/10.1080/22797254.2021.2002726

Rassam, D. W., Peeters, L., Pickett, T., Jolly, I., & Holz, L. (2013). Accounting for surface-groundwater interactions and their uncertainty in river and groundwater models: A case study in the Namoi River, Australia. Environmental Modelling and Software, 50, 108–119. https://doi.org/10.1016/j.envsoft.2013.09.004

Rao, N. S., Ravindra, B., risk, J. W.-H. and ecological, & 2020, undefined. (2020). Geochemical and health risk evaluation of fluoride rich groundwater in Sattenapalle Region, Guntur district, Andhra Pradesh, India. Taylor & Francis, 26(9), 2316–2348. https://doi.org/10.1080/10807039.2020.1741338

Ravichandran, R., Ayyavoo, R., Rajangam, L., Madasamy, N., Murugaiyan, B., & Shanmugam, S. (2022). Identification of groundwater potential zone using analytical hierarchical process (AHP) and multi-criteria decision analysis (MCDA) for Bhavani river basin, Tamil Nadu, southern India. Groundwater for Sustainable Development, 18, 100806. https://doi.org/10.1016/J.GSD.2022.100806

Razandi, Y., Pourghasemi, H. R., Neisani, N. S., & Rahmati, O. (2015). Application of analytical hierarchy process, frequency ratio, and certainty factor models for groundwater potential mapping using GIS. Earth Science Informatics, 8(4), 867–883. https://doi.org/10.1007/s12145-015-0220-8

Regenspurg, S., Alawi, M., Blöcher, G., Börger, M., Kranz, S., Norden, B., & Vieth, H. (2018). Impact of drilling mud onchemistry and microbiology of an Upper Triassic groundwater after drilling and testing an exploration well for aquifer thermal energy storage in Berlin (Germany). *Environ Earth Sci*, 77. https://doi.org/10. 1007/s12665-018-7696-8

Reimann, C., Bjorvatn, K., Frengstad, B., Melaku, Z., Tekle-Haimanot, R., & Siewers, U. (2003). Drinking water quality in the Ethiopian section of the East African Rift Valley I—data and health aspects. Science of The Total Environment, 311(1–3), 65–80. https://doi.org/10.1016/S0048-9697(03)00137-2

Remondino, F., Guilhot, D., Cannas, V., Ammirati, L., Chirico, R., Martire, D. Di, & Mondillo, N. (2022). Application of Multispectral Remote Sensing for Mapping Flood-Affected Zones in the Brumadinho Mining District (Minas Gerais, Brasil). Remote Sensing 2022, Vol. 14, Page 1501, 14(6), 1501. https://doi.org/10.3390/RS14061501

Renzullo, L. J., van Dijk, A. I. J. M., Perraud, J. M., Collins, D., Henderson, B., Jin, H., Smith, A. B., & McJannet, D. L. (2014). Continental satellite soil moisture data assimilation improves root-zone moisture analysis for water resources assessment. Journal of Hydrology, 519(PD), 2747–2762. https://doi.org/10.1016/j.jhydrol.2014.08.008

Ren, J., Yang, J., Wu, F., Sun, W., Xiao, X., & Xia, J. (Cecilia). (2023). Regional thermal environment changes: Integration of satellite data and land use/land cover. *IScience*, *26*(2), 105820. https://doi.org/10.1016/J.ISCI.2022.105820

Rideal, E. K. (1940). A MEMORIAL LECTURE DELIVERED BEFORE THE CHEMICAL SOCIETY ON APRIL 4TH.

Riché, B., Hachileka, E., Awuor, C., report, A. I., & 2009, undefined. (2009). Climate related vulnerability and adaptive capacity in Ethiopia's Borana and Somali communities. Cakex.Org. Retrieved from https:// www.cakex.org/sites/default/files/climate_ethiopia_communities_0.pdf

Rodgers, P., Soulsby, C., Waldron, S., & Tetzlaff, D. (2005). Using stable isotope tracers to assess hydrological flow paths, residence times and landscape influences in a nested mesoscale catchment. Hydrology and Earth System Sciences, 9(3), 139–155. https://doi.org/10.5194/hess-9-139-2005

Rodríguez-Rodríguez, M., Fernández-Ayuso, A., Hayashi, M., & Moral-Martos, F. (2018). Using water temperature, electrical conductivity, and pH to characterize surface-groundwater relations in a shallow Ponds System (Doñana National Park, SW Spain). Water (Switzerland), 10(10), 1–13. https://doi.org/10.3390/w10101406

Romilly, T. G., & Gebremichael, M. (2011). Evaluation of satellite rainfall estimates over Ethiopian river basins. Hydrology and Earth System Sciences, 15(5), 1505–1514. https://doi.org/10.5194/hess-15-1505-2011

Rout, C., environmental, A. S.-I. journal of, & 2011, undefined. (2011). Assessment of drinking water quality: A case study of Ambala cantonment area, Haryana, India. Indianjournals.Com, 2(2). https://www.indianjournals.com/ijor.aspx?target=ijor:ijes&volume=2&issue=2&article=049

Rozanski, K., Araguás-Araguás, L., Gonfiantini, R., Rozanski, K., Araguas-Araguas, L., & Gonftanttni, R. (1993). Isotopic Patterns in Modern Global Precipitation. Article in Journal of Geophysical Research Atmospheres, 78. https://doi.org/10.1029/GM078p0001

Roy, P., Chakrabortty, R., Chowdhuri, I., Malik, S., Das, B., & Pal, S. C. (2020). Development of different machine learning ensemble classifier for gully erosion susceptibility in Gandheswari watershed of West Bengal, India (pp. 1–26). Retrieved from https://doi.org/10.1007/978 981 15 3689 2_1

Ruidas, D., Pal, S. C., Islam, A. R. M. T., & Saha, A. (2021). Characterization of groundwater potential zones in water-scarce hardrock regions using data driven model. Environmental Earth Sciences, 80(24). https://doi.org/10.1007/S12665-021-10116-8

Rusydi, A. F. (2018). Correlation between conductivity and total dissolved solid in various type of water: A review. IOP Conference Series: Earth and Environmental Science, 118(1). https://doi.org/10.1088/1755-1315/118/1/012019

Saade, J., Atieh, M., Ghanimeh, S., & Golmohammadi, G. (2021). Modeling Impact of Climate Change on Surface Water Availability Using SWAT Model in a Semi-Arid Basin: Case of El Kalb River, Lebanon. Hydrology 2021, Vol. 8, Page 134, 8(3), 134. https://doi.org/10.3390/HYDROLOGY8030134

Saaty, T. L. (2002). Decision making with the analytic hierarchy process. Scientia Iranica, 9(3), 215–229. Retrieved from https://doi.org/10.1504/ijssci.2008. 017590

Saaty, T. L., & Katz, J. M. (1990). How to make a decision: The analytic hierarchy process? European Journal of Operational Research, 48.

Saaty, T. L. (1987). A new macroeconomic forecasting and policy evaluation method using the analytic hierarchy process. Moth/Modelling, 9(5).

Saaty, T. L., & Katz, J. M. (1994). Theory and methodology highlights and critical points in the theory and application of the analytic hierarchy process. *74*.

Sarikhani, R., Kamali, Z., Dehnavi, A. G., & Sahamieh, R. Z. (2014). Correlation of lineaments and groundwater quality in Dasht-e-Arjan Fars, SW of Iran. *Environmental Earth Sciences*, *72*(7), 2369–2387. https://doi.org/10. 1007/s12665-014-3146-4

Sachdeva, S., & Kumar, B. (2021). Comparison of gradient boosted decision trees and random forest for groundwater potential mapping in Dholpur (Rajasthan), India. Stochastic Environmental Research and Risk Assessment, 35(2), 287–306. https://doi.org/10.1007/S00477-020-01891-0/TABLES/6

Safaei, M., Jafari, R., Datta, P., Bashari, H., Pothier, D., & Koch, B. (2021). Spatial scale effect of Sentinel-2, Landsat OLI, and MODIS imagery in the assessment of landscape condition of Zagros mountains. Https://Doi.Org/10.1080/10106049.2021.1914745, 37(18), 5345–5362. https://doi.org/10.1080/10106049.2021.1914745

Sameen, M. I., Pradhan, B., & Lee, S. (2019). Self-Learning Random Forests Model for Mapping Groundwater Yield in Data-Scarce Areas. Natural Resources Research, 28(3), 757–775. https://doi.org/10.1007/s11053-018-9416-1

Saranya, T., & Saravanan, S. (2023). Assessment of groundwater vulnerability using analytical hierarchy process and evidential belief function with DRASTIC parameters, Cuddalore, India. International Journal of Environmental Science and Technology, 20(2), 1837–1856. https://doi.org/10.1007/S13762-022-03944-Z/FIGURES/13

Saravanan, S., Pitchaikani, S., Thambiraja, M., Sathiyamurthi, S., Sivakumar, V., Velusamy, S., & Shanmugamoorthy, M. (2023). Comparative assessment of groundwater vulnerability using GIS-based DRASTIC and DRASTIC-AHP for Thoothukudi District, Tamil Nadu India. Environmental Monitoring and Assessment, 195(1), 1–19. https://doi.org/10.1007/S10661-022-10601-Y/FIGURES/7

Şarlak, N., & Mahmood Agha, O. M. A. (2018). Spatial and temporal variations of aridity indices in Iraq. Theoretical and Applied Climatology, 133(1–2), 89–99. https://doi.org/10.1007/S00704-017-2163-0/FIGURES/4

Seeyan, S., Merkel, B., & Abo, R. (2014). Investigation of the relationship between groundwater level fluctuation and vegetation cover by using NDVI for Shaqlawa Basin, Kurdistan Region-Iraq. Journal of Geography and Geology, 6(3), 187.

Senatilleke, U., Abeysiriwardana, H., Makubura, R. K., Anwar, F., & Rathnayake, U. (2022). Estimation of Potential Evapotranspiration across Sri Lanka Using a Distributed Dual-Source Evapotranspiration Model under Data Scarcity. Advances in Meteorology, 2022. https://doi.org/10.1155/2022/6819539

Semaw, F., Zeleke, G., & Balew, A. (2022). Evaluating flood risk management practices and vulnerability mapping in Alawuha watershed (North Wollo Zone, Ethiopia) using GIS and remote sensing. Applied Geomatics, 14(2), 347–367. https://doi.org/10.1007/S12518-022-00429-Z/TABLES/7

Seifu, K., Lamb, H., Telford, R., Leng, M., & Mohammed, U. (2002). Lake-Groundwater realtionships oxy gene isotope balance and climate sensitivity of the Bishoftu Crater Lakes,Ethiopia. 261–275

Seifu, T., Ayenew, T. T. A., & T A Woldesenbet. (2023). Groundwater potential mapping using GIS and remote sensing with multi-criteria decision-making in Shinile sub-basin, eastern Ethiopia.

Seifu, T. K., Ayenew, T., Woldesenbet, T. A., & Alemayehu, T. (2022). Identification of groundwater potential sites in the drought-prone area using geospatial techniques at Fafen-Jerer sub-basin, Ethiopia. Https://Doi.Org/10.1080/24749508.2022.2141993

Seleshi, Y., & Zanke, U. (2004). Recent changes in rainfall and rainy days in Ethiopia. International Journal of Climatology, 24(8), 973–983. Retrieved from https://doi.org/10.1002/JOC.1052

Senapati, U., & Das, T. K. (2022). GIS based comparative assessment of groundwater potential zone using MIF and AHP techniques in Cooch Behar district, West Bengal. Applied Water Science, 12(3). Retrieved from https://doi.org/10.1007/s13201 02101509

Şener, E. (2023). Appraisal of groundwater pollution risk by combining the fuzzy AHP and DRASTIC method in the Burdur Saline Lake Basin, SW Turkey. Environmental Science and Pollution Research, 30(8), 21945–21969. https://doi.org/10.1007/S11356-022-23651-Z/FIGURES/13

Senthilkumar, M., Gnanasundar, D., & Arumugam, R. (2019). Identifying groundwater recharge zones using remote sensing & GIS techniques in Amaravathi aquifer system

Schoeman, J., Allan, C., & Finlayson, C. M. (2014). A new paradigm for water? A comparative review of integrated, adaptive and ecosystem-based water management in the Anthropocene. International Journal of Water Resources Development, 30(3), 377–390. https://doi.org/10.1080/07900627.2014.907087

Shah, R. A., & Lone, S. A. (2019). Hydrogeomorphological mapping using geospatial techniques for assessing the groundwater potential of Rambiara river basin, western Himalayas. Applied Water Science, 9(3), 1–11. https://doi.org/10.1007/s13201-019-0941-9

Shayannejad, M., Ghobadi, M., & Ostad-Ali-Askari, K. (2022). Modeling of Surface Flow and Infiltration During Surface Irrigation Advance Based on Numerical Solution of Saint–Venant Equations Using Preissmann's Scheme. Pure and Applied Geophysics, 179(3), 1103–1113. https://doi.org/10.1007/S00024-022-02962-9/TABLES/5

Sheikha-BagemGhaleh, S., Babazadeh, H., Rezaie, H., & Sarai-Tabrizi, M. (2023). The effect of climate change on surface and groundwater resources using WEAP-MODFLOW models. Applied Water Science, 13(6), 1–15. https://doi.org/10.1007/S13201-023-01923-4/FIGURES/9

Shimizu, K., Murakami, W., Furuichi, T., & Estoque, R. C. (2023). Mapping Land Use/Land Cover Changes and Forest Disturbances in Vietnam Using a Landsat Temporal Segmentation Algorithm. *Remote Sensing*, *15*(3), 851. https://doi.org/10.3390/RS15030851/S1

Shiru, M. S., Chung, E. S., Shahid, S., & Wang, X. jun. (2022). Comparison of precipitation projections of CMIP5 and CMIP6 global climate models over Yulin, China. Theoretical and Applied Climatology, 147(1–2), 535–548. https://doi.org/10.1007/S00704-021-03823-6/FIGURES/6

Singh, A., Srivastav, S. K., Kumar, S., & Chakrapani, G. J. (2015). A modified-DRASTIC model (DRASTICA) for assessment of groundwater vulnerability to pollution in an urbanized environment in Lucknow, India. Environmental Earth Sciences, 74(7), 5475–5490. https://doi.org/10.1007/S12665-015-4558-5/TABLES/10

Singh, S., Raju, N. J., Gossel, W., & Wycisk, P. (2016). Assessment of pollution potential of leachate from the municipal solid waste disposal site and its impact on groundwater quality, Varanasi environs, India. Arabian Journal of Geosciences, 9(2), 1–12. https://doi.org/10.1007/S12517-015-2131-X/FIGURES/4

Sidhu, N., Rishi, M., & Urban, R. H. (2013). Groundwater quality variation with respect to aquifer dispositioning in urbanized watershed of Chandigarh, India. Researchgate.Net.

Singh, U. V., Abhishek, A., Singh, K. P., Dhakate, R., & Singh, N. P. (2013). Groundwater quality appraisal and its hydrochemical characterization in Ghaziabad (a region of indo-gangetic plain), Uttar Pradesh, India. Applied Water Science 2013 4:2, 4(2), 145–157. https://doi.org/10.1007/S13201-013-0137-7

Singh, S. K., Singh, C. K., & Mukherjee, S. (2010). Impact of land-use and land-cover change on groundwater quality in the Lower Shiwalik hills: A remote sensing and GIS based approach. Central European Journal of Geosciences, 2(2), 124–131. https://doi.org/10.2478/v10085-010-0003-x

Singh, A. (2014). Groundwater resources management through the applications of simulation modeling: A review. *Science of the Total Environment*, *499*, 414–423. https://doi.org/10.1016/j.scitotenv.2014.05.048

Singer, M. B., Asfaw, D. T., Rosolem, R., Cuthbert, M. O., Miralles, D. G., MacLeod, D., Quichimbo, E. A., & Michaelides, K. (2021). Hourly potential evapotranspiration at 0.1° resolution for the global land surface from 1981-present. Scientific Data 2021 8:1, 8(1), 1–13. https://doi.org/10.1038/s41597-021-01003-9

Smail, R. Q. S., & Dişli, E. (2023). Assessment and validation of groundwater vulnerability to nitrate and TDS using based on a modified DRASTIC model: a case study in the Erbil Central Sub-Basin, Iraq. Environmental Monitoring and Assessment, 195(5), 567. https://doi.org/10.1007/s10661-023-11165-1

Smedley, P. (2001). Groundwater quality: Ethiopia. http://bgs.ac.uk/downloads/browse.cfm?sec=9&cat=11...

Solomon, T. (2013). Rationale and capacity of pastoral community innovative adaptation to climate change in Ethiopia. Retrieved from https://www.africa portal.org/publications/rationale and capacity of pastoral community innovative adaptation to climate change in Ethiopia/

Sommer, B., Boggs, D. A., Boggs, G. S., van Dijk, A., & Froend, R. (2016). Spatio-temporal patterns of evapotranspiration from groundwater-dependent vegetation. *Ecohydrology, 9*(8), 1620-1629.

Souza Filho, C. R., & Drury, S. A. (1997). Remote sensing strategies for lithological mapping of pan African assemblages in arid environments: a case study in Eritrea, NE Africa. Boletim IG-USP. Série Científica, 28(0), 1. https://doi.org/10.11606/issn.2316-8986.v28i0p1-22

Starbuck, C. A., Dickson, B. G., & Chambers, C. L. (2022). Informing wind energy development: Land cover and topography predict occupancy for Arizona bats. PLOS ONE, 17(6), e0268573. https://doi.org/10.1371/JOURNAL.PONE.0268573

S. B., Carlier, C., Cochand, F., Hunkeler, D., & Brunner, P. (2020). Lithological and tectonic control on groundwater contribution to stream discharge during low-flow conditions. *Water (Switzerland)*, 12. https:// doi.org/10.3390/w12030821

Stefanidis, S., & Alexandridis, V. (2021). Precipitation and Potential Evapotranspiration Temporal Variability and Their Relationship in Two Forest Ecosystems in Greece. Hydrology 2021, Vol. 8, Page 160, 8(4), 160. https://doi.org/10.3390/HYDROLOGY8040160

Stelling, J. M., Slesak, R. A., Windmuller-Campione, M. A., & Grinde, A. (2023). Effects of stand age, tree species, and climate on water table fluctuations and estimated evapotranspiration in managed peatland forests. Journal of Environmental Management, 339, 117783. https://doi.org/10.1016/J.JENVMAN.2023.117783

Srivastava, A., Kumari, N., & Maza, M. (2020). Hydrological response to agricultural land use heterogeneity using variable infiltration capacity model. Water Resources Management, 34(12), 3779–3794. Retrieved from https://doi.org/10.1007/s11269 02002630 4

Stone, R. J. (2014). Climate Change and Climate Variability Same difference ? Soil Management Issues Related to Food Production and Environmental Quality as a Consequence of Climate Change and Variability, February.

Straffelini, E., & Tarolli, P. (2023). Climate change-induced aridity is affecting agriculture in Northeast Italy. Agricultural Systems, 208, 103647. https://doi.org/10.1016/J.AGSY.2023.103647

Subramani, T., Rajmohan, · N, Elango, · L, Rajmohan, N., & Elango, L. (2010). Groundwater geochemistry and identification of hydrogeochemical processes in a hard rock region, Southern India. Springer, 162(1–4), 123–137. https://doi.org/10.1007/s10661-009-0781-4

Sun, T., Cheng, W., Abdelkareem, M., & Al-Arifi, N. (2022). Mapping Prospective Areas of Water Resources and Monitoring Land Use/Land Cover Changes in an Arid Region Using Remote Sensing and GIS Techniques. https://doi.org/10.3390/W14152435

Swain, S., Taloor, A. K., Dhal, L., Sahoo, S., & Al-Ansari, N. (2022). Impact of climate change on groundwater hydrology: a comprehensive review and current status of the Indian hydrogeology. Applied Water Science 2022 12:6, 12(6), 1–25. https://doi.org/10.1007/S13201-022-01652-0

Tabari, H. (2020). Climate change impact on flood and extreme precipitation increases with water availability. Scientific Reports, 10(1). https://doi.org/10.1038/s41598-020-70816-2

Tabari, H., & Aghajanloo, M. B. (2013). Temporal pattern of aridity index in Iran with considering precipitation and evapotranspiration trends. International Journal of Climatology, 33(2), 396–409. https://doi.org/10.1002/JOC.3432

Tadesse, A., Moges, M. A., Lijalem, D., Dagnew, D. C., Taffese, T., Belete, M. A., Tilahun, S. A., & Steenhuis, T. S. (2008). Assessment of nitrate concentration in drinking water sources in rural areas of Ethiopia.

Tadese, M., Kumar, L., Atmosphere, & R. K. (2020). Long-term variability in potential evapotranspiration, water availability and drought under climate change scenarios in the Awash River Basin, Ethiopia. Mdpi.Com. https://doi.org/10.3390/atmos11090883

Tadesse, Y., Amsalu, A., Billi, P., & Fazzini, M. (2018). A new early warning drought index for Ethiopia. Journal of Water and Climate Change, 9(3), 624–630. https://doi.org/10.2166/wcc.2018.105

Tadesse, N., Nedaw, D., Woldearegay, K., Gebreyohannes, T., & Steenbergen, F. Van. (2015). Groundwater management for irrigation in the raya and kobo valleys, Northern Ethiopia. International Journal of Earth Sciences and Engineering, 8(3), 1104–1114.

Tadesse, D., Suryabhagavan, K. V., Nedaw, D., & Hailu, B. T. (2022). A model-based flood hazard mapping in Itang District of the Gambella region, Ethiopia. *Https://Doi.Org/10.1080/24749508.2021.2022833*.

Taghavi, N., Niven, R. K., Paull, D. J., & Kramer, M. (2022). Groundwater vulnerability assessment: A review including new statistical and hybrid methods. Science of The Total Environment, 822, 153486. https://doi.org/10.1016/J.SCITOTENV.2022.153486

Taheri, K., Missimer, T. M., Bayatvarkeshi, M., Mahmoudi Sivand, S., Fathi, S., Toranjian, A., & Dehghan Manshadi, B. (2023). An intrinsic vulnerability approach to assess an overburden alluvial aquifer exposure to sinkhole-prone area; results from a Central Iran case study. Https://Doi.Org/10.1080/10106049.2023.2168068

Taheri, K., Regional, K., Authority, W., Missimer, T. M., Maleki, A., Omidipour, R., & Bahrami, J. (2021). Assessment of Alluvial Aquifer Intrinsic Vulnerability by a Generic Drastic Model. https://doi.org/10.21203/rs.3.rs-525916/v1

Tamil Nadu, South India. Sustainable Environment Research, 1(1), 1–9. Retrieved from https://doi.org/10.1186/S42834 0190014 7/TABLES/3

Tanguy, M., Chevuturi, A., Marchant, B. P., Mackay, J. D., Parry, S., & Hannaford, J. (2023). How will climate change affect spatial coherence of streamflow and groundwater droughts in Great Britain? Environmental Research Letters. https://doi.org/10.1088/1748-9326/ACD655

Tanimu, J. J., Hamada, M., Hassan, M., Kakudi, H. A., & Abiodun, J. O. (2022). A Machine Learning Method for Classification of Cervical Cancer. Electronics (Switzerland), 11(3).https://doi.org/10.3390/electronics11030463

Tariq, A., Yan, J., Gagnon, A. S., Riaz Khan, M., & Mumtaz, F. (2022). Mapping of cropland, cropping patterns and crop types by combining optical remote sensing images with decision tree classifier and random forest. https://doi.org/10.1080/10095020.2022.2100287

Tasgara, T. D., & Kumar, B. (2023). Assessment of land use/land cover change impact on streamflow: a case study over upper Guder Catchment, Ethiopia. *Sustainable Water Resources Management*, *9*(1), 1–12. https://doi.org/10.1007/S40899-022-00783-1/TABLES/11

Tatebe, H., Ogura, T., Nitta, T., Komuro, Y., Ogochi, K., Takemura, T., Sudo, K., Sekiguchi, M., Abe, M., Saito, F., Chikira, M., Watanabe, S., Mori, M., Hirota, N., Kawatani, Y., Mochizuki, T., Yoshimura, K., Takata, K., O'Ishi, R., … Kimoto, M. (2019). Description and basic evaluation of simulated mean state, internal variability, and climate sensitivity in MIROC6. Geoscientific Model Development, 12(7), 2727–2765. https://doi.org/10.5194/gmd-12-2727-2019

Taye, M. T., Willems, P., & Block, P. (2015). Implications of climate change on hydrological extremes in the Blue Nile basin: A review. Journal of Hydrology: Regional Studies, 4, 280–293. https://doi.org/10.1016/J.EJRH.2015.07.001

Taylor, R. G., Koussis, A. D., & Tindimuguya, C. (2009). Groundwater and climate in Africa - A review. Hydrological Sciences Journal, 54(4), 655–664. https://doi.org/10.1623/hysj.54.4.655

Tegos, A., Stefanidis, S., Cody, J., & Koutsoyiannis, D. (2023). On the Sensitivity of Standardized-Precipitation-Evapotranspiration and Aridity Indexes Using Alternative Potential Evapotranspiration Models. Hydrology 2023, Vol. 10, Page 64, 10(3), 64. https://doi.org/10.3390/HYDROLOGY10030064

Tegos, A., Ziogas, A., Bellos, V., & Tzimas, A. (2022). Forensic Hydrology: A Complete Reconstruction of an Extreme Flood Event in Data-Scarce Area. Hydrology 2022, Vol. 9, Page 93, 9(5), 93. https://doi.org/10.3390/HYDROLOGY9050093

Telford, R. J., & Lamb, H. F. (1999). Groundwater-Mediated Response to Holocene Climatic Change Recorded by the Diatom Stratigraphy of an Ethiopian Crater Lake. http://www.idealibrary.com

Terwey, J. L. (1984). Isotopes in groundwater hydrology (Sudan). Challenges in African Hydrology and Water Resources. Proc. Harare Symposium, 1984, 144, 155–160

Thanh, N. N., Chotpantarat, S., Trung, N. H., Ngu, N. H., & Muoi, L. Van. (2022). Mapping groundwater potential zones in Kanchanaburi Province, Thailand by integrating of analytic hierarchy process, frequency ratio, and random forest. Ecological Indicators, 145, 109591. https://doi.org/10.1016/J.ECOLIND.2022.109591

Thamaga, K. H., Dube, T., & Shoko, C. (2022). Evaluating the impact of land use and land cover change on unprotected wetland ecosystems in the arid-tropical areas of South Africa using the Landsat dataset and support vector machine. *Https://Doi.Org/10.1080/10106049.2022.2034986*, *37*(25), 10344–10365. https://doi.org/10.1080/10106049.2022.2034986

Thornthwaite, C. W. (1948). An Approach toward a Rational Classification of Climate. Geographical Review, 38(1), 55. https://doi.org/10.2307/210739

Tian, Y., Zheng, Y., Wu, B., Wu, X., Liu, J., & Zheng, C. (2015). Modeling surface water-groundwater interaction in arid and semi-arid regions with intensive agriculture. Environmental Modelling and Software, 63(January), 170–184. https://doi.org/10.1016/j.envsoft.2014.10.011

Tian, X., Tang, C., Wu, X., Yang, J., Zhao, F., & Liu, D. (2023). The global spatial-temporal distribution and EOF analysis of AOD based on MODIS data during 2003–2021. Atmospheric Environment, 302, 119722. https://doi.org/10.1016/J.ATMOSENV.2023.119722

Tigabu, T. B., Wagner, P. D., Hörmann, G., Kiesel, J., & Fohrer, N. (2021). Climate change impacts on the water and groundwater resources of the Lake Tana Basin, Ethiopia. Journal of Water and Climate Change, 12(5), 1544–1563. https://doi.org/10.2166/WCC.2020.126

Tilahun, K., & Merkel, B. J. (2010). Assessment of groundwater vulnerability to pollution in dire dawa, Ethiopia using drastic. Environmental Earth Sciences, 59(7), 1485–1496. https://doi.org/10.1007/S12665-009-0134-1/FIGURES/11

Tilahun, K. (2006). The characterisation of rainfall in the arid and semi-arid regions of Ethiopia. Water SA, 32(3), 429-436.

Tisseuil, C., Vrac, M., Lek, S., & Wade, A. J. (2010). Statistical downscaling of river flows. Journal of Hydrology, 385(1–4), 279–291. https://doi.org/10.1016/j.jhydrol.2010.02.030

Toma, M. B., Belete, M. D., & Ulsido, M. D. (2023). Historical and future dynamics of land use land cover and its drivers in Ajora-Woybo watershed, Omo-Gibe basin, Ethiopia. *Natural Resource Modeling*, *36*(1), e12353. https://doi.org/10.1111/NRM.12353

Trajkovic, S., Gocic, M., Pongracz, R., & Bartholy, J. (2019). Adjustment of Thornthwaite equation for estimating evapotranspiration in Vojvodina. Theoretical and Applied Climatology, 138, 1231-1240.

Tran, T. V., Bruce, D., Huang, C. Y., Tran, D. X., Myint, S. W., & Nguyen, D. B. (2023). Decadal assessment of agricultural drought in the context of land use land cover change using MODIS multivariate spectral index time-series data. https://doi.org/10.1080/15481603.2022.2163070

T.Segele, M.Leslie, & J.Lamb. (2009). Evaluation and adaptation of a regional climate model for the Horn of Africa: rainfall climatology and interannual variability. International Journal of Climatology, 2029(March 2008), 2011–2029. https://doi.org/10.1002/joc

Tolche, A. D., Gurara, M. A., Pham, Q. B., & Anh, D. T. (2021). Modelling and accessing land degradation vulnerability using remote sensing techniques and the analytical hierarchy process approach. Https://Doi.Org/10.1080/10106049.2021.1959656.

Tummala, V. M. R., & Ling, H. (1996). Sampling distribution of the random consistency index of the analytic hierarchy process (AHP). Journal of Statistical Computation and Simulation, 55(1–2), 121–131. Retrieved from https://doi.org/10.1080/00949659 608811754

Tu, Z., & Yang, Y. (2022). On the Estimation of Potential Evaporation Under Wet and Dry Conditions. Water Resources Research, 58(4), e2021WR031486. https://doi.org/10.1029/2021WR031486

Tu, Z., Zhou, Y., Zhou, J., Han, S., Liu, J., Liu, J., Sun, Y., & Yang, F. (2023). Identification and Risk Assessment of Priority Control Organic Pollutants in Groundwater in the Junggar Basin in Xinjiang, P.R. China. International Journal of Environmental Research and Public Health 2023, Vol. 20, Page 2051, 20(3), 2051. https://doi.org/10.3390/IJERPH20032051

Tyralis, H., Papacharalampous, G., & Langousis, A. (2019). A Brief Review of Random Forests for Water Scientists and Practitioners and Their Recent History in Water Resources. Water 2019, Vol. 11, Page 910, 11(5), 910. https://doi.org/10.3390/W11050910

Ty, T. Van, Lavane, K., Nguyen, P. C., Downes, N. K., Nam, N. D. G., Minh, H. V. T., & Kumar, P. (2022). Assessment of Relationship between Climate Change, Drought, and Land Use and Land Cover Changes in a Semi-Mountainous Area of the Vietnamese Mekong Delta. Land 2022, Vol. 11, Page 2175, 11(12), 2175. https://doi.org/10.3390/LAND11122175

Ullah, S., You, Q., Sachindra, D. A., Nowosad, M., Ullah, W., Bhatti, A. S., Jin, Z., & Ali, A. (2022). Spatiotemporal changes in global aridity in terms of multiple aridity indices: An assessment based on the CRU data. https://doi.org/10.1016/J.ATMOSRES.2021.105998

Umar, M., Khan, S. N., Arshad, A., Aslam, R. A., Khan, H. M. S., Rashid, H., Pham, Q. B., Nasir, A., Noor, R., Khedher, K. M., & Anh, D. T. (2022). A modified approach to quantify aquifer vulnerability to pollution towards sustainable groundwater management in Irrigated Indus Basin. Environmental Science and Pollution Research, 29(18), 27257–27278. https://doi.org/10.1007/S11356-021-17882-9/FIGURES/11

United Nations Environment Programme., Middleton, Nick., & Thomas, D. S. G. (1997). World atlas of desertification.. ed. 2. 182. https://doi.org/10.3/JQUERY-UI.JS

Urry, J. (2015). Climate Change and Society. Why the Social Sciences Matter, 45–59. https://doi.org/10.1057/9781137269928_4/COVER

Van der Meer, F. D., van der Werff, H. M. A., van Ruitenbeek, F. J. A., Hecker, C. A., Bakker, W. H., Noomen, M. F., van der Meijde, M., Carranza, E. J. M., de Smeth, J. B., & Woldai, T. (2012). Multi- and hyperspectral geologic remote sensing: A review. International Journal of Applied Earth Observation and Geoinformation, 14(1), 112–128. https://doi.org/10.1016/j.jag.2011.08.002

Vardhan, K. H., Kumar, P. S., & Panda, R. C. (2019). A review on heavy metal pollution, toxicity and remedial measures: Current trends and future perspectives. Journal of Molecular Liquids, 290, 111197. https://doi.org/10.1016/J.MOLLIQ.2019.111197

Viste, E., Korecha, D., & Sorteberg, A. (2013). Recent drought and precipitation tendencies in Ethiopia. Theoretical and Applied Climatology, 112(3–4), 535–551. https://doi.org/10.1007/S00704-012-0746-3/TABLES/1

Wakejo, W. K., Meshesha, B. T., Habtu, N. G., & Mekonnen, Y. G. (2022). Anthropogenic nitrate contamination of water resources in Ethiopia: an overview. In Water Supply (Vol. 22, Issue 11, pp. 8157–8172). IWA Publishing. https://doi.org/10.2166/ws.2022.377

Wallén, C. C. (1967). Aridity Definitions and their Applicability. Geografiska Annaler: Series A, Physical Geography, 49(2–4), 367–384. https://doi.org/10.1080/04353676.1967.11879765

Walter, J., Chesnaux, R., Cloutier, V., & Gaboury, D. (2017). The influence of water/rock− water/clay interactions and mixing in the salinization processes of groundwater. Journal of Hydrology: Regional Studies, 13, 168-188. https://doi.org/10.1016/j.ejrh.2017.07.004

Wang, F., & Tian, D. (2022). On deep learning-based bias correction and downscaling of multiple climate models simulations. Climate Dynamics, 59(11–12), 3451–3468. https://doi.org/10.1007/S00382-022-06277-2/FIGURES/14

Wang, H., Khayatnezhad, M., & Youssefi, N. (2022). Using an optimized soil and water assessment tool by deep belief networks to evaluate the impact of land use and climate change on water resources. Concurrency and Computation: Practice and Experience, 34(10), e6807. https://doi.org/10.1002/CPE.6807

Wang, H., Qi, Y., Lian, X., Zhang, J., Yang, R., & Zhang, M. (2022). Effects of climate change and land use/cover change on the volume of the Qinghai Lake in China. Journal of Arid Land, 14(3), 245–261. https://doi.org/10.1007/S40333-022-0062-4/METRICS

Watts, G., Battarbee, R. W., Bloomfield, J. P., Crossman, J., Daccache, A., Durance, I., Elliott, J. A., Garner, G., Hannaford, J., Hannah, D. M., Hess, T., Jackson, C. R., Kay, A. L., Kernan, M., Knox, J., Mackay, J., Monteith, D. T., Ormerod, S. J., Rance, J., … Wilby, R. L. (2015). Climate change and water in the UK – past changes and future prospects. 39(1), 6–28. https://doi.org/10.1177/0309133314542957

Wei, H., Liang, X., Liu, S., Liu, M., & Water, C. X.-. (2020). Hydrochemical evolution of groundwater in Dehui, China. Mdpi.Com. https://doi.org/10.3390/w12123378

Wei, A., Bi, P., Guo, J., Lu, S., & Li, D. (2021). Modified DRASTIC model for groundwater vulnerability to nitrate contamination in the Dagujia river basin, China. Water Supply, 21(4), 1793-1805. https://doi.org/10.2166/ws.2021.018

Whaley-Martin, K. J., Mailloux, B. J., van Geen, A., Bostick, B. C., Ahmed, K. M., Choudhury, I., & Slater, G. F. (2017). Human and livestock waste as a reduced carbon source contributing to the release of arsenic to shallow Bangladesh groundwater. Science of The Total Environment, 595, 63–71. https://doi.org/10.1016/J.SCITOTENV.2017.03.234

Wilhite, D. A., Svoboda, M. D., & Hayes, M. J. (2007). Understanding the complex impacts of drought: A key to enhancing drought mitigation and preparedness. Water Resources Management, 21(5), 763–774. https://doi.org/10.1007/S11269-006-9076-5/METRICS

Wilson, J. P., John P., & Gallant, J. C. (2000). Terrain analysis: Principles and applications. Hoboken, NJ: Wiley.

Worku, G., Teferi, E., Bantider, A., Dile, Y. T., & Taye, M. T. (2018). Evaluation of regional climate models performance in simulating rainfall climatology of Jemma sub-basin, Upper Blue Nile Basin, Ethiopia. Dynamics of Atmospheres and Oceans, 83(June), 53–63. https://doi.org/10.1016/j.dynatmoce.2018.06.002

World Health Organization. (2016). Protecting surface water for health: identifying, assessing and managing drinking-water quality risks in surface-water catchments.

Wu, W. Y., Lo, M. H., Wada, Y., Famiglietti, J. S., Reager, J. T., Yeh, P. J. F., Ducharne, A., & Yang, Z. L. (2020). Divergent effects of climate change on future groundwater availability in key mid-latitude aquifers. Nature Communications, 11(1), 1–9. https://doi.org/10.1038/s41467-020-17581-y

Worqlul, A. W., Jeong, J., Dile, Y. T., Osorio, J., Schmitter, P., Gerik, T., Srinivasan, R., & Clark, N. (2017). Assessing potential land suitable for surface irrigation using groundwater in Ethiopia. Applied Geography, 85, 1–13. https://doi.org/10.1016/j.apgeog.2017.05.010

Xiao, Y., Xiao, D., Hao, Q., Liu, K., Wang, R., Huang, X., Liao, X., & Zhang, Y. (2021). Accessible Phreatic Groundwater Resources in the Central Shijiazhuang of North China Plain: Perspective From the Hydrogeochemical Constraints. Frontiers in Environmental Science, 9, 747097. https://doi.org/10.3389/FENVS.2021.747097/BIBTEX

Xue, J., Anderson, M. C., Gao, F., Hain, C., Knipper, K. R., Yang, Y., Kustas, W. P., Yang, Y., Bambach, N., McElrone, A. J., Castro, S. J., Alfieri, J. G., Prueger, J. H., McKee, L. G., Hipps, L. E., & del Mar Alsina, M. (2022). Improving the spatiotemporal resolution of remotely sensed ET information for water management through Landsat, Sentinel-2, ECOSTRESS and VIIRS data fusion. Irrigation Science, 40(4–5), 609–634. https://doi.org/10.1007/S00271-022-00799-7/FIGURES/14

Xiong, C., & Ren, Y. (2023). Arctic sea ice melt pond fraction in 2000–2021 derived by dynamic pixel spectral unmixing of MODIS images. *ISPRS Journal of Photogrammetry and Remote Sensing*, *197*, 181–198. https://doi.org/10.1016/J.ISPRSJPRS.2023.01.023

Yamusa, I. B., Yamusa, Y. B., Danbatta, U. A., & Najime, T. (2018). Geological and structural analysis using remote sensing for lineament and lithological mapping. IOP Conference Series: Earth and Environmental Science, 169(1). https://doi.org/10.1088/1755-1315/169/1/012082

Yan, R., Cai, Y., Li, C., Wang, X., & Liu, Q. (2019). Hydrological responses to climate and land use changes in a watershed of the Loess Plateau, China. Sustainability (Switzerland), 11(5). https://doi.org/10.3390/su11051443

Yang, R., Suhail, H. A., Gourbet, L., Willett, S. D., Fellin, M. G., Lin, X., Gong, J., Wei, X., Maden, C., Jiao, R., & Chen, H. (2020). Early Pleistocene drainage pattern changes in Eastern Tibet: Constraints from provenance analysis, thermochronometry, and numerical modeling. Earth and Planetary Science Letters, 531, 115955. https://doi.org/10.1016/J.EPSL.2019.115955

Yang, Y., Chen, R., Han, C., & Liu, Z. (2021). Evaluation of 18 models for calculating potential evapotranspiration in different climatic zones of China. Agricultural Water Management, 244. https://doi.org/10.1016/j.agwat.2020.106545

Yang, S., Song, S., Li, F., Yu, M., Yu, G., Zhang, Q., Cui, H., Wang, R., & Wu, Y. (2022). Vegetation coverage changes driven by a combination of climate change and human activities in Ethiopia, 2003–2018. *Ecological Informatics*, *71*, 101776. https://doi.org/10.1016/J.ECOINF.2022.101776

Yang, Y. M., Wang, B., Cao, J., Ma, L., & Li, J. (2020). Improved historical simulation by enhancing moist physical parameterizations in the climate system model NESM3.0. Climate Dynamics, 54(7–8), 3819–3840. https://doi.org/10.1007/S00382-020-05209-2/FIGURES/19

Yariyan, P., Avand, M., Omidvar, E., Pham, Q. B., Linh, N. T. T., & Tiefenbacher, J. P. (2022). Optimization of statistical and machine learning hybrid models for groundwater potential mapping. *Geocarto International*, *37*(13), 3877–3911. https://doi.org/10. 1080/10106049.2020.1870164

Yasin, H. M., Zeebaree, S. R. M., Sadeeq, M. A. M., Ameen, S. Y., Ibrahim, I. M., Zebari, R. R., Ibrahim, R. K., & Sallow, A. B. (2021). IoT and ICT based Smart Water Management, Monitoring and Controlling System: A Review. Asian Journal of Research in Computer Science, 42–56. https://doi.org/10.9734/AJRCOS/2021/V8I230198

Yeboah, K. A., Akpoti, K., Kabo-bah, A. T., Ofosu, E. A., Siabi, E. K., Mortey, E. M., & Okyereh, S. A. (2022). Assessing climate change projections in the Volta Basin using the CORDEX-Africa climate simulations and statistical bias-correction. Environmental Challenges, 6, 100439. https://doi.org/10.1016/J.ENVC.2021.100439

Yeh, H. F., Lee, C. H., & Hsu, K. C. (2011). Oxygen and hydrogen isotopes for the characteristics of groundwater recharge: a case study from the Chih-Pen Creek basin, Taiwan. Environmental Earth Sciences, 62, 393-402. https://doi.org/10.1007/s12665-010-0534-2

Yi, H., Zhang, X., He, L., He, J., Tian, Q., Zou, Y., & An, Z. (2023). Detecting the impact of the "Grain for Green" program on land use/land cover and hydrological regimes in a watershed of the Chinese Loess Plateau over the next 30 years. *Ecological Indicators*, *150*, 110181. https://doi.org/10.1016/J.ECOLIND.2023.110181

Yifru, B. A., Chung, I. M., Kim, M. G., & Chang, S. W. (2021). Assessing the Effect of Land/Use Land Cover and Climate Change on Water Yield and Groundwater Recharge in East African Rift Valley

using Integrated Model. Journal of Hydrology: Regional Studies, 37, 100926. https://doi.org/10.1016/J.EJRH.2021.100926

Yoo, C., Im, J., Cho, D., Lee, Y., Bae, D., & Sismanidis, P. (2022). Downscaling MODIS nighttime land surface temperatures in urban areas using ASTER thermal data through local linear forest. International Journal of Applied Earth Observation and Geoinformation, 110, 102827. https://doi.org/10.1016/J.JAG.2022.102827

Young, R. A., & Haveman, R. H. (1985). Chapter 11 Economics of water resources: a survey. Handbook of Natural Resource and Energy Economics, 2(C), 465–529. https://doi.org/10.1016/S1573-4439(85)80018-X

Yousif, M., & El-Aassar, A. H. M. (2018). Rock-water interaction processes based on geochemical modeling and remote sensing applications in hyper-arid environment: cases from the southeastern region of Egypt. Bulletin of the National Research Centre, 42, 1-23.

Yuan, W., Liu, Q., Song, S., Lu, Y., Yang, S., Fang, Z., & Shi, Z. (2023). A climate-water quality assessment framework for quantifying the contributions of climate change and human activities http://creativecommons.org/licenses/by/4.0/

Yukimoto, S., Kawai, H., Koshiro, T., Oshima, N., Yoshida, K., Urakawa, S., Tsujino, H., Deushi, M., Tanaka, T., Hosaka, M., Yabu, S., Yoshimura, H., Shindo, E., Mizuta, R., Obata, A., Adachi, Y., & Ishii, M. (2019). The Meteorological Research Institute Earth System Model Version 2.0, MRI-ESM2.0: Description and Basic Evaluation of the Physical Component. Journal of the Meteorological Society of Japan. Ser. II, 97(5), 931–965. https://doi.org/10.2151/JMSJ.2019-051

Zarei, A. R., & Mahmoudi, M. R. (2021). Assessing the Influence of PET Calculation Method on the Characteristics of UNEP Aridity Index Under Different Climatic Conditions throughout Iran. Pure and Applied Geophysics, 178(8), 3179–3205. https://doi.org/10.1007/S00024-021-02786-Z/TABLES/7

Zerssa, G., Feyssa, D., Kim, D. G., & Eichler-Löbermann, B. (2021). Challenges of smallholder farming in Ethiopia and opportunities by adopting climate-smart agriculture. *Agriculture (Switzerland)*, *11*, 1–26. https:// doi.org/10.3390/agriculture11030192

Zhang, H., Sekhari, A., Ouzrout, Y., & Bouras, A. (2014). Deriving consistent pairwise comparison matrices in decision making methodologies based on linear programming method. Journal of Intelligent and Fuzzy Systems, 27(4). Retrieved from https://doi. org/10.3233/IFS 141164ï

Zhu, Q., Guo, X., Deng, W., Guan, Q., Zhong, Y., Zhang, L., & Li, D. (2022). Land-Use/Land-Cover change detection based on a Siamese global learning framework for high spatial resolution remote sensing imagery. *ISPRS Journal of Photogrammetry and Remote Sensing*, *184*, 63–78

LIST OF APPENDIXES

Appendix Figures

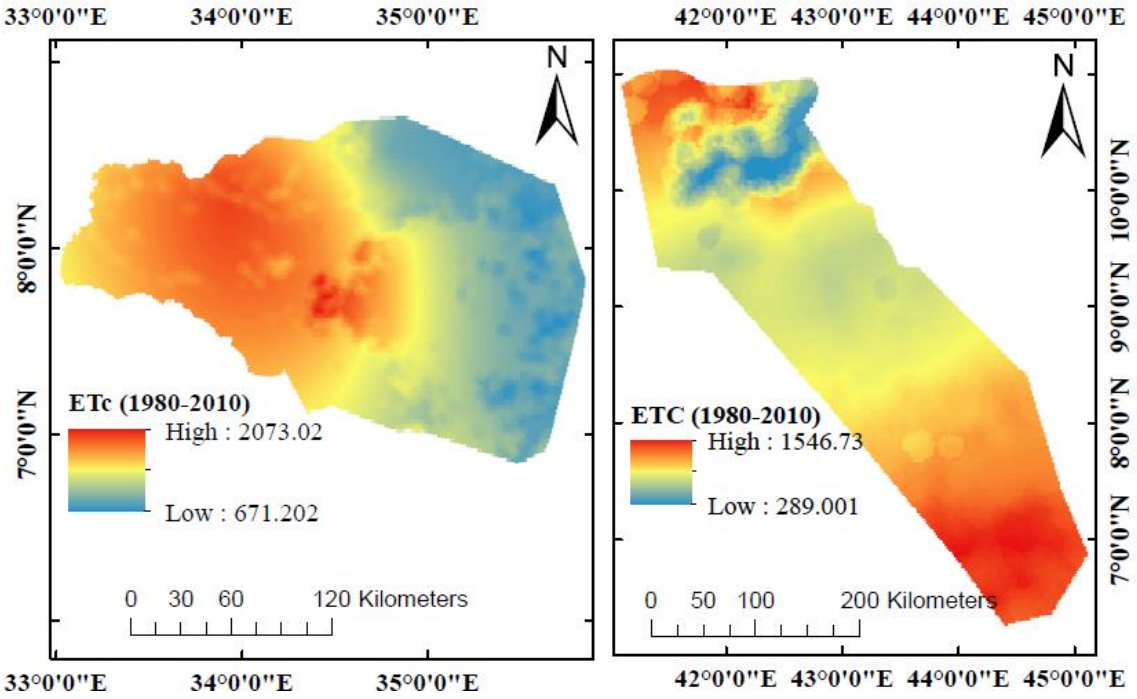

Figure A7.1 Crop evapotranspiration for the historical period

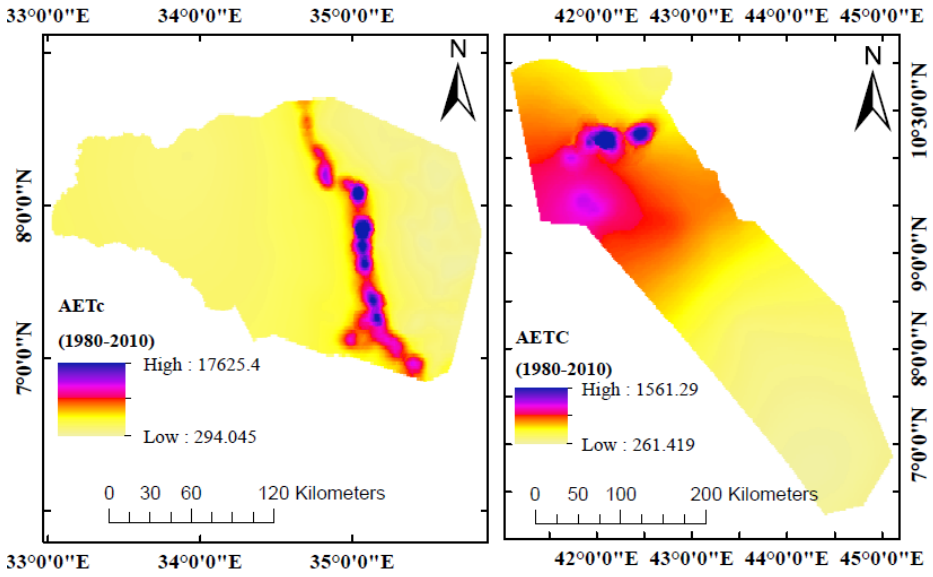

Figure A7.2 Actual crop evapotranspiration for the historical period

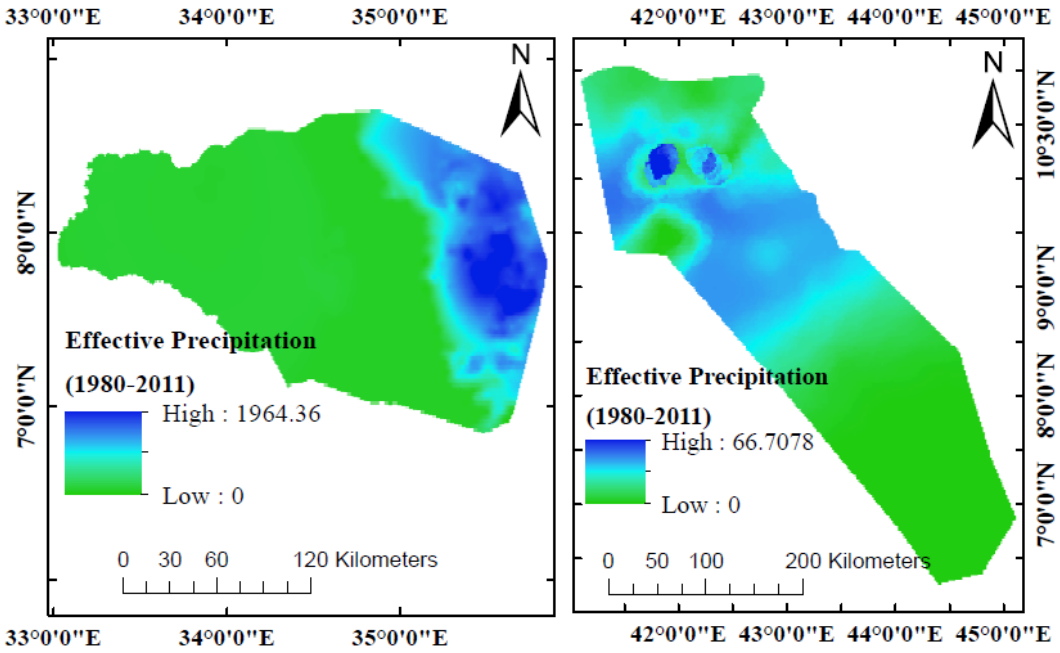

Figure A7.3 Effective precipitation for the historical period

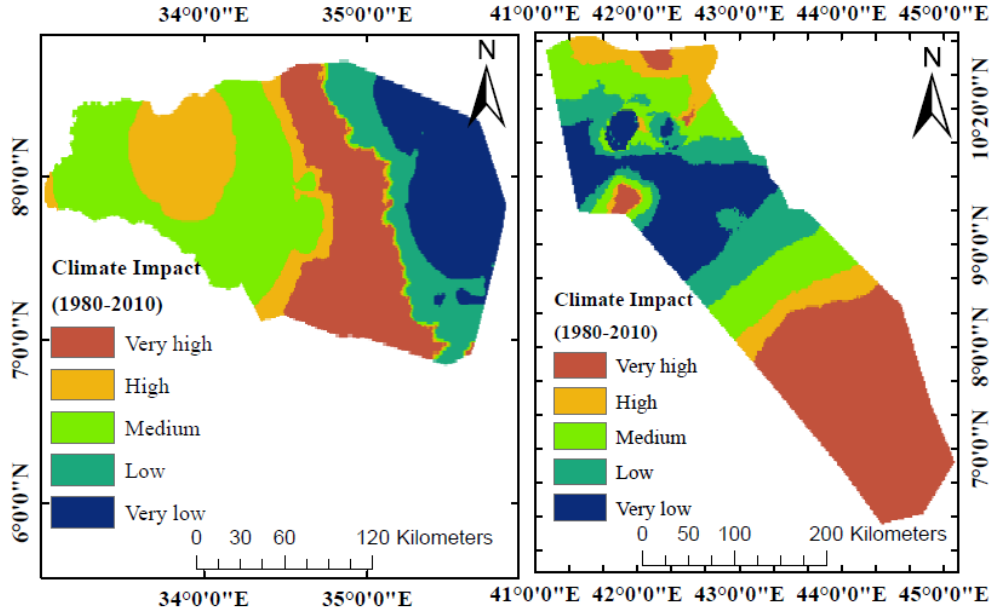

Figure A7.4 Climate effect on groundwater for the historical period

Appendix Tables

Table A4.1 Saaty's pair-wise comparison nine-point scale for AHP preference

Scale	**Numerical rating**	**Rescpirocal**
Extreame importance	9	1/9
Very Extremely strongly importance	8	1/8
Very strongly importance	7	1/7
Strongly to very strongly importance	6	1/6
Strongly importance	5	1/5
Moderate to strongly importance	4	1/4
Moderatly importance	3	1/3
Equally to moderatly importance	2	1/2
Equally importance	1	1/1

Table A 4.2 Pair wise comparison matrix table (Fafen-Jerer)

	RF	**Gm**	**Ge**	**Slope**	**LD**	**LUC**	**DD**	**soil**	**TWI**	**TRI**
RF	1	1	2	3	3	5	5	7	5	7
Gm	1/1	1	3	3	5	5	5	6	7	7
Ge	1/2	1/3	1	1	3	3	5	5	5	7
Slope	1/3	1/3	1/1	1	1	2	3	3	5	5
LD	1/3	1/5	1/3	1/1	1	1	3	3	5	5
LUC	1/5	1/5	1/3	1/2	1/1	1	1	3	3	5
DD	1/5	1/5	1/5	1/3	1/3	1/1	1	1	3	3
soil	1/7	1/6	1/5	1/3	1/3	1/3	1/1	1	3	3
TWI	1/5	1/7	1/5	1/5	1/5	1/3	1/3	1/3	1	1
TRI	1/7	1/7	1/7	1/5	1/5	1/5	1/3	1/3	1/1	1

Table A 4.3 Pair wise comparison matrix (Gambela)

	RF	Geom	Geo	LD	Slope	soil	LULC	DD	NDVI	TWI	TRI
RF	1										
Geom	0.33	1									
Geo	0.33	0.33	1								
LD	0.2	0.33	1	1							
Slope	0.2	0.2	0.33	1	1						
soil	0.2	0.2	0.33	0.5	1	1					
LULC	0.14	0.2	0.2	0.33	0.33	1	1				
DD	0.14	0.14	0.2	0.33	0.33	0.33	1	1			
NDVI	0.14	0.14	0.2	0.2	0.2	0.33	0.33	0.33	1		
TWI	0.13	0.13	0.14	0.2	0.2	0.2	0.33	0.33	1	1	
TRI	0.11	0.13	0.14	0.14	0.14	0.2	0.2	0.33	0.5	1	1

Table A 4.4 Pair wise comparison matrix table (Shinile)

	G	Gm	RF	Slope	LD	LULC	DD	Soil	TWI	TRI
G	1	3	3	3	3	5	5	6	5	7
Gm	0.33	1	3	3	3	5	5	5	6	7
RF	0.33	0.33	1	1	3	3	5	5	5	7
Slope	0.33	0.33	1	1	1	2	3	3	5	5
LD	0.33	0.33	0.33	1	1	1	3	3	5	5
LULC	0.2	0.2	0.33	0.5	1	1	1	3	3	5
DD	0.2	0.2	0.2	0.33	0.33	1	1	1	3	3
Soil	0.17	0.2	0.2	0.33	0.33	0.33	1	1	3	3
TWI	0.2	0.17	0.2	0.2	0.2	0.33	0.33	0.33	1	1
TRI	0.14	0.14	0.14	0.2	0.2	0.2	0.33	0.33	1	1

Table A4.5 Random consistency index table

N	3	4	5	6	7	8	9	10	11	12	13	14	15
RCI	0.58	0.9	1.12	1.24	1.32	1.41	1.45	1.49	1.51	1.48	1.56	1.57	1.59

Table A4.6 The calculated weight of thematic layers for the Fafen-Jerer sub-basin

	Criteria	**Weight**	**Sub-classes**	**Ranks**	**0verall weightage**
1	Rainfall	22	281-341	1	22
			342-445	2	44
			446-585	3	66
			586-720	4	88
			721-884	5	110
2	Geomorphology	25	Mountains	1	25
			Hills and high ridge	2	50
			Plain area	4	100
			Shallow valley	5	125
			U-shaped valley	5	125
3	Geology	15	Alluvial and lacustrine deposits(Q)	5	75
			Jessoma Formation (Pj)	2	30
			Hamanlei Formation (Jh)	3	45
			Adigrat Formation (Ja)	2	30
			Ashangi Formation(P2a)	4	60
			Gabredarre Formation (Jg)	3	45
			Urandab Formation (Ju)	3	45
			Alghe Group (ARI)	1	15

Table A4.6 Continued

4	Lineaments Density	9	0-0.146	1	9
			0.147-0.292	2	18
			0.293-0.438	3	27
			0.439-0.584	4	36
			0.585-0.73	5	45
5	Slope	10	Level slope	5	50
			Gentle sloping	4	40
			Strong slope	3	30
			Moderate steep	2	20
			Very steep	1	10
6	Soil texture	4	Clay	1	4
			Loam	3	12
			Loamy sand	5	20
			Sandy loam	4	16
7	Land use land cover	6	Forest Land	5	30
			Agricultural land	5	30
			Shrub land	3	18
			Build up area	2	12
			Rock out crop	1	6
			Grass Land	4	24
8	Drainage Density	5	0-0.18	5	25
			0.181-0.359	4	20
			0.36-0.539	3	15
			0.54-0.719	2	10
			0.72-0.898	1	5
9	Topographic Wetness Index	2	2.67-7.02	1	2
			7.03-8.79	2	4
			8.8-11.3	3	6
			11.4-14.7	4	8
			14.8-25.3	5	10
10	Topographic Roughness Index	2	0.111-0.364	5	10
			0.365-0.471	4	8
			0.472-0.566	3	6
			0.567-0.675	2	4
			0.678-0.889	1	2

Table A4.7 The calculated weight of thematic layers for the Gambela plain

Criteria	**Sub-class**	**weight**	**Ranks**	**Overall weights**
Rainfall (mm/year)	809.7	28	2	56
	928.85		3	84
	1025.7		4	112
	1113.275		5	140
Geomorphology	Canyons	21	5	105
	Shallow Valleys		4	84
	Plain areas		4	84
	Local ridges		2	42
	Mideslope ridges and Mesas		1	21
Geology	Alluvial and lacustrine deposits(Q)	13	5	65
	Baro Group (ARb)		1	13
	Birbir Group (PR2b)		4	52
	Enticho Sandstone (Pzt)		3	39
	Late to post - tectonic granite(gt3)		2	26
	Makonnen Basalts (PNmb)		4	52
Slope	Level to gentle slope	8	5	40
	Moderate sloping		4	32
	Strong slope		3	24
	Moderate steep		2	16
	Steep to very steep		1	8
Drainage density	0_0.00457	4	5	20
	0.0458_0.124		4	16
	0.125_0.207		3	12
	0.208_0.309		2	8
	0.31_0.555		1	4

Table A4.7 Continued

LULC	Water body	5	5	25
	Wet lands		5	25
	Forest Land		4	20
	Agricultural land		4	20
	Grass Land		3	15
	Shrub land		3	15
	Sandy area		4	20
	Build up area		1	5
	Rock out crop		1	5
Lineaments density	0-0.057	9	1	9
	0.058-0.167		2	18
	0.168-0.297		3	27
	0.298-0.455		4	36
	0.456-0.733		5	45
Soil	Clay	6	2	12
	Loam		3	18
	Loamy sand		5	30
NDVI	-0.43	2	1	2
	0.128-0.236		2	4
	0.237-0.337		3	6
	0.338-0.451		4	8
	0.452-0.731		5	10
TWI	2.41-7.58	2	1	2
	7.59-9.33		2	4
	9.34-11.6		3	6
	11.7-14.9		4	8
	15-24.7		5	10
TRI	0.111-0.309	2	5	10
	0.31-0.437		4	8
	0.438-0.556		3	6
	0.557-0.665		2	4
	0.686-0.889		1	2

Table A4.8 The calculated weight of thematic layers for the Shinile sub-basin

Criteria	Weight	Sub-class	Ranks	Overall weights
Geology	26	Alluvial and lacustrine deposits(Q)	5	130
		Undifferentiated alluvial	5	130
		Basalts flows	4	104
		Jessoma Formation (Pj)	3	78
		Hamanlei Formation (Jh)	3	78
		Adigrat Formation (Ja)	2	52
		Ashangi Formation(P2a)	2	52
		Afar series	4	104
		Amba Aradom formation	3	78
		Chilalo Formation (Nc)	2	52
		Delaha Formation (Ndb)	2	52
		Alghe Group (ARI)	1	26
Geomorphology	21	Valley	5	105
		open slope	4	84
		plain	4	84
		hills	2	42
		mountains	1	21
Rainfall	14	426-521	1	14
		522-585	2	28
		586-631	3	42
		632-676	4	56
		677-798	5	70
Slope	10	Level to gentle	5	50
		Moderate sloping	4	40
		Strong sloping	3	30
		moderate steep	2	20
		steep to very steep	1	10
Lineaments Density	9	0.0-0.146	1	9
		0.147-0.292	2	18
		0.293-0.438	3	27
		0.439-0.584	4	36
		0.585-0.73	5	45

Table A4.8 Continued

LULC	7	Agricultural land	5	35
		Shrub land	3	21
		Build up land	2	14
		Rock outcrop	1	7
		Grassland	4	28
		Bare land	1	7
Drainage density	5	0.1-0.18	5	25
		0.181-0.359	4	20
		0.36-0.539	3	15
		0.54-0.719	2	10
		0.72-0.898	1	5
soil	4	clay	1	4
		loam	3	12
		loamy sand	5	20
		sandy loam	4	16
Topographic wetness index	2	2.67-7.02	1	2
		7.03-8.79	2	4
		8.8-11.3	3	6
		11.4-14.7	4	8
		14.8-25.3	5	10
Topographic roughness index	2	0.111-0.364	5	10
		0.365-0.471	4	8
		0.472-0.566	3	6
		0.567-0.675	2	4
		0.678-0.889	1	2

Table A6.1 The vulnerability index results of removal of each of the modified DRASTIC parameters (Fafen-Jerer)

Parameters removal	Minimum	Mean	Maximum	Standard Deviation (SD)
D	103	136.01	194	19.64
R	90	145.49	206	22.12
A	97	138.28	218	30.52
S	90	153.10	230	29.85
T	105	156.20	237	30.34
I	75	132.05	237	31.47
C	95	149.77	230	30.09
L	103	145.74	197	23.79
LULC	101	152.10	233	30.10

Table A6.1Map removal sensitivity calculation (Fafen-Jerer)

Parameters removal	Minimum	Mean	Maximum	Standard Deviation (SD)
D	0.014	1.78	5.625	1.36
R	0.027	1.41	5.916	1.13
A	0.027	1.22	5.36	0.85
S	0.027	1.02	2.7	0.60
T	0.15	1.39	3.4	0.66
I	0.014	1.97	4.18	1.08
C	0.014	1.05	3.65	0.87
L	0.027	1.24	7.23	1.12
LULC	0.014	0.94	3.48	0.69

Table A6.3 The vulnerability index results of removal of each of the modified DRASTIC parameters (Gambela)

Parameters Removal	Minimum	Mean	Maximum	Standard Deviation (SD)
D	20	142.95	203	20.26
R	18	159.22	228	18.64
A	23	151.08	218	23.44
S	20	169.99	234	20.37
T	22	170.22	239	22.53
I	23	130.94	198	23.62
C	17	166.68	218	17.37
L	21	172.01	226	21.08
LULC	22	166.88	233	22.92

Table A6.4 Map removal sensitivity calculation (Gambela)

Parameters Removal	Minimum	Mean	Maximum	Standard Deviation (SD)
D	0.014	2.006	3.68	1.17
R	0	1.264	5.81	0.87
A	0.027	1.065	2.32	0.56
S	0.61	1.388	2.03	0.32
T	0.61	1.418	2.61	0.39
I	0.014	3.501	4.33	0.91
C	0.305	1.51	2.403	0.52
L	0.027	1.689	2.58	0.49
LULC	0.167	1	2.44	0.45

Table A6.5 The vulnerability index results of removal of each of the modified DRASTIC parameters (Shinile)

Parameters Removal	Minimum	Mean	Maximum	Standard Deviation (SD)
D	81	157.68	222	25.509
R	85	151.21	206	21.808
A	79	146.69	213	23.268
S	89	162.36	231	24.333
T	90	167.62	242	25.547
I	80	135.19	200	23.491
C	88	153.41	213	22.443
L	90	158.43	203	24.053
LULC	86	162.5	232	25.513

Table A6.6 Map removal sensitivity calculation (Shinile)

Parameters Removal	Minimum	Mean	Maximum	Standard Deviation (SD)
D	0	0.956	7.3	0.976
R	0.013	1.456	9.3	1.144
A	0	1.154	3.8	0.522
S	0.28	0.916	2.2	0.354
T	0.3	1.573	3.25	0.543
I	0	2.627	4.26	1.371
C	0	0.873	2.32	0.634
L	0.28	1.626	3.8	0.893
LULC	0.04	1.229	8.6	0.982

Table A7.1The climate change effect on groundwater of western catchment

			Effective precipitation (mm)				
			0-20	21-60	61-1200	1201-2000	2001-2650
		Effect	very high	high	medium	low	very low
De Martone Aridity Index							
Extremely	DMI>55	Very low	medium	medium	low	low	very low
Very humid	35≤DMI≤55	Low	high	medium	medium	low	low
Humid	28≤DMI<35	Medium	high	high	medium	medium	low
Semi-humid	24≤DMI<28	High	very high	high	high	medium	medium
Mediterranean	20≤DMI<24	Very high	very high	very high	high	high	medium
			Climate change effect				
			very high	high	medium	low	very low

Table A7.2 The climate change effect on groundwater of the eastern catchment

			Effective precipitation (mm)				
			0-10	11-20	21-40	41-60	61-89.4
		Effect	very high	high	medium	low	very low
De Martone Aridity Index							
Humid	28≤DMI<35	Very low	medium	medium	low	low	very low
Semi-humid	24≤DMI<28	Low	high	medium	medium	low	low
Mediterranean	20≤DMI<24	Medium	high	high	medium	medium	low
Semi-arid	10≤DMI<20	High	very high	high	high	medium	medium
Arid	DMI<10	Very high	very high	very high	high	high	medium
			Climate change effect				
			very high	high	medium	low	very low

Dissertation Approval Sheet

Addis Ababa University

Ethiopian Institute of Water Resources

As a member of the Board of Examiners of the PhD dissertation Open Defense Examination, this is to certify that the dissertation prepared by Tesema Kebede Seifu entitled "Characterization of Major Alluvial Aquifers of Ethiopia and Determination of their Vulnerability to Climate Variability and Land Use Changes" submitted in the fulfillment of the requirement for Degree of Doctor of Philosophy in Water Resources Engineering and Management (Specialization in Groundwater Management) meets the accepted standards concerning originality and quality.

Approved by the Board of Examiners:

Dr.Samuel Dagalo (Asso. Prof.)		18 May, 2024
External Examiner	Signature	date
Dr. Solomon Gebreyohannis (Asso. Prof.)	#Solomon Gebreyohannis	23/5/2024
Internal Examiner	Signature	date
Dr. Behailu Birhanu (Asso. Prof.)		25/5/2024
Internal Examiner	Signature	Date
Dr. Haileyesus Belay (Asst. Prof.)		27/5/2024
Chairperson	Signature	Date
Prof. Tenalem Ayenew (Prof. Dr.)		27/5/2024
Main Advisor	Signature	Date
Dr. Tilahun Derib (Asst. Prof.)		
EIWR Coordinator	Signature	Date

Document Viewer

Turnitin Originality Report

Processed on: 26-Nov-2023 12:25 EAT
ID: 2231760750
Word Count: 66571
Submitted: 1

PhD Thesis Tesema By Tesema Kebede

Similarity Index	Similarity by Source
24%	Internet Sources: 24% Publications: 2% Student Papers: 4%

exclude quoted | exclude bibliography | exclude small matches | mode: overview (classic) report | print | refresh | download

checked by zelelee Agide (PhD) 29/11/23

2% match (Internet from 31-Oct-2023)
https://downloads.hindawi.com/journals/ijac/2023/7454137.pdf

1% match (Internet from 23-Aug-2023)
http://carpcoll.csmb.gov.cn

1% match (Internet from 15-May-2023)
https://ayan.iitg.ac.in

1% match (Internet from 16-May-2020)
https://www.nrc.ch/sites/nrc.ch/files/uploads/2019/09/Final_report.pdf

1% match ("Groundwater Resource Development and Planning in the Semi-Arid Region", Springer Science and Business Media LLC, 2021)
"Groundwater Resources Development and Planning in the Semi-Arid Region", Springer Science and Business Media LLC, 2021

1% match (Swamim, Jayant Nath Tripathi, Irjesh Sankar, Surya Prakash Tiwari. "Groundwater potential mapping in Trans Yamuna Region, Prayagraj, using combination of geospatial technologies and AHP method", Environmental Monitoring and Assessment, 2023)
Swamim, Jayant Nath Tripathi, Irjesh Sankar, Surya Prakash Tiwari. "Groundwater potential mapping in Trans Yamuna Region, Prayagraj, using combination of geospatial technologies and AHP method", Environmental Monitoring and Assessment, 2023

1% match ("Geostatistics and Geospatial Technologies for Groundwater Resources in India", Springer Science and Business Media LLC, 2021)
"Geostatistics and Geospatial Technologies for Groundwater Resources in India", Springer Science and Business Media LLC, 2021

<1% match (student papers from 16-Jul-2023)
Class: MSc thesis
Assignment: MSc thesis Final
Paper ID: 2131760750

<1% match (student papers from 10-Sep-2023)
Submitted to Addis Ababa University on 2021-09-10

<1% match (student papers from 29-May-2023)
Submitted to Addis Ababa University on 2023-05-29

<1% match (student papers from 16-Jul-2023)
Class: MSc thesis
Assignment: MSc thesis Final
Paper ID: 2131764219

<1% match (student papers from 07-Oct-2023)
Submitted to Addis Ababa University on 2023-10-07

<1% match (student papers from 22-Aug-2023)
Submitted to Addis Ababa University on 2023-08-22

<1% match (student papers from 08-Jun-2023)
Submitted to Addis Ababa University on 2023-06-08

<1% match (Internet from 19-Dec-2022)
https://www.cotalog.cglar.org/dbtw-wpd/exec/dbtwpub.dll?AC=SEE_ALSO&BG=&BU=http%3A%2F%2Fwww.catalog.cglar.org%2Fexec%2Fmsc.htm&DF=WWW+expand&DL=16DT=&EF=&EL=16ES=16&nnd%2Fexec%2Fdbtwpub.dll&XP=

<1% match (Internet from 25-Dec-2022)
https://www.catalog.cglar.org/dbtw-wpd/exec/dbtwpub.dll?AC=SEE_ALSO&BG=&BU=http%3A%2F%2Fwww.catalog.cglar.org%2Fexec%2Fmsc.htm&DF=WWW+expand&DL=&DT=&EF=&EL=16ES=&nnd%2Fexec%2Fdbtwpub.dll&XP=

<1% match (Internet from 25-Dec-2022)
https://www.catalog.cglar.org/dbtw-wpd/exec/dbtwpub.dll?AC=SEE_ALSO&BG=&BU=http%3A%2F%2Fwww.catalog.cglar.org%2Fexec%2Fmsc.htm&DF=WWW+expand&DL=&DT=&EF=&EL=16ES=&nnd%2Fexec%2Fdbtwpub.dll&XP=

<1% match (Internet from 25-Dec-2022)